APC/C^{Cdh1} Contributes to Maintenance of Genome Stability by Targeting the DNA-end Resection Factor CtIP

Dissertation

zur

Erlangung der naturwissenschaftlichen Doktorwürde
(Dr. sc. nat.)

vorgelegt der

Mathematisch-naturwissenschaftlichen Fakultät

der

Universität Zürich

von

Lorenzo Lafranchi

von

Monteceneri/Medeglia TI

Promotionskomitee

Prof. Dr. Alessandro A. Sartori (Vorsitz und Leitung der Dissertation)

Dr. Izabela Sumara

Prof. Dr. Claus M. Azzalin

Prof. Dr. Ian J. Frew

Zürich, 2015

Zusammenfassung

Alle Zellen besitzen Mechanismen, um ihr Erbmaterial vor Schäden, die durch Substanzen endogenen oder exogenen Ursprungs verursacht werden zu schützen. Wenn Schäden in der DNA nicht adäquat repariert werden, können sie zum Zelltod oder sogar zu Mutationen und damit zur Entstehung von Krebs führen. Um dies zu verhindern, sind die Zellen mit einem komplexen System ausgestattet, welches DNA-Schäden erkennt und repariert, dem „DNA damage response"-System. Der zellulären Reaktion auf DNA-Schäden durch das DDR-System liegt ein komplexes Netzwerk von Signalkaskaden zugrunde, welches die Läsionen erkennt und durch posttranslationale Modifikationen, wie Phosphorylierung und Ubiquitinierung, verschiedene Reparaturmechanismen aktiviert. Dabei ist die DDR auch für die Aktivierung der Zellzyklus-Kontrollpunkte verantwortlich, wodurch ein genügend grosses Zeitfenster zur Reparatur des Schadens gewährleistet und gleichzeitig die Replikation der fehlerhaften DNA gestoppt wird.

DNA-Doppelstrangbrüche (DSBs) zählen zu den gefährlichsten Schäden, die entweder durch Fehler während der DNA-Replikation oder durch Exposition der Zellen gegenüber mutagenen Substanzen entstehen können. Zur Reparatur von DSBs hat die Zelle hauptsächlich zwei Mechanismen entwickelt: nicht-homologes Verknüpfen von DNA-Enden (NHEJ) und homologe Rekombination (HR). NHEJ ist der vorrangige Reparaturmechanismus für DSBs in menschlichen Zellen und findet während des gesamten Zellzyklus statt. Im Gegensatz dazu ist für HR die homologe Sequenz des intakten Schwesterchromatids als Matrize erforderlich. Deshalb ist die Reparatur durch HR zwar fehlerfrei, aber auf die S/G_2-Phase des Zellzyklus beschränkt. Während der S/G_2-Phase sind NHEJ und HR konkurrierende Reparaturwege und die Wahl des richtigen Mechanismus ist entscheidend für die Erhaltung der genomischen Stabilität der Zelle. Werden die DSBs in dieser Phase nicht richtig prozessiert, können chromosomale Translokationen und Krebs die Folge sein.

HR wird durch die Resektion der DNA-Enden des Strangbruches eingeleitet und bestimmt somit den Reparaturweg, welcher wiederum streng durch den Zellzyklus reguliert wird. Das humane CtIP-Protein ist ein Schlüsselfaktor für die Initiierung der Resektion, dessen Aktivität durch verschiedene post-translationale Modifikationen kontrolliert wird. Zusätzlich wird die Proteinmenge von CtIP während der G_1-Phase

reduziert und während der S/G_2-Phase des Zellzyklus erhöht. Im ersten Teil meiner Dissertation charakterisiere ich einen neuen Mechanismus zur Regulierung der Proteinstabilität von CtIP während des Zellzyklus. Ich zeige, dass die APC/C^{Cdh1} E3 Ubiquitin Ligase für den Proteasom-abhängigen Abbau von CtIP während der G_1 verantwortlich ist. CtIP interagiert mit Hilfe eines hochkonservierten KEN Box-Motivs mit dem APC/C Co-Aktivator Cdh1. Die Mutation der KEN Box (CtIP-K467A) verhindert die Interaktion und beeinträchtigt die Poly-ubiquitinierung von CtIP. Dementsprechend ist die CtIP-K467A-Mutante nach dem Austreten aus der Mitose stabiler als die wildtyp-Form des Proteins.

Wenn Zellen DNA-schädigenden Substanzen ausgesetzt werden, kann APC/C^{Cdh1} auch in der S/G_2-Phase aktiviert werden und ist an der Aufrechterhaltung des G_2/M Zellzyklus-Kontrollpunkts beteiligt. Im zweiten Teil der Studie zeige ich, dass CtIP nicht nur in der G_1-Phase, sondern nach DNA-Schäden auch in der S/G_2-Phase durch APC/C^{Cdh1} poly-ubiquitiniert und somit für den proteasomalen Abbau markiert wird. Überexpression der CtIP-KEN Box Mutante führt, genauso wie die Inhibierung des APC/C Komplex nach DNA-Schäden in S/G_2, zu einer verstärkten Resektion von DNA-Enden bei einer gleichzeitigen Verringerung von HR. Möglicherweise ist in diesen Zellen der darauffolgende Schritt, nämlich die Rekrutierung der Rad51 Rekombinase beeinträchtigt, weil die CtIP-KEN Box Mutante nicht von den prozessierten DNA Enden beseitigt werden kann. Interessanterweise haben wir eine ähnliche Beeinträchtigung in der Rekrutierung von Rad51 und in HR auch in Cdh1-defizienten Zellen beobachtet.

Zusammengefasst deuten diese Ergebnisse darauf hin, dass APC/C^{Cdh1} den Abbau von CtIP während der G_1-Phase sowie nach DNA-Schäden in der G_2-Phase des Zellzyklus kontrolliert und dadurch entscheidend an der Wahl des geeigneten DSB-Reparaturwegs beteiligt ist. Diese Studie beschreibt eine neue Rolle für die APC/C Ubiquitin Ligase bei dem Erhalt der genomischen Stabilität, unter anderem durch die Kontrolle der Stabilität des DNA-Reparatur Faktors CtIP.

Summary

Our genome is constantly exposed to endogenous and exogenous agents causing DNA damage. Unrepaired lesions can lead to cell death or, even more hazardous for an organism, misrepaired DNA damage can result in genomic instability and promote tumorigenesis. To counteract genomic instability, cells are equipped with a multifaceted system to efficiently signal and repair defects in DNA: the DNA damage response (DDR). Upon detection of genomic lesions, the DDR activates DNA repair pathways through a cascade of post-translational modifications including phosphorylation and ubiquitiylation. Moreover, the DDR is responsible for the activation of cell cycle checkpoints thereby allowing time for DNA repair to occur.

DNA double-strand breaks (DSBs) are particularly cytotoxic lesions, which can arise either during replicative stress or from exposure to DNA damaging agents. Cells can deal with DSBs through two major repair pathways: non-homologous end joining (NHEJ) and homologous recombination (HR). NHEJ is the predominant pathway in human cells and acts throughout the cell cycle, while HR only takes place in S/G_2 phase when the intact sister chromatid is available as a template to allow homology-directed repair. Thus, during S and G_2 phases of the cell cycle, NHEJ and HR compete for DSB repair. Choosing the suitable mechanism is pivotal for genome stability maintenance, because inappropriately repaired DSBs have the potential to trigger chromosomal translocations that may result in various diseases including cancer.

HR is initiated through the resection of broken DNA ends, a process determining DSB repair pathway choice and, thus, tightly regulated during the cell cycle. The activity of the key DNA-end resection factor CtIP for instance is controlled by various post-translational modifications. Moreover, CtIP protein levels are low during G_1 and increase in S/G_2 phases of the cell cycle. In the first part of my PhD thesis, I characterized a novel regulatory mechanism responsible for the cell cycle fluctuations of CtIP, by showing that the APC/C^{Cdh1} ubiquitin ligase targets CtIP for proteasome-dependent degradation following mitotic exit. In addition, I discovered that the APC/C co-activator Cdh1 interacts with CtIP through an evolutionary conserved KEN box motif, mutation of which (CtIP-K467A) abrogates CtIP-Cdh1 interaction and impairs CtIP polyubiquitylation. Consequently, we found that the CtIP-K467A mutant is more stable throughout G_1 compared to the wild-type CtIP protein.

Summary

Upon treatment with genotoxic agents, APC/C^{Cdh1} is transiently activated during G_2 phase and is involved in the maintenance of the G_2/M checkpoint. In the second part of my study, I demonstrated that, besides in unperturbed G_1 cells, CtIP is polyubiquitylated and targeted for degradation by the APC/C^{Cdh1} after DNA damage in G_2. In irradiated G_2 cells, we observed that CtIP-K467A causes disproportionate DNA-end resection, resulting in reduced HR efficiency. As a possible mechanistic explanation for these phenotypes, CtIP-K467A is defective in being cleared from sites of DSBs. Hence the loading of the Rad51 recombinase, an event occurring downstream of DNA-end resection, is impaired in the CtIP-K467A mutant cells. Interestingly, I observed a similar defect in Rad51 recruitment to DSBs and, thus, a decrease in HR in Cdh1-depleted cells.

Taken together, we hypothesize that APC/C^{Cdh1}-mediated degradation of CtIP, both during G_1 and after DNA damage in G_2, contributes in limiting DNA-end resection and therefore choosing the appropriate DSB repair pathway. In summary, this study describes a novel role for the APC/C ubiquitin ligase in the maintenance of genome stability, at least partially, by controlling the stability of the DNA-end resection factor CtIP.

Table of contents

1 Introduction

1.1 Cancer and genome instability

Cancer is a widely used term, which can be employed to indicate an evil or destructive phenomenon that is hard to contain or eradicate [1]. The word originated in the medical field, in which cancer indicates a heterogeneous disease arising from abnormal cells, which acquired the capacity to divide without control and ultimately invade other tissues. Cancer is not just one disease but many diseases that can originate from cells belonging to any tissue of the body. There are more than 100 different types of cancer [2] and with 8.2 million deaths in 2012 they account for the leading causes of death worldwide. Despite the huge efforts to understand and restrict cancer incidence, 14.1 million new cancer cases were diagnosed in 2012 [3]. The “war on cancer” was initiated in the seventies to improve the understanding of cancer biology and to develop more effective cancer treatments [4]. Over the years, cancer research generated a huge amount of data, which help the treatment of some forms of cancer, but mainly demonstrate the complexity of this disease. The main challenge in treating cancer is that it arises from inside the body making a targeted approach extremely challenging.

In the year 2000, Hanahan and Weinberg, tried to identify underlying principles, which are common to all cancer cells [5]. Accordingly to the authors, the acquired capabilities of cancer cells are self-sufficiency in growth signals, insensitivity to antigrowth signals, evading apoptosis, limitless replicative potential, sustained angiogenesis and tissue invasion or metastasis. Virtually, all cancers must acquire these six capabilities, but they can arise in different ways, both mechanistically and chronologically. The work is based on the observations that cancer is enabled by dynamic changes occurring in the human genome, eventually leading to mutations. The genes that, if mutated, play a role in tumorigenesis are categorized as oncogenes, which acquire a dominant gain-of-function or tumor suppressors, which result in a recessive loss-of-function. Accumulation of mutations enables the cells to acquire the above-mentioned hallmarks that allow them to overcome intrinsic and extrinsic control mechanisms, which in healthy tissues restrict cellular proliferation. Therefore, genome instability and mutations are defined as main enabling characteristics of cancer. In a more recent review, the same authors refine their

model by suggesting tumor-promoting inflammation to be a second enabling characteristic, which fosters multiple hallmarks [6].

Genome instability is observed in almost all human cancers, whereas “normal” human cells are equipped with complex genome maintenance systems, which allow them to deal with DNA lesions and avoid mutations. In fact, despite cells experience tens of thousands of DNA lesions per day, the rate of spontaneous-arising mutations is extremely low [7, 8]. There are different types of DNA lesions and they can arise following exogenous or endogenous challenges. For example, various environmental agents, such as the ultraviolet (UV) component of sunlight, ionizing radiation (IR) and genotoxic chemicals are able to disrupt the DNA integrity. Moreover, normal metabolic processes, such as cellular respiration, can indirectly damage the DNA through the production of reactive oxygen species [9]. Finally, the chemical structure of DNA can degenerate over time, affecting the original information [10]. Even if they are highly different, all lesions affect the integrity of the DNA structure, thereby interfering with vital cellular processes like DNA transcription and replication. Therefore, the majority of lesions are in principle able to kill a cell. Therefore, cells must be capable of detecting, signaling and repairing DNA lesions though a complex network of interconnected pathways, named the DNA damage response (DDR). Errors occurring during the detection and the repair process can easily lead to the introduction of mutations in the genomic information. As discussed above, for a multicellular organism, mutations can have consequences that are even more detrimental than those of cellular death, namely causing various disorders including cancer. Generally, acquisition or genetic predisposition to mutations in genome caretaker genes, such as DDR factors, increase the overall rate of mutations, thereby causing genome instability and paving the way for carcinogenesis [11, 12].

1.1.1 DNA repair pathways

Cells evolved different repair pathways to deal with the wide variety of lesions that can arise in their DNA. For example, the nucleotide excision repair (NER) pathway is responsible for repairing UV-induced cyclobutane-pyrimidine dimers (CPDs) and 6-4 photoproducts (6-4PPs). Two sub-pathways of NER, with partly different substrate specificity, are responsible for detecting the lesions either using a global genome approach (GG-NER) or focusing on damages that block elongating RNA polymerases (TCR, transcription coupled repair). Base excision repair (BER) is the main actor in dealing with metabolic-induced damages, such as 8-oxoguanine or

DNA methylation, hydroxylation and deamination. Different damage-specific glycosylases are involved in the recognition and removal of the modified bases, leaving an abasic side that is addressed by the APE1 endonuclease. The following repair process overlaps with single-strand DNA break (SSB) repair and requires the combined action of nucleases, polymerases and ligases. A central player in SSB repair is the poly-adenosine-diphosphate-ribose (PAR) polymerase (PARP). After damage detection, PARP catalyzes the formation of PAR chains, which enable the recruitment of proteins required for repair. Mismatch repair (MMR) recognizes and repair insertion/deletion loops and nucleotide mis-pairing occurring during DNA replication. After detection of a lesion, the DNA is incised in close proximity and then repaired by various downstream factors. Homologous recombination (HR) and non-homologous end joining (NHEJ) are the two principal mechanisms used to repair DNA double-strand breaks (DSBs).

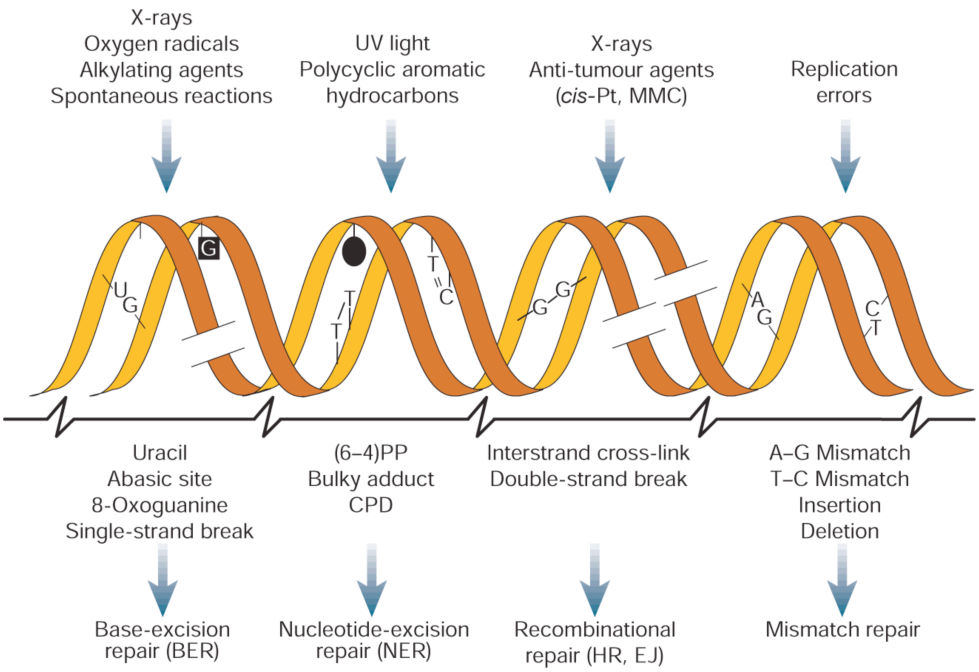

Figure 1 DNA damage and repair mechanisms. Different DNA damaging agents (top) induce a variety of DNA lesions (middle), which are addressed by dedicated repair mechanisms (bottom). Adapted from [8].

Cells are not able to directly repair all DNA damages. Translesion synthesis (TLS) is a repair tolerance system that permits to bypass DNA lesions. TLS is achieved by the use of dedicated DNA polymerases with a less stringent base-pair requirement than replicative polymerases. Interestingly, the different repair pathways are tightly interconnected and some lesions (e.g. a SSB) can be introduced to the DNA by the repair process and then be addressed by the specific repair pathway. The Fanconi

anemia (FA) pathway is a well-established example where different DNA repair pathways co-operate to repair cross-linked DNA (interstrand cross-link, ICL). The FA pathway is composed by a set of genes (15 so far) that have been identified to be mutated in patients, which display hypersensitivity towards cross-linking chemicals, such as mitomycin C (MMC) or cisplatin. Apart of the core components of the FA pathway, ICL repair requires the action of proteins belonging to the NER, HR and TLS pathways.

1.1.2 The DNA damage response

The DNA damage response is a multifaceted system that permits to properly signal and deal with damaged DNA. Although the repair processes per-se differ between the various classes of lesions, they are usually controlled by a common signaling program. Detection of DNA damage leads to the activation of one of the three apical kinases, belonging to the family of phosphatidylinositol 3-kinase-like protein kinases (PIKKs) [13]. ATM (ataxia telangiectasia mutated) and DNA-PK (DNA-dependent protein kinase) become activated following detection of DSBs by the Mre11-Rad50-Nbs1 (MRN) complex or the Ku70-Ku80 heterodimer, respectively [14-16]. ATR (ataxia telangiectasia and Rad3-related) is activated by the presence of ssDNA coated by the Replication Protein A (RPA) complex and requires the presence of the ATR-interacting protein (ATRIP), Rad17 and the 9-1-1 (Rad9, Rad1, Hus1) complex [17, 18]. Proteomics analysis showed that DNA-PK activity is restricted to few proteins, whereas ATM and ATR target more than 700 substrates [19, 20]. Active ATM/ATR/DNA-PK phosphorylate serine 139 of the histone variant H2AX at chromatin regions surrounding DSB sites [7]. Phosphorylated H2AX, called γH2AX, can now be recognized by phosphopeptide-binding BRCT (BRCA1 C terminus) domains, which are present in many proteins involved in the DDR. One of these proteins, MDC1, is a large adaptor protein, which directly binds γH2AX and serves as a docking site for the recruitment of different factors amplifying the DDR [21, 22]. Importantly, MDC1 recruits RNF8, a RING-domain E3 ubiquitin ligase that initiates a ubiquitylation cascade by forming K63-linked ubiquitin chains on different histone protein variants [23-25]. RNF168 then binds to ubiquitylated histones and amplifies RNF8-dependent ubiquitylation events, which is necessary for the recruitment of different chromatin-associated repair mediators such as 53BP1, BRCA1 and TopBP1 [26-28]. Generally, DNA repair mediators help sustaining damage-induced signaling. For example, TopBP1 binds phosphorylated 9-1-1

complex and thereby boosts the activity of ATR [29]. Other examples of mediator proteins are 53BP1 and BRCA1, which play an antagonistic role during the initial stages of DSB repair. Two well-studied targets of the ATR and ATM signaling cascade are the checkpoint kinases 1 and 2 (Chk1 and Chk2), respectively [30]. Claspin, another mediator protein, is required for Chk1 stability and mediating its association and activation by ATR [31, 32]. In turn, Chk1 and Chk2 inhibit main components of the cell cycle machinery to delay cell cycle progression, allowing time for repair (see below). Besides activating DNA damage checkpoints, ATM/ATR directly phosphorylate repair proteins leading to their activation and recruitment to the site of damage (see chapter 1.6).

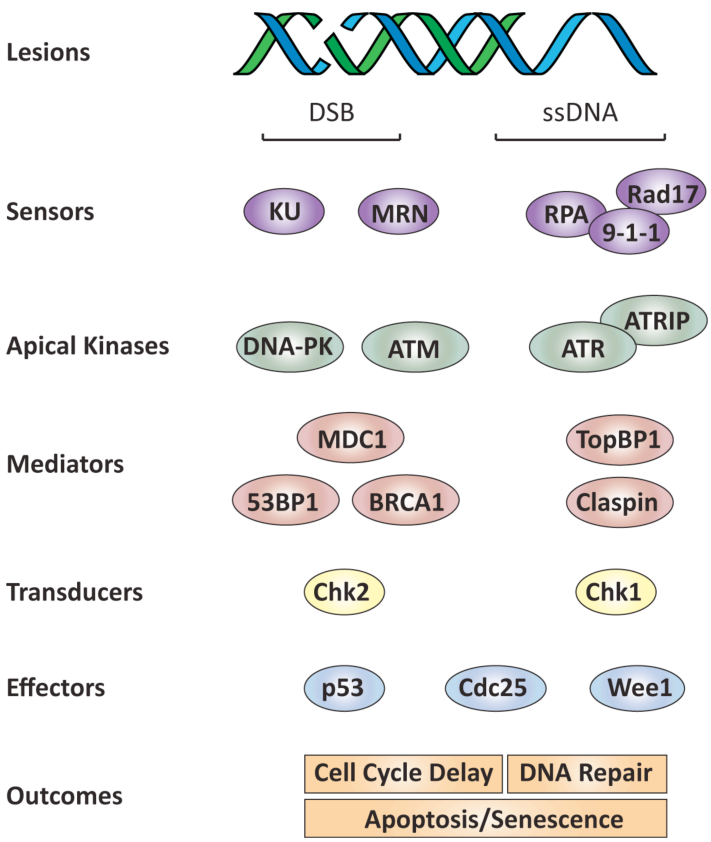

Figure 2 The DNA damage response. Detection of DNA lesions by specialized sensor proteins results in the activation of one of the three apical kinases (ATM, ATR or DNA-PK). Mediator proteins are involved in the activation or in the amplification of the signaling cascade, which finally result in the activation of the two diffusible transducer kinases (Chk1 and Chk2). Effector proteins modulate the activity of cell cycle regulators, transiently blocking cell cycle progression, allowing time for the repair to occur. In case of severe DNA damage, DDR activation results in senescence or apoptosis. Adapted from [33].

Mutations in various proteins involved at different steps of the DDR cause a predisposition to tumor development. For example, ATM mutations observed in patients suffering from ataxia telangiectasia (A-T), result in an increased risk of

developing thymic lymphoma and other cancers [34]. A-T cells are impaired in checkpoint activation upon DNA damage, a condition that contributes to genome instability and favors tumorigenesis. Similar phenotypes are also observed in patients suffering from the Nijmegen breakage syndrome, which is caused by mutations in the gene encoding for the Nbs1 protein [35]. These patients also suffer of immunodeficiency, due to inefficient V(D)J recombination and class switch recombination (CSR). Moreover, mutations in genes encoding for NHEJ proteins can facilitate lymphomagenesis due to the increased rate of transpositions that is caused by unrestrained alt-NHEJ [36]. Finally, germline mutations in the BRCA1, BRCA2 or PALB2 genes predispose the carrier to develop breast and ovarian cancer [37, 38].

1.2 The cell cycle

The cell cycle is an ordered sequence of events, which result in the duplication of a cell. Indeed, proliferating cells are constantly cycling through a growth or gap phase (G_1), a phase in which the DNA is replicated (S phase), a second growth phase (G_2) and, finally, the division into two daughter cells (M phase or mitosis).

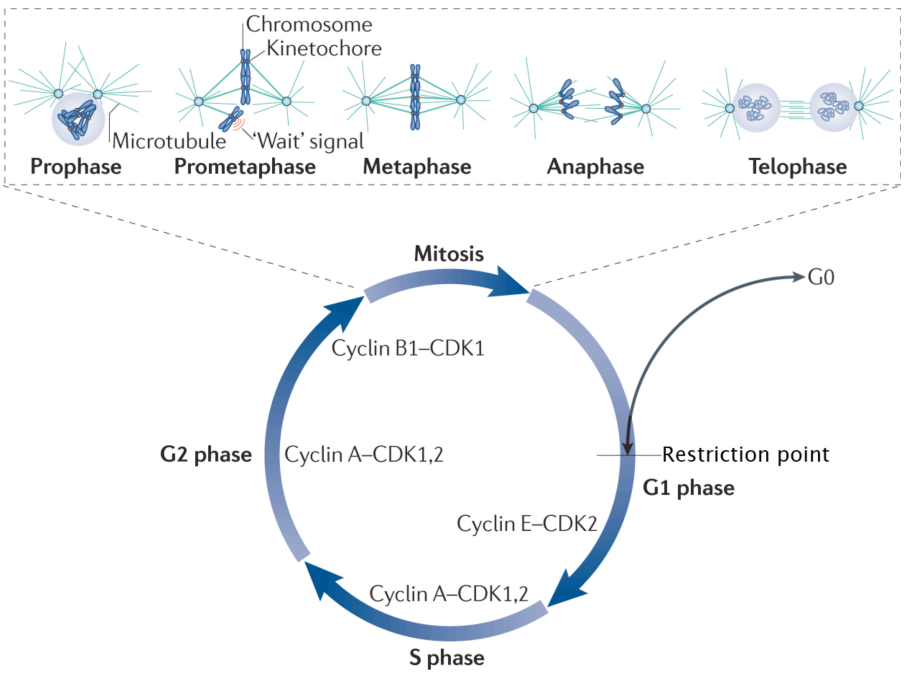

Figure 3 The cell cycle. The various phases of the cell cycle –G_1, S, G_2 and mitosis– are depicted. Dedicated cyclin-CDK complexes control each phase. Passage through the restriction point in G1 phase commits cells to enter S phase and complete the cell cycle. An expanded view of mitosis is shown at the top of the figure. In prophase, the chromosomes condense and the nuclear envelope breaks down. In prometaphase, the chromosomes attach to the mitotic spindle, and any unattached chromosomes generate a "wait" signal. In metaphase, all the chromosomes attach, and the "wait" signal is turned off. In anaphase, the

sister chromatids separate, and in telophase the DNA decondenses, the nuclear envelope reforms and the two daughter cells form by cytokinesis. Adapted from [41].

Transitions between the different phases are orchestrated by cyclin-dependent kinases (CDKs), which are controlled by dedicated activating subunits, called cyclins [39]. The human genome encodes for 11 CDKs and 9 CDK-like proteins, but the main cell cycle transitions are regulated by a few, highly conserved CDKs [40]. Moreover, higher eukaryotes express different isoforms of the various cyclins (e.g. cyclin B1-3), which perform slightly different cellular functions.

In case of growth stimuli, D-type cyclins are synthesized. D-type cyclins activate CDK4/6 allowing progression through G_1 phase, by phosphorylating different members of the retinoblastoma (Rb) protein family and therefore suppressing their anti-proliferative activity. Hyperphosphorylation of Rb releases inhibition of E2F, which results in transcription of E-, A- and B-type cyclins and of E2F itself. The fast increase in E-type cyclins, ensure a positive feedback loop, which generates a rapid rise in E2F-dependent transcription, which is now sustained alone by CDK2-cyclin E complexes. This point is known as “restriction point” and the cells can afterwards undergo cell division, independently of mitogen stimulation. In addition to maintain Rb phosphorylation, the activity of CDK2-cyclin E complexes is essential for initiating DNA replication through loading of the mini chromosome maintenance (MCM) complex to origins of replication. Right after origin firing, E-type cyclins are rapidly degraded to avoid re-replication of DNA and the slow accumulating A-type cyclins ensure the maintenance of high CDK2 activity. CDK2-cyclin A complexes phosphorylate numerous proteins that are required for proper completion and exit from S phase [40]. During G_2, A-type cyclins are degraded in a ubiquitin-dependent manner, whereas B-type cyclins are actively synthesized to sustain CDK1 activation. CDK1-cyclin B complexes are the main drivers of the extensive reorganization required for mitosis. Indeed, activity of CDK1-cyclin B complexes permit Golgi fragmentation, nuclear envelope breakdown, chromosome condensation and formation of the mitotic spindle [42]. Other important kinases orchestrating mitotic progression belong to the Aurora and Polo-like kinase (Plk) families. Finally, inactivation of CDK1-cyclin B complexes and mitotic kinases is required for proper completion of mitosis and re-establishment of G_1 phase. Inactivation of the various mitotic regulators is accomplished by ubiquitylation and proteosomal degradation supported by the anaphase-promoting complex, also known as cyclosome (APC/C).

1.2.1 Cell cycle checkpoints

To ensure that the various processes belonging to a cell cycle phase are completed before proceeding into the next one, the cells evolved different control mechanisms. These mechanisms are called cell cycle checkpoints and permit to temporarily arrest cell cycle progression at different critical transitions. The G_1/S checkpoint, or restriction point, is an important commitment point for the cells, because they have to decide whether initiate a further round of cell division or stop proliferating and enter a quiescence state (G_0). The next checkpoint is placed during DNA replication (intra-S checkpoint) and, in case of DNA damage or other problems, it can decrease the speed of the replication machinery to ensure faithful completion of DNA synthesis. If the problems persist, cells can activate the G_2/M checkpoint, which blocks cells from entering mitosis with damaged DNA. If the previous checkpoint has been satisfied and cells enter mitosis, the last control is performed by the spindle assembly checkpoint SAC (see chapter 1.4.2), which prevents chromosome separation until each chromosome is properly attached to the mitotic spindle and aligned on the metaphase plate.

In order to block cell cycle progression, the checkpoint inhibits CDK activity in different ways [40]. CDKs can be inactivated by phosphorylation of two amino acids located in the ATP binding loop by Wee1 and Myt1 kinases. These inhibitory phosphorylations are reverted by the activity of the Cdc25 family of phosphatases (Cdc25A-C) [43]. Additionally, two families of CDK inhibitors (CKI) have been described: the Cip/Kip family ($p21^{Cip1}$, $p27^{Kip1}$, $p57^{Kip2}$) and the INK4 family ($p16^{INK4a}$, $p15^{INK4b}$, $p18^{INK4c}$, $p19^{INK4d}$) [44, 45]. These two families differ in their way of action; in fact Cip/Kip binds and inhibits CDK-cyclin complexes, whereas INK4 acts on monomeric CDK4/6.

1.2.1.1 DNA damage checkpoints

As mentioned above, Chk1 and Chk2 are responsible for the fast activation of a checkpoint following DNA damage. This rapid response mainly relies on the transmission of the signal by phosphorylation of multiple substrates. The role of Chk1 is conserved from yeast to human and both homologues operate by the same molecular mechanisms. Chk1 is essential for induction of the checkpoint response and needs to be in complex with Claspin in order to be efficiently activated by ATR [32, 46]. Blocking Cdc25 phosphatase activity is a fast mean to arrest the cell cycle in

response to DNA damage. In brief, following DNA damage, Chk1-dependent phosphorylation of Cdc25A enables its recognition and polyubiquitylation by the $SCF^{\beta TrCP}$ E3 ligase [47]. The resulting rapid degradation of Cdc25A results in increased phosphorylation and, thus, inhibition of CDK2 or CDK1 activity, ultimately triggering cell cycle arrest [48]. Moreover, also Cdc25B and Cdc25C are phosphorylated by Chk1/2 which promotes the binding of 14-3-3 proteins to block Cdc25B/C activity [49, 50]. Chk2 is the human homolog of yeast proteins Cds1 and Rad53. These two kinases are structurally different, but they share some overlapping substrates [51]. In higher eukaryotes, Chk2 is functionally redundant with ATM in checkpoint activation, but it plays a major role in regulating proapoptotic pathways [52, 53]. Indeed, ATM and Chk2 phosphorylate and activate the tumor suppressor p53, which is involved in the long-term damage response that can trigger senescence or apoptosis [54, 55]. Interestingly, Cdc25B- and Cdc25C-deficient mice are able to activate the G_2/M checkpoint, indicating that damage checkpoints are regulated by redundant pathways [56]. For example, after becoming activated in response to DNA damage, Chk1 phosphorylates and activates Wee1, which, in turn, directly phosphorylates CDK1 and CDK2 [57]. Moreover, in case of exposure to IR occurring during G_1 phase, rapid degradation of cyclin D1 ensures arrest at the G_1/S transition [58, 59].

The checkpoint response not only has to be fast, but it also has to last long enough to give time to the cells to efficiently repair the damage. Pathways ensuring checkpoint maintenance rely on transcriptional changes in many target genes [51]. For example, after genotoxic stress, p53 becomes highly modified by different posttranslational modifications, including phosphorylation by ATM/ATR/DNA-PK and by Chk1/Chk2. Modified p53 is no longer bound by its inhibitor Mdm2 and, after tetramerization, p53 activates the promoters of multiple target genes [60, 61]. One of these target genes is the CDK-inhibitor p21, which is able to bind and inhibit CDK2-cyclin E and CDK4-cyclin A complexes, blocking the G_1/S transition [62, 63]. In a similar fashion, p21 inhibits CDK1-cyclin B complexes, retaining cells from entering mitosis [64]. p53 is involved in the G_2/M checkpoint also in a p21-independent manner, by transcriptionally repressing different mitotic inducers, such as cyclin B and Plk1 [65] [66].

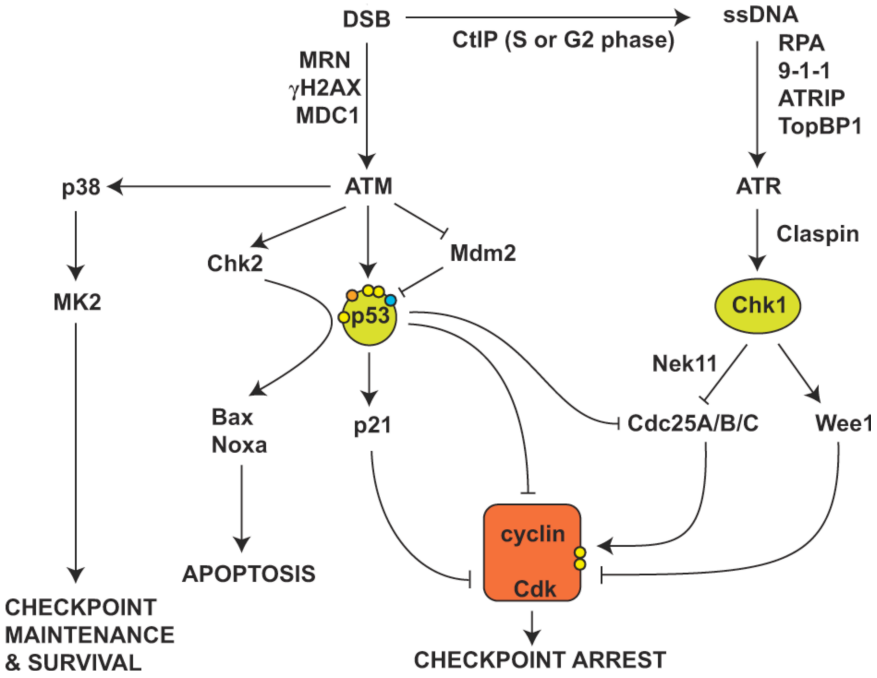

Figure 4 DNA damage checkpoint activation. Detection of DNA lesions leads to the activation of ATM and ATR kinases and a downstream signaling cascade, resulting in the inactivation of cell cycle progression. ATM signaling stabilizes p53, which, in cooperation with its transcriptional target p21, enables the inhibition of CDK-cyclin complexes (depicted as red box). Similarly, ATR activates Chk1, which, by inhibiting the Cdc25 phosphatases and activating the Wee1 kinase, inhibits CDK activity. ATM is also involved in the activation of p38 and Chk2, which are responsible for checkpoint maintenance and apoptosis. Chk1 and p53, in green, are key players in DNA damage checkpoint signaling. Yellow dots indicate phosphorylation, whereas orange and blue dots indicate other posttranslational modification. Adapted from [51].

Interestingly, p53 levels oscillate in response to DNA damage and the oscillatory pattern highly depend on the type and the extent of damage [67, 68]. During G_1, the DNA damage-induced response is mainly dependent on the activity of p53 and cancer cells that are compromised in p53 activation fail to establish a G_1 arrest. Nevertheless, these cells are proficient for the G_2/M checkpoint, indicating that alternative pathways ensure the maintenance of checkpoint signaling [69]. In this line, the p38/MK2 pathway has been shown to play a primary role to ensure survival of p53-deficient cells after induction of DNA damage [70]. In fact, after checkpoint initiation through the Chk1 pathway, p38/MK2 is needed for maintaining its activation [71] and deficiency in MK2 and p53 results in synthetic lethality [72]. Since checkpoints need to remain active until the damage is fully repaired, DNA repair factors are directly involved in checkpoint maintenance. For example, CtIP-driven DNA-end resection plays a critical role in sustaining ATR signaling and maintenance of the G_2/M checkpoint [73]. Moreover, depletion of BRCA2 or its interaction partner

PALB2 results in premature checkpoint termination, which allows damage-bearing cells to enter mitosis [74, 75].

1.2.1.2 Checkpoint recovery

Once the DNA lesions are successfully repaired, cells need to re-enter the cell cycle in a process called checkpoint recovery. Since checkpoint activation causes the inactivation or degradation of many cell cycle regulators, they need to be re-established for re-entering the cell cycle. Nevertheless, during checkpoint recovery, the cell cycle machinery works differently than during unperturbed cell cycle progression and some proteins acquire different roles [76]. For example, Plk1 depletion does not affect mitotic entrance in cycling cells but it completely blocks checkpoint recovery [77]. Phosphorylation of Plk1 by Aurora A, sustained by its cofactor Bora, is required to fully activate the kinase in late G_2 [78-80]. In response to DNA damage, Plk1 phosphorylation is inhibited and, at a later timepoint, the protein is targeted for degradation by APC/C^{Cdh1} [81, 82]. Following the repair of the lesion, Plk1 promotes recovery by inducing nuclear import of Cdc25B/C and inhibiting Chk2 activity [83-85]. Moreover, Plk1-induced phosphorylation of Wee1 and claspin cause their $SCF^{\beta TrCP}$-dependent degradation [86-88].

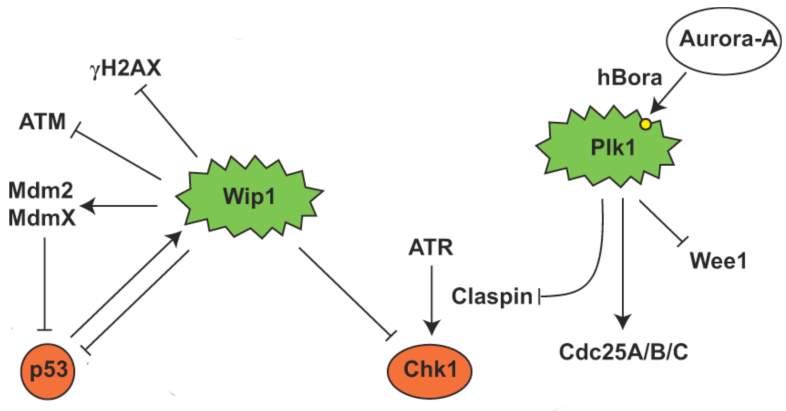

Figure 5 DNA damage checkpoint recovery. After DNA repair, Plk1 phosphorylates Wee1 and claspin enabling their degradation. Plk1 activity is also required for the re-activation of the Cdc25 phosphatases. Multiple proteins are also dephosphorylated by the activity of Wip1, which leads to the silencing of the checkpoint. Green indicates active proteins, whereas red indicates the inactivation of the main players of the checkpoint signaling. Adapted from [51].

Plk1 activity is essential but not sufficient for checkpoint recovery and different phosphatases are reverting checkpoint-induced phosphorylation events [89]. One of these phosphatases, Wip1, plays a central role during checkpoint recovery and its depletion results in prolonged checkpoint activation [90]. Interestingly, Wip1 activity is

directed towards pS/T-Q sites in target proteins, which are specifically phosphorylated by ATM/ATR, and it has been shown that Wip1 dephosphorylates several proteins involved in the DDR [51]. After a genotoxic insult, Wip1 levels are increased in a p53-dependent manner and they hence limit the amplitude of the checkpoint [91]. Moreover, Wip1 dephosphorylates p53 and Mdm2, facilitating the interaction between the two proteins and therefore promoting p53 proteolysis [92, 93]. Noteworthy, p53 inactivation is critical for checkpoint recovery. Indeed, inhibition of ATM/ATR, Chk1/Chk2 and p38 is not sufficient to promote recovery in Wip1-depleted cells, whereas cells lacking p53 and Wip1 recover normally. Importantly, Wip1 activity is necessary throughout the checkpoint response to maintain the levels of cell cycle regulators above a critical threshold and therefore enable cells to recover from the arrest even after long periods of activation [90].

1.2.1.3 Cellular senescence

In case the DNA damage is particularly severe, cells may undergo programmed cell death (apoptosis) or initiate a different program, which leads to an irreversible cell cycle arrest. This state is called senescence and, in contrast to quiescence, cannot be reverted by altering the cellular environment *in vitro*, for example by removing cell contact inhibition or adding nutrients [94]. The factors determining the outcome of the DDR activation are still unclear, but the cell type and the kind of damage, as well as the intensity and the duration of the signal seem to be major determinants [95]. Senescence was observed for the first time *in vitro*, due to the exhaustion of the replicative capacity of human fibroblasts. Indeed, cultured fibroblasts do not duplicate infinitely, but they arrest after a limited and reproducible number of populations doublings (the so called Hayflick limit) [96]. This replicative senescence is mainly due to telomere attrition, which occurs at every DNA replication and that, once telomeres reach a critical length, triggers DDR activation [94]. As discussed in the previous chapter, checkpoint maintenance is dependent on the activity of p53 and its downstream effector p21. p21 expression has been suggested to negatively regulate p53-dependent apoptosis: high p21 levels often result in senescence, whereas a response involving low p21 expression results most likely in apoptosis [97]. Prolonged checkpoint activation leads to the upregulation of p16, which, beside acting as a CDK inhibitor, activates the transcriptional regulator Rb [98, 99]. Rb, cooperating with heterochromatin proteins, drives heterochromatization and stable repression of E2F-responsive genes, causing the appearance of peculiar

heterochromatic regions called senescence-associated heterochromatic foci (SAHF) [100]. However, SAHF is not a common feature of senescent cells [101] and since not all the senescent cells display all the phenotypes so far associated to this state, they are mainly identified through a combination of characteristics [102]. Histochemical staining for senescence-associated β-galactosidase (SA-βgal) is commonly used as a marker, because this enzyme is highly expressed in lysosomes accumulating in senescent cells [103, 104]. Interestingly, apoptosis leads to the rapid elimination of cells by phagocytes in an inflammation-independent manner, whereas senescent cells release growth factors and different cytokines [105, 106]. This senescence-associated secretory phenotype (SASP) can establish a prolonged paracrine signaling, which influences in both beneficial and detrimental manner the surrounding tissue. For example, SASP can result in maintaining the senescence state, clearing the senescence cells, or promoting a pro-tumorigenic phenotype [97].

1.3 The ubiquitin-proteasome system

Targeted proteolysis through the ubiquitin-proteasome system (UPS) is a highly regulated process that allows the removal of proteins, thereby restricting their activity. The UPS is involved in virtually any cellular process, which depends on regulation of intracellular proteins by degradation [107]. For example, the periodic degradation of cyclins and CKIs by the UPS system allows the strict control of CDKs, permitting tight regulation of cell cycle progression. In fact, in contrast to phosphorylation, ubiquitin-mediated degradation is an irreversible mechanism that ensures the unidirectionality of the cell cycle [108]. Ubiquitin is a small, 76 amino acids long protein that is covalently linked to substrates through the sequential activity of three enzymes. Modified substrates can then be bound by the 26S proteasome complex, which is responsible for the lysis of the proteins [109]. Ubiquitin is first bound by a specific E1 activating enzyme, which activates the C-terminal residue of ubiquitin in an ATP-dependent manner. Activated ubiquitin is next transferred to an E2 ubiquitin-conjugating enzyme and, finally, a E3 ubiquitin ligase is mediating the binding of ubiquitin to the target protein. In this last step, the carboxyl group of the C-terminal glycine of ubiquitin, is covalently linked to the ε-amino group of a lysine present in the substrate protein [110]. Several rounds of this sequential reaction, lead to the formation of long ubiquitin chains in which each ubiquitin is bound to a specific lysine, or the N-terminal residue, of the previous ubiquitin. Totally, there are 7 lysine

residues in ubiquitin (K6, K11, K27, K29, K33, K48 and K63) and specific linkages through all of them have been reported to occur in cells [111]. The synthesis of particular ubiquitin chain linkages appears to be a function of the specific E2s and the E2-E3 combinations involved in the process [112]. Structural characterization of various chain types revealed that the different linkages results in distinct chain conformations, which can be more open or compact [113]. Moreover, the type of linkage between ubiquitins within a chain determines the functional outcome of the modification. For example, if polyubiquitylation occurs through lysine 11 or 48 (K11 and K48, respectively) the substrate is recognized and subsequently degraded by the 26S proteasome. Differently, monoubiquitylation or K63-linked polyubiquitylation of a substrate specifies non-proteolytic fates, while the precise outcome of other chain linkages is less understood [114]. Finally, ubiquitylation can be reverted by the activity of deubiquitinating enzymes (DUBs), which can remove ubiquitin molecules from a chain, or directly from the substrate [115].

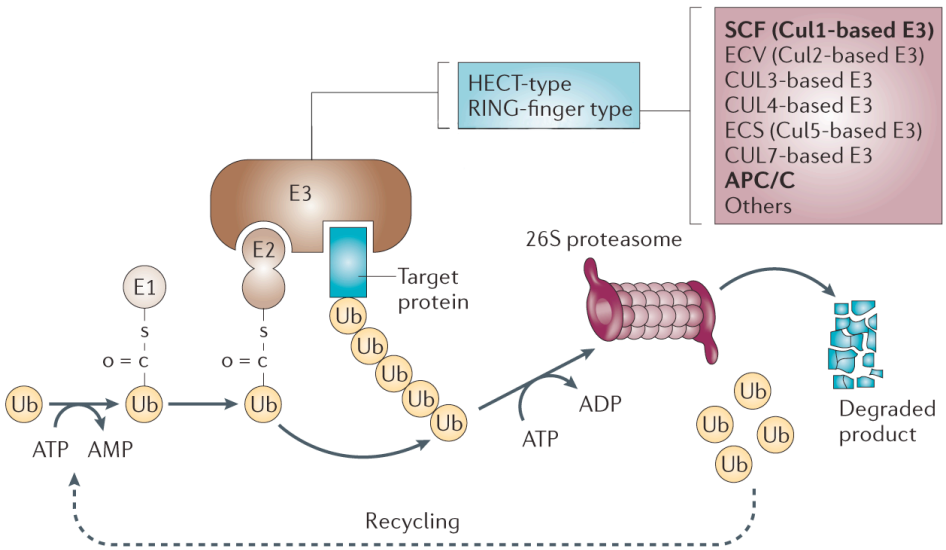

Figure 6 The ubiquitin-proteasome system. Ubiquitin is attached to the substrate protein in a three-step reaction. Firstly, the E1 ubiquitin-activating enzyme binds ubiquitin in an ATP-dependent manner. Secondly, ubiquitin is transferred to the E2 ubiquitin-conjugating enzyme and, finally, attached to the substrate by the E3 ubiquitin ligase. Repetition of this cycle leads to the formation of a polyubiquitin chain. The 26S proteasome recognizes and lyses polyubiquitylated proteins in an ATP-dependent manner. At the top of the scheme, the different families of E3 ligases are shown. Adapted from [116].

Mammalian cells express two E1, at least 38 different E2 and 600-1000 E3 enzymes. E2 enzymes play a central role during ubiquitylation of substrates, because they determine the linkage specificity and length of ubiquitin chains. Moreover, they can strongly influence the processivity of chain formation [117]. Nevertheless, the E3

ligases are pivotal in directing the activity of E2 enzymes toward the right substrate. Depending on their homology domains, the E3 ubiquitin ligases can be subdivided in to two major families: HECT (homologous to E6-AP C-terminus) and RING (really interesting new gene) E3 ligases [118]. Other than possessing different functional domains, these enzymes perform their function in distinct manners. HECT ligases form a transient linkage to ubiquitin before transferring it to the substrate, whereas RING ligases mainly act as scaffolds and mediate the passage of ubiquitin from the E2 to the substrate by bringing them in close proximity [119, 120]. To date, more than 600 RING proteins are annotated for human cells [121]. A canonical RING domain is composed by spaced cysteine and histidine residues, coordinated to a specific conformation by Zinc atoms [120]. RING domain-containing proteins can act as monomers, dimers or multi-subunit complexes and one of the best-studied multi-subunit RING ligases belong to the cullin-RING ligase (CRL) superfamily. In their minimal conformation, CRLs are composed of a backbone, consisting of one out of several cullin isoforms, which binds through its C-terminus to a RING-containing protein, whereas the N-terminus is linked to a substrate-recognizing module. Two prominent examples are the SCF and the APC/C E3 ligases, which play a central role during cell cycle progression. SCF complexes are cullin 1-based and contain the small RING protein Rbx1. The linker protein Skp1 and a F-box motif adaptor protein form their substrate recognition modules. The majority of F-box proteins contain protein–protein interaction motifs, such as WD-40 and leucine-rich repeats, which are involved in substrate binding [122].

1.4 The anaphase-promoting complex

The anaphase-promoting complex or cyclosome (APC/C) is an evolutionary-conserved multisubunit E3 ligase [123]. In mammals it comprises 15 subunits, however the basic organization resembles the one of the SCF complex. Apc2 is the cullin-like scaffold subunit and it is connected to the Apc11 RING protein, which is responsible for recruiting specific E2 enzymes. Cell cycle-dependent and mutually exclusive association with two co-activators, Cdc20 and Cdh1, is a prerequisite for APC/C capability of binding to its substrates [124]. Both proteins are characterized by the presence of an N-terminal “IR-tail”, which is important for their binding to Apc3, and a WD40 domain, which mediates the interaction with the substrates [125, 126]. Apc3, similarly to other structural subunits of APC/C, contains different

tetratricopeptide repeats (TPRs), which are involved in intra- and inter-molecular interactions [127, 128]. Substrate-binding capacity of the complex, also requires the Apc10 subunit, which is positioned close to the co-activators [129-131]. The presence of Apc10 is also important for stimulating the processivity of the complex [132].

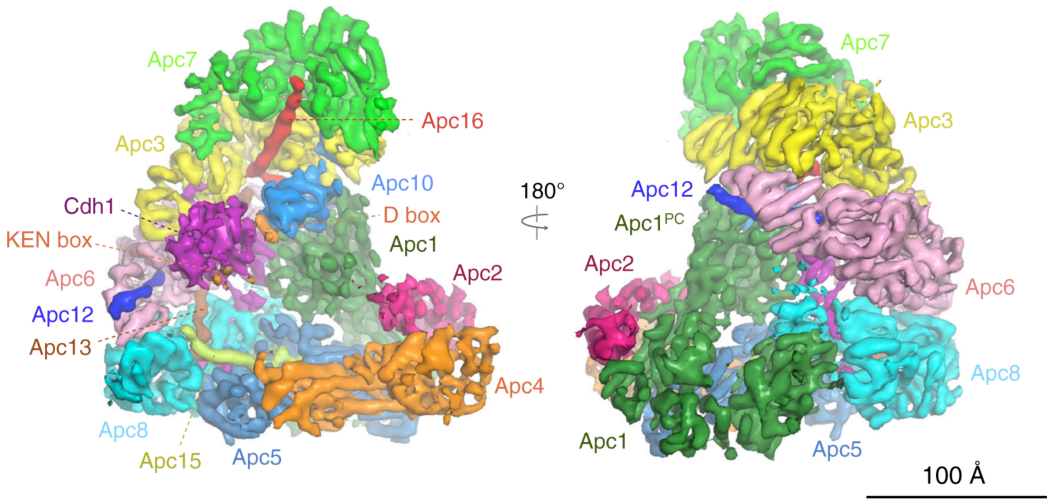

Figure 7 Structure of the APC/C. Electron microscopy based reconstruction of human APC/C, in complex with its co-activator Cdh1 and a substrate protein. The different subunits are color-coded. The "platform", in the lower part of the complex, comprises subunits Apc1, 4, 5 and 15, whereas the "arc lamp" is form by Apc3, 6, 7, 8, 12, 13 and 16. In the central cavity is possible to identify the substrate recognition module (Cdh1 and Apc10) and the substrate protein (in orange). Adapted from [123].

Electron microscopy studies showed that the complex is organized in an asymmetrical triangular shape, composed of an outer wall surrounding a central cavity. The complex can be conceptually divided in two large domains, known as "platform" and "arc lamp" (also called "TPR lobe"). The catalytic subunits (Apc2 and Apc11) are positioned at one end of the platform, whereas at the other end the arc lamp is mounted, which bears the substrate-recognizing module (Apc10 and Cdc20/Cdh1). The two domains possess a high degree of conformational flexibility bringing the catalytic and substrate-recognition motifs in close proximity upon binding of the co-activators [123, 133, 134]. This conformational change enhances the catalytic activity of the APC/C and depends on the N-terminal region of the co-activators [135]. In human cells, APC/C assembles atypical K11-linked conjugates to drive proteasomal degradation and mitotic exit. Indeed, APC/C activation during mitosis correlates with and increased abundance of K11 linkages and this boost is dependent on the E2 Ube2S [136, 137]. APC/C initiates chain formation by using the E2 Ube2C (also known as UbcH10), which synthesizes K11, K48 or K63 linkages

[138, 139]. However, chain extension by Ube2C is inefficient and elongation is taken over by Ube2S, which specifically catalyzes K11 linkages [140-142]. Interestingly, it has been recently shown that the combined activity of these two E2 enzymes generates branched ubiquitin chains, which enhance substrate recognition by the proteasome [143].

1.4.1 Two co-activators provide specificity to the APC/C

The two co-activators, Cdc20 and Cdh1, are responsible for directing the APC/C towards specific substrates. Structural insights into the mechanisms of degron recognition showed that the co-activators collaborate with the Apc10 subunit to properly bind substrates [130, 144]. Through their WD40 domains, which folds in a propeller-like structure, the co-activators have the capacity of recognizing two conserved degrons present in most of the APC/C substrates: the destruction box (D-box) and the KEN box. The D-box was initially identified as a nine amino acid-long motif present in the N-terminal region of cyclin B, mediating its degradation [145]. However, RxxL seems to be the minimal consensus motif required for the recognition of a substrate [146]. The second degron is simply formed by the three amino acids K-E-N, but a more extended consensus motif is facilitating substrate recognition [147, 148]. Despite the identification of different non-canonical destruction signals, such as the A-box present in Aurora A, KEN and D-boxes are regarded as the major APC/C recognition motifs [146, 149]. No particular structural organization is required for the region surrounding the degron, but the presence of additional binding motifs in the substrates facilitates their recruitment [41].

1.4.2 APC/C function and regulation during the cell cycle

The APC/C, in conjunction with its co-activators, controls the degradation of various cell cycle regulators. Therefore, periodic activation and inactivation of the APC/C is required to organize cell cycle progression. This becomes particularly important during mitosis to ensure that the daughter cells inherit an equal set of chromosomes. During unperturbed cell cycle progression, the APC/C is inactive from late G_1 phase until mitosis and this allows the accumulation of its substrates, many of which are needed to enable DNA replication and mitosis. Both co-activators are already transcribed and translated during S/G_2 but their interaction with the APC/C is prevented by several mechanisms [150]. For example, in vertebrate cells, E2F

activation at the G_1/S transition drives the expression of the early mitotic inhibitor 1 (Emi1), which blocks APC/C activity [151, 152]. Another, more conserved mechanism, exploits in an ingenious fashion the activity of the different CDKs. In fact, Cdc20 only interacts with APC/C when several subunits are phosphorylated at various sites, which is mediated by the mitotic CDK1-cyclin B complexes and Plk1 [153]. Activity of CDK1-cyclin B complexes is particularly important to enable Cdc20 binding and APC/C activation [154]. Noteworthy, phosphorylation of the APC/C subunits is not required for Cdh1 binding [155]. Nevertheless, in S/G_2 and early mitotic phases Cdh1 is phosphorylated by CDK2-cyclin A complexes and this blocks the association of Cdh1 with APC/C [155, 156]. In budding yeast, mutating the CDK sites enables Cdh1 to activate the APC/C during mitosis and renders Cdc20 dispensable [157]. Whether phosphorylation is the principal mechanism of APC/C activation in mitosis is unclear. Some studies proposed that Plk1-dependent phosphorylation of Emi1 and its subsequent $SCF^{\beta TrCP}$-dependent degradation is also needed to enable APC/C activation [158, 159]. However, overexpression of a non-degradable form of Emi1 or inhibiting Plk1 activity does not block APC/C activation [153, 160, 161].

APC/C activation occurs early in mitosis and has to be coordinated with chromosome attachment to the mitotic spindle and their alignment on the metaphase plate. In fact, one prominent target of the APC/C is securin, which binds and inactivates separase, a protease able to cleave the Scc1 cohesin subunit responsible for chromatid cohesion. Securin degradation results in loss of cohesion and detachment of the sister chromatids, which, if occurring prematurely, results in aneuploidy [162]. The spindle assembly checkpoint (SAC) controls chromosome segregation by blocking Cdc20, and hence the APC/C, until all the kinetochores are correctly attached to the mitotic spindle. Briefly, after nuclear envelope break down, unattached kinetochores recruit four SAC proteins (Mad1, Mad2, BubR1 and Mps1) [41]. Here, Mad1-Mad2 catalyze a conformational change in a second Mad2 protein, which then firmly binds and inhibits Cdc20. This transient SAC activation can be prolonged in case the cell is experiencing problems with kinetochore attachment. Robust Cdc20 inhibition is achieved by the further binding of Mad2-Cdc20 to Bub3 and BubR1, forming the mitotic checkpoint complex (MCC), which can be free or APC/C-bound [163]. When all kinetochores are attached to the spindle microtubules, the SAC is satisfied and APC/C is reactivated in order for mitosis to proceed. In this regard, Cdc20 auto-ubiquitylation has been proposed to occur in an Apc15-

dependent manner, resulting in MCC disassembly and its dissociation from the APC/C [164]. Moreover, p31^{comet} disrupts the Mad2-BubR1 interaction, releasing the sequestered Cdc20 [165].

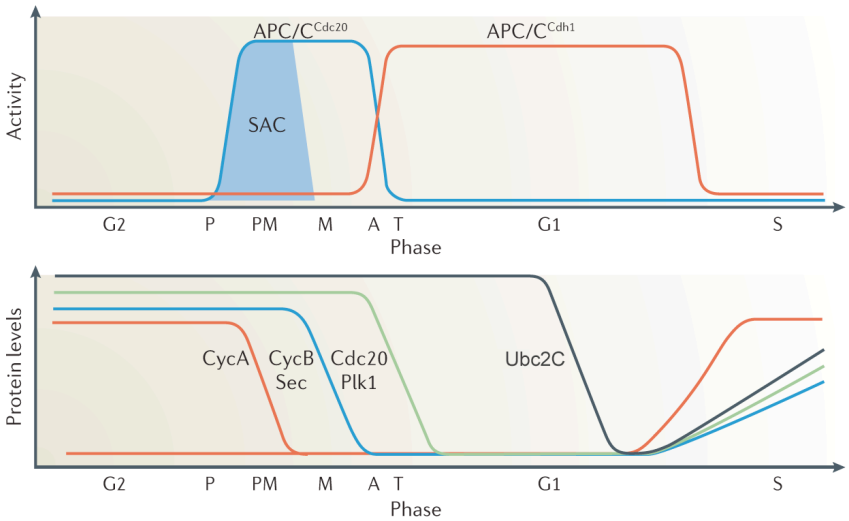

Figure 8 Activation of the APC/C during the cell cycle. APC/C becomes activated in prophase (P) by binding of Cdc20, but its activity towards cyclin B and securin is retained until metaphase (M) by the spindle assembly checkpoint (SAC). However, some substrates, such as cyclin A, are already degraded during prometaphase (PM). During anaphase (A) and telophase (T), APC/C^{Cdh1} is activated and mediates the destruction of additional mitotic regulators, such as Cdc20 and Plk1. APC/C^{Cdh1} remains active throughout G1 and during this time window degrades different substrates, including its own E2 ubiquitin-conjugating enzyme (Ubc2C). Adapted from [150].

Securin and cyclin B1 degradation is initiated after the last kinetochore is attached to the mitotic spindle, enabling APC/C^{Cdc20} activation [166]. Cdc20 is essential for the degradation of these two factors and loss of Cdc20 causes embryonic lethality in mice at the two-cell stage [167]. An absolute metaphase block is also achieved in human cell lines by depleting Cdc20 to very low levels [168, 169]. Once securin and cyclin B1 are degraded to a sufficient level, APC/C activity is directed towards a broader range of substrates, including those with KEN boxes, such as Plk1, Aurora kinases and Cdc20 itself [170]. This is partially achieved by switching the co-adaptors in APC/C from Cdc20 to Cdh1. Mitotic progression results in decreased CDK levels and activation of the Cdc14 phosphatase, enabling Cdh1 dephosphorylation and leading to the formation of the APC/C^{Cdh1} complex [171-173]. Interestingly, depletion of Cdh1 stabilizes Aurora kinases, but does not affect Plk1 or Cdc20 degradation indicating that APC/C^{Cdc20} activity is sufficient for sustaining mitotic exit [174, 175]. After its activation, APC/C^{Cdh1} substrates are degraded in a sequential order during mitotic exit [176]. An *in vitro* study suggests that this sequential degradation is

achieved through an intrinsic property of the APC/C in promoting polyubiquitin chain formation [177]. On one hand, polyubiquitylation of “early” substrates occurs in a processive manner requiring a single APC/C-binding event to obtain a long chain and resulting in efficient proteasome-dependent clearance of the protein. On the other hand, “late”” substrates are modified in a distributive fashion, requiring multiple rounds of APC/C binding and hence more time to become polyubiquitylated and degraded [177].

Even if Cdh1 seems to play a secondary role during mitosis, this APC/C co-activator plays an important role during G_1 phase. Indeed, APC/C^{Cdh1} activity during G_1 is required to keep S phase and M phase cyclins at low levels, retaining their accumulation until the cells decide to commit for another round of division. Interestingly, deletion of the Apc2 subunit of the APC/C in quiescent hepatocytes results in their re-entry in the cell cycle without requirement for proliferative stimuli [178]. Moreover, loss of Cdh1 results in the premature accumulation of cyclin A, which leads to unscheduled DNA replication [174, 175]. Other than by targeting cyclin A, APC/C^{Cdh1} delays S phase by promoting degradation of Skp2, which is an adaptor of the SCF complex, targeting the CKI p27 for degradation. Therefore, stabilization of Skp2 in Cdh1-deficient cells, results in the de-stabilization of p27 and an increase in CDK activity that promotes premature initiation of DNA replication [179, 180]. Furthermore, the transcription factor and proto-oncogene Ets2 is stabilized in absence of Cdh1, resulting in increased cyclin D1 levels and enhanced proliferation [181, 182]. Under normal conditions, once cells decide to replicate, the APC/C activity is inhibited by a loop comprising different mechanisms. As mentioned above, Emi1 is a major player in promoting APC/C inhibition and is expressed at the G_1/S transition in an E2F-dependent manner [183]. Additionally, APC/C^{Cdh1} directly promotes the degradation of Ubc2C, its E2 ubiquitin-conjugating enzyme, and initiates the auto-ubiquitylation of Cdh1 [184, 185]. Finally, increasing CDK activity, results in phosphorylation of Cdh1 and its release from the APC/C complex [156]. Later in S phase, the $SCF^{\beta TrCP}$ complex targets phosphorylated Cdh1 for degradation [186, 187].

1.4.3 APC/C^{Cdh1} involvement in cancer and in the DDR

APC/C^{Cdh1} restricts the proliferative capacity of cells, by targeting various cell cycle regulators for degradation. Due to their essential role in cell cycle regulation, most germline knockout mice targeting the APC/C pathway are embryonic lethal. Cdh1 has

also been reported to be overexpressed in malignant but not benign tumor types [188]. Nevertheless, Cdh1 is often downregulated or lost in human cancers and Cdh1 heterozygosity in mice results in increased susceptibility to spontaneous tumors formation [82, 175, 189, 190]. Moreover, Cdh1-deficient cells have aberrant chromosome numbers, including highly aneuploid cells with 100–150 chromosomes and high number of chromosome breaks [175]. Interestingly, loss of Cdh1 causes an increase in γH2AX foci even in absence of exogenous genotoxic treatment [174]. As a first indication in this direction, it was shown that after irradiation of S phase cells, Cdh1 becomes integrated in the APC/C, forming a catalytically active complex. Moreover, Cdh1-deficient cells are unable to maintain a G_2 arrest after IR, but no difference between wild-type and Cdh1-deficient cells is observed if UV-irradiation is used [191]. Activation of the APC/C^{Cdh1} in response to DNA damage during G_2 was shown to depend on the release of the Cdc14B phosphatase from the nucleoli. This enables Cdc14B to de-phosphorylate Cdh1, resulting in the activation of the APC/C^{Cdh1} complex, which finally leads to the degradation of Plk1 and the stabilization of the G_2/M checkpoint. Interestingly, not all targets of the APC/C^{Cdh1} are degraded under these conditions and it was suggested that USP28 is involved in counteracting APC/C activity [82]. Further experiments performed in Cdc14-deficient cells showed that those cells are proficient in the maintenance of the G_2/M checkpoint following IR, but require longer time to repair DSBs. Moreover, depletion of Cdh1 does not affect the capacity of the cells to activate the G_2/M checkpoint [192].

Full activation of APC/C^{Cdh1} is part of the long-term response to IR and requires the activation of p53 and its transcriptional target p21. Stabilization of p21 results in the degradation of the Emi1 inhibitor and the consequent activation of APC/C^{Cdh1}. Interestingly, also in this case, Cdc14B plays a secondary role for APC/C^{Cdh1} activation following genotoxic stress [193, 194]. Recently, different groups showed that in non-transformed cells, following p53 activation in G_2, APC/C^{Cdh1}-dependent degradation of cyclin B1 determines the irreversible withdrawal from the cell cycle and the establishment of a senescence state [195-197]. Moreover, it was shown that damage-induced activation of the APC/C^{Cdh1} is responsible for the degradation of two major histone methyltransferases, G9a and GLP, involved in the silencing of euchromatic genes. This event results in the expression of IL-6/IL-8, which are pro-inflammatory cytokines produced and secreted by senescent cells [198]. In summary, upon DNA damage in G_2, Cdc14B-dependent dephosphorylation of Cdh1 promotes

the prompt activation of a fraction of APC/C^{Cdh1}, which is directed towards a subset of substrates. Prolonged exposure to DNA damage, leads to p53 activation, resulting in the p21-dependent degradation of Emi1, enabling the full activation of APC/C^{Cdh1} and the establishment of senescence.

1.5 DNA double-strand breaks

DNA double-strand breaks (DSBs) arise when both DNA strands of the double helix break simultaneously in close proximity. Although they occur much less frequently than other kinds of DNA lesions, they pose a severe challenge to the cells as they can trigger genome rearrangements [28]. It has been shown that one single DSB can be lethal to radiosensitive mutants of budding yeast [199]. DSBs emerge because of endogenous or exogenous challenges. Replication is a major endogenous source of DSBs, since prolonged replication fork stalling at unrepaired DNA lesions can result in fork collapse and DSB formation. In this regard, treatment of cells with PARP inhibitors (e.g. olaparib) prevents detection and repair of SSBs, which are converted into DSBs during replication. In addition, various exogenous DNA damaging agents, such as IR and certain anti-cancer drugs, can induce DSBs. One important class of genotoxic drugs leading to DSB formation are DNA topoisomerase inhibitors. DNA topoisomerases solve topological problems associated with DNA replication, transcription, recombination, and chromatin remodeling by introducing temporary single- or double-strand breaks in the DNA [200]. Inhibition of a topoisomerase blocks the re-sealing of the nicked DNA, inducing a permanent break in the DNA. Topoisomerase type II inhibitors (e.g. Etoposide) directly induce DSBs, whereas inhibitors of type I topoisomerases (e.g. Camptothecin) cause SSBs, which give rise to DSBs during S phase. Moreover, different endonucleases, such as I-SceI, FokI or Cas9, can be used to induce DSBs at precise locations in the genome and, recently, different genome-editing methods, which rely on endonuclease-induced cuts, have been developed [201].

DSB formation is also occurring in different physiological settings. For example, during meiosis, DSBs are induced and repaired by HR in order to increase genetic diversity. Other examples are the programmed DSBs that are induced at different stages of lymphocyte development to increase antibody and T cells receptor diversity. Early in development of B and T lymphocytes, rearrangement of the V(D)J region is initiated by RAG1 and RAG2, which introduce DSBs at specific recognition

sites. Repair through c-NHEJ (see below) favors the production of highly different antibody variable regions [202]. The second programmed DNA recombination process takes place in mature B cells. Class switch recombination (CSR) is initiated by the activation-induced cytidine deaminase (AID), which favor DSB formation in defined switch regions. Also in this case, the broken ends are repaired by c-NHEJ and recombination with a different region, leads to the formation of different classes of antibodies (e.g. IgG, IgE or IgA) [203].

1.6 DSB repair pathways

Cells have evolved two major pathways dedicated to DSB repair: homology-directed repair (HDR) and non-homologous end joining (NHEJ). Both of them can additionally be subcategorized in homologous recombination (HR) versus single-strand annealing (SSA) and classical NHEJ (c-NHEJ) versus alternative NHEJ (alt-NHEJ), respectively [28]. HR and SSA require the formation of longer stretches of ssDNA, that are exposed in a nucleolytic process defined as DNA-end resection and that prevents repair through NHEJ [204-206]. In fact, alt-NHEJ only requires short stretches of ssDNA, whereas c-NHEJ does not require resection of the broken ends. Generally, these different requirements make the initiation and extent of DSB end processing a main decisional event in DSB repair pathway choice. The choice between the different repair pathways is influenced by various circumstances, as for instance the cell cycle stage [207]. Repair based on the use of a homology sequence template (HR, SSA), are mainly restricted to the S/G_2 phases of the cell cycle. The temporal restriction of HDR is controlled both at the transcriptional and post-transcriptional level. For instance, the expression of many HR factors including Rad51 and BRCA1 is cell cycle-dependent, being much lower in G_0/G_1 than in S/G_2 [208, 209]. In addition, CDKs, the key orchestrators of cell cycle, play an important role in the regulation of multiple HR components, especially of those involved in DNA-end resection [210]. CDK activity has been shown to be essential for DNA-end resection and HR both in yeast and vertebrate cells [211-213]. In human cells, Chk1 activation requires CDK activity and the formation of RPA-coated ssDNA, mainly occurring in an MRN-dependent manner. Moreover, also the direct ATM-dependent activation of ATR is restricted to S/G_2 [213]. Interestingly, CDK2 plays a redundant role for cell cycle progression, but the specific inhibition of this kinase results in defective checkpoint signaling and DSB repair [214].

1.6.1 Non-homologous end joining

c-NHEJ does not require sequence homology for repairing the broken chromosomes and, in mammalian cells, is the main pathway for the repair of DSBs [215]. It is active throughout the cell cycle and it covers a particularly important role during G_0/G_1 phases [216]. c-NHEJ seems to be a relatively simple pathway, because it joins DNA ends by ligation without requirement of searching for an homologous template. Interestingly, this pathway is also able to re-ligate ends that are not blunt or complementary, indicating that the proteins involved are capable of "clean-up" modified nucleotides which may be present at the broken ends, in particular after IR. Even though c-NHEJ appears to have higher fidelity than alt-NHEJ, repair through this pathway can cause short deletions/insertions and translocations, especially in case of "dirty" broken DNA ends [217, 218].

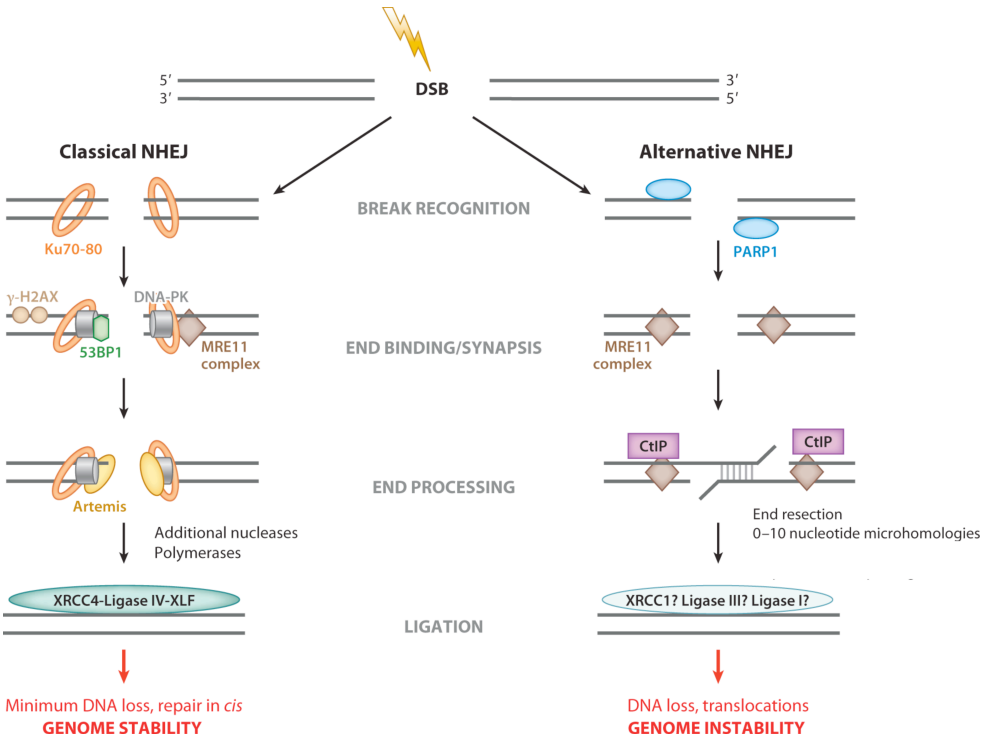

Figure 9 Non-homologous end joining. Schematic comparison of the classical (c) and alternative (alt) NHEJ repair pathways. c-NHEJ is initiated by binding of the Ku heteroduplex to the broken DNA and the subsequent recruitment of the DNA-PK kinase. After short processing of the DNA ends, the break is re-sealed by action of the XRCC4-Ligase IV-XLF complex. Events involved in alt-NHEJ are less defined, but MRN/CtIP-dependent DNA-end resection is required to expose sequences containing microhomologies, which facilitate the repair process. Adapted from [233]

Binding of the Ku70/80 heterodimer protects the DNA ends from possibly aberrant processing and enables the recruitment of DNA-PKcs [219, 220]. After its recruitment, DNA-PKcs promotes phosphorylation of different substrates, such as

Ku, Artemis, XRCC4, ligase IV and XLF [221]. Generally, inactivation of DNA-PKcs kinase activity is detrimental for cells and cause hypersensitivity toward DSB-inducing agents and severely interfere with V(D)J recombination [222, 223]. DNA-PKcs sits on a terminal DNA region, promoting contact between two opposing ends: an event that seems to be important for the full activation of the kinase [221, 224, 225]. The *in trans* autophosphorylation of DNA-PKcs across the break causes changes in the kinase structure, which help its dissociation and increase accessibility for processing enzymes and ligases to the DNA ends [219, 226]. The majority of DSBs require limited DNA end processing before ligation and different enzymes are able to perform this task. For example, Artemis is able to process ssDNA overhangs or opening DNA hairpins, which are generated during V(D)J recombination [227-230]. Following a limited end processing step, DNA polymerases are required to fill in nucleotide gaps prior to DNA ligation. Three members of the polymerase X family have been associated with c-NHEJ in mammalian cells: pol λ, pol μ and the terminal deoxynucleotidyl transferase (TdT) [231]. The final step of the repair process is the ligation of the broken ends, performed by the XRCC4-ligase IV-XLF complex [232].

alt-NHEJ was initially believed to be a backup system used by cells deficient for c-NHEJ factors, but was afterwards observed also in c-NHEJ-proficient cells [234-237]. alt-NHEJ is often characterized by excessive deletions and presence of microhomologies at the junctions. Importantly, alt-NHEJ is much less faithful than c-NHEJ and deficiency of c-NHEJ factors increases the number of alt-NHEJ-driven chromosomal translocations [238-240]. The precise mechanisms of alt-NHEJ remain unclear, but a resection step seems to be required to expose regions of microhomology, which are then used during the repair process. In this regard, depletion of CtIP or Mre11 decreases the amount of chromosomal translocation in cells lacking Ku70 or XRCC4 [236, 241, 242]. After DNA-end resection, DNA ligase III appears to promote re-ligation, in combination with its cofactor XRCC1. Moreover, in absence of ligase III and IV, ligase I was proposed to mediate ligation in a microhomology-independent manner [243, 244].

1.6.2 Homology-directed repair

Homology-directed repair (HDR) mechanisms use homologous sequences present in the genome as a template for repairing DSBs. A characteristic feature of these repair mechanisms is the exposure of relatively long stretches of ssDNA, which are used for homology search and recombination. Two distinct mechanisms of HDR

have been described in mammalian cells: homologous recombination (HR) and single-strand annealing (SSA). Since ssDNA is an intermediate for both HR and SSA, these two DSB repair pathways compete with each other and deficiency for some HR factors facilitates SSA repair [245]. HR is directed toward the homologous sequences present in the sister chromatid and restore the genetic information in a faithful manner [246]. Nevertheless, recombination with sequences of the homologous chromosome potentially leads to loss of heterozygosity (LOH) [247]. In somatic cells, the repair of DSBs through HR is restricted to the S/G_2 phases of the cell cycle, with a peak of usage during S phase [216, 248, 249]. SSA involves the annealing of complementary single-stranded tails formed at repetitive sequences, such as ALU repeats, and is therefore considered to be highly mutagenic [250]. SSA has been suggested to be a significant pathway causing translocations in human cancers [251, 252].

1.6.2.1 DNA-end resection

Long stretches of ssDNA are generated by 5' to 3' nucleolytic resection of DNA ends, resulting in 3' single-stranded tails. DNA-end resection is a major decision-making process for the usage of the different pathways [253]. Mainly based on data coming from yeast studies, a two-step model has been proposed for DSB resection in eukaryotic cells.

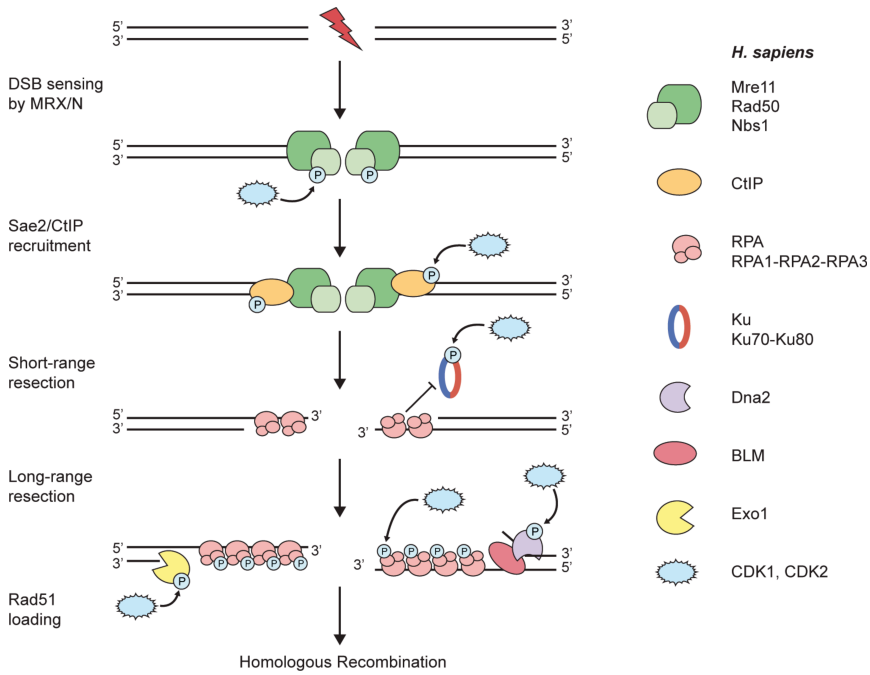

Figure 10 DNA-end resection. During S/G_2 phases of the cell cycle, DSB repair via HR is initiated by DNA-end resection. Initial short-range resection is carried out by the MRX/N complex and Sae2/CtIP. Next, long-range resection is catalyzed either by the 5′-3′

exonuclease Exo1 or the helicase Sgs1/BLM in conjunction with the endonuclease Dna2. After formation, ssDNA is rapidly coated by RPA. Once adequate stretches of ssDNA are formed, RPA is replaced by Rad51 that is required for strand invasion of the sister chromatid and further downstream steps in HR. Adapted from [210].

The MRX complex, in combination with Sae2, initially resects the DNA ends to create a short 3' overhang. Extension of the ssDNA track is subsequently performed by Sgs1-Dna2 and Exo1 [205, 254, 255]. Since Mre11 possesses endonuclease and 3' to 5' exonuclease activity, which is opposite to the direction in which DNA-end resection occurs, a bidirectional model has been proposed [256-258]. In this model, MRX nicks the DNA at 15-20 nt from the end in a Sae2-dependent manner. This event creates an entry point for MRX, which then resects the DNA towards the ends. In the meantime, Exo1 and Sgs1-Dna2 extend the ssDNA tracks in the opposite direction. Interestingly, in the absence of Ku, CDK1 activity is dispensable for the initiation of resection by MRX-Sae2, but is still needed for long-range resection by Exo1 or Sgs1-Dna2 [259].

In higher eukaryotes, initial resection is performed by CtIP, the proposed Sae2 homologue, in conjunction with the MRN complex [260, 261]. Interestingly, and in contrast to Sae2, CtIP has been reported to possess nuclease activity [258, 262, 263]. The observation that the active site is outside the evolutionarily conserved C-terminus of the protein, opens the possibility that CtIP possesses more functions than its yeast counterpart [264]. Similar to what has been observed in yeast, ssDNA overhangs are expanded by the Sgs1 homologue BLM, in combination with Dna2 and Exo1 [265]. The so-formed ssDNA tracks at broken ends can extend up to several kilobases and they are promptly coated by the ssDNA binding protein RPA [266]. RPA is an evolutionarily conserved, heterotrimeric complex consisting of RPA1, RPA2, and RPA3. Owing to its high ssDNA binding affinity, RPA is required for most aspects of DNA metabolism including replication, repair and recombination [267]. Different studies have also implicated RPA in promoting long-range resection through stimulation of both Exo1- and Sgs1-Dna2-dependent pathways [268-270].

1.6.2.2 Homologous recombination

After the formation of long stretches of ssDNA, the repair process can be completed. For this to occur, ssDNA-bound RPA has to be substituted by the recombinase protein Rad51, however the high affinity of RPA for ssDNA interferes with this process. Therefore, mammalian cells possess diverse accessory factors,

such as BRCA2 and PALB2, which facilitate this exchange [271]. Once the Rad51 nucleoprotein filament is formed, it promotes homology search and strand invasion. During synapsis formation, Rad51 facilitates the contact between the invading ssDNA and the homologous DNA duplex, in a structure called displacement loop (D-loop) [272]. Finally, repair synthesis can be performed, using the invading strand as primer and the donor duplex as template. The required polymerases remain elusive *in vivo*, but polymerase η and other TLS polymerases were shown to fulfill this role *in vitro* [273, 274].

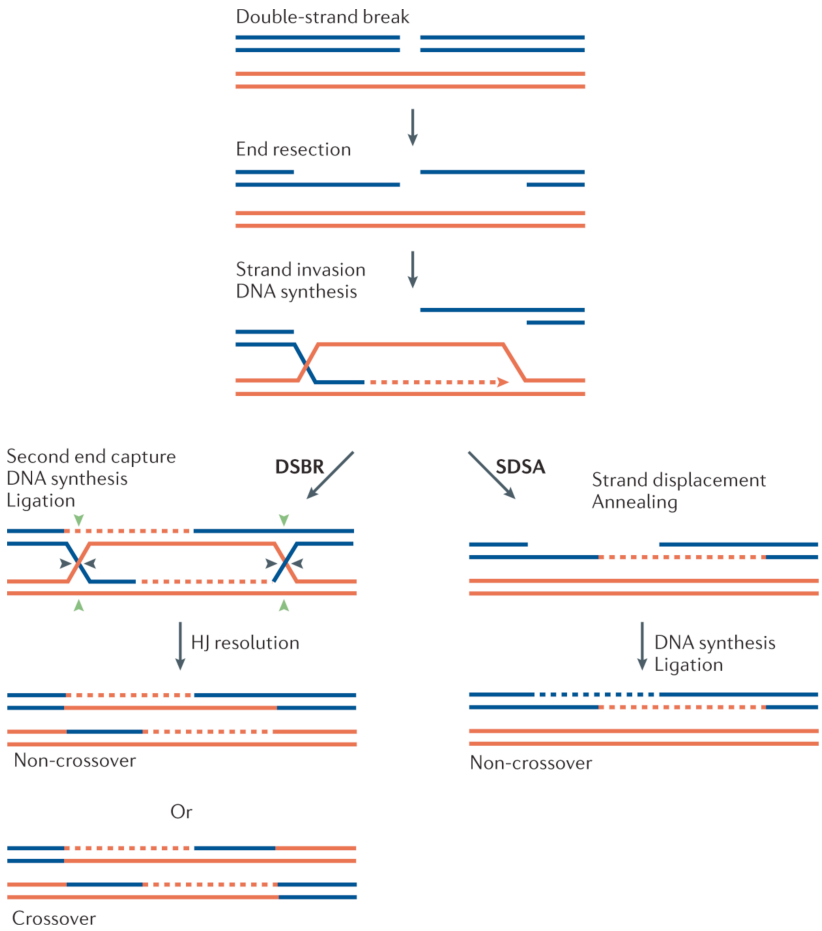

Figure 11 DSB repair through HR. Repair is initiated by resection of a DSB to provide 3′ ssDNA overhangs, which enable strand invasion into a homologous sequence. In DSBR, after DNA synthesis the second DSB end is captured to form an intermediate with two Holliday junctions (HJs). After gap-repair DNA synthesis and ligation, the structure is resolved forming a non-crossover or a crossover product. Alternatively, in SDSA, the newly synthesized strand is displaced and after annealing to the other break end, gap-filling DNA synthesis and ligation take place. SDSA forms exclusively non-crossover products. Adapted from [271].

Downstream repair events can occur in different ways, leading to the formation of variable outcomes. On the one hand, during canonical DSB repair (DSBR), the second DNA end is captured, leading to the formation of a double Holliday junction (dHJ), of which endonucleolytic cleavage produces either crossover or non-crossover

products. Different structure-specific endonucleases, including Mus81/Eme1, Slx1-Slx4 and Gen1, are able to cut HJs *in vitro* and have been proposed to act as "resolvases" in mammalian cells [275]. dHJs can also be dissolved and exclusively generate non-crossover products. Dissolution requires the BLM helicase, topoisomerase III α and RMI1-2 complex, which act in concert to permit branch migration and decatenation of the interlinked strands of the two HJs [276]. On the other hand, in case of synthesis-dependent strand annealing (SDSA), the newly synthetized strand is displaced and re-annealed to the second DNA end, forming a non-crossover product. SDSA is the preferred pathway during mitotic recombination, whereas both pathways are used during meiotic recombination [277]. In case resection occurs within highly repetitive DNA sequences, repair can occur through SSA. This pathway is Rad51-independent and relies on the activity of Rad52, which anneals the exposed sequences, leading to deletion of intervening regions [272].

1.7 CtIP

CtIP, also known as Rbbp8, is an 897 amino acid-long protein, whose primary amino acids sequence is significantly conserved among mammals. Moreover, the C-terminal region of CtIP is extremely conserved from yeast to human and is crucial for DNA-end resection during the initial steps of HR [261, 278-280]. CtIP was first described as a transcription cofactor, interacting with the transcriptional repressor CtBP (thereby the name CtIP, which stands for CtBP interacting protein) and Rb (hence the name RBBP8, which stands for retinoblastoma-binding protein 8) [281-283]. CtBP acts as a transcriptional corepressor of several tumor suppressors, such as E-cadherin, p16, p15 and PTEN, indicating a strong association with tumorigenesis and tumor progression [284]. It was further shown that the Rb/E2F pathway stimulates CtIP expression at the G_1/S transition and that CtIP itself interacts with Rb, modulating its own promoter activity but also those of other E2F-responsive genes, such as cyclin D1 [285, 286]. CtIP contains a LECEE motif, which mediates its interaction with Rb and other members of the same family: p107 and p130. Interestingly, ablation of CtIP in MEFs results in Rb hypophosphorylation and inhibition of the G_1/S transition, but the underlying mechanism remains unresolved [287]. One possible explanation is that CtIP is involved in p130-mediated transcriptional repression by recruiting CtBP to specific promoters, one of which is encoding a direct regulator of Rb [281, 288]. Moreover, CtIP is interacting with

members of the Ikaros family, which are Krüppel-like zinc finger transcription factors involved in lymphoid development and differentiation [289]. Interestingly, deregulated expression of these proteins is often associated with leukemia [290]. Inactivation of both CtIP alleles in mice results in early embryonic lethality at stage E4, whereas heterozygous $CtIP^{-/+}$ mice are viable but prone to the development of multiple tumors, which result in a shorter lifespan. Noteworthy, among the different types of tumors observed in $CtIP^{-/+}$ mice, B and T cells lymphomas were the prevalent ones [287]. Lymphomas were shown to result from a MYC translocation, rendering this transcription factor hyperactive and hence driving the expression of different oncogenes [291]. One example is the overexpression of the oncogenic miRNA 17~92 cluster, containing the miR-19a/b members [292], which were shown to control the levels of CtIP protein [293]. CtIP is ubiquitously expressed in different cell types with the highest levels observed in thymus and testis, in line with its role during meiotic recombination [283]. Even if CtIP has been suggested to be a tumor suppressor itself, no strong evidences support so far this hypothesis. For example, analysis of different human cancer cell lines derived from various tissues did not identify homozygous deletions of the CtIP gene. Nevertheless numerous mutations in CtIP sequence have been identified in those samples [283, 288].

1.7.1 Cell cycle regulation of CtIP

CtIP and its yeast orthologs Ctp1/Sae2 play a central role in the initiation of DNA-end resection during DSB repair. In fission yeast, Ctp1 is absent during G_0/G_1 and its expression coincides with the initiation of DNA replication. This simple regulatory mechanism clearly restricts Ctp1 activity to the S/G_2 phases of the cell cycle [280]. Differently, in budding yeast, CDK1 activity is required to phosphorylate Sae2 at Ser-267 and this event is strictly required for Sae2 activity [278, 294]. Higher vertebrates seem to rely on a combination of both these regulatory mechanisms. In fact, CtIP levels were shown to be low in quiescent G_0 cells and increased during S/G_2 phases of the cell cycle [295]. Interestingly, the strong fluctuation in CtIP protein levels is not accompanied by a similar change in mRNA levels, suggesting a post-translational regulatory mechanism [286, 295]. In addition, similar to the phosphorylation of Ser-267 in Sae2, CDKs are required to phosphorylate Thr-847 within the evolutionarily conserved C-terminus of CtIP to promote DNA-end resection [296]. Interestingly, in cells expressing a phospho-mimicking mutant (CtIP-T847E), resection can take place even in absence of active CDK1, yet not to the same extent as in normal cells.

Therefore, additional CDK sites, on CtIP itself or on other proteins, are probably required for optimal resection [210, 297]. Along these lines, it was recently proposed that phosphorylation of additional CDK sites in the central region of CtIP is required for DNA-end resection. Phosphorylation of this cluster seems to be needed for ATM-dependent phosphorylation of CtIP through its association with Nbs1 [298]. Moreover, the CDK-dependent activation of CtIP has recently been challenged by the observation that in response to DSBs occurring during G_1, Plk3 can substitute CDKs in phosphorylating CtIP at Thr-847. This phosphorylation triggers CtIP activity, promoting DNA-end resection events that result in alt-NHEJ and increased chromosomal translocations [299].

CDKs are also responsible for phosphorylating CtIP at Ser-327 enabling CtIP to interact with the E3 ligase BRCA1, which promotes CtIP polyubiquitylation and chromatin recruitment [300-302]. Ser-327 phosphorylation is CDK2-dependent and facilitated by the interaction of CtIP with Mre11, which binds to both proteins, bringing them in close proximity [303]. The CtIP-BRCA1 interaction is mediated by the BRCT domain of BRCA1 and has been initially proposed to facilitate the interaction of these two proteins with MRN, and hence to promote efficient DNA-end resection [301, 302]. However, other groups have recently reported that CtIP-dependent resection does not require BRCA1 interaction [304, 305]. In fact, it was already shown that CtIP is able to directly bind DNA [306]. An additional layer of complexity to the cell cycle-regulation of CtIP was added by the recent discovery that CDK-dependent phosphorylation of Thr-315 during S/G_2, enables the interaction between PIN1 and CtIP [307]. PIN1 is a phosphorylation-specific peptidyl-prolyl cis/trans isomerase (PPIase), which mediates the interconversion between the two conformations (*cis/trans*) that can be adopted by proline bonds in proteins. PPIases-induced conformational changes not only control protein folding but also protein functions (Lu et al., 2007) [308]. Interestingly, after binding to Thr-315, PIN1 isomerizes the bond between Ser-276, which is phosphorylated by an as-yet-unknown kinase, and the following proline. CtIP isomerization results in its ubiquitylation and subsequent proteasomal degradation. Disruption of this regulatory circuit results in aberrant hyperresection of the broken DNA ends, which blocks NHEJ and favors error-prone homology-directed repair [307].

2 Aim of the study

DSBs are particularly cytotoxic lesions because, if left unrepaired, they can lead to cell death. Furthermore, misrepaired DSBs can trigger genome instability and foster tumorigenesis. HR exploits homologous sequences present in the sister chromatid to repair DSBs in an error-free fashion. The temporal restriction of HR repair to S/G_2 mainly concerns factors involved in the initial step of HR, known as DNA-end resection. Human CtIP is essential for the initiation of DNA-end resection, and its activity is controlled by various post-translational modifications.

The aim of my PhD project was to characterize a novel regulatory circuit by the APC/C E3 ligase, controlling the stability of CtIP during cell cycle progression and in response to DSBs.

CtIP protein levels are low during G_1 and increased during S/G_2 phase. However, the mechanism behind these fluctuations has never been elucidated. The APC/C^{Cdh1} ubiquitin ligase is active during G_1 and drive the proteasome-dependent degradation of different substrates containing two characteristic degron motifs: the D- and KEN boxes. We identified two evolutionary conserved KEN boxes of CtIP *in silico* and we set out to investigate whether APC/C^{Cdh1} controls CtIP levels during cell cycle progression. Furthermore, upon treatment with genotoxic agents, APC/C^{Cdh1} was shown to be transiently activated during G_2 phase. The observation that $Cdh1^{-/-}$ mice have elevated levels of DNA damage and chromosomal aberrations suggests a more direct involvement of the APC/C^{Cdh1} in the regulation of DSB repair. However, direct mechanistic insights into how the APC/C^{Cdh1} ubiquitin ligase connects the cell cycle machinery to DNA repair is still lacking. Besides investigating the regulation of CtIP during G_1, we also addressed the question whether APC/C^{Cdh1} targets CtIP for degradation following DNA damaging events during G_2.

The results of this study were included in an article that was recently published in the peer-review scientific journal “The EMBO Journal”. The manuscript is part of the result section (chapter 3.1).

3 Results

3.1 APC/C^{Cdh1} controls CtIP stability during the cell cycle and in response to DNA damage

Article published in “the EMBO Journal”, 2014

Authors:
Lorenzo Lafranchi, Rolf H. de Boer, Elisabeth G.E. de Vries, Shao-En Ong, Marcel A.T.M. van Vugt and Alessandro A. Sartori

Contributions:
LL and HRdB performed experiments, analyzed the data, and edited the manuscript. SEO performed mass spectrometry analyses. EGEdV edited the manuscript. AAS and MATMvV directed and supervised the studies, analyzed the data, and wrote the manuscript.

Specifically, I performed the experiments shown in figures 2C-D, 4A-E, 5A-C, 7D and 8A-F and in the supplementary figures 2A-C, 4B and D, 5A, 6A-B, 7A-B and 8D. Moreover, I generated all the Flp-In T-REx U2OS and HEK293 cell lines expressing GFP-CtIP mutants (wild-type, K467A and T847A) that were used throughout the study.
HRdB performed the other experiments included in the manuscript.

Article

TRANSPARENT PROCESS

THE EMBO JOURNAL

APC/C^{Cdh1} controls CtIP stability during the cell cycle and in response to DNA damage

Lorenzo Lafranchi[1,†], Harmen R de Boer[2,†], Elisabeth GE de Vries[2], Shao-En Ong[3], Alessandro A Sartori[1,*] & Marcel ATM van Vugt[2,**]

Abstract

Human cells have evolved elaborate mechanisms for responding to DNA damage to maintain genome stability and prevent carcinogenesis. For instance, the cell cycle can be arrested at different stages to allow time for DNA repair. The APC/C^{Cdh1} ubiquitin ligase mainly regulates mitotic exit but is also implicated in the DNA damage-induced G_2 arrest. However, it is currently unknown whether APC/C^{Cdh1} also contributes to DNA repair. Here, we show that Cdh1 depletion causes increased levels of genomic instability and enhanced sensitivity to DNA-damaging agents. Using an integrated proteomics and bioinformatics approach, we identify CtIP, a DNA-end resection factor, as a novel APC/C^{Cdh1} target. CtIP interacts with Cdh1 through a conserved KEN box, mutation of which impedes ubiquitylation and downregulation of CtIP both during G_1 and after DNA damage in G_2. Finally, we find that abrogating the CtIP–Cdh1 interaction results in delayed CtIP clearance from DNA damage foci, increased DNA-end resection, and reduced homologous recombination efficiency. Combined, our results highlight the impact of APC/C^{Cdh1} on the maintenance of genome integrity and show that this is, at least partially, achieved by controlling CtIP stability in a cell cycle- and DNA damage-dependent manner.

Keywords Cdh1; cell cycle; CtIP; DNA damage; DNA double-strand break repair

Subject Categories Cell Cycle; DNA Replication, Repair & Recombination; Post-translational Modifications, Proteolysis & Proteomics

DOI 10.15252/embj.201489017 | Received 16 May 2014 | Revised 7 September 2014 | Accepted 30 September 2014

Introduction

Our genome is constantly exposed to various forms of endogenous and exogenous insults provoking different types of DNA lesions, which can promote tumorigenesis. To maintain genomic integrity, the DNA damage response (DDR) activates cell cycle checkpoints to slow cell cycle progression, thereby allowing time for appropriate repair (Jackson & Bartek, 2009). DNA double-strand breaks (DSBs) are the most cytotoxic lesions induced by ionizing radiation (IR) and certain anticancer drugs. Cells have evolved two major DSB repair mechanisms: non-homologous end-joining (NHEJ) and homologous recombination (HR) (Lieber, 2010).

In the G_0/G_1 phase of the cell cycle, NHEJ is the preferred mechanism for DSB repair (Lieber, 2010). In this process, DNA ends are joined without the requirement for a homologous sequence, making NHEJ potentially mutagenic. In contrast, cells that have entered S phase can use the sister chromatid as a template for high-fidelity DSB repair through HR (Aylon *et al*, 2004; Ferreira & Cooper, 2004; Sonoda *et al*, 2006). NHEJ and HR are mutually exclusive pathways since DNA-end resection, which generates long stretches of single-stranded DNA (ssDNA), commits cells to HR and prevents repair by NHEJ. Mechanisms controlling DSB repair pathway choice are under vigorous investigation (Chapman *et al*, 2012). The temporal restriction of HR repair to S/G_2 is controlled both at the transcriptional and post-transcriptional level. The expression of many HR factors including Rad51, Rad54, and Brca1 is cell cycle-dependent, being much lower in G_0/G_1 than in S/G_2 (Gudas *et al*, 1996; Yamamoto *et al*, 1996). In addition, cyclin-dependent kinases (CDKs), core components of the cell cycle machinery, play an important role in DSB repair pathway choice through phosphorylation of multiple HR components, including members of the MRN complex as well as Brca1 and Brca2 (Esashi *et al*, 2005; Ayoub *et al*, 2009; Falck *et al*, 2012). CDK-mediated regulation of DSB repair occurs mainly at the level of DNA-end resection (Aylon *et al*, 2004; Ira *et al*, 2004; Henderson *et al*, 2006; Jazayeri *et al*, 2006; Johnson *et al*, 2011). Human CtIP is essential for the initiation of DNA-end resection, and its function in this process is controlled by various post-translational modifications including phosphorylation, ubiquitylation, and acetylation (Sartori *et al*, 2007; Huertas & Jackson, 2009; Kaidi *et al*, 2010; Steger *et al*, 2013).

Likewise, targeted proteolysis through the ubiquitin-proteasome system (UPS) is a highly regulated process that allows the removal of potentially harmful proteins, thereby restricting their activity. The anaphase-promoting complex/cyclosome (APC/C) is an E3 ubiquitin

1 Institute of Molecular Cancer Research, University of Zurich, Zurich, Switzerland
2 Department of Medical Oncology, University Medical Center Groningen, University of Groningen, Groningen, The Netherlands
3 Department of Pharmacology, University of Washington, Seattle, WA, USA
*Corresponding author. Tel: +41 446353473; Fax: +41 446353484; E-mail: sartori@imcr.uzh.ch
**Corresponding author. Tel: +31 50 3619554; Fax: +31 50 3614862; E-mail: m.vugt@umcg.nl
†These authors contributed equally to this work

ligase involved in cell cycle regulation and becomes activated upon sequential binding to the Cdc20 and Cdh1 adaptor proteins (Peters, 2006; Pesin & Orr-Weaver, 2008). Cdc20 is associated with the APC/C during early mitosis and principally regulates mitotic progression, whereas Cdh1 interacts with the APC/C from late mitosis onwards until the following G_1/S transition (Kramer *et al*, 2000; Peters, 2006). In most cases, APC/C^{Cdh1} interacts with its substrates through the recognition of a short consensus motif called the KEN box (Pfleger & Kirschner, 2000; Pines, 2011). During S/G_2 phase, premature APC/C activation is at least in part prevented through CDK-mediated phosphorylation of Cdh1, which hinders association of Cdh1 with the APC/C (Lukas *et al*, 1999; Kramer *et al*, 2000; Miller *et al*, 2006).

As a first indication of APC/C^{Cdh1} playing a role in the DDR, *CDH1*$^{-/-}$ chicken DT40 cells failed to maintain a G_2 arrest after IR (Sudo *et al*, 2001). In addition, activation of the APC/C^{Cdh1} in response to DNA damage during G_2 phase was shown to depend on the Cdc14B phosphatase and to result in the degradation of Polo-like kinase 1 (Plk1) (Bassermann *et al*, 2008; Wiebusch & Hagemeier, 2010). Upon completion of DSB repair, Cdk1 and Plk1 are reactivated to allow cell cycle progression from G_2 into mitosis (van Vugt *et al*, 2004). Further experiments performed in Cdc14B-deficient cells showed that those cells are unable to repair DSBs even if they efficiently arrest in G_2 (Mocciaro *et al*, 2010). However, direct participation of the APC/C^{Cdh1} in the regulation of DSB repair has never been reported. The observation that Cdh1-depleted cells or *Cdh1*$^{-/-}$ mice have elevated levels of DNA damage and chromosomal aberrations (García-Higuera *et al*, 2008; Sigl *et al*, 2009; Delgado-Esteban *et al*, 2013) strengthens this notion, but direct mechanistic insights into how the APC/C^{Cdh1} ubiquitin ligase connects the cell cycle machinery to DNA repair is still lacking and the responsible substrates remain elusive.

In this study, we show that inactivation of Cdh1 results in genomic instability in different human cell lines. Moreover, Cdh1-depleted cells are hypersensitive toward DNA-damaging agents and display reduced Rad51 foci upon IR treatment. Making use of an integrated proteomics and bioinformatics approach, we identify the DNA-end resection factor CtIP as a novel substrate of the APC/C^{Cdh1} E3 ubiquitin ligase. CtIP–Cdh1 interaction is mediated by an evolutionary conserved KEN box and is required for the downregulation of CtIP protein levels both after mitotic exit and in late S/G_2 in response to DNA damage. U2OS cells inducibly expressing a CtIP KEN box mutant exhibit increased DNA-end resection capacity, which correlates with a decrease in HR and hypersensitivity to PARP inhibition. Together, our data describe a novel regulatory role for the APC/C^{Cdh1} in DNA repair, at least in part by limiting CtIP-dependent DNA-end resection activity in late S/G_2 phases of the cell cycle.

Results

Cdh1 depletion provokes DNA damage and hypersensitivity to DSB-inducing agents

To analyze the role of APC/C^{Cdh1} in the maintenance of genome stability, we stably suppressed Cdh1 in non-transformed, immortalized human retina pigment epithelium (hTERT-RPE-1), HeLa cervical cancer, and MCF7 breast cancer cells using lentiviral shRNAs (Fig 1A). Sustained downregulation of Cdh1 over the course of 5 days resulted in approximately twofold increase of cells in G_2/M phase accompanied by elevated levels of γ-H2AX (Fig 1A–C). Also, Cdh1 depletion resulted in upregulation of p53 in RPE-1 and MCF7 cells (Fig 1A and Supplementary Fig S1). Combined, these results are indicative of DNA damage accumulation in Cdh1-depleted cells, even in the absence of genotoxic agents, which is in line with observations in other cell types (García-Higuera *et al*, 2008; Sigl *et al*, 2009; Delgado-Esteban *et al*, 2013; Eguren *et al*, 2013). We next analyzed the distribution of cells over the various mitotic stages to address whether the acquisition of DNA damage caused by Cdh1 downregulation translates into aberrant mitotic progression. While Cdh1 depletion in MCF7 cells did not significantly alter the distribution of the various mitotic phases, it gave rise to a higher frequency of bridging chromosomes in anaphase (Fig 1D). Such abnormal chromosome segregation events are frequently observed in cells that exhibit G_2/M checkpoint or DNA repair defects (French *et al*, 2006; Acilan *et al*, 2007; Chan *et al*, 2007; Laulier *et al*, 2011).

This prompted us to examine whether Cdh1 depletion leads to increased sensitivity to DNA-damaging agents. Clonogenic survival assays showed that Cdh1-depleted MCF7 cells are hypersensitive to IR (Fig 2A). Notably, the colonies of irradiated Cdh1-depleted cells were considerably smaller compared to control-depleted cells (Fig 2A). In line with these results, we found that shRNA-mediated depletion of Cdh1 reduced cell survival after treatment with doxorubicin, a chemotherapeutic compound inducing DSBs (Fig 2B).

We next examined whether DSB repair mechanisms are affected by Cdh1 depletion. Since cell cycle status significantly influences the mode of DSB repair, we made use of the FUCCI system which allows to specifically analyze S/G_2 cells without employing synchronization protocols (Supplementary Fig S2A) (Sakaue-Sawano *et al*, 2008). First, Cdh1 depletion did not affect IR-induced phosphorylation of KAP1 at S824, an early event in the DNA damage response (Fig 2C) (White *et al*, 2006; Ziv *et al*, 2006). Interestingly, however, Cdh1-depleted cells displayed significantly reduced numbers of Rad51 foci at both 2 and 5 h after irradiation, without affecting Rad51 levels (Fig 2C and D, and Supplementary Fig S2B). In contrast, 53BP1 foci numbers remained largely unaffected by the absence of Cdh1 (Fig 2D and Supplementary Fig S2C). Taken together, our results demonstrate that Cdh1 ensures genome stability, promotes survival under conditions of DNA damage, and influences the dynamics of IR-induced Rad51 foci formation, indicative of a regulatory function of Cdh1 in HR.

Proteomic analysis of potential Cdh1 targets

We next set out to identify APC/C^{Cdh1} substrates that contribute to the role of Cdh1 in maintaining genome stability. To select for potential candidates, we focused on two selection criteria. Firstly, we screened for proteins that are downregulated when APC/C^{Cdh1} activity is turned on after mitotic exit using quantitative mass spectrometry. Secondly, we analyzed the primary amino acid sequence of each of those downregulated proteins for the presence of so-called D-boxes and KEN boxes, through which Cdh1 recruits targets to the APC/C (Pfleger *et al*, 2001; Liu *et al*, 2012). To identify proteins that are degraded during the mitosis-to-G_1 transition, we treated cells with nocodazole, a reversible microtubule-depolymerizing agent that activates the spindle assembly checkpoint, thereby causing cells to

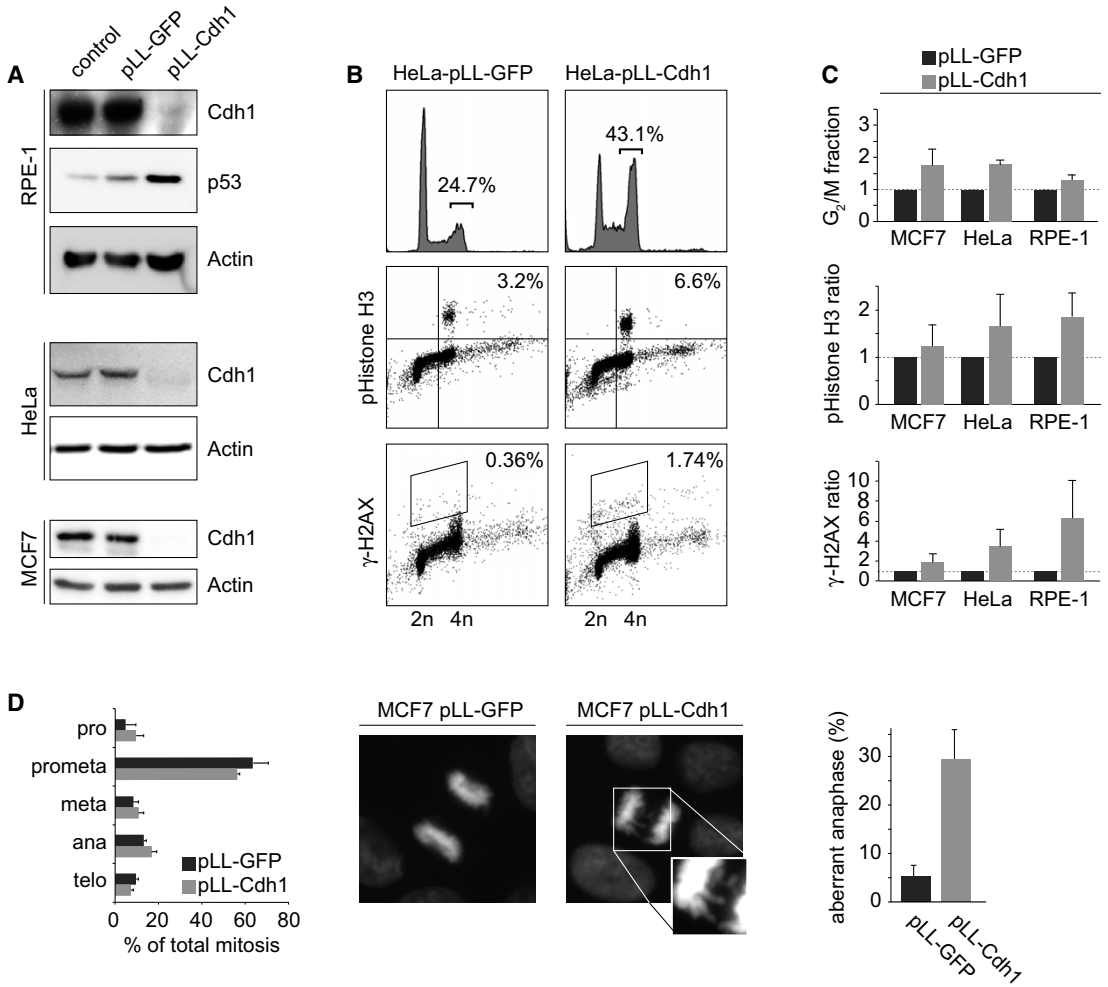

Figure 1. Cdh1 depletion results in genomic instability.

A RPE-1, HeLa, and MCF7 cells were infected with pLL-GFP or pLL-Cdh1 lentiviral shRNAs, and puromycin-resistant cells were harvested at 5 days after virus infection. Immunoblotting was performed with anti-Cdh1, anti-p53, and anti-actin antibodies.

B HeLa cells treated as in (A) were harvested in ice-cold ethanol and co-stained for γ-H2AX and phospho-histone H3 along with propidium iodide before analysis by flow cytometry. Plots of at least 10,000 events are shown. Percentages indicate average amounts of G_2/M cells, phospho-histone H3-positive cells, and γ-H2AX-positive cells.

C RPE-1, HeLa, and MCF7 cells were treated as in (B), and averages and standard deviations for three independent experiments are indicated for G_2/M content, phospho-histone H3-positive cells, and γ-H2AX-positive cells.

D MCF7 cells were infected with the indicated shRNA viruses, grown on glass coverslips and stained with DAPI. From three experiments, at least 200 mitoses were scored per condition. Anaphase figures were scored separately for the presence of lagging chromosomes. Averages and standard deviations are indicated. Representative examples are indicated.

arrest in prometaphase. Subsequent removal of nocodazole allows cells to synchronously exit mitosis along with APC/C^{Cdh1} activation. To compare protein abundance before and after mitotic exit, RPE-1 cells were grown in DMEM containing either light or heavy isotope-labeled amino acids (Ong *et al*, 2002). Cells cultured in light medium were lysed directly after nocodazole incubation, whereas cells in heavy medium were harvested at 2.5 h after being released from mitotic arrest (Fig 3A and B). In addition, a label-swap experiment was performed with the SILAC labeling reversed. Cell lysates were then mixed in a 1:1 ratio and analyzed by mass spectrometry. We measured relative up- or downregulation of > 3,300 proteins in G_1 compared to M phase (Supplementary Data S1). To interrogate the quality of our data set, we assessed whether specific pathways were predominantly affected during mitotic exit. To this end, protein entries were converted to gene entries and enrichment was tested using Gene set enrichment analysis (GSEA) (Subramanian *et al*, 2005). As expected, "cell cycle" and "mitotic" pathways were significantly downregulated during mitotic exit (Fig 3C). In

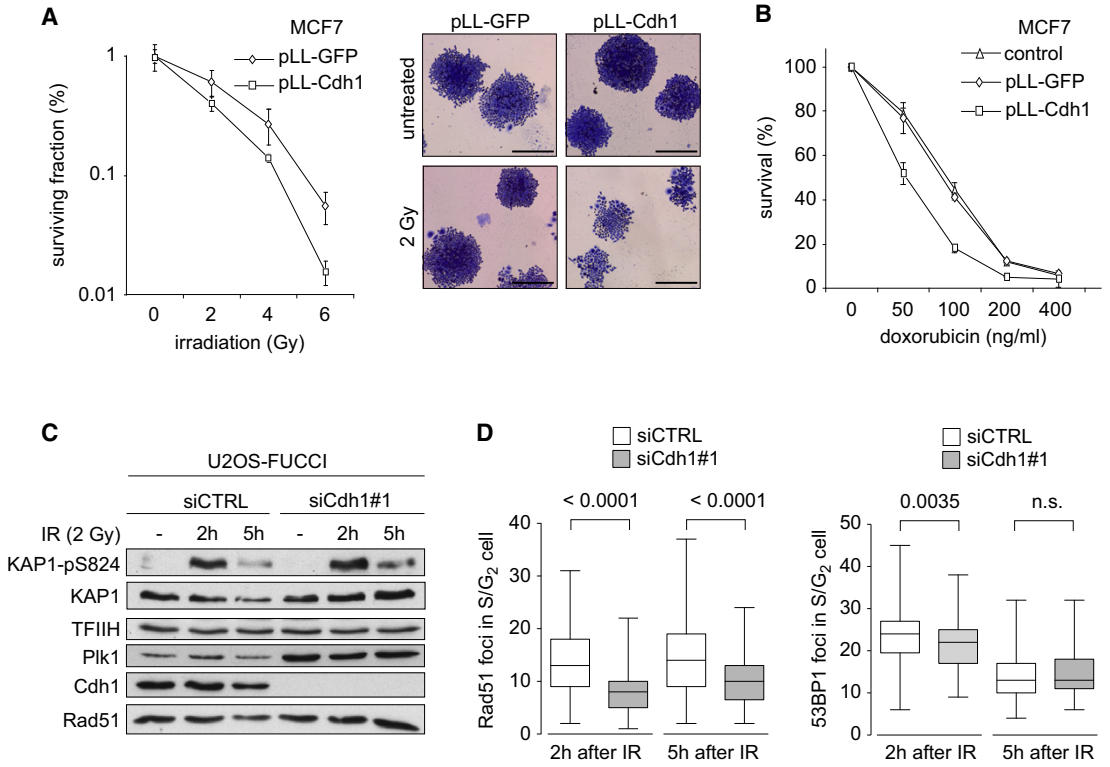

Figure 2. Cdh1 depletion sensitizes to DNA-damaging agents and affects recruitment of DNA repair components.

A MCF7 cells were infected with the indicated shRNAs and selected with puromycin. pLL-GFP- or pLL-Cdh1-infected MCF7 cells were plated in 6-well plates and subsequently irradiated with the indicated amounts of ionizing radiation. Surviving colonies were stained, and relative amounts of colony numbers compared to non-irradiated cells are shown. Averages and standard deviations of three independent experiments are shown.

B pLL-GFP- or pLL-Cdh1-infected MCF7 cells were plated in 96-well plates and subsequently treated with the indicated amounts of doxorubicine for 4 days. Cellular viability was assessed using MTT conversion, and untreated cells were used as a reference. Averages and standard deviations of three independent experiments are shown.

C At 48 h after siRNA transfection, U2OS-FUCCI cells were irradiated (2 Gy). At 2 or 5 h after treatment, whole-cell extracts were prepared and analyzed by Western blotting with the indicated antibodies.

D U2OS-FUCCI cells treated as in (C) were prepared for 53BP1 and Rad51 immunofluorescence. Graphs show the amounts of 53BP1 or Rad51 foci in S/G_2 cells. At least 120 cells from three independent experiments were counted for each condition, and data are presented as box plots with whiskers representing the minimal and maximal values. Unpaired Student's *t*-tests (two-sided) were done to compare control-depleted and Cdh1-depleted conditions. Representative images can be found in Supplementary Fig S2B and C.

contrast, proteins involved in translation and transcription were upregulated, in line with observations that chromatin is re-established after mitosis and that translational and transcriptional processes are inactive during mitosis and need to be re-initiated upon mitotic exit (Fig 3C) (Prescott & Bender, 1963; Bonneau & Sonenberg, 1987).

Our data set for proteins that were considerably downregulated after mitotic exit included various known APC/C^{Cdh1} targets such as p15-PAF, cyclin B1, Plk1, UbcH10, Aurora A, and Aurora B (Fig 3D and Supplementary Fig S3A) (Pfleger *et al*, 2001; Littlepage & Ruderman, 2002; Taguchi *et al*, 2002; Lindon & Pines, 2004; Rape & Kirschner, 2004; Nguyen *et al*, 2005; Stewart & Fang, 2005; Emanuele *et al*, 2011). As expected, both KEN box and D-box motifs were significantly enriched in proteins downregulated during mitotic exit compared to the entire proteomic data set (Fig 3E) (Liu *et al*, 2012). When we applied "DNA damage response" (see Supplementary Table S1 for list of Gene Ontology terms) as a functional criterion for proteins downregulated during mitotic exit containing a conserved destruction motif, we discovered various proteins involved in the maintenance of genomic integrity including Rif1, Smc5, Mdc1, CtIP, and Top2A (Fig 3F). DNA topoisomerase 2-alpha was recently discovered as a novel Cdh1 substrate (Eguren *et al*, 2014). Interestingly, Rif1 has been reported to act as a 53BP1 effector protein, antagonizing the role of BRCA1 in promoting CtIP-dependent resection and HR (Kumar & Cheok, 2014). However, sequence analysis revealed that none of the predicted functional destruction motifs in human Rif1 were evolutionary conserved, whereas both putative KEN boxes in human CtIP were highly conserved in vertebrates (Supplementary Fig S3). Therefore, we decided to focus on the DNA-end resection factor CtIP as a potential target of the APC/C^{Cdh1} involved in the maintenance of genomic integrity.

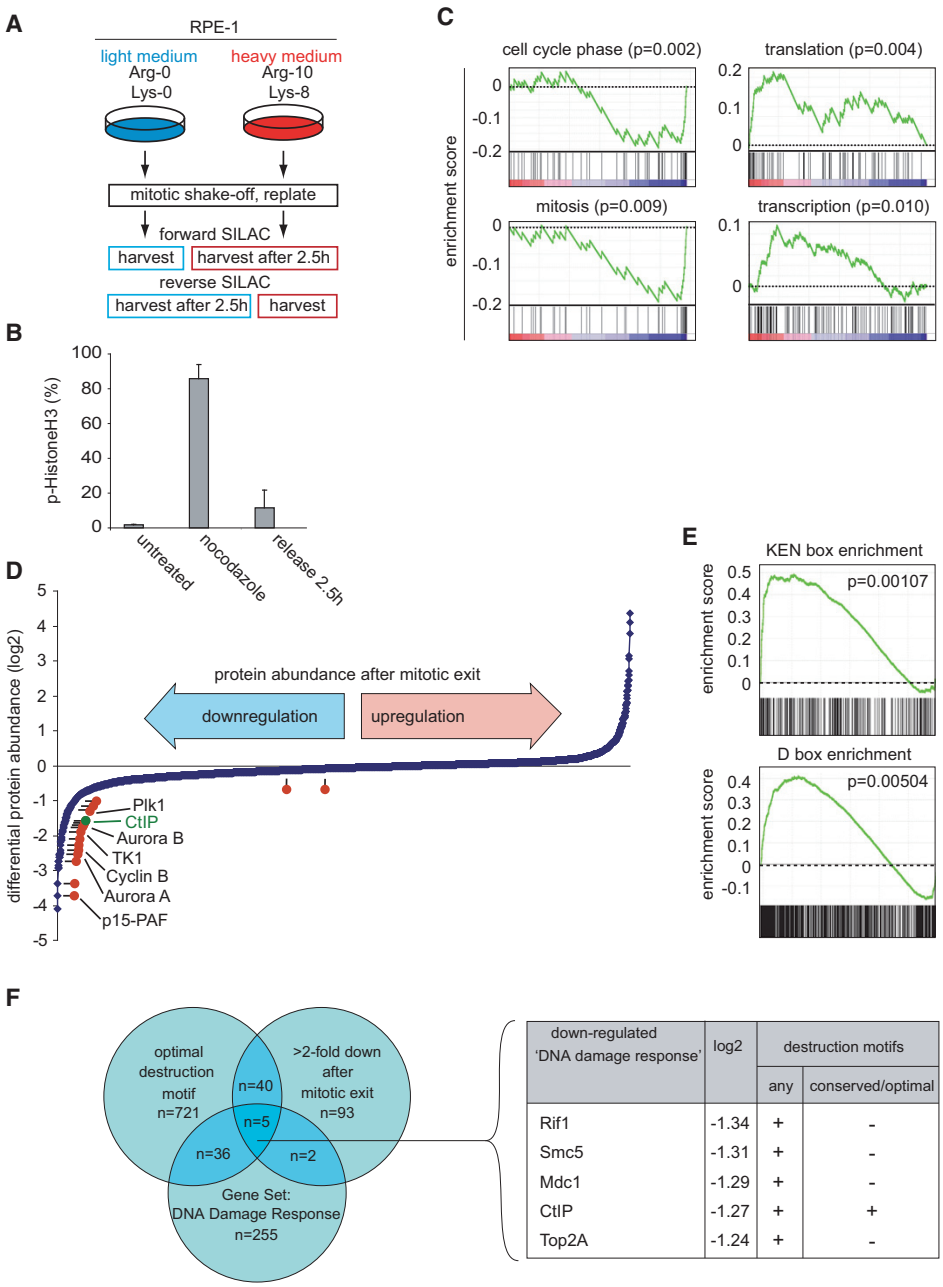

down-regulated 'DNA damage response'	log2	destruction motifs	
		any	conserved/optimal
Rif1	-1.34	+	-
Smc5	-1.31	+	-
Mdc1	-1.29	+	-
CtIP	-1.27	+	+
Top2A	-1.24	+	-

Figure 3. A combined proteomics/bioinformatics approach to identify potential APC/C^{Cdh1} substrates.

A Overview of mass spectrometry analysis of changes in protein abundance during mitotic exit. RPE-1 cells were grown in "light" or "heavy" SILAC media and treated with nocodazole. Mitotic cells were obtained by shake-off and were directly lysed or replated in nocodazole-free medium and lysed after 2.5 h. Alternatively, treatments were swapped ("reverse SILAC"). Cell lysates were mixed 1:1 and analyzed by mass spectrometry.

B RPE-1 cells were treated and harvested in parallel to (A) and were stained for phospho-histone H3/Alexa-488.

C Gene set enrichment analysis (GSEA) of SILAC results. Indicated pathways are significantly affected during mitotic exit.

D Log2-transformed ratios are indicated for the > 3,300 proteins that were identified both in forward and in reverse SILAC. Negative ratios indicate downregulation during mitotic exit. Established APC/C^{Cdh1} targets are indicated in red.

E GPS-ARM software was used to identify D-box or KEN box sequences in mass spectrometry hits. GSEA was used to assess enrichment for destruction motif-containing proteins within downregulated proteins.

F Venn diagram indicating proteins that are downregulated at least twofold, contain any destruction motif, and belong to the "DNA damage response/DNA repair" gene set.

CtIP is a substrate of APC/C^{Cdh1} during mitotic exit

Confirming our mass spectrometry data, we observed that CtIP protein levels decreased when RPE-1 cells exit mitosis following release from a nocodazole-induced prometaphase arrest (Fig 4A–C). Notably, CtIP downregulation followed a pattern similar to that of Plk1, a known APC/C^{Cdh1} substrate (Fig 4A–C) (Lindon & Pines, 2004). This was not due to nocodazole-induced microtubule depolymerization, as cells released from a mitotic block induced by Eg5 inhibition showed a similar behavior with regard to CtIP levels (Supplementary Fig S4A). Likewise, when cells were enriched at the G_2/M transition using the reversible Cdk1 inhibitor RO-3306, and subsequently followed during exit from mitosis, we observed that CtIP protein levels gradually decreased (Fig 4D). Interestingly, under these different synchronization conditions, we repeatedly noticed that CtIP migrates much slower in mitotic cells compared to G_1 cells. We find that this shift is mainly attributed to phosphorylation, but further work is needed to explore whether there is a functional interplay between CtIP phosphorylation and stability during exit from mitosis (Supplementary Fig S4B).

In line with the APC/C^{Cdh1} targeting CtIP for proteasomal degradation, we observed increased CtIP protein levels after transfecting RPE-1 and U2OS cells with Cdh1 siRNA oligos (Fig 4E and Supplementary Fig S4C and D), which was not due to altered cell cycle distribution profiles (Supplementary Fig S4C and D). Analogously, treatment of asynchronously growing RPE-1 cells with the small molecule APC/C inhibitor proTAME (Zeng *et al*, 2010) stabilized CtIP as well as Plk1, albeit not to the same extent as treatment with the proteasome inhibitor MG-132 (Fig 4F). Importantly, both MG-132 and proTAME clearly blocked CtIP and Plk1 degradation after cells synchronously exit mitosis and enter G_1 phase (Fig 4G and Supplementary Fig S4E). Taken together, our findings indicate that CtIP is targeted by APC/C^{Cdh1} during mitotic exit.

CtIP interacts with Cdh1 through a conserved KEN box

CtIP contains two conserved KEN box motifs, which are believed to be recognized exclusively by APC/C^{Cdh1} (Pfleger & Kirschner, 2000), but only the second one between amino acids 467 and 469 matches the recently reported consensus KEN box sequence ([D/N]-K-E-N-x-x-P) (Fig 5A) (He *et al*, 2013). To test whether any of the two KEN box motifs are functional, HEK293T cells were transfected with HA-Cdh1, along with FLAG-CtIP mutated in one or both KEN box motifs. Whereas CtIP-wt and CtIP-K179A are efficiently co-immunoprecipitated with HA-Cdh1, mutating the second putative KEN box in CtIP (K467A) abolished its interaction with Cdh1 (Fig 5B). Furthermore, only GFP-CtIP-wt, but not GFP-CtIP-K467A, was efficiently co-immunoprecipitated with endogenous Cdh1 (Supplementary Fig S5A). To strengthen these observations, we subjected HeLa nuclear extracts to GST-CtIP pull-down assays and found that endogenous Cdh1 interacts with wild-type recombinant CtIP, but not with the CtIP-K467A mutant (Fig 5C). Moreover, this was unlikely due to improper protein folding of bacterially expressed GST-CtIP-K467A, as the mutant full-length protein was still able to pull-down Mre11 (Fig 5C). These results were confirmed using a CtIP fragment covering both KEN box motifs (166–487), indicating that the coiled coil domain (45–160) and the conserved Sae2-like C-terminal domain (790–897) of CtIP are not required for Cdh1 interaction (Fig 5A and C).

The APC/C is a multi-subunit E3 ubiquitin ligase that, once activated by either Cdc20 or Cdh1, mediates ubiquitin- and proteasome-dependent degradation of key cell cycle regulatory proteins (Peters, 2006). Since CtIP was recently shown to be poly-ubiquitylated and degraded by the proteasome (Steger *et al*, 2013), we next addressed whether Cdh1 may promote CtIP ubiquitylation. To this end, we transfected His-ubiquitin into HEK293 cells inducibly expressing GFP-CtIP and analyzed the level of CtIP ubiquitylation after Ni-NTA pull-down. Remarkably, depletion of Cdh1 using two independent siRNAs severely impaired CtIP ubiquitylation (Fig 5D). Furthermore, the conjugation of ubiquitin chains was largely abolished in the CtIP-K467A KEN box mutant compared to CtIP-wt, further indicating that CtIP is a substrate of APC/C^{Cdh1} (Fig 5E). To test whether the conserved KEN box is required for CtIP degradation during mitotic exit, we performed time-lapse fluorescence microscopy with U2OS cells harboring siRNA-resistant inducible GFP-tagged CtIP-wt or CtIP-K467A (Fig 5F). These cell lines progressed through the cell cycle with similar kinetics and expressed comparable levels of GFP-tagged CtIP upon doxycycline addition (Supplementary Fig S5B). Importantly, whereas the fluorescence intensity of nuclear CtIP-wt slowly decreased after exit from mitosis, CtIP-K467A levels remained relatively constant throughout the entire time course (Fig 5F). Combined, our data suggest that CtIP interacts with Cdh1 through a conserved KEN box motif and this interaction promotes CtIP poly-ubiquitylation and degradation in an APC/C^{Cdh1}-dependent manner.

Figure 4. CtIP is a substrate of the APC/C^{Cdh1} during mitotic exit.

A RPE-1 cells were left untreated (asynchronous, "AS") or treated with nocodazole for 16 h. Mitotic cells were obtained by shake-off and replated in nocodazole-free medium for indicated time periods. Cells were stained for phospho-histone H3 and propidium iodide, and at least 10,000 events were analyzed by flow cytometry. Averages and standard deviations of three experiments are shown.

B Same cells as in (A) were immunoblotted for the indicated proteins.

C Western blots as shown in (B) were quantified, and averages and standard deviations of three independent experiments are shown.

D RPE-1 cells were treated for 18 h with the Cdk1 inhibitor RO-3306 (5 μM) to enrich for G_2 cells. Subsequently, cells were washed 3 times with warm culture medium, and 1 h later, mitotic cells were collected by mitotic shake-off (t = 0 h). At the indicated time points after replating, cells were harvested and further analyzed as in (A) and (B).

E Asynchronously growing RPE-1 cells were transfected with indicated siRNAs for 48 h and processed for immunoblotting with the indicated antibodies. Western blots were quantified, and averages and standard deviations of three independent experiments are shown.

F RPE-1 cells were cultured for 3 h in proTAME (12 μM), MG-132 (5 μM), or solvent controls. Whole-cell lysates were immunoblotted for the indicated proteins (left panel). Average Western blot intensities and standard deviations of three independent experiments are shown (right panel).

G Mitotic RPE-1 cells were obtained by mitotic shake-off after nocodazole treatment. Cells were replated, and after 1 h, proTAME (12 μM) or MG-132 (5 μM) or solvent was added to the culture medium. At 1 or 2.5 h after treatment, cells were harvested for Western blot analysis with the indicated antibodies. Western blots of a representative experiment are indicated (left panel). In parallel, cells were fixed in ethanol and stained for phospho-histone H3 and propidium iodide, and at least 10,000 events were analyzed by flow cytometry. Averages and standard deviations of three independent experiments are shown (right panel).

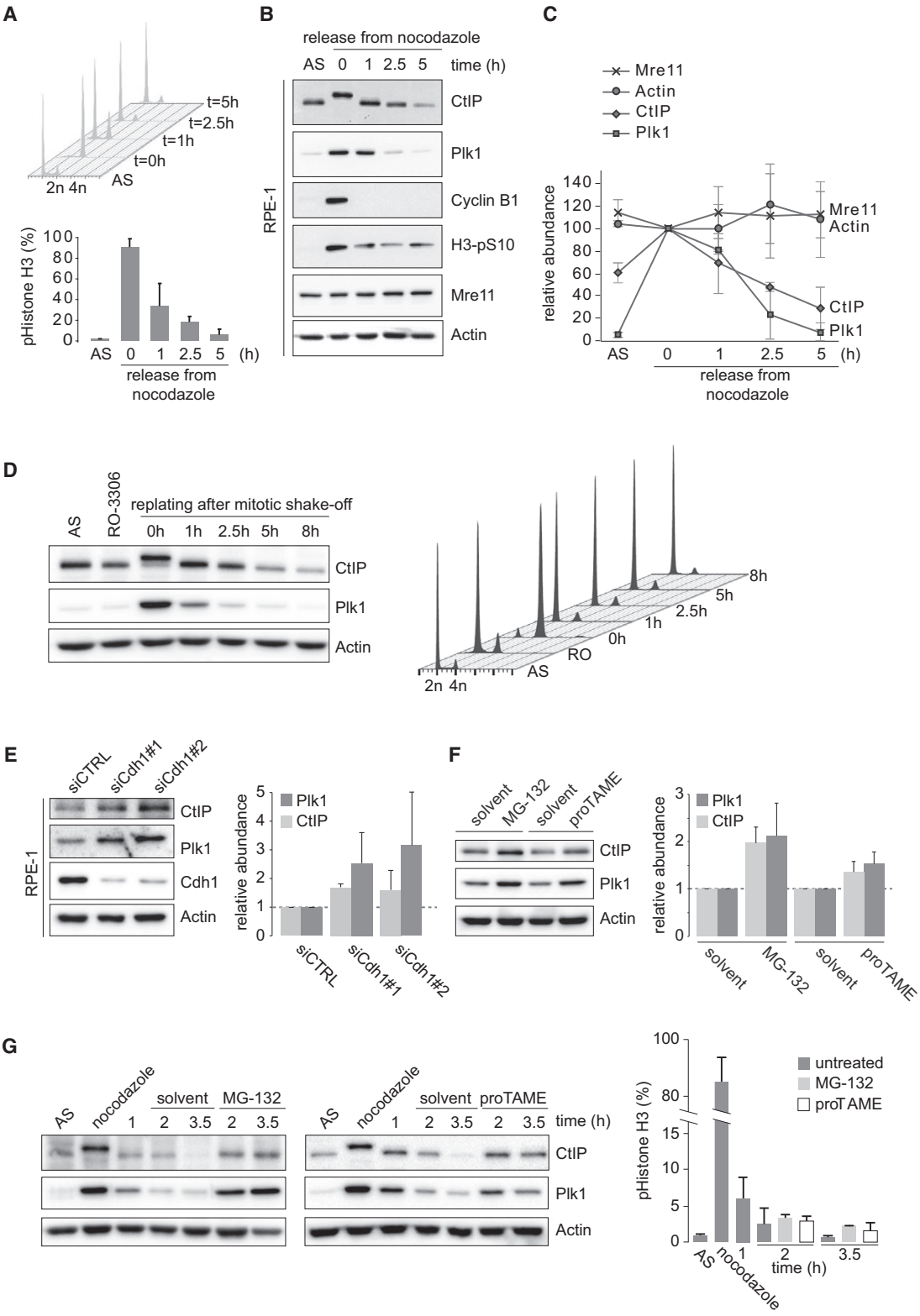

Figure 4.

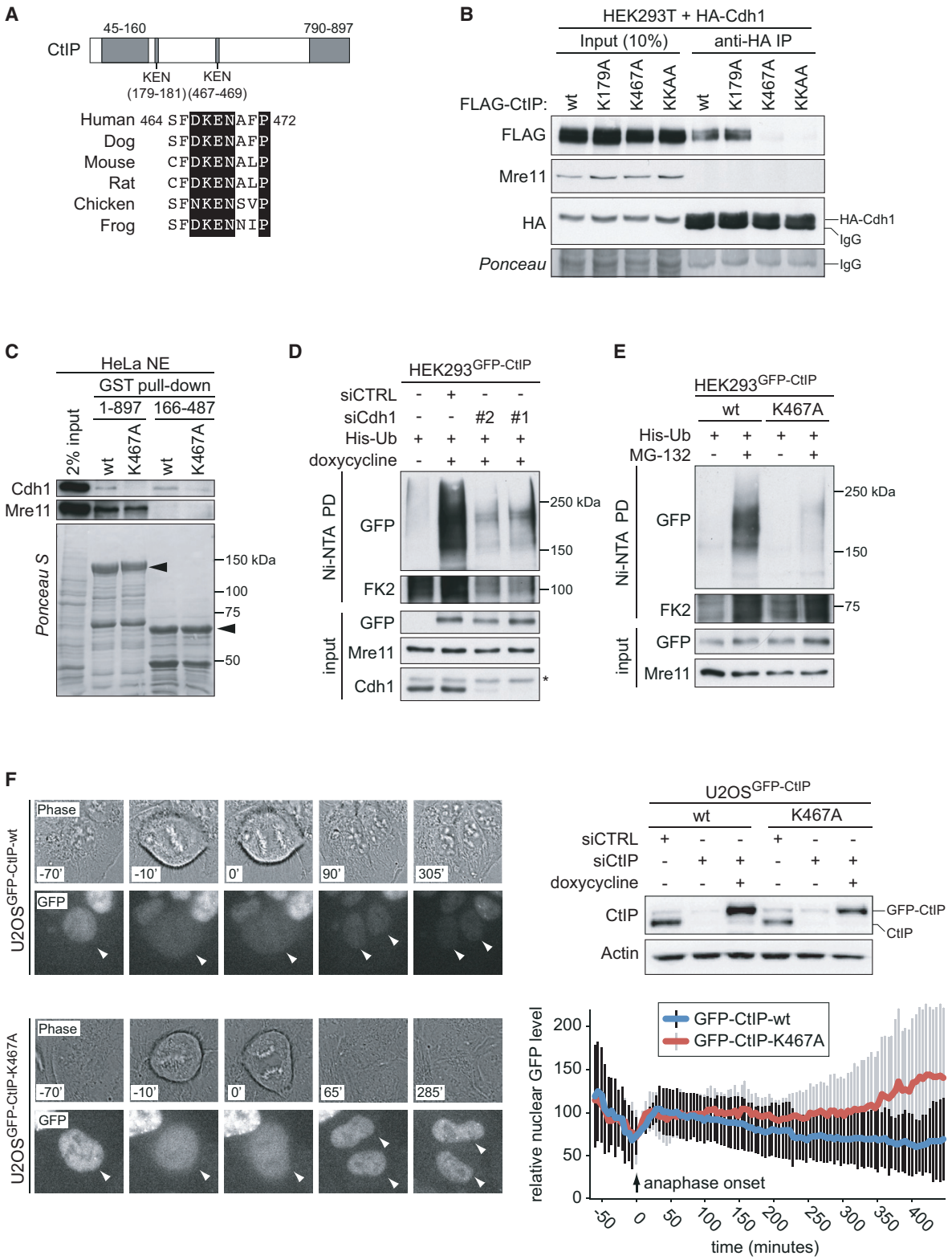

Figure 5.

APC/C promotes CtIP degradation in response to DSBs

Since APC/C^{Cdh1} has been described to be activated in G_2 phase after DNA damage (Sudo *et al*, 2001; Bassermann *et al*, 2008), we decided to investigate whether CtIP is also targeted by the APC/C under these conditions. To this end, we synchronized U2OS cells at the G_1/S transition using a single thymidine treatment and then allowed cells to re-enter the cell cycle. At 7 h after the release, G_2-enriched cells were irradiated at low (2 Gy) or high dose (10 Gy) and analyzed after 2 and 5 h by Western blotting (Fig 6A). Whereas CtIP levels only slightly decreased at 5 h after 2 Gy, CtIP downregulation in response to 10 Gy occurred to an extent that was similar to that of Claspin, a previously reported APC/C^{Cdh1} substrate (Fig 6B) (Bassermann *et al*, 2008). These changes did not represent post-mitotic degradation of CtIP, as judged by comparable cell cycle profiles (Fig 6A). Importantly, CtIP and Claspin levels were partially restored when proTAME was added to the cells immediately after IR (Fig 6B), indicating that the APC/C is responsible for CtIP degradation in G_2-irradiated cells. Similar results were obtained after treatment of G_2-enriched cells with doxorubicin (Supplementary Fig S6A and B). Interestingly, we noticed that proTAME treatment led to an increase in RPA2 phosphorylation following IR (Fig 6B, lane 7), while other DNA damage signaling events including Chk1 and Chk2 phosphorylation remained largely unaffected. In line with a requirement for the APC/C in CtIP degradation after DNA damage in G_2 cells, ubiquitylation of endogenous CtIP in response to IR was significantly reduced in presence of proTAME (Fig 6C).

To strengthen these findings, we monitored GFP-CtIP-wt fluorescent intensity following irradiation of G_2 cells using live-cell imaging. Consistent with our Western blot data, CtIP levels drop to approximately 50% starting at 4 h after IR (Fig 6D and Supplementary Fig S6C). Also in this case, the observed CtIP downregulation was not due to post-mitotic degradation, since none of the analyzed cells entered mitosis during the entire time-lapse experiments, most likely due to a strong G_2-arrest produced by 10 Gy (data not shown). In line with our previous observation, GFP-CtIP-wt levels in cells co-treated with proTAME remained constant throughout the analyzed time frame, supporting our hypothesis that the APC/C is required for CtIP downregulation in response to DNA damage in G_2 cells (Fig 6D and Supplementary Fig S6C). Altogether, these data suggest that CtIP is degraded after DSB induction in G_2 and that this regulatory mechanism is dependent on APC/C activity.

CtIP–Cdh1 interaction is required for CtIP downregulation after DNA damage and clearance of IR-induced CtIP foci

Having established that CtIP is degraded in an APC/C-dependent manner in response to DNA damage, we wanted to test whether this requires physical interaction between Cdh1 and CtIP. Quantitative live-cell imaging revealed that a functional KEN box is crucial for IR-induced downregulation of CtIP, since GFP-CtIP-K467A levels remained stable throughout the entire time course (Fig 7A and B). Strikingly, we observed that CtIP-K467A IR-induced foci (IRIF) persisted, whereas CtIP-wt IRIF were resolved over time, indicating that APC/C^{Cdh1} facilitates the spatiotemporal release of CtIP from damaged chromatin (Fig 7C). Analysis of GFP-CtIP localization in response to laser micro-irradiation further confirmed that both CtIP-wt and CtIP-K467A are efficiently recruited to microlaser-generated DSB tracks, and overlap with γ-H2AX-decorated chromatin (Supplementary Fig S7A).

To further investigate the role of Cdh1–CtIP interaction in response to DNA damage, we isolated monoclonal cell lines, inducibly expressing siRNA-resistant GFP-CtIP-wt and GFP-CtIP-K467A. Importantly, expression of GFP-CtIP-wt rescued DNA-end resection defects caused by CtIP depletion, as judged by the restoration of RPA2 phosphorylation at S4/S8 in response to IR treatment (Supplementary Fig S7B) (Sartori *et al*, 2007). The DNA-end resection capacity of CtIP was previously shown to be required for the maintenance of IR-induced G_2 arrest (Kousholt *et al*, 2012). In line with this report, depletion of CtIP did not interfere with checkpoint initiation, but did result in defective checkpoint maintenance (Supplementary Fig S7C). Notably, expression of either GFP-CtIP-wt or GFP-CtIP-K467A rescued the checkpoint maintenance defect (Supplementary Fig S7C), suggesting that CtIP-K467A is proficient in DNA-end resection. In addition, we did not find any significant defects in initiation and maintenance of the IR-induced G_2 checkpoint upon Cdh1 depletion (Supplementary Fig S7D).

In agreement with CtIP-K467A mutant cells being checkpoint proficient, irradiation resulted in robust activation of ATM and ATR, as assessed by Chk2 and Chk1 phosphorylation, respectively (Fig 7D). Moreover, both CtIP-wt and CtIP-K467A were able to promote RPA2 phosphorylation, with the KEN box mutant being slightly more efficient than the wt, whereas expression of the resection-deficient CtIP-T847A mutant largely

Figure 5. CtIP interacts with Cdh1 through a conserved KEN box.

A Schematic representation of human CtIP protein with its coil-coiled domain (45–160), Sae2-like domain (790–897), and putative KEN boxes (179–181 and 467–469). Conservation of KEN box at 467 is shown for the indicated species.

B HEK293T cells were transfected with HA-Cdh1 in combination with indicated FLAG-CtIP plasmids. Cells lysates were used for anti-HA immunoprecipitations. Western blotting was performed with the indicated antibodies for whole-cell lysate or immunoprecipitations.

C HeLa nuclear extract (NE) was incubated with GST fusion proteins with the indicated full-length (1–897) CtIP variants or CtIP fragment (166–487) variants. GST pull-downs were immunoblotted for Mre11 and Cdh1.

D HEK293 Flp-In T-REx cells were induced to express GFP-CtIP-wt using doxycycline and were transfected with His-tagged ubiquitin ("His-Ub") along with control siRNA or Cdh1 siRNA. Before lysis, cells were treated with proteasome inhibitor MG-132 for 4 h. Cell lysates were used for Ni-NTA precipitations. Total cell lysates ("input") and Ni-NTA pull-downs ("PD") were immunoblotted for the indicated proteins.

E HEK293 Flp-In T-REx cells were induced to express GFP-CtIP-wt or GFP-CtIP-K467A and transfected with His-tagged ubiquitin ("His-Ub"), and treated with proteasome inhibitor MG-132 for 4 h. Cell lysates were subsequently used for Ni-NTA pull-down. Total cell lysates ("input") and Ni-NTA pull-downs ("PD") were immunoblotted for the indicated proteins.

F U2OS Flp-In T-REx cells were induced to express GFP-CtIP-wt or GFP-CtIP-K467A and were transfected with control siRNA or siCtIP. Cell lysates were processed for immunoblotting for CtIP and actin (upper right panel). U2OS cells were then imaged every 5 min for GFP expression or phase contrast using live-cell microscopy. Representative stills from live-cell imaging are shown, in which anaphase onset was used as a reference time point (left panels). Quantifications of the average nuclear GFP signal from time-lapse movies are indicated for GFP-CtIP-wt (n = 12) and GFP-CtIP-K467A (n = 18) (lower right panel).

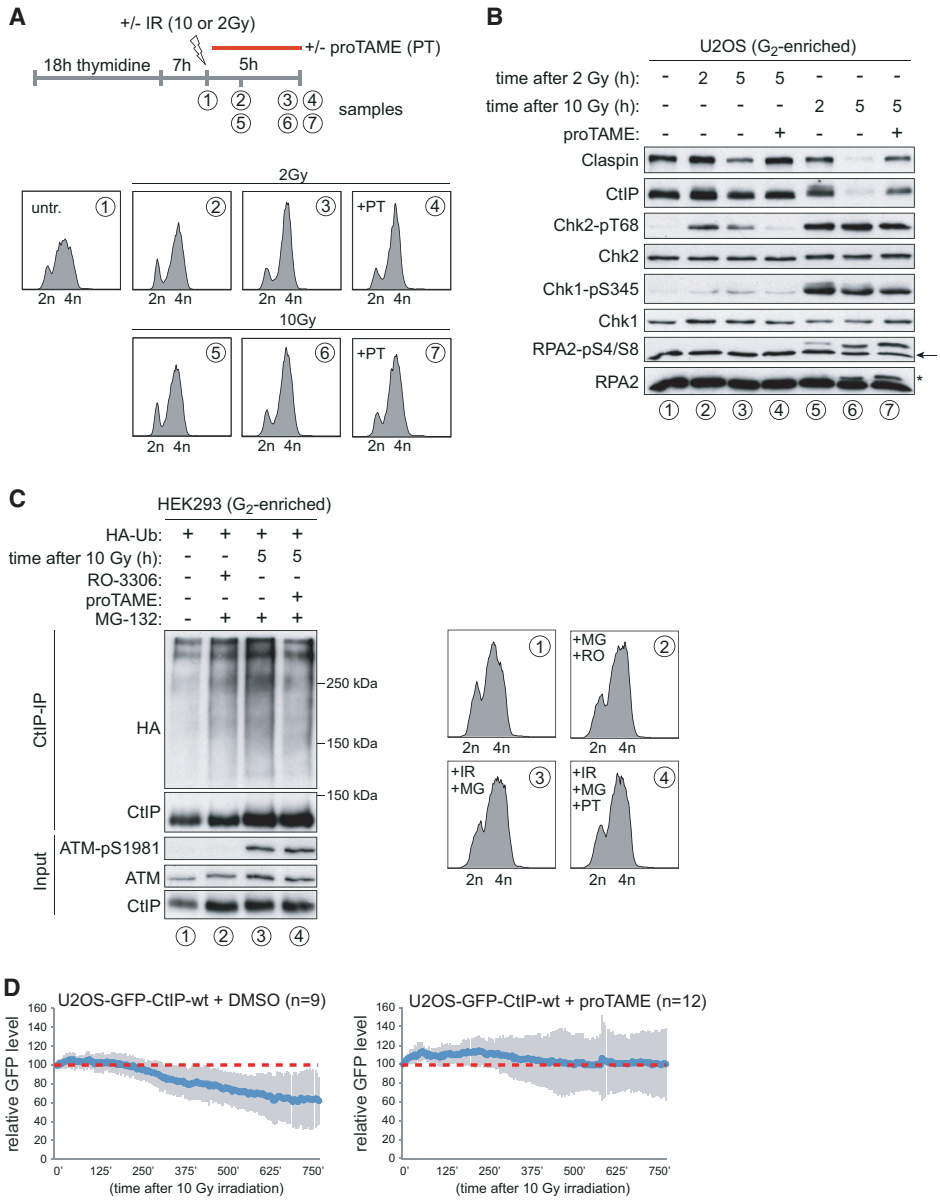

Figure 6. CtIP is degraded in response to DNA damage in G_2 phase in an APC/C-dependent manner.

A U2OS cells were synchronized using a single thymidine block with 2 mM thymidine for 18 h. Seven hours after release, cells enriched in G_2 phase were either fixed directly (lane 1) or exposed to low (2 Gy) or high dose (10 Gy) of IR and harvested at the indicated time points following irradiation. Where indicated, cells were treated with the APC inhibitor proTAME (20 μM) immediately after irradiation. Cells were stained with DAPI and analyzed by flow cytometry.

B Cells were treated as in (A) and lysed in RIPA buffer for immunoblotting with the indicated antibodies. The anti-RPA2 blot was reprobed with anti-pRPA2-S4/S8 antibody. The arrow indicates leftover signals of the unmodified RPA2 protein. The asterisk indicates hyperphosphorylated RPA2.

C HEK293 cells were transfected with HA-tagged ubiquitin ("HA-Ub"). Thirty hours post-transfection, cells were synchronized using a single thymidine block with 2 mM thymidine for 18 h. Five hours after the release, cells enriched in late S/G_2 phase were either lysed directly (lane 1), or further incubated for 5 h in the presence of CDK1 inhibitor RO-3306 (9 μM) to keep cells in G_2 (lane 2), or irradiated with 10 Gy in the absence (lane 3) or presence (lane 4) of the APC inhibitor proTAME (20 μM) and lysed after 5 h. Where indicated, cells were treated with MG-132 (20 μM) for 5 h before lysis. Samples were then further processed for immunoprecipitation using a polyclonal anti-CtIP antibody as indicated in Materials and Methods. Cell cycle profiles of corresponding samples are indicated on the right.

D U2OS Flp-In T-REx cells were induced to express GFP-CtIP-wt and transfected with CtIP siRNA. Cells were subsequently synchronized by thymidine incubation for 24 h and released from thymidine for 8 h. At 8 h after release, cells were treated with DMSO or proTAME (12 μM), subsequently irradiated with 10 Gy, and imaged using fluorescence time-lapse microscopy. Representative stills of GFP and DIC movies are presented in Supplementary Fig S6C. Averages and standard deviations of total nuclear GFP intensity are indicated from 9 and 12 movies for DMSO-treated and proTAME-treated cells, respectively.

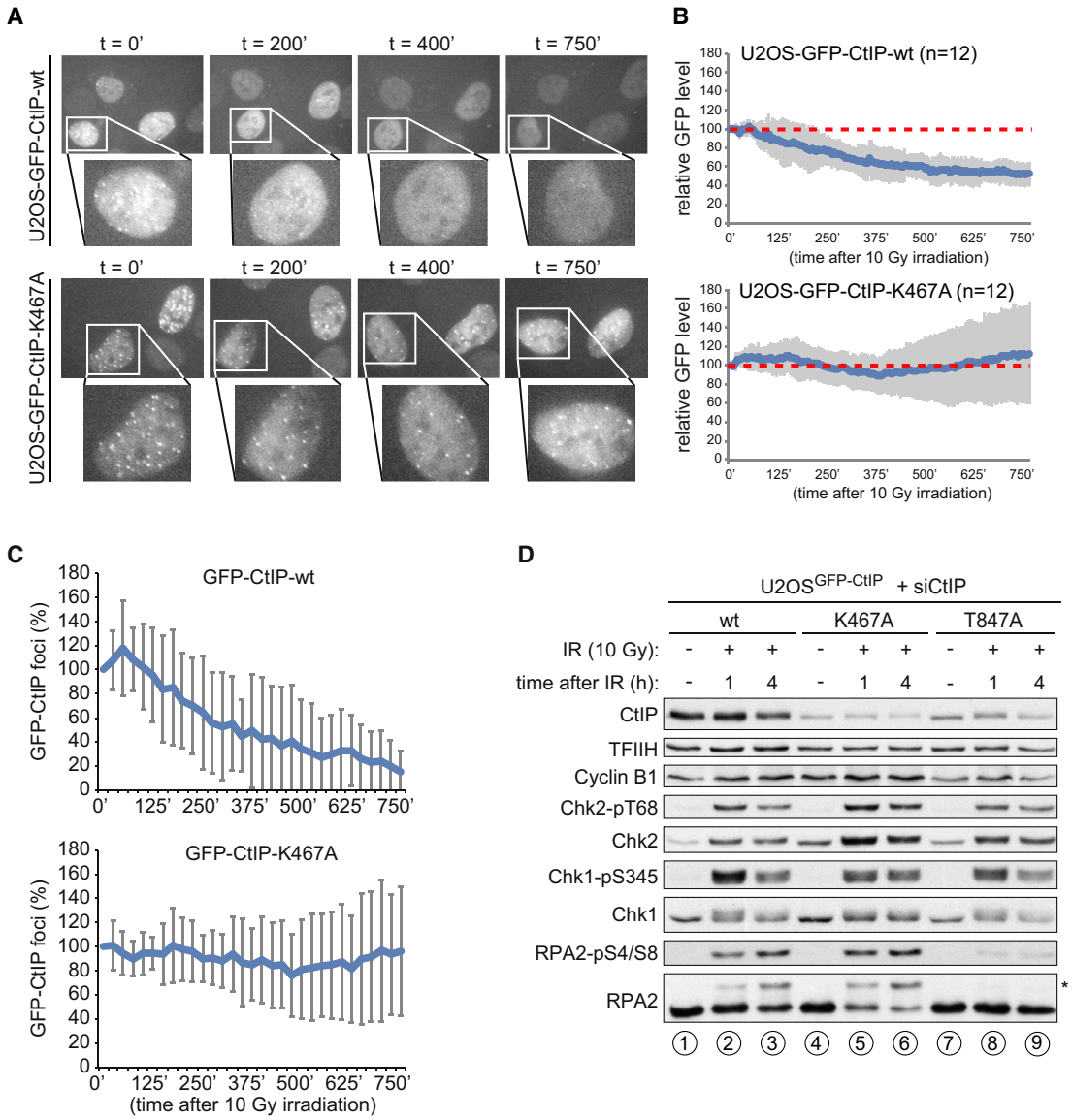

Figure 7. CtIP–Cdh1 interaction is not required for CtIP recruitment to sites of DNA damage and initiation of DNA-end resection.

A U2OS Flp-In T-REx cells were induced to express GFP-CtIP-wt or GFP-CtIP-K467A and transfected with CtIP siRNA. Cells were subsequently synchronized by thymidine incubation for 24 h and released for 8 h. GFP-CtIP-wt and GFP-CtIP-K467A were expressed to similar degree, and expression of GFP-CtIP-wt or GFP-CtIP-K467A did not alter cell cycle progression as judged by flow cytometry (Supplementary Fig S5B). Cells were then irradiated with 10 Gy and imaged using fluorescence time-lapse microscopy. Representative stills are indicated for GFP and DIC images.

B Quantifications of time-lapse movies from (A). Averages and standard deviations of total nuclear GFP intensity are indicated from 12 movies for each cell line.

C In the same experiment as described in (A), numbers of GFP-CtIP foci per nucleus were counted and plotted as a percentage of GFP-CtIP foci at the start of imaging. Averages and standard deviations of 15 movies per cell line are indicated.

D U2OS Flp-In T-REx clones stably expressing doxycycline-inducible GFP-CtIP-wt, GFP-CtIP-T847A, and GFP-CtIP-K467A were transfected with siCtIP. At 24 h post-transfection, cells were cultivated in the absence or presence of doxycycline. At 48 h post-transfection, cells were mock-treated or harvested at the indicated time points following irradiation (10 Gy). Whole-cell lysates were immunoblotted using the indicated antibodies.

abolished RPA2 phosphorylation (Fig 7D) (Huertas & Jackson, 2009). These data suggest that CtIP–Cdh1 interaction is not required for DNA-end resection, but may control the proper timing of resection.

The CtIP–Cdh1 interaction facilitates homology-directed repair

The above findings prompted us to test whether CtIP–Cdh1 interaction plays a role in DSB repair. To this end, we analyzed the repair

of I-*Sce*I-induced DSBs in HEK293 cell lines containing two different reporters measuring HR (DR-GFP) and total NHEJ (EJ5-GFP). As shown previously, CtIP depletion interfered with HR, and led to a slight increase in total NHEJ (Fig 8A and B) (Bennardo *et al*, 2008). Importantly, these effects could be rescued by expression of siRNA-resistant FLAG-CtIP-wt (Fig 8A and B). Interestingly, expression of the K467A mutant did not rescue HR, but caused a similar decrease as compared to the DNA-end resection-defective T847A mutant (Fig 8A and B). Surprisingly, unlike T847A, we observed that expression of K467A does not lead to a significant increase in total NHEJ (Fig 8C). The observation that CtIP-K467A impaired homology-directed repair but does not result in compensation through NHEJ, suggested a dominant negative effect of the KEN box mutant. To test this hypothesis, FLAG-CtIP constructs were transfected into HEK293 DR-GFP cells without siRNA-mediated depletion of endogenous CtIP. Indeed, expression of CtIP-K467A caused a reduction in HR, whereas expression of CtIP-wt or CtIP-T847A did not significantly alter HR (Fig 8D). Taken together, these results suggest that abolishing the interaction between CtIP and Cdh1 does not interfere with the initiation of DNA-end resection, which would otherwise increase NHEJ efficiency. Instead, after resection has been initiated, the CtIP–Cdh1 interaction appears to be required for the proper execution of downstream HR events.

Defective HR was previously shown to result in increased sensitivity to PARP inhibition (Bryant *et al*, 2005; Farmer *et al*, 2005). In line with a defect in HR, we observed that cells inducibly expressing GFP-CtIP-K467A showed elevated sensitivity to the PARP inhibitor olaparib, although not as pronounced as in GFP-CtIP-T847A mutant cells (Fig 8E). Notably, depletion of Cdh1 also resulted in an elevated sensitivity to PARP inhibition (Fig 8E). However, GFP-CtIP-K467A-expressing cells did not display hypersensitivity to IR or doxorubicin treatment, indicating that the inability of Cdh1 to interact with CtIP cannot explain all phenotypic responses associated with Cdh1 loss in combination with DNA damage (Supplementary Fig S8A–C).

Besides decreased DNA-end resection capacity, also excessive or temporally unrestricted resection may potentially impair HR. Since we have observed that CtIP is targeted by the APC/C for proteasomal degradation after DNA damage in G_2, we monitored DNA-end resection in wt and K467A mutant cells that had been synchronized in G_2 prior to IR (Fig 8F and Supplementary Fig S8D). Clearly, expression of GFP-CtIP-K467A resulted in elevated levels of RPA2 phosphorylation at S4/S8, indicative of hyper-resection. This matched our earlier observation of elevated levels of RPA2 phosphorylation upon proTAME treatment in irradiated cells (Fig 6B). Remarkably, increased RPA2 phosphorylation in GFP-CtIP-K467A-expressing cells coincided with lower amounts of Rad51 being recruited to damaged chromatin (Fig 8F). Combined, these data suggest that CtIP–Cdh1 interaction is involved in limiting DSB resection, which probably allows correct assembly of Rad51–ssDNA nucleoprotein filaments, to facilitate HR.

Discussion

The response to DSBs is tightly regulated during the cell cycle. As a consequence, deregulated cell cycle control may lead to aberrant DSB repair and ensuing genomic instability. An example thereof is provided by the APC/C^{Cdh1} cell cycle regulator, as genetic inactivation of Cdh1 in either mouse embryonic fibroblasts or primary human cells has been shown to cause elevated levels of DNA damage and chromosomal instability. We could recapitulate these findings in Cdh1-depleted human cell lines of different origins. Moreover, we were able to extend these findings and demonstrate that depletion of Cdh1 results in hypersensitivity to DSB-inducing agents and negatively affects Rad51 IRIF formation. Concerning potential APC/C substrates responsible for these effects, Rhp54 (the fission yeast ortholog of Rad54) and Rad17 were shown to be degraded by the APC/C (Trickey *et al*, 2008; Zhang *et al*, 2010). However, when Rad54 was investigated in other species, no APC/C-dependent degradation was observed, and the degradation of Rad17 by the APC/C appeared to be UV-induced and appeared to control checkpoint duration rather than DNA repair. Finally, Cdh1 was reported to control the duration of the G_2 cell cycle arrest in response to DSBs by targeting Polo-like kinase 1 (Plk1) for proteolytic degradation (Wäsch & Engelbert, 2005; Bassermann *et al*, 2008; Engelbert *et al*, 2008). So far, it remained elusive, however, whether the APC/C^{Cdh1} also contributes to the regulation of DSB repair.

Using a proteomics analysis of mitotic exit combined with bioinformatics analysis of the presence of KEN and D-box motifs, we have identified a number of candidate APC/C^{Cdh1} substrates. Several of the putative Cdh1 targets play key roles in the regulation of DSB repair, including Rif1, MDC1, SMC5, and CtIP. Detailed *in silico* analysis of multiple protein sequences for the conservation of putative KEN and D-box motifs guided us to focus on CtIP as a previously unrecognized APC/C^{Cdh1} substrate. Human CtIP contains two conserved KEN box motifs, but only the second KEN box strongly matches the consensus sequence recently proposed by Barford and colleagues (He *et al*, 2013) and is required for Cdh1–CtIP interaction. In addition to being targeted by the APC/C^{Cdh1} for proteasomal degradation in G_1, we discovered that CtIP protein levels are controlled by the APC/C^{Cdh1} prior to mitotic entry in response to DSBs. Concerning the activation of the APC/C^{Cdh1} in response to DNA damage in G_2 cells, we noted that APC/C^{Cdh1} activation is achieved most efficiently after high levels of DNA damage. This implies that especially under conditions provoking high amounts of DNA damage, such as after chemotherapy or radiotherapy, the APC/C^{Cdh1} may acquire new functions, which under these circumstances may determine cell fate and genomic integrity.

Due to its crucial role in initiating DNA-end resection, CtIP is essential for homology-directed repair of DSBs (Sartori *et al*, 2007; Bennardo *et al*, 2008). DNA-end resection dictates the choice between HR and NHEJ and is thus proposed to be tightly regulated during the cell cycle (Ferretti *et al*, 2013). For instance, CtIP phosphorylation at T847 by cyclin-dependent kinases represents a key step toward the commencement of DNA-end resection and, consequently, a CtIP-T847A mutant abrogates HR (Huertas & Jackson, 2009). Here, we show that a CtIP KEN box mutant (K467A) compromises HR to a similar extent as the T847A mutant, indicating that the interaction between Cdh1 and CtIP facilitates HR. NHEJ requires only very limited DSB processing and is therefore not suitable for repairing DSBs which have undergone extensive resection. In other words, NHEJ can only compensate for HR in cells that are defective in DNA-end resection (Shibata *et al*, 2011). This is in line with our results showing that CtIP-T847A results in higher levels of NHEJ. In contrast, we find that CtIP-K467A does not lead to a concomitant

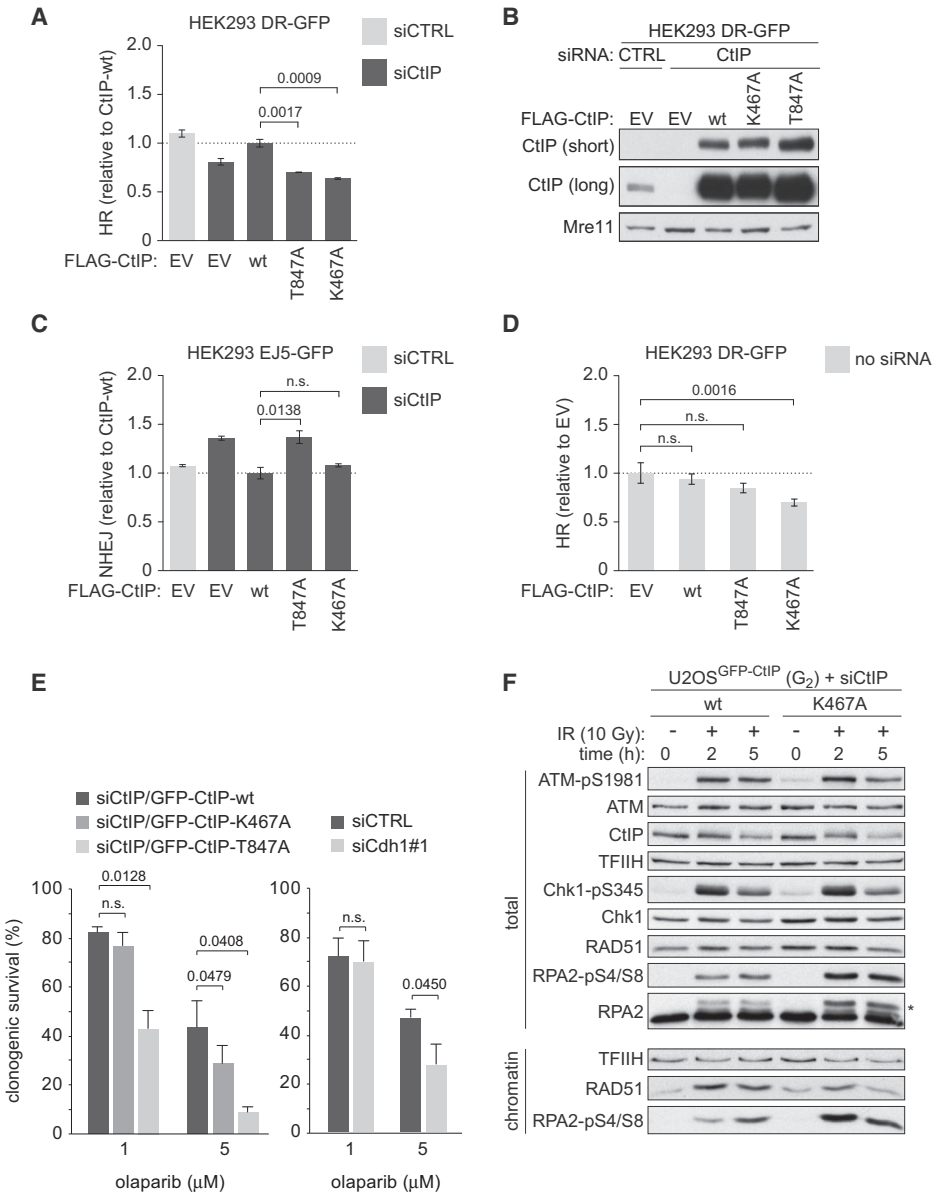

Figure 8. CtIP–Cdh1 interaction limits DNA-end resection and is required for homologous recombination repair.

A–D HEK293 cell lines stably harboring DNA repair reporters for HR (DR-GFP; A, B, and D), or NHEJ (EJ5-GFP; C) were transfected with control siRNA, or with CtIP siRNA in combination with the indicated siRNA-resistant FLAG-CtIP plasmids. After 24 h, cells were transfected with the I-*Sce*I-expression plasmid, and 48 h later, GFP positivity was assessed by flow cytometry. Averages and standard deviations of three independent experiments are indicated. In (B), representative Western blots for (A) are shown. Lysates were immunoblotted using anti-CtIP and anti-Mre11 antibodies. HEK293-DR-GFP cells (D) were co-transfected with the indicated siRNA-resistant FLAG-CtIP plasmids together with the I-*Sce*I-expression plasmid. 48 h later, GFP positivity was assessed by flow cytometry.

E U2OS-GFP-CtIP-wt, U2OS-GFP-CtIP-K467A, or U2OS-GFP-CtIP-T847A clones were transfected with siCtIP and were induced to express GFP-CtIP-wt, GFP-CtIP-K467, or GFP-CtIP-T847A at 24 h after transfection. Cells were replated for clonogenic survival 48 h after transfection and treated with the indicated olaparib concentrations. Alternatively, U2OS cells were transfected with siCdh1#1 and replated for clonogenic survival at 48 h after transfection in the presence of the indicated concentrations of olaparib. Standard error of the means of three experiments is shown. Statistical analysis was done using Student's *t*-tests (n.s. indicates not significant).

F U2OS Flp-In T-REx clones stably expressing doxycycline-inducible GFP-CtIP-wt, and GFP-CtIP-K467A were transfected with siCtIP, and protein expression was simultaneously induced by adding doxycycline. After 6 h, cells were synchronized using a single thymidine block for 18 h. Seven hours after release, cells enriched in S/G_2 phase (see Supplementary Fig S8D for cell cycle profiles) were mock-treated or harvested at the indicated time points following irradiation. RIPA whole-cell lysates or chromatin-enriched fractions were immunoblotted using the indicated antibodies.

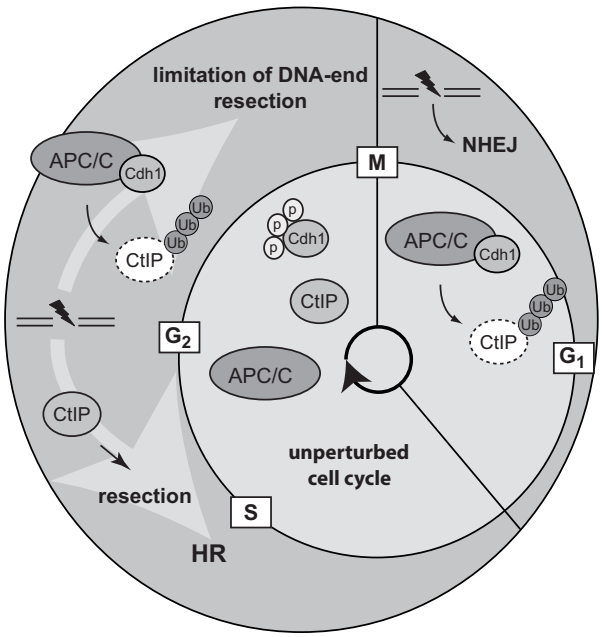

Figure 9. Model of cell cycle- and DNA damage-dependent regulation of CtIP by the APC/C^{Cdh1}.
The central area represents unperturbed cell cycle, when CtIP is degraded after mitotic exit by the APC/C^{Cdh1}. Cells in G_0/G_1 lack CDK activity, which precludes phosphorylation and consequent activation of CtIP. Post-mitotic CtIP degradation by the APC/C^{Cdh1} E3 ubiquitin ligase may contribute to prevent unscheduled DNA-end resection in G_0/G_1 phase. In response to DSBs in S/G_2 phase, CtIP promotes DNA-end resection to facilitate HR repair. In response to high levels of DSBs, CtIP is initially recruited to DSBs to resect DNA ends and promote HR repair. In a late response to high levels of DNA damage, the APC/C^{Cdh1} promotes ubiquitin-dependent proteolysis of CtIP. Downregulation of CtIP by the APC/C^{Cdh1} promotes its clearance from DSBs and prevents excessive DNA-end resection, a prerogative for proper homology-directed repair.

increase in NHEJ, suggesting that resection has occurred in those cells. In fact, CtIP-K467A-expressing cells irradiated in G_2 display even heightened levels of DNA-end resection compare to CtIP-wt cells, but are partially impaired in promoting efficient Rad51 recruitment to damaged chromatin, which is similar to what we observed in Cdh1-depleted cells. Moreover, reduced HR efficiency of K467A mutant cells is in line with our data of decreased survival upon PARP inhibition.

Combined, our data support a model in which APC/C^{Cdh1} activity is involved in negatively regulating the stability of CtIP both after mitotic exit in unperturbed cells and after DNA damage in G_2 (Fig 9). Moreover, we speculate that the APC/C^{Cdh1} is required at a late stage within the HR process, after initiation of resection has occurred and NHEJ is no longer an option for DSB repair. One possibility is that APC/C^{Cdh1} mediates clearance of CtIP IRIF through ubiquitin-mediated degradation, thereby limiting resection to amounts of ssDNA that can be handled by the downstream recombination machinery. A similar mechanism has been recently reported by Choi *et al* for the regulation of nuclear PTEN, in which Cdh1 promotes the removal of PTEN from chromatin during mitotic exit (Choi *et al*, 2014).

Our observations that Rad51 IRIF are decreased in Cdh1-depleted G_2 cells, that CtIP-K467 IRIF persist much longer, and that Rad51 loading onto damaged chromatin is compromised in G_2-enriched cells expressing the CtIP KEN box mutant are in line with a role for APC/C^{Cdh1}-dependent CtIP degradation in controlling HR. In its role of keeping DNA-end resection in check, the APC/C^{Cdh1} may play a similar function in G_1 and G_2. In response to DNA breaks in G_1 cells, the end resection machinery cannot be activated due to lack of CDK activity. In this context, APC/C^{Cdh1}-mediated degradation of CtIP may serve as a backup mechanism to prevent unscheduled end resection. In G_2 cells, on the other hand, end resection is required for error-free DSB repair by HR. Here, APC/C^{Cdh1}-mediated degradation of CtIP, after initial resection has been performed, may be required to limit end resection to levels that optimally facilitate HR repair.

Materials and Methods

Cell culture

hTERT-immortalized retinal pigment epithelium (RPE-1), U2OS, U2OS-FUCCI, and HEK293T cells were grown in DMEM (Gibco, Life Technologies). MCF7 cells were cultured in RPMI (Gibco, Life Technologies). HeLa cells were cultured in DMEM/Ham's F12 (1:1) medium (Gibco, Life Technologies). All culture media were supplemented with 10% fetal calf serum (FCS), 100 units/ml penicillin, and 100 μg/ml streptomycin. U2OS and HEK293 Flp-In T-REx cells were grown in DMEM supplemented with 10% Tet system approved FCS, 100 U/ml penicillin, 100 mg/ml streptomycin, 125 μg/ml hygromycin B, and 12.5 μg/ml blasticidin S.

IR was given using a CIS international/IBL 637 irradiator equipped with a cesium^{137} source (dose rate: 0.01083 Gy/s), or using a Faxitron X-ray device. For serum starvation experiments, RPE-1 cells were initially plated in medium containing 10% FCS and were washed with phosphate-buffered saline (PBS) at 24 h after plating and subsequently cultured without serum for another 24 h. After serum starvation, serum was added to a final concentration of 20%. At the time of serum addition, bromodeoxyuridine (BrdU) was added to a final concentration of 10 μM to measure replication onset. If indicated, cells were treated with 5 μM of the proteasome inhibitor MG-132 (Sigma-Aldrich, St. Louis, MO), 250 nM of the microtubule polymerization inhibitor nocodazole (Sigma-Aldrich), 5 μM of the Eg5 inhibitor *S*-trityl-L-cysteine (STLC, Sigma-Aldrich), 5 μM of the Cdk1 inhibitor RO-3306 (Axon Medchem, Groningen, the Netherlands), or with the APC/C inhibitor proTAME (Zeng *et al*, 2010) at a final concentration of 12 or 20 μM. ProTAME was kindly provided by Randy King, Harvard Medical School, Boston MA, or obtained from Boston Biochem.

Generation of stable GFP-CtIP cell lines

The Flp-In T-REx system (Invitrogen, Life Technologies) was used to generate cell lines stably expressing different siRNA-resistant GFP-CtIP constructs in an inducible manner. The GFP-CtIP-containing pcDNA5/FRT/TO vector and the Flp recombinase expression plasmid pOG44 were mixed in a 1:9 ratio and transfected into Flp-In T-REx 293 (Invitrogen, Life Technologies) and Flp-In T-REx U2OS (a kind gift of Daniel Durocher, University of Toronto) cells using

FuGENE 6 transfection reagent (Promega) at 60% confluency. After 6 h, medium was exchanged to fresh DMEM and cells were incubated at 30°C (6% CO_2). Two days later, cells were replated at different dilutions in 10-cm plates. After 24 h, the medium was supplemented with 250 μg/ml hygromycin B and 12.5 μg/ml blasticidin S. The medium was replaced every 2–3 days, and cells were selected for approximately 2 weeks. Resistant colonies were picked and further characterized as single clones or pooled to generate bulk cultures. All cell lines were screened for inducible GFP-CtIP expression by both immunofluorescence microscopy and immunoblotting. To induce expression of GFP-CtIP, cells were treated with 0.5 or 1 μg/ml doxycycline (Dox) for 24 h as indicated.

Immunoprecipitation and GST pull-down

For immunoprecipitation and glutathione S-transferase (GST) pull-down assays, cells were lysed in NP-40 extraction buffer (50 mM Tris–HCl, pH 7.5, 120 mM NaCl, 1 mM EDTA, 6 mM EGTA, 15 mM sodium pyrophosphate, 1% NP-40), supplemented with phosphatase inhibitors (20 mM NaF, 1 mM sodium orthovanadate) and protease inhibitors (1 mM benzamidine and 0.1 mM phenylmethylsulfonyl fluoride (PMSF)), and clarified by centrifugation at 20,000 *g*. HeLa nuclear extracts (HNE) were purchased from Ipracell (Belgium). Generation of the GST–CtIP constructs was described previously (Sartori *et al*, 2007). GST fusion plasmids were grown in BL21 RIL (CodonPlus) *Escherichia coli* (Stratagene), and recombinant proteins were expressed by incubating the bacteria for 24 h at 16°C after the addition of 100 μM IPTG. After centrifugation, the bacterial pellet was resuspended in cold PBS, supplemented with 1% Triton X-100 and protease inhibitors (1 mM PMSF, 1 mM benzamidine, and Roche protease inhibitor cocktail). After sonication and centrifugation, GST-tagged proteins were purified from soluble extracts using Glutathione Sepharose 4 Fast Flow beads (GE Healthcare). GST fusion proteins bound to glutathione beads were mixed with 1 mg of HeLa nuclear extract and incubated for 1 h at 4°C in 1 ml of TEN100 buffer (20 mM Tris–HCl (pH 7.4), 0.1 mM EDTA, and 100 mM NaCl). Beads were then washed three times with NTEN500 buffer (0.5% NP-40, 0.1 mM EDTA, 20 mM Tris–HCl (pH 7.4), and 500 mM NaCl) and once with TEN100 buffer. Recovered complexes were boiled in SDS sample buffer and analyzed by SDS–PAGE followed by immunoblotting.

Immunoprecipitating antibodies were added to the cell lysates and incubated overnight at 4°C. After 2 h incubation with protein A or protein G beads, precipitated immunocomplexes were washed four times with lysis buffer or three times with TNE buffer (50 mM Tris–HCl (pH 7.4), 100 mM NaCl, 0.1 mM EDTA) containing 1% Triton X-100 and once with TNE buffer, boiled in SDS sample buffer, and loaded on an SDS–polyacrylamide gel. Proteins were analyzed by immunoblotting as described below.

In vivo ubiquitylation assays

HEK293 Flp-In T-REx GFP-CtIP cells were transfected with His-ubiquitin using the FuGENE 6 transfection reagent (Promega), and after 24 h, GFP-CtIP expression was induced with 1 μg/ml Dox. After 24 h, cells were treated for 4 h with 20 μM MG-132 and then washed and scraped in 500 μl of ice-cold PBS. 2% of the cell suspension was used for direct Western blot analysis. The remaining cells were lysed in "buffer A" (6 M guanidine–HCl, 0.1 M Na_2HPO_4/NaH_2PO_4, pH 8.0, 10 mM imidazole), and lysates were incubated with Ni^{2+}-NTA agarose beads for 3 h under rotation at room temperature. The beads were washed two times with buffer A, two times with "buffer A/TI" (1 volume buffer A: 3 volume buffer "TI" (25 mM Tris–HCl, pH 6.8, and 20 mM imidazole)), and two times with buffer TI. Bound proteins were eluted by boiling the beads in 2× SDS sample buffer supplemented with 250 mM imidazole and analyzed by immunoblotting. In case of siRNA treatment, cells were first transfected with the indicated siRNA and after 24 h transfected with His-ubiquitin using the FuGENE6 transfection reagent (Promega). At the same time, GFP-CtIP expression was induced with 1 μg/ml Dox, and after 24 h, samples were processed as described above.

To analyze ubiquitylation of endogenous CtIP, HEK293 cells were transfected with HA-ubiquitin using the FuGENE 6 transfection reagent (Promega) and enriched in S/G_2 phase of the cell cycle by releasing them from a single thymidine block. After treatment, cells were lysed in (5 mM Tris–HCl (pH 7.5), 5 mM DTT, 1% SDS) and boiled for 5 min (El-Shemerly *et al*, 2005). After sonication, samples were clarified by centrifugation and diluted 4 times with NP-40 buffer supplemented with phosphatase inhibitors (20 mM NaF, 1 mM sodium orthovanadate), protease inhibitors (1 mM benzamidine and 0.1 mM phenylmethylsulfonyl fluoride (PMSF)), and the deubiquitinases inhibitor N-ethylmaleimide (NEM, 20 mM). Immunoprecipitation was performed overnight at 4°C, using a polyclonal rabbit antibody (612L, raised against CtIP N-terminus, a kind gift of Prof. Richard Baer, Columbia University). After 2 h incubation with protein A beads, precipitated immunocomplexes were washed three times with NTEN500 buffer and once with TEN100 buffer, boiled in SDS sample buffer, and loaded on an SDS–polyacrylamide gel. After transfer, membranes were incubated for 30 min at 4°C in denaturing buffer (6 M guanidine–HCl, 20 mM Tris–HCl (pH 7.5), 1 mM PMSF, and 5 μM β-mercaptoethanol) as described in Penengo *et al* (2006). After extensive washing with TBS-Tween buffer, membranes were incubated with the appropriate antibody and further processed as described below.

Immunoblotting

If not specified otherwise, cell extracts were prepared in Laemmli buffer (4% SDS, 20% glycerol, 120 mM Tris–HCl pH 6.8). If indicated, cells were lysed in RIPA buffer (50 mM Tris–HCl, pH 7.5, 1% NP-40, 0.25% sodium deoxycholate, 150 mM NaCl, 1 mM EDTA, and 0.1% SDS) supplemented with phosphatase and protease inhibitors. Proteins were resolved by SDS–PAGE and transferred to nitrocellulose. Immunoblots were performed using the appropriate antibodies, and proteins were visualized using the ECL detection system (Amersham). Primary antibodies used in this study are listed in Supplementary Table S2. The anti-Claspin antibody was a kind gift of Dr. Raimundo Freire, University of Tenerife) and was described previously (Semple *et al*, 2007).

When indicated, a Triton X-100-insoluble (chromatin-enriched) fraction was isolated as described in Peña-Diaz *et al* (2012). Briefly, cells were rinsed twice in cold PBS and incubated for 5 min on ice in pre-extraction buffer (25 mM HEPES (pH 7.9), 50 mM NaCl, 1 mM EDTA, 3 mM $MgCl_2$, 300 mM sucrose, 0.5% Triton X-100, and protease inhibitors). After buffer removal and rinsing in PBS,

adherent cellular material was harvested by scraping it into Laemmli buffer. The chromatin-enriched fraction was then heat denatured, sonicated, and analyzed by immunoblotting.

HR and NHEJ DNA repair assays

DSB repair efficiency by HR or NHEJ was measured in DR-GFP or EJ5-GFP HEK293 cell lines as described previously (Bennardo *et al*, 2008). Briefly, 0.6×10^6 cells were plated in 6-well plates (poly-L-lysine coated) and, after 24 h, cells were transfected with siRNA oligos (40 nM). The next day, 0.24×10^6 cells were reseeded in 12-well plates. At 48 h after siRNA transfection, cells were either mock-transfected or transfected with 0.6 μg I-*Sce*I expression plasmid (pCBASce) in combination with 0.2 μg of the appropriate FLAG-tagged CtIP constructs (pcDNA3) using 1.6 μl of JetPrime (Polyplus). At 4 h after plasmids transfection, media were replaced and a second transfection with siRNA oligos (15 nM) was performed. Alternatively, cells were only transfected with 0.6 μg I-*Sce*I expression plasmid (pCBASce) in combination with 0.2 μg of the appropriate FLAG-tagged CtIP constructs (pcDNA3) using 1.6 μl of JetPrime (Polyplus). At 48 h after I-*Sce*I transfection, cells were analyzed for GFP expression by flow cytometry on a CyAn ADP 9 (Dako).

Laser micro-irradiation

Laser micro-irradiation to generate DSBs in a defined nuclear region was performed as described previously (Lukas *et al*, 2003; Bekker-Jensen *et al*, 2006). Briefly, 24 h before irradiation, culture medium was supplemented with 10 μM BrdU. Around 100 cells were micro-irradiated at room temperature (a procedure lasting around 10 min) using the MMI CELLCUT system containing a UVA laser of 355 nm (Molecular Machines and Industries, Zurich, Switzerland). The laser intensity was set to 50% energy output, and each cell was generally exposed to the laser beam for < 300 ms (Meerang *et al*, 2011).

DNA plasmids and RNA interference

Plasmids were transfected by using either the standard calcium phosphate method or FuGENE 6 (Promega) according to manufacturer's instructions. The epitope-tagged expression vectors for human CtIP have been described previously (Yu *et al*, 2006; Sartori *et al*, 2007). The HA-tagged expression vector for human Cdh1 was described previously and was purchased from Addgene (plasmid #11596) (Pfleger *et al*, 2001). The pcDNA3.1-6×His-ubiquitin plasmid was a kind gift of Matthias Peter (ETH Zurich, Switzerland), whereas the HA-ubiquitin plasmid was described previously and purchased from Addgene (plasmid #18712) (Kamitani *et al*, 1997). All CtIP point mutants were introduced by site-directed mutagenesis using Expand Long Template PCR System (Roche) and confirmed by sequencing. shRNA interference for Cdh1 in RPE-1, MCF7, or HeLa cells was performed using lentiviral infection with control pLL3.7-GFP (targeting sequence: 5′-GGCATCAAGGTGAACTTCA-3′) or pLL3.7-Cdh1 (targeting sequence: 5′-GGATTAACGAGAATGA GAA-3′; provided by r, University of Freiburg, Germany) (Engelbert *et al*, 2008). To this end, HEK293T cells were transfected with the pLL3.7 plasmids along with the packaging plasmids pCMV-VSVG, pCMV-dR8.2 (provided by Robert Weinberg, MIT, Cambridge, MA), and pAdVAntage (Promega) in a 4:3:1:0.5 ratio. Virus-containing supernatant was harvested at 24 and 48 h after transfection, filtered through a 0.45-μM syringe filter, and used to infect target cells, which were subsequently selected with 1 μg/ml puromycin. Analysis of stable Cdh1-depleted cells was done at 5 days post-infection.

For transient siRNA experiments, RPE-1, MCF7, HeLa, or U2OS cells were plated in 6-well plates and transfected with the indicated amounts of siRNA oligos (40 nM final concentration of oligos) using Oligofectamine or Lipofectamine RNAiMAX using manufacturer's guidelines (Invitrogen, Life Technologies). In brief, medium was replaced with Opti-MEM (Gibco, Life Technologies) prior to incubation with siRNAs and Oligofectamine for 4 h. Thereafter, medium containing FCS (10% final concentration) was added and cells were analyzed at 48 or 72 h after transfection. siRNA oligos targeting Cdh1 #1 (5′-GGATTAACGAGAATGAGAAdTdT-3′), Cdh1 #2 (5′-AA TGAGAAGTCTCCCAGTCAGdTdT-3′), CtIP (5′-GCUAAACAGGAACG AAUCTTdTdT-3′) (Sartori *et al*, 2007), or luciferase (5′-CGUACGCG GAAUACUUCGAdTdT-3′) were purchased from Ambion (Life Technologies) or Microsynth (Balgach, Switzerland). In addition, "medium GC duplex" control siRNA (Cat. No: 12935-300) was purchased from Ambion (Life Technologies).

SILAC and mass spectrometry

For SILAC experiments, RPE-1 cells were cultured in ready-to-use light and heavy DMEM media, containing light or heavy arginine and lysine ("R0K0 DMEM" with $^{12}C_6$-L-arginine and $^{12}C_6$-L-lysine or "R10K8 DMEM" with $^{13}C_6$-L-arginine and $^{13}C_6$-L-lysine, respectively) and supplemented with dialyzed FBS. Media were obtained from Silantes (Munich, Germany). SILAC labeling was performed as previously described by Ong and Mann (Ong *et al*, 2002). Briefly, RPE-1 cells were cultured in normal media or complete heavy DMEM medium containing 10% dialyzed FBS for at least 10 cell doublings (5 passages) to allow full incorporation of both labeled amino acids within the proteome. Cells were subsequently treated with nocodazole for 16 h (250 ng/ml) and collected by mitotic shake-off. Cells were washed three times in pre-warmed PBS and replated in the absence of nocodazole. Immediately after replating or 2.5 h after replating, cells were harvested by trypsinization, snap-frozen in liquid nitrogen, and resuspended in lysis buffer (6 M urea and 2 M thio-urea). A label-swap replicate was also performed where SILAC states and harvesting conditions were reversed (Fig 3A). To determine protein concentration in lysates, 10 μl lysate was added to 150 μl of 660 nM protein assay reagent (Pierce). Equal amounts of protein from R0K0 and R10K8 were mixed, reduced with 1 mM DTT, and alkylated with 8 mM iodoacetamide. Proteins were separated on SDS–PAGE 4–12% gradient gels and visualized by staining by Coomassie staining. Gel lanes were divided into eight slices and proteins digested with an in-gel digestion protocol with trypsin. Peptides were desalted on C18 StageTips and loaded on a 10-cm-long 360 μm O.D. by 75 μm I.D. column packed with 3 μm ReproSil-Pur C18 AQ 3beads (Dr. Maisch, Germany) with an Agilent 1100 nano-flow pump and autosampler. A 60 min gradient from 3 to 35% acetonitrile containing 1% formic acid at 200 nl/min was applied to elute peptides for analysis in the LTQ-Orbitrap-Velos (Thermo, Bremen) in a Top5 CID data-dependent acquisition mode. Peptide identification and quantification was performed using MaxQuant v.1.1.1.14 with the IPI human database ver. 3.70 with

variable modifications of oxidized methionine and acetylated protein N-termini. Cysteines were carbamidomethylated. Peptide and protein FDR was set at 1%.

Flow cytometry

Cells were harvested at the indicated time points after treatment and fixed in ice-cold 70% ethanol. Cells were stained with rabbit anti-phospho-histone H3 antibody, mouse anti-MPM-2, and/or mouse anti-γ-H2AX (details of used antibodies are in Supplementary Table S2), subsequently stained with Alexa488-conjugated and Alexa647-conjugated secondary antibodies (Molecular Probes, 1:300), and counterstained with propidium iodide/RNase (Sigma). Samples were analyzed on a FACS-Calibur (Becton Dickinson) equipped with Cell Quest software. Per sample, a minimum of 10^4 events was analyzed and indicated results show averages and standard deviations of three independent experiments.

Immunofluorescence microscopy

MCF7, MEFs, or HeLa cells were cultured on glass coverslips and, if indicated, were irradiated at 24 h after plating. After treatment, cells were fixed in formaldehyde (3.7% in PBS) for 15 min at room temperature. After washing with PBS, cells were permeabilized with Triton X-100 (0.1% in PBS) for 5 min at room temperature. After extensive washing, cells were stained with mouse anti-Cdh1, mouse anti-p53 diluted in PBS, 0.05%Tween-20, 2.5%BSA for 16 h at 4°C. After extensive washing, cells were stained with Alexa488-, Alexa568-, or Alexa647-conjugated secondary antibodies for 30 min at room temperature and counterstained with DAPI. Images were obtained using a Leica DM6000B microscope, equipped with 63× immersion lens (PL-S-APO, numerical aperture: 1.30) and Xenon light source using LAS-AF software (Leica).

Alternatively, U2OS-FUCCI cells were grown on glass coverslips and, at different time points after treatment, fixed directly in 4% formaldehyde (w/v) in PBS for 15 min as described previously (Eid *et al*, 2010). After incubation with rabbit anti-Rad51 or rabbit anti-53BP1 and appropriate secondary antibodies the coverslips were mounted and sealed with Vectashield (Vector Laboratories) containing DAPI. Images were acquired on a Leica DMRB fluorescence microscope.

For live-cell microscopy, stable U2OS cells were plated in chambered coverglass 8-well plates (LabTek-II, Nunc). At 24 h before imaging, GFP-CtIP expression was induced by adding doxycycline to a final concentration of 1 μg/ml. GFP and DIC images were obtained every 5 min on a DeltaVision Elite microscope, equipped with a CoolSNAP HQ2 camera, 40× immersion objective (U-APO 340, numerical aperture: 1.35). In the Z-plane, 12 images were acquired at 0.5-μm interval, which were subsequently deconvolved using SoftWorx 5.5 software (Applied Precision). Nuclear fluorescence intensity was quantified using ImageJ software.

Clonogenic and short-term survival assays

HeLa or MCF7 cells were cultured in 6-well plates. One day after plating, cells were irradiated with 1, 2, or 4 Gy. When surviving colonies were approximately 50 cells in size, cells were fixed and stained using methanol/acidic acid/water in a 5:2:3 ratio, supplemented with 0.01% Coomassie brilliant blue. Surviving fractions were calculated using the plating efficiencies with non-irradiated conditions as a reference. Shown averages are from three experiments, with three replicates each. Alternatively, clonal U2OS cells expressing GFP-CtIP variants were transfected with siRNAs and, if indicated, were treated with doxycycline 24 h later to induce expression of GFP-CtIP. At 48 h after transfection, cells were trypsinized and replated in 6-well plates. During replating, indicated doses of doxorubicin or the PARP inhibitor olaparib (Axon Medchem, Groningen, the Netherlands) were added. To test whether Cdh1-depleted cells also are more sensitive to PARP inhibition, U2OS cells were transfected with siCdh1#1, and after 48 h, cells were replated in the presence of olaparib. Statistical testing was done using the Student's *t*-test.

For short-term survival assays, 2,000 cells were plated in 96-wells plates and treated at 24 h after plating. At 4 days after treatment initiation, 20 μl of 3-(4,5-dimethylthiazol-2-yl)-2,5-diphenyltetrazolium bromide (MTT) was added to the culture medium to a final concentration of 5 mg/ml for 3 h. Formazan crystals were dissolved in DMSO, and absorbance was analyzed at 520 nM using a Bio-Rad benchmark III microtiter spectrophotometer. Survival was calculated as a percentage of untreated cells.

Gene set enrichment analysis (GSEA) and destruction motif analysis

GSEA was performed with GSEA 2.0 (Broad Institute, Cambridge, MA) (Mootha *et al*, 2003; Subramanian *et al*, 2005). A significance threshold was set at a nominal *P*-value of 0.05 and a false discovery rate (FDR) of 0.30. In our analysis, we transformed protein names from SILAC MS analysis to HUGO gene symbols and tested enrichment in Kyoto Encyclopedia of Genes and Genomes (KEGG), Gene Map Annotator and Pathway Profiler (GenMAPP) (Dahlquist *et al*, 2002; Kanehisa *et al*, 2012), and the BioCarta database (http://www.biocarta.com). Within the set of identified proteins from the SILAC MS analysis, we used GPS-ARM (Liu *et al*, 2012) to identify proteins with a D-box or a KEN box using a threshold setting of "high" for D-boxes and "medium" for KEN boxes. Subsequently, GSEA was used to test for enrichment of KEN box or D-box containing proteins in the downregulated fraction. FDR rates of 0.25 were used in combination with 10,000 permutations. Conservation of KEN or D-boxes was done using Clustal Omega. In order to identify proteins related to the DNA damage response and DNA damage repair, a combined list of genes was compiled by merging the following Gene Ontology gene sets (see also Supplementary Table S1): GO:0006302 ("double-strand break repair); GO:0006974 ("cellular response to DNA damage stimulus"); GO:0000077 ("DNA damage checkpoint"); and GO:0000724 ("double-strand repair via homologous recombination"). In total, 255 genes were included in this combined gene set (Supplementary Table S1), which in Fig 3 is referred to as "DNA damage response".

Supplementary information for this article is available online: http://emboj.embopress.org

Acknowledgements

We thank Dr. Rudolf Fehrmann, Dr. Małgorzata Krajewska, and Anne Margriet Heijink for technical help and Dr. Floris Foijer for help with

live-cell microscopy. We are grateful to Dr. Jeremy Stark, Dr. Robert Weinberg, Dr. Ralph Waesch, Dr. Stefano Ferrari, Dr. Randy King, Dr. Richard Baer, Dr. Raimundo Freire, and Dr. Matthias Peter for providing reagents. We thank Chris Soon Heng Tan and Rob Wolthuis for helpful discussions. This research was supported by an NWO-VIDI grant (016.136.334) and Dutch Cancer Society grant (RUG-2011-5093) to M.A.T.M.v.V, an ERC Advanced Grant to E.G.E.d.V (ERC-2011-293445). Alessandro A. Sartori is supported by the Vontobel-Stiftung. Lorenzo Lafranchi is supported by grants of the Swiss National Science Foundation (31003A_135507 to A.A.S) and the Promedica Stiftung (to A.A.S).

Author contributions

LL and HRdB performed experiments, analyzed the data, and edited the manuscript. SEO performed mass spectrometry analyses. EGEdV edited the manuscript. AAS and MATMvV directed and supervised the studies, analyzed the data, and wrote the manuscript.

Conflict of interest

The authors declare that they have no conflict of interest.

References

Acilan C, Potter DM, Saunders WS (2007) DNA repair pathways involved in anaphase bridge formation. *Genes Chromosom Cancer* 46: 522 – 531

Aylon Y, Liefshitz B, Kupiec M (2004) The CDK regulates repair of double-strand breaks by homologous recombination during the cell cycle. *EMBO J* 23: 4868 – 4875

Ayoub N, Rajendra E, Su X, Jeyasekharan AD, Mahen R, Venkitaraman AR (2009) The carboxyl terminus of Brca2 links the disassembly of Rad51 complexes to mitotic entry. *Curr Biol* 19: 1075 – 1085

Bassermann F, Frescas D, Guardavaccaro D, Busino L, Peschiaroli A, Pagano M (2008) The Cdc14B-Cdh1-Plk1 axis controls the G2 DNA-damage-response checkpoint. *Cell* 134: 256 – 267

Bekker-Jensen S, Lukas C, Kitagawa R, Melander F, Kastan MB, Bartek J, Lukas J (2006) Spatial organization of the mammalian genome surveillance machinery in response to DNA strand breaks. *J Cell Biol* 173: 195 – 206

Bennardo N, Cheng A, Huang N, Stark JM (2008) Alternative-NHEJ is a mechanistically distinct pathway of mammalian chromosome break repair. *PLoS Genet* 4: e1000110

Bonneau AM, Sonenberg N (1987) Involvement of the 24-kDa cap-binding protein in regulation of protein synthesis in mitosis. *J Biol Chem* 262: 11134 – 11139

Bryant HE, Schultz N, Thomas HD, Parker KM, Flower D, Lopez E, Kyle S, Meuth M, Curtin NJ, Helleday T (2005) Specific killing of BRCA2-deficient tumours with inhibitors of poly(ADP-ribose) polymerase. *Nature* 434: 913 – 917

Chan K-L, North PS, Hickson ID (2007) BLM is required for faithful chromosome segregation and its localization defines a class of ultrafine anaphase bridges. *EMBO J* 26: 3397 – 3409

Chapman JR, Taylor MRG, Boulton SJ (2012) Playing the end game: DNA double-strand break repair pathway choice. *Mol Cell* 47: 497 – 510

Choi BH, Pagano M, Huang C, Dai W (2014) Cdh1, a substrate-recruiting component of anaphase-promoting complex/cyclosome (APC/C) ubiquitin E3 ligase, specifically interacts with phosphatase and tensin homolog (PTEN) and promotes its removal from chromatin. *J Biol Chem* 289: 17951 – 17959

Dahlquist KD, Salomonis N, Vranizan K, Lawlor SC, Conklin BR (2002) GenMAPP, a new tool for viewing and analyzing microarray data on biological pathways. *Nat Genet* 31: 19 – 20

Delgado-Esteban M, García-Higuera I, Maestre C, Moreno S, Almeida A (2013) APC/C-Cdh1 coordinates neurogenesis and cortical size during development. *Nat Commun* 4: 2879

Eguren M, Porlan E, Manchado E, García-Higuera I, Cañamero M, Fariñas I, Malumbres M (2013) The APC/C cofactor Cdh1 prevents replicative stress and p53-dependent cell death in neural progenitors. *Nat Commun* 4: 2880

Eguren M, Álvarez-Fernández M, García F, López-Contreras AJ, Fujimitsu K, Yaguchi H, Luque-García JL, Fernandez-Capetillo O, Muñoz J, Yamano H, Malumbres M (2014) A synthetic lethal interaction between APC/C and topoisomerase poisons uncovered by proteomic screens. *Cell Rep* 6: 670 – 683

Eid W, Steger M, El-Shemerly M, Ferretti LP, Peña-Diaz J, König C, Valtorta E, Sartori AA, Ferrari S (2010) DNA end resection by CtIP and exonuclease 1 prevents genomic instability. *EMBO Rep* 11: 962 – 968

El-Shemerly M, Janscak P, Hess D, Jiricny J, Ferrari S (2005) Degradation of human exonuclease 1b upon DNA synthesis inhibition. *Cancer Res* 65: 3604 – 3609

Emanuele MJ, Ciccia A, Elia AEH, Elledge SJ (2011) Proliferating cell nuclear antigen (PCNA)-associated KIAA0101/PAF15 protein is a cell cycle-regulated anaphase-promoting complex/cyclosome substrate. *Proc Natl Acad Sci USA* 108: 9845 – 9850

Engelbert D, Schnerch D, Baumgarten A, Wäsch R (2008) The ubiquitin ligase APC(Cdh1) is required to maintain genome integrity in primary human cells. *Oncogene* 27: 907 – 917

Esashi F, Christ N, Gannon J, Liu Y, Hunt T, Jasin M, West SC (2005) CDK-dependent phosphorylation of BRCA2 as a regulatory mechanism for recombinational repair. *Nature* 434: 598 – 604

Falck J, Forment JV, Coates J, Mistrik M, Lukas J, Bartek J, Jackson SP (2012) CDK targeting of NBS1 promotes DNA-end resection, replication restart and homologous recombination. *EMBO Rep* 13: 561 – 568

Farmer H, McCabe N, Lord CJ, Tutt ANJ, Johnson DA, Richardson TB, Santarosa M, Dillon KJ, Hickson I, Knights C, Martin NMB, Jackson SP, Smith GCM, Ashworth A (2005) Targeting the DNA repair defect in BRCA mutant cells as a therapeutic strategy. *Nature* 434: 917 – 921

Ferreira MG, Cooper JP (2004) Two modes of DNA double-strand break repair are reciprocally regulated through the fission yeast cell cycle. *Genes Dev* 18: 2249 – 2254

Ferretti LP, Lafranchi L, Sartori AA (2013) Controlling DNA-end resection: a new task for CDKs. *Front Genet* 4: 99

French JD, Dunn J, Smart CE, Manning N, Brown MA (2006) Disruption of BRCA1 function results in telomere lengthening and increased anaphase bridge formation in immortalized cell lines. *Genes Chromosom Cancer* 45: 277 – 289

García-Higuera I, Manchado E, Dubus P, Cañamero M, Méndez J, Moreno S, Malumbres M (2008) Genomic stability and tumour suppression by the APC/C cofactor Cdh1. *Nat Cell Biol* 10: 802 – 811

Gudas JM, Li T, Nguyen H, Jensen D, Rauscher FJ, Cowan KH (1996) Cell cycle regulation of BRCA1 messenger RNA in human breast epithelial cells. *Cell Growth Differ* 7: 717 – 723

He J, Chao WCH, Zhang Z, Yang J, Cronin N, Barford D (2013) Insights into degron recognition by APC/C coactivators from the structure of an Acm1-Cdh1 complex. *Mol Cell* 50: 649 – 660

Henderson KA, Kee K, Maleki S, Santini PA, Keeney S (2006) Cyclin-dependent kinase directly regulates initiation of meiotic recombination. *Cell* 125: 1321 – 1332

Huertas P, Jackson SP (2009) Human CtIP mediates cell cycle control of DNA end resection and double strand break repair. *J Biol Chem* 284: 9558 – 9565

Ira G, Pellicioli A, Balijja A, Wang X, Fiorani S, Carotenuto W, Liberi G, Bressan D, Wan L, Hollingsworth NM, Haber JE, Foiani M (2004) DNA end resection, homologous recombination and DNA damage checkpoint activation require CDK1. *Nature* 431: 1011 – 1017

Jackson SP, Bartek J (2009) The DNA-damage response in human biology and disease. *Nature* 461: 1071 – 1078

Jazayeri A, Falck J, Lukas C, Bartek J, Smith GCM, Lukas J, Jackson SP (2006) ATM- and cell cycle-dependent regulation of ATR in response to DNA double-strand breaks. *Nat Cell Biol* 8: 37 – 45

Johnson N, Li Y-C, Walton ZE, Cheng KA, Li D, Rodig SJ, Moreau LA, Unitt C, Bronson RT, Thomas HD, Newell DR, D'Andrea AD, Curtin NJ, Wong K-K, Shapiro GI (2011) Compromised CDK1 activity sensitizes BRCA-proficient cancers to PARP inhibition. *Nat Med* 17: 875 – 882

Kaidi A, Weinert BT, Choudhary C, Jackson SP (2010) Human SIRT6 promotes DNA end resection through CtIP deacetylation. *Science* 329: 1348 – 1353

Kamitani T, Kito K, Nguyen HP, Yeh ET (1997) Characterization of NEDD8, a developmentally down-regulated ubiquitin-like protein. *J Biol Chem* 272: 28557 – 28562

Kanehisa M, Goto S, Sato Y, Furumichi M, Tanabe M (2012) KEGG for integration and interpretation of large-scale molecular data sets. *Nucleic Acids Res* 40: D109 – D114

Kousholt AN, Fugger K, Hoffmann S, Larsen BD, Menzel T, Sartori AA, Sørensen CS (2012) CtIP-dependent DNA resection is required for DNA damage checkpoint maintenance but not initiation. *J Cell Biol* 197: 869 – 876

Kramer ER, Scheuringer N, Podtelejnikov AV, Mann M, Peters JM (2000) Mitotic regulation of the APC activator proteins CDC20 and CDH1. *Mol Biol Cell* 11: 1555 – 1569

Kumar R, Cheok CF (2014) RIF1: a novel regulatory factor for DNA replication and DNA damage response signaling. *DNA Repair* 15: 54 – 59

Laulier C, Cheng A, Stark JM (2011) The relative efficiency of homology-directed repair has distinct effects on proper anaphase chromosome separation. *Nucleic Acids Res* 39: 5935 – 5944

Lieber MR (2010) The mechanism of double-strand DNA break repair by the nonhomologous DNA end-joining pathway. *Annu Rev Biochem* 79: 181 – 211

Lindon C, Pines J (2004) Ordered proteolysis in anaphase inactivates Plk1 to contribute to proper mitotic exit in human cells. *J Cell Biol* 164: 233 – 241

Littlepage LE, Ruderman JV (2002) Identification of a new APC/C recognition domain, the A box, which is required for the Cdh1-dependent destruction of the kinase Aurora-A during mitotic exit. *Genes Dev* 16: 2274 – 2285

Liu Z, Yuan F, Ren J, Cao J, Zhou Y, Yang Q, Xue Y (2012) GPS-ARM: computational analysis of the APC/C recognition motif by predicting D-boxes and KEN-boxes. *PLoS ONE* 7: e34370

Lukas C, Sørensen CS, Kramer E, Santoni-Rugiu E, Lindeneg C, Peters JM, Bartek J, Lukas J (1999) Accumulation of cyclin B1 requires E2F and cyclin-A-dependent rearrangement of the anaphase-promoting complex. *Nature* 401: 815 – 818

Lukas C, Falck J, Bartkova J, Bartek J, Lukas J (2003) Distinct spatiotemporal dynamics of mammalian checkpoint regulators induced by DNA damage. *Nat Cell Biol* 5: 255 – 260

Meerang M, Ritz D, Paliwal S, Garajova Z, Bosshard M, Mailand N, Janscak P, Hübscher U, Meyer H, Ramadan K (2011) The ubiquitin-selective segregase VCP/p97 orchestrates the response to DNA double-strand breaks. *Nat Cell Biol* 13: 1376 – 1382

Miller JJ, Summers MK, Hansen DV, Nachury MV, Lehman NL, Loktev A, Jackson PK (2006) Emi1 stably binds and inhibits the anaphase-promoting complex/cyclosome as a pseudosubstrate inhibitor. *Genes Dev* 20: 2410 – 2420

Mocciaro A, Berdougo E, Zeng K, Black E, Vagnarelli P, Earnshaw W, Gillespie D, Jallepalli P, Schiebel E (2010) Vertebrate cells genetically deficient for Cdc14A or Cdc14B retain DNA damage checkpoint proficiency but are impaired in DNA repair. *J Cell Biol* 189: 631 – 639

Mootha VK, Lepage P, Miller K, Bunkenborg J, Reich M, Hjerrild M, Delmonte T, Villeneuve A, Sladek R, Xu F, Mitchell GA, Morin C, Mann M, Hudson TJ, Robinson B, Rioux JD, Lander ES (2003) Identification of a gene causing human cytochrome c oxidase deficiency by integrative genomics. *Proc Natl Acad Sci USA* 100: 605 – 610

Nguyen HG, Chinnappan D, Urano T, Ravid K (2005) Mechanism of Aurora-B degradation and its dependency on intact KEN and A-boxes: identification of an aneuploidy-promoting property. *Mol Cell Biol* 25: 4977 – 4992

Ong S-E, Blagoev B, Kratchmarova I, Kristensen DB, Steen H, Pandey A, Mann M (2002) Stable isotope labeling by amino acids in cell culture, SILAC, as a simple and accurate approach to expression proteomics. *Mol Cell Proteomics* 1: 376 – 386

Peña-Diaz J, Bregenhorn S, Ghodgaonkar M, Follonier C, Artola-Borán M, Castor D, Lopes M, Sartori AA, Jiricny J (2012) Noncanonical mismatch repair as a source of genomic instability in human cells. *Mol Cell* 47: 669 – 680

Penengo L, Mapelli M, Murachelli AG, Confalonieri S, Magri L, Musacchio A, Di Fiore PP, Polo S, Schneider TR (2006) Crystal structure of the ubiquitin binding domains of rabex-5 reveals two modes of interaction with ubiquitin. *Cell* 124: 1183 – 1195

Pesin JA, Orr-Weaver TL (2008) Regulation of APC/C activators in mitosis and meiosis. *Annu Rev Cell Dev Biol* 24: 475 – 499

Peters J-M (2006) The anaphase promoting complex/cyclosome: a machine designed to destroy. *Nat Rev Mol Cell Biol* 7: 644 – 656

Pfleger CM, Kirschner MW (2000) The KEN box: an APC recognition signal distinct from the D box targeted by Cdh1. *Genes Dev* 14: 655 – 665

Pfleger CM, Lee E, Kirschner MW (2001) Substrate recognition by the Cdc20 and Cdh1 components of the anaphase-promoting complex. *Genes Dev* 15: 2396 – 2407

Pines J (2011) Cubism and the cell cycle: the many faces of the APC/C. *Nat Rev Mol Cell Biol* 12: 427 – 438

Prescott DM, Bender MA (1963) Autoradiographic study of chromatid distribution of labeled DNA in two types of mammalian cells *in vitro*. *Exp Cell Res* 29: 430 – 442

Rape M, Kirschner MW (2004) Autonomous regulation of the anaphase-promoting complex couples mitosis to S-phase entry. *Nature* 432: 588 – 595

Sakaue-Sawano A, Kurokawa H, Morimura T, Hanyu A, Hama H, Osawa H, Kashiwagi S, Fukami K, Miyata T, Miyoshi H, Imamura T, Ogawa M, Masai H, Miyawaki A (2008) Visualizing spatiotemporal dynamics of multicellular cell-cycle progression. *Cell* 132: 487 – 498

Sartori AA, Lukas C, Coates J, Mistrik M, Fu S, Bartek J, Baer R, Lukas J, Jackson SP (2007) Human CtIP promotes DNA end resection. *Nature* 450: 509 – 514

Semple JI, Smits VAJ, Fernaud J-R, Mamely I, Freire R (2007) Cleavage and degradation of Claspin during apoptosis by caspases and the proteasome. *Cell Death Differ* 14: 1433 – 1442

Shibata A, Conrad S, Birraux J, Geuting V, Barton O, Ismail A, Kakarougkas A, Meek K, Taucher-Scholz G, Löbrich M, Jeggo PA (2011) Factors determining DNA double-strand break repair pathway choice in G2 phase. *EMBO J* 30: 1079 – 1092

Sigl R, Wandke C, Rauch V, Kirk J, Hunt T, Geley S (2009) Loss of the mammalian APC/C activator FZR1 shortens G1 and lengthens S phase but has little effect on exit from mitosis. *J Cell Sci* 122: 4208 – 4217

Sonoda E, Hochegger H, Saberi A, Taniguchi Y, Takeda S (2006) Differential usage of non-homologous end-joining and homologous recombination in double strand break repair. *DNA Repair* 5: 1021 – 1029

Steger M, Murina O, Hühn D, Ferretti LP, Walser R, Hänggi K, Lafranchi L, Neugebauer C, Paliwal S, Janscak P, Gerrits B, Del Sal G, Zerbe O, Sartori AA (2013) Prolyl isomerase PIN1 regulates DNA double-strand break repair by counteracting DNA end resection. *Mol Cell* 50: 333 – 343

Stewart S, Fang G (2005) Destruction box-dependent degradation of aurora B is mediated by the anaphase-promoting complex/cyclosome and Cdh1. *Cancer Res* 65: 8730 – 8735

Subramanian A, Tamayo P, Mootha VK, Mukherjee S, Ebert BL, Gillette MA, Paulovich A, Pomeroy SL, Golub TR, Lander ES, Mesirov JP (2005) Gene set enrichment analysis: a knowledge-based approach for interpreting genome-wide expression profiles. *Proc Natl Acad Sci USA* 102: 15545 – 15550

Sudo T, Ota Y, Kotani S, Nakao M, Takami Y, Takeda S, Saya H (2001) Activation of Cdh1-dependent APC is required for G1 cell cycle arrest and DNA damage-induced G2 checkpoint in vertebrate cells. *EMBO J* 20: 6499 – 6508

Taguchi SI, Honda K, Sugiura K, Yamaguchi A, Furukawa K, Urano T (2002) Degradation of human Aurora-A protein kinase is mediated by hCdh1. *FEBS Lett* 519: 59 – 65

Trickey M, Grimaldi M, Yamano H (2008) The anaphase-promoting complex/cyclosome controls repair and recombination by ubiquitylating Rhp54 in fission yeast. *Mol Cell Biol* 28: 3905 – 3916

van Vugt MATM, Bràs A, Medema RH (2004) Polo-like kinase-1 controls recovery from a G2 DNA damage-induced arrest in mammalian cells. *Mol Cell* 15: 799 – 811

Wäsch R, Engelbert D (2005) Anaphase-promoting complex-dependent proteolysis of cell cycle regulators and genomic instability of cancer cells. *Oncogene* 24: 1 – 10

White DE, Negorev D, Peng H, Ivanov AV, Maul GG, Rauscher FJ (2006) KAP1, a novel substrate for PIKK family members, colocalizes with numerous damage response factors at DNA lesions. *Cancer Res* 66: 11594 – 11599

Wiebusch L, Hagemeier C (2010) p53- and p21-dependent premature APC/C-Cdh1 activation in G2 is part of the long-term response to genotoxic stress. *Oncogene* 29: 3477 – 3489

Yamamoto A, Taki T, Yagi H, Habu T, Yoshida K, Yoshimura Y, Yamamoto K, Matsushiro A, Nishimune Y, Morita T (1996) Cell cycle-dependent expression of the mouse Rad51 gene in proliferating cells. *Mol Gen Genet* 251: 1 – 12

Yu X, Fu S, Lai M, Baer R, Chen J (2006) BRCA1 ubiquitinates its phosphorylation-dependent binding partner CtIP. *Genes Dev* 20: 1721 – 1726

Zeng X, Sigoillot F, Gaur S, Choi S, Pfaff KL, Oh D-C, Hathaway N, Dimova N, Cuny GD, King RW (2010) Pharmacologic inhibition of the anaphase-promoting complex induces a spindle checkpoint-dependent mitotic arrest in the absence of spindle damage. *Cancer Cell* 18: 382 – 395

Zhang L, Park C-H, Wu J, Kim H, Liu W, Fujita T, Balasubramani M, Schreiber EM, Wang X-F, Wan Y (2010) Proteolysis of Rad17 by Cdh1/APC regulates checkpoint termination and recovery from genotoxic stress. *EMBO J* 29: 1726 – 1737

Ziv Y, Bielopolski D, Galanty Y, Lukas C, Taya Y, Schultz DC, Lukas J, Bekker-Jensen S, Bartek J, Shiloh Y (2006) Chromatin relaxation in response to DNA double-strand breaks is modulated by a novel ATM- and KAP-1 dependent pathway. *Nat Cell Biol* 8: 870 – 876

Legends to Supplementary Figures:

Supplementary Figure S1:

MCF-7 cells were infected with pLL-GFP or pLL-Cdh1 and selected with puromycin. Cells were grown on glass coverslips, fixed with 3.7% formaldehyde in PBS and stained with anti-p53 and DAPI. Ten microscopic fields were counted for p53 positivity. Averages and standard deviations of 10 fields of cells are indicated.

Supplementary Figure S2:

A. Schematic representation of the FUCCI system, which was used in the experiments depicted in Figures 2C and 2D. In these cells, fragments of geminin and Cdt1 are tagged with fluorescent reporters, which allow the discrimination of G_1 and S/G_2 cells. **B/C.** U2OS-FUCCI cells treated as described in Figure 2C were prepared for Rad51 (panel B) and 53BP1 (panel C) immunofluorescence. Shown are representative images of the different time-points. Scale bars correspond to 20 μm.

Supplementary Figure S3:

A. Indicated are established substrates of the APC/C^{Cdh1} that were identified in our mass spectrometry analysis. Log2-transformed ratios between t=2.5 and t=0 hours after release from nocodazole-mediated mitotic arrest are indicated. Literature references to these APC/C^{Cdh1} are provided in Table S3.

B. Proteins that were downregulated at least 1.0 (log2-transformed SILAC ratios) and were part of the 'DNA Damage response' (see Supplementary Table S2), were queried for the presence of KEN or D-box destruction motifs. To this end, GPS-ARM software (Liu *et al*, 2012) was used to identify D-boxes and KEN boxes. Open orange squares represent any D-box, whereas filled orange squares represent an optimal D-box. Likewise, open green squares represent any KEN box, whereas filled green squares represent optimal KEN box motifs. Subsequently, protein sequences from orthologs from indicated species were aligned using Clustal Omega (www.ebi.ac.uk/Tools/msa/clustalo/) using default settings. Boxes indicate evolutionary conserved destruction motifs. Grey filled boxes indicated evolutionary conservation of an optimal destruction motif. Numbers above destruction motifs indicate the amino acid location of the start position of the destruction motif in the human sequence.

Supplementary Figure S4:

A. RPE-1 cells were treated for 18 hours with *S*-Trityl-L-Cysteine (STLC, 5 μM) and mitotic cells were collected by shake-off. Mitotic cells were subsequently washed with warm culture medium and subsequently replated. Total cell lysates were immunoblotted with anti-CtIP, anti-Plk1 and anti-Actin. In parallel to obtaining total cell lysates, cells were fixed in ethanol and stained for the mitotic marker MPM-2. Representative plots are shown. **B.** HeLa cells were left untreated (asynchronous, "AS") or were treated with nocodazole (75 ng/ml) for 14 hours. Subsequently, cells were lysed in RIPA buffer, containing 0.1% SDS; PMSF and benzamidine. Next, the samples of asynchronous or nocodazole-treated cells were incubated for 30 minutes in the absence or presence of λ-phosphatase ("λ-PPase"). Control samples treated with a combination of λ-PPase and inhibitors (50 mM EDTA and 10 mM sodium orthovanadate) were included. **C.** U2OS cells were transfected with indicated siRNAs and total cell lysates were made at 48 hours after transfection. Western blotting was performed with indicated antibodies. In parallel, cells were fixed in ethanol, stained with PI/RNAse and subsequently analyzed by flow cytometry. **D.** RPE-1 cells were treated as described for Figure 4D. In parallel to making total cell lysates for Western blotting, cells were fixed in ethanol and stained for anti-phospho-HistoneH3/Alexa-488 in combination with PI/RNAse. Representative DNA profiles and phospho-

Histone-H3 plots are shown. Numbers indicate averages and standard deviations of phospho-Histone-H3 content from three independent experiments. **E.** RPE-1 cells were treated as for Figure 4F. In parallel to obtaining total cell lysates, cells were fixed in ethanol and stained for phospho-Histone-H3. Representative plots are shown.

Supplementary Figure S5:

A. HEK293 Flp-In T-REx cells were induced to express GFP-CtIP-wt or GFP-CtIP-K467A using doxycycline. Cell lysates were used for Cdh1 immunoprecipitations. Total cell lysates ('input') and Cdh1 immunoprecipitations ('anti-Cdh1 IP') were immunoblotted for indicted proteins. **B.** Polyclonal U2OS Flp-In T-REx cells were induced to express GFP-CtIP-wt (upper panels) or GFP-CtIP-KA (middle panels) using doxycycline for 24 hours. Subsequently, cells were synchronized using a single thymidine block. After release from the thymidine treatment, cells were treated with nocodazole (250 ng/ml) and at indicated time points, cells were harvested, fixed in ethanol and stained for the mitotic marker MPM-2. Lower panels: Cells were treated as for upper and middle panels. At the moment of thymidine wash-out, cells were fixed in ethanol and levels of GFP-CtIP-wt or GFP-CtIP-KA were assessed using flow cytometry. Black lines indicate untreated cells, green lines indicate doxycycline-treated cells.

Supplementary Figure S6:

A. U2OS cells were synchronized for 18 hours using thymidine (2 mM). Cells were then released from the S-phase block to allow progression towards G_2. At 7 hours post-release, cells were treated with doxorubicin ('dox', 0.5 μM) for 1 hour. Subsequently, fresh (dox-free) medium was added, and cells were left untreated or were treated with proTAME ('PT', 20 μM) for 5 hours. At indicated time points, cells were fixed and analyzed for cell cycle distribution. **B.** Same cells as in panel A were lysed in RIPA buffer at indicated time points. Whole cell extracts were analyzed by immunoblotting with indicated antibodies. ('short') and ('long') depict short and long exposures of the same membrane, respectively. '*' indicate phosphorylated species of proteins. **C.** U2OS Flp-In T-REx cells were induced to express GFP-CtIP-wt using doxycycline (1μg/ml) for 24 hours. Subsequently, cells were synchronized using a single thymidine block. At 8 hours after release, cells were treated with DMSO or

proTAME (12 μM), subsequently irradiated with 10 Gy, and imaged using fluorescence time-lapse microscopy. Representative stills of GFP and DIC movies are indicated.

Supplementary Figure S7:

A. Polyclonal U2OS Flp-In T-REx cells were induced to express GFP-CtIP-wt or GFP-CtIP-K467A using doxycycline. Lysates were immunoblotted using anti-CtIP and anti-TFIIH. In parallel**,** U2OS Flp-In T-REx cells were induced to express GFP-CtIP-wt or GFP-CtIP-K467A and subsequently micro-irradiated. Cells were then fixed and stained for γ-H2AX to visualize laser-induced DNA damage. **B.** Monoclonal U2OS-GFP-CtIP-wt were transfected with CtIP siRNA, and if indicated, cells were induced to express GFP-CtIP-wt using doxycycline (0.5 μg/ml). Cells were irradiated with 10 Gy and harvested after 1 or 4 hours. Total cell lysates were immunoblotted with indicated antibodies. '*' indicates phosphorylated species of proteins. **C.** Monoclonal U2OS-GFP-CtIP-wt or U2OS-GFP-CtIP-K467A cells were transfected with indicated siRNA. If indicated, cells were induced to express GFP-CtIP-wt or GFP-CtIP-K467A using doxycycline (0.5 μg/ml and 1 μg/ml respectively). 24 hours after transfection. At 48 hours after transfection, cells were harvested, and total cell lysates were immunoblotted for CtIP and Actin. 'Short ex' indicates short exposure and 'long ex' indicates long exposure. In parallel, cells were irradiated (2 Gy) at 48 hours after transfection, and nocodazole was added 1.5 hours after irradiation to trap cells in mitosis. Samples were fixed in ethanol at 4 hours and 8 hours after irradiation, stained with the mitotic marker MPM-2 in combination with propidium iodide/RNAse treatment and subsequently analyzed by flow cytometry. Percentages of mitotic cells are indicated. Averages and standard deviations of three experiments are indicated. **D.** U2OS cells were transfected with siCTRL or siCdh1 and treated as for panel C. Lysates were blotted using anti-Cdh1 and anti-Actin.

Supplementary Figure S8:

A-C. Monoclonal U2OS-GFP-CtIP-wt, U2OS-GFP-CtIP-K467A and U2OS-GFP-CtIP-T847A cells were transfected with siCtIP and were induced to express GFP-CtIP-wt (0.5 μg/ml doxycycline), GFP-CtIP-K467 or GFP-CtIP-T847A (1 μg/ml

Supplementary Figure S1

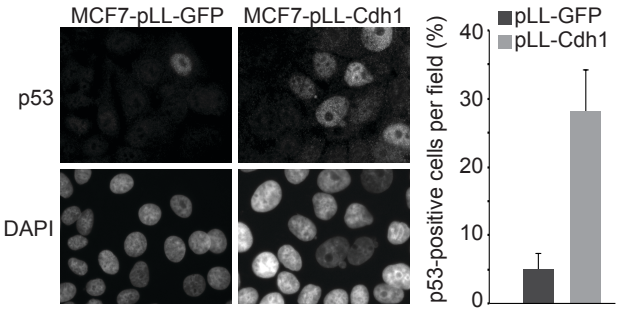

Supplementary Figure S2

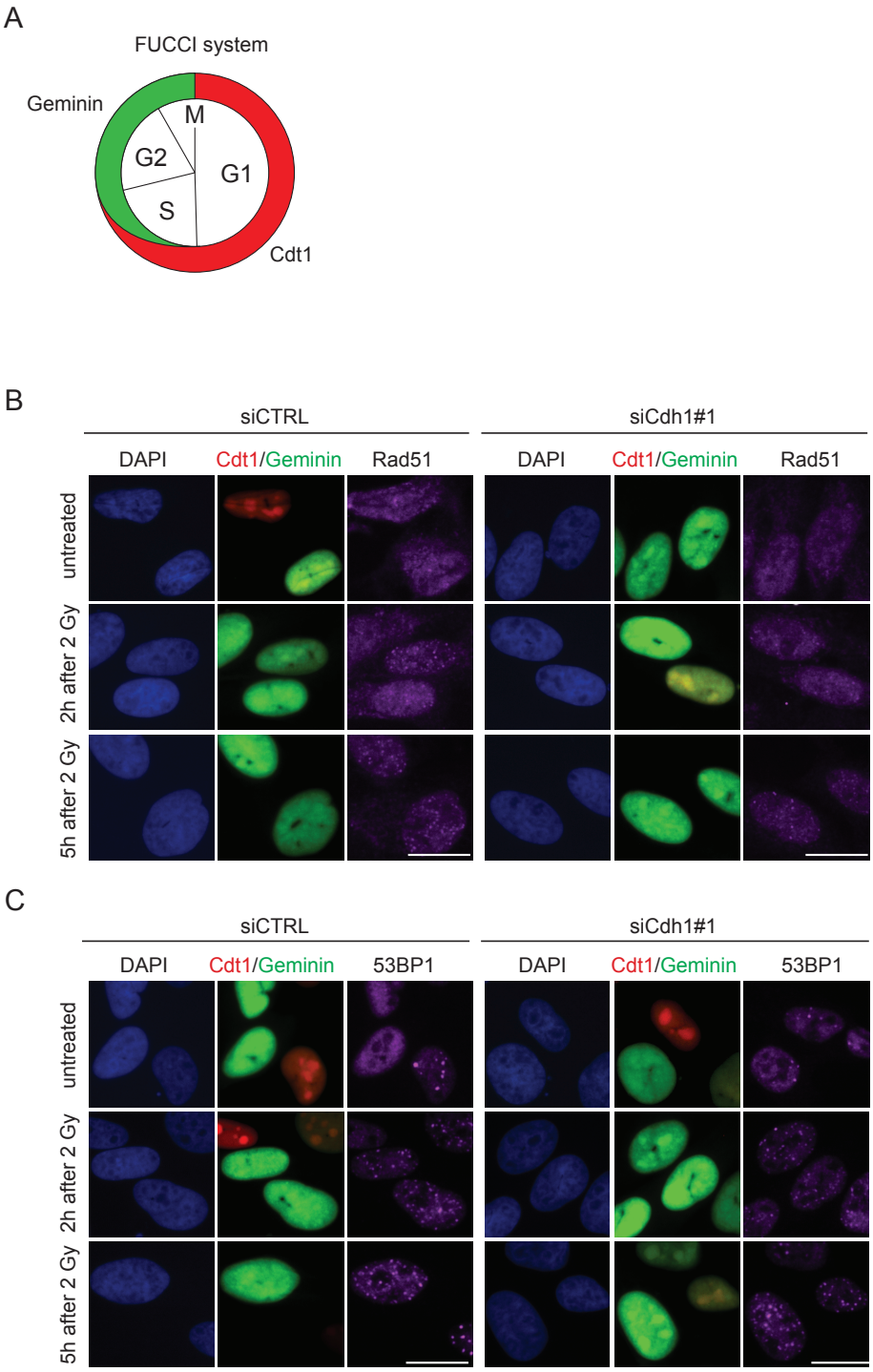

Supplementary Figure S3

A

known APC/C substrate	Gene symbol	log2
P15-PAF	KIAA0101	-3.71
CKAP2	CKAP2	-3.36
KIFC1	KIFC1/HSET	-2.74
Aurora kinase A	AURKA	-2.57
Cyclin B	CCNB	-2.31
Cenp-F	CENPF	-2.29
ECT2	ECT2	-1.88
Thymidine kinase	TK1	-1.57
UbcH10	UBCH10	-1.49
Anillin	ANLN	-1.46
Kif11/Eg5	KIF11	-1.39
Aurora kinase B	AURKB	-1.37
Bub1	BUB1	-1.25
Polo-like kinase-1	PLK	-1.08
KIF2C/MCAK	KIF2C	-0.98
GTSE-1	GTSE1	-0.84
NDC80/Hec1	NDC80	-0.05
Thymidylate kinase	DTYMP	-0.02

B

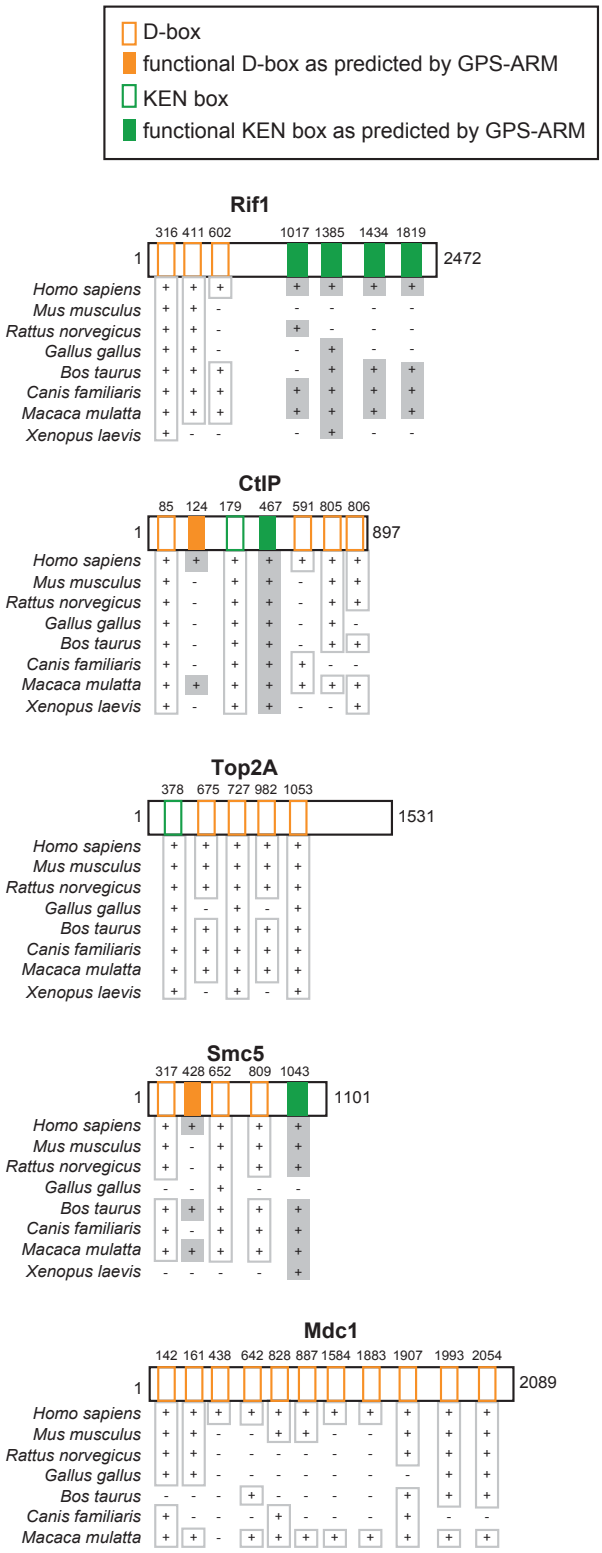

Supplementary Figure S4

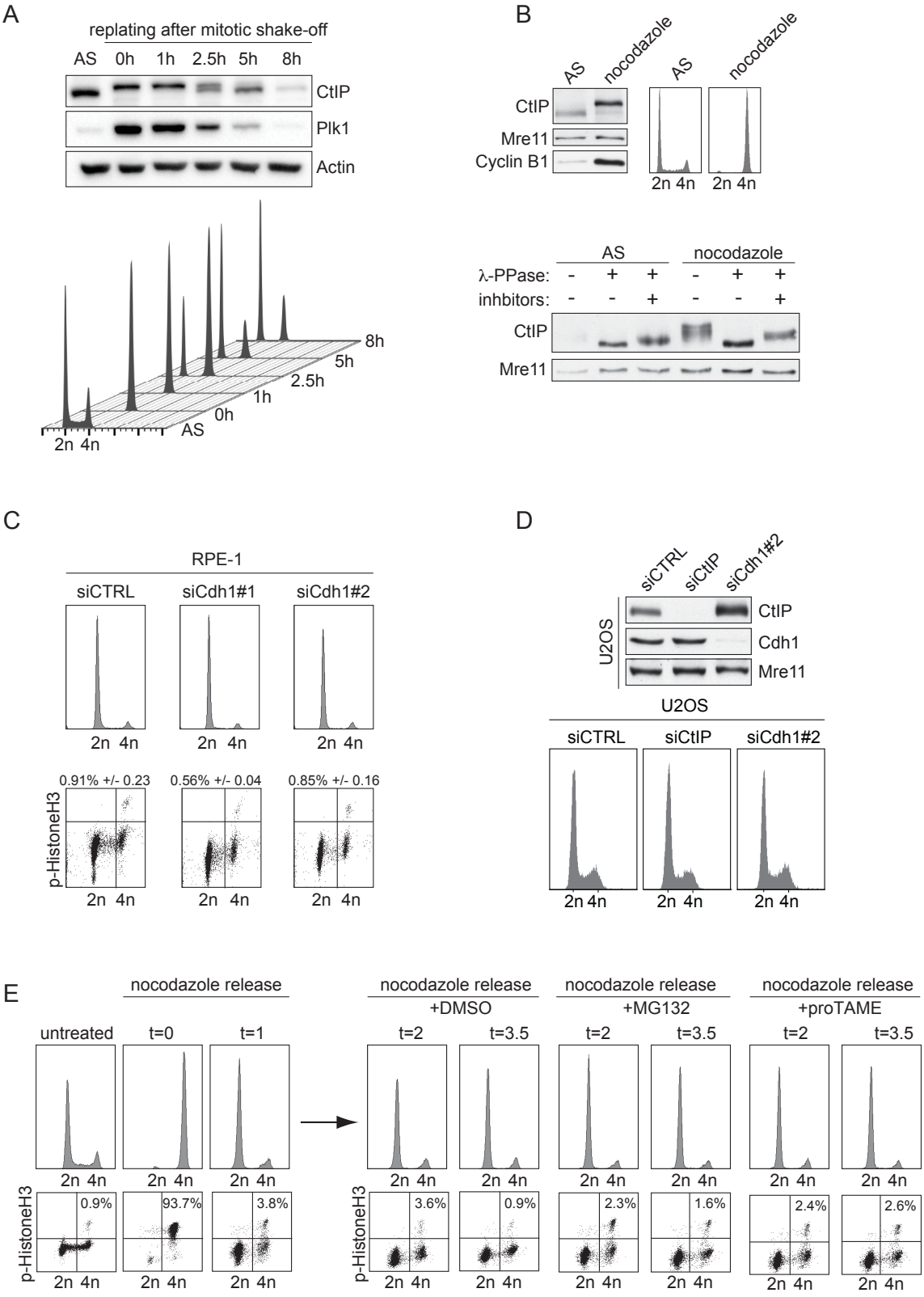

Supplementary Figure S5

A

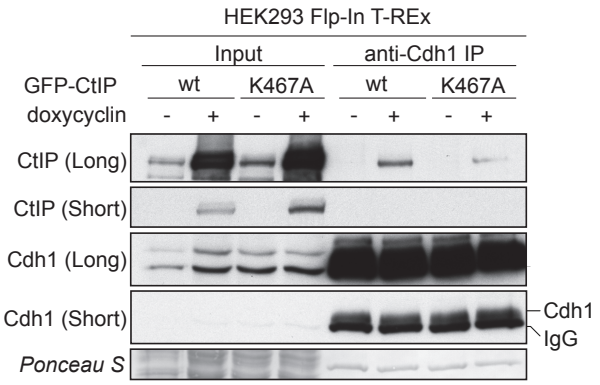

B

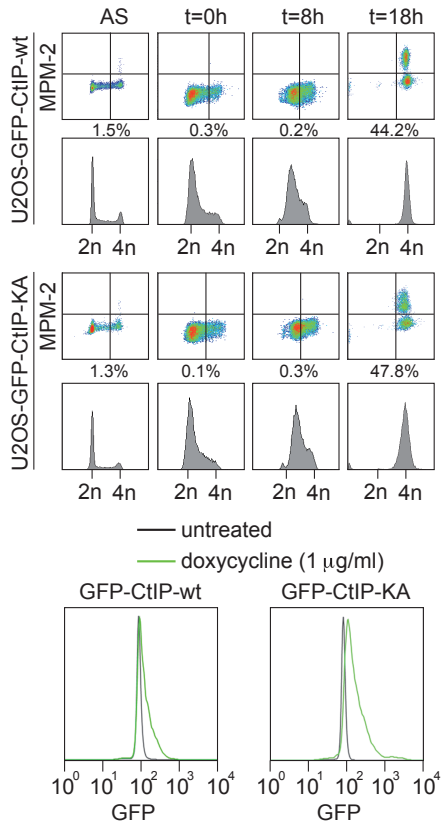

Supplementary Figure S7

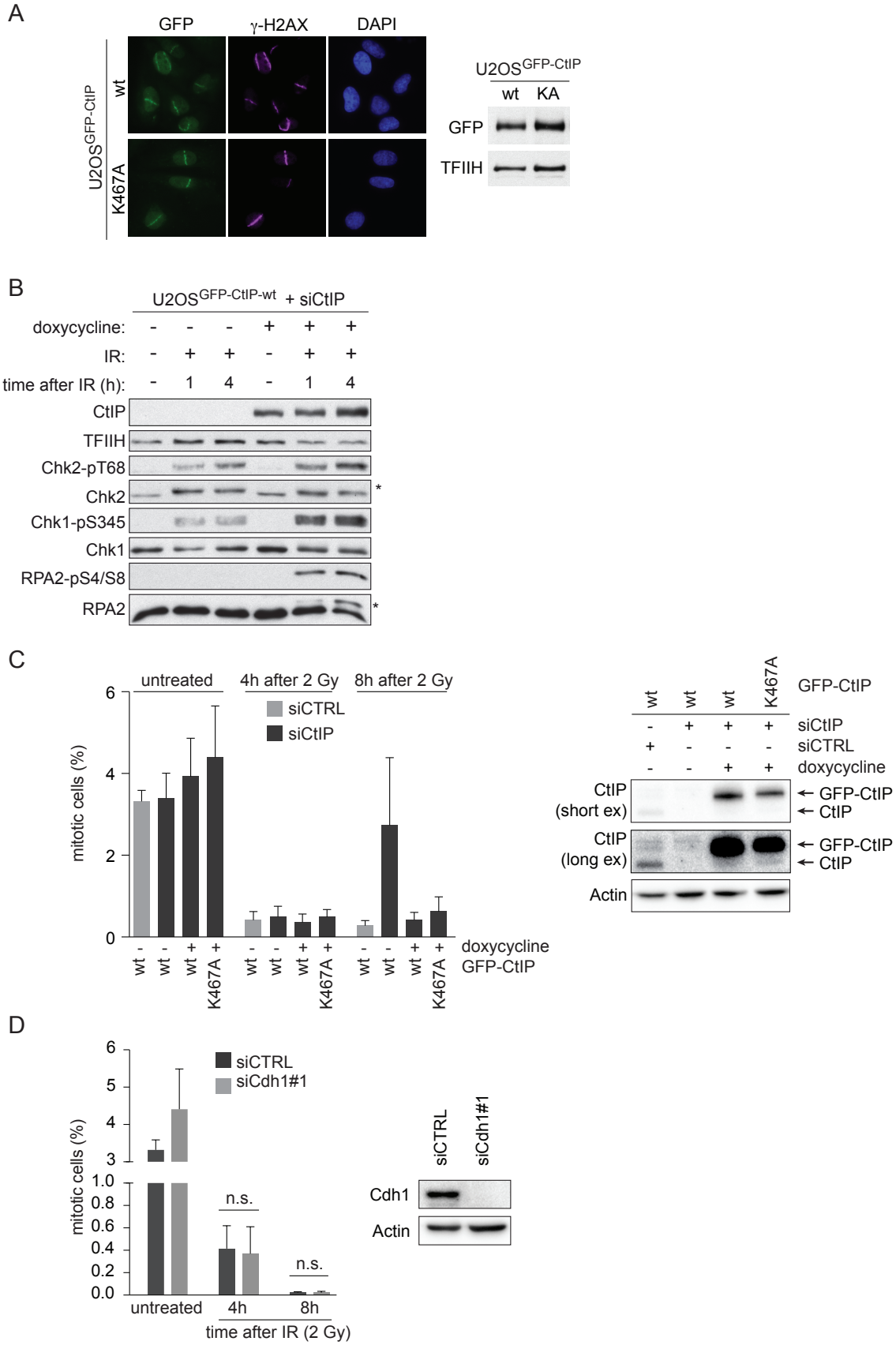

Supplementary Figure S8

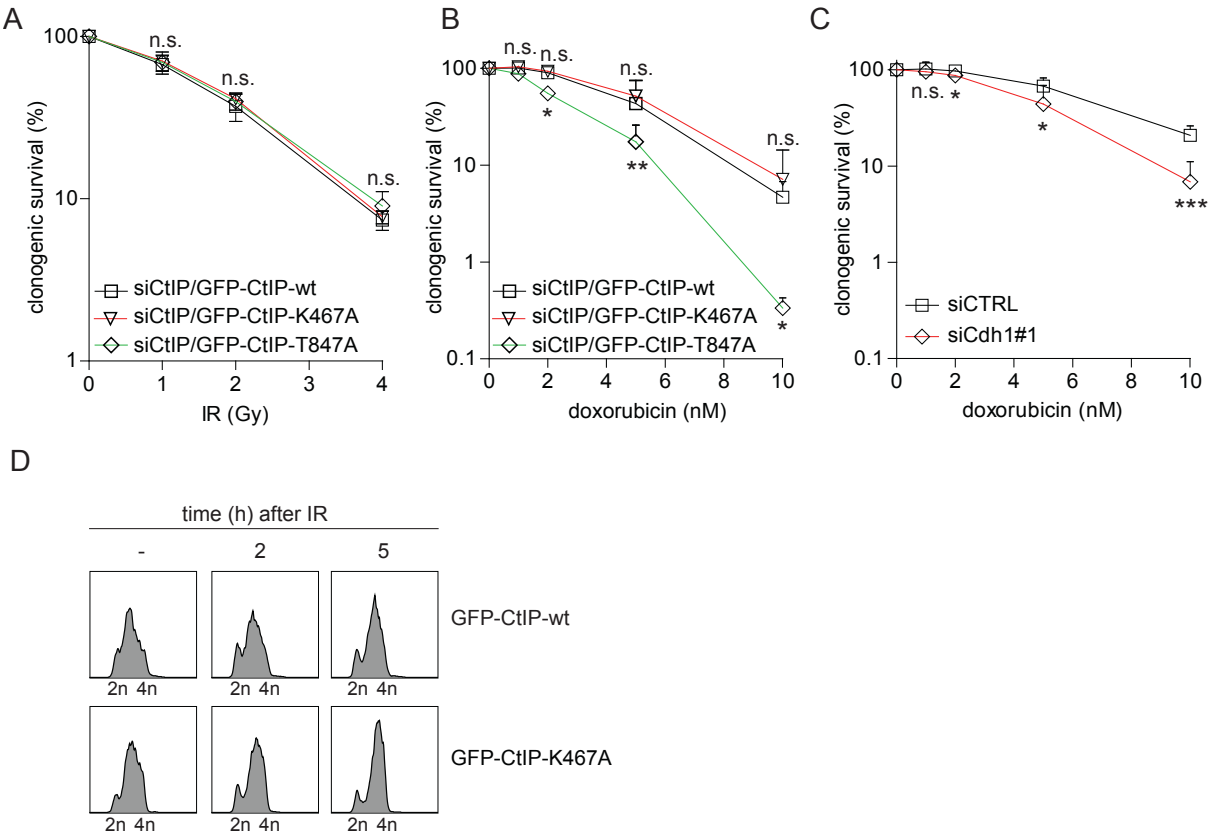

Uniprot iden	Gene symbol	Gene Ontology terms	Description	Gene symbol aliases
Q9NY61	AATF	GO:0006974	Protein AATF	AATF|AATF_HUMAN|CHE1|DED|HSPC277
P00519	ABL1	GO:0006974	Tyrosine-protein kinase ABL1	ABL|ABL1|ABL1_HUMAN|JTK7
Q9H9F9	ACTR5	GO:0006302	Actin-related protein 5	ACTR5|ARP5|ARP5_HUMAN
Q9BT30	ALKBH7	GO:0006974	Alpha-ketoglutarate-dependent dioxyg	ABH7|ALKB7_HUMAN|ALKBH7|SPATA11|UNQ6002/PRO34564
Q96BT7	ALKBH8	GO:0006974	Alkylated DNA repair protein alkB hom	ABH8|ALKB8_HUMAN|ALKBH8
Q9NUS5	AP5S1	GO:0000724	AP-5 complex subunit sigma-1	AP5S1|AP5S1_HUMAN|C20orf29
O43299	AP5Z1	GO:0000724	AP-5 complex subunit zeta-1	AP5Z1|AP5Z1_HUMAN|KIAA0415|SPG48
O00213	APBB1	GO:0006974; GO:0006302	Amyloid beta A4 precursor protein-bin	APBB1|APBB1_HUMAN|FE65|RIR
R4GMU6	APC	GO:0006974	Adenomatous polyposis coli protein	APC|R4GMU6_HUMAN
Q8N2Z9	APITD1	GO:0006974	Centromere protein S	APITD1|CENPS|CENPS_HUMAN|FAAP16|MHF1
Q8IW19	APLF	GO:0006974; GO:0006302	Aprataxin and PNK-like factor	APLF|APLF_HUMAN|C2orf13|PALF|XIP1
Q7Z2E3	APTX	GO:0006974; GO:0006302	Aprataxin	APTX|APTX_HUMAN|AXA1
Q9UBL3	ASH2L	GO:0006974	Set1/Ash2 histone methyltransferase c	ASH2L|ASH2L1|ASH2L_HUMAN
Q96QE3	ATAD5	GO:0006974	ATPase family AAA domain-containing p	ATAD5|ATAD5_HUMAN|C17orf41|FRAG1
P15336	ATF2	GO:0006974	Cyclic AMP-dependent transcription fa	ATF2|ATF2_HUMAN|CREB2|CREBP1
Q13315	ATM	GO:0006974; GO:0000077; GO:000	Serine-protein kinase ATM	ATM|ATM_HUMAN
O43313	ATMIN	GO:0006974	ATM interactor	ATMIN|ATMIN_HUMAN|KIAA0431|ZNF822
Q13535	ATR	GO:0006974; GO:0000077	Serine/threonine-protein kinase ATR	ATR|ATR_HUMAN|FRP1
Q8WXE1	ATRIP	GO:0000077	ATR-interacting protein	AGS1|ATRIP|ATRIP_HUMAN
Q9NWV8	BABAM1	GO:0006302	BRISC and BRCA1-A complex member 1	BABA1_HUMAN|BABAM1|C19orf62|HSPC142|MERIT40|NBA1
Q99728	BARD1	GO:0006974	BRCA1-associated RING domain protein	BARD1|BARD1_HUMAN
Q16520	BATF	GO:0006974	Basic leucine zipper transcriptional fact	BATF|BATF_HUMAN
Q07812	BAX	GO:0006974	Apoptosis regulator BAX	BAX|BAX_HUMAN|BCL2L4
Q9UIG0	BAZ1B	GO:0006974; GO:0006302	Tyrosine-protein kinase BAZ1B	BAZ1B|BAZ1B_HUMAN|WBSC10|WBSCR10|WBSCR9|WSTF
Q9BXH1	BBC3	GO:0006974	Bcl-2-binding component 3	BBC3|BBC3_HUMAN|PUMA
P10415	BCL2	GO:0006974	Apoptosis regulator Bcl-2	BCL2|BCL2_HUMAN
P20749	BCL3	GO:0006974	B-cell lymphoma 3 protein	BCL3|BCL3_HUMAN|BCL4|D19S37
P41182	BCL6	GO:0006974	B-cell lymphoma 6 protein	BCL5|BCL6|BCL6_HUMAN|LAZ3|ZBTB27|ZNF51
P54132	BLM	GO:0006974; GO:0000724	Bloom syndrome protein	BLM|BLM_HUMAN|RECQ2|RECQL3
P38398	BRCA1	GO:0006974; GO:0000724; GO:000	Breast cancer type 1 susceptibility prot	BRCA1|BRCA1_HUMAN|RNF53
E9PIQ1	BRCA2	GO:0000724; GO:0006302	Breast cancer type 2 susceptibility prot	BRCA2|E9PIQ1_HUMAN
P46736	BRCC3	GO:0006302	Lys-63-specific deubiquitinase BRCC36	BRCC3|BRCC36|BRCC3_HUMAN|C6.1A|CXorf53
O60885	BRD4	GO:0006974	Bromodomain-containing protein 4	BRD4|BRD4_HUMAN|HUNK1
Q9NXR7	BRE	GO:0006974; GO:0006302	BRCA1-A complex subunit BRE	BRCC45|BRE|BRE_HUMAN
Q9BX63	BRIP1	GO:0000077; GO:0006302	Fanconi anemia group J protein	BACH1|BRIP1|FANCJ|FANCJ_HUMAN
Q8TDC3	BRSK1	GO:0006974	Serine/threonine-protein kinase BRSK1	BRSK1|BRSK1_HUMAN|KIAA1811|SAD1|SADB
P78543	BTG2	GO:0006974	Protein BTG2	BTG2|BTG2_HUMAN|PC3
B4DMA1	C11orf82	GO:0006974	Nitric oxide-inducible gene protein	B4DMA1_HUMAN|C11orf82
C9JXR7	CASP3	GO:0006974	Caspase-3 subunit p12	C9JXR7_HUMAN|CASP3
P55211	CASP9	GO:0006974	Caspase-9	CASP9|CASP9_HUMAN|MCH6
Q8N163	CCAR2	GO:0006974	Cell cycle and apoptosis regulator prote	CCAR2|CCAR2_HUMAN|DBC1|KIAA1967
P24385	CCND1	GO:0006974	G1/S-specific cyclin-D1	BCL1|CCND1|CCND1_HUMAN|PRAD1
O75909	CCNK	GO:0006974	Cyclin-K	CCNK|CCNK_HUMAN|CPR4
Q96FF9	CDCA5	GO:0006302	Sororin	CDCA5|CDCA5_HUMAN
P38936	CDKN1A	GO:0006974	Cyclin-dependent kinase inhibitor 1	CAP20|CDKN1|CDKN1A|CDN1A_HUMAN|CIP1|MDA6|PIC1|SDI1|WAF1
Q96MT8	CEP63	GO:0000077	Centrosomal protein of 63 kDa	CEP63|CEP63_HUMAN
Q9BRQ6	CHCHD6	GO:0006974	Coiled-coil-helix-coiled-coil-helix domai	CHCH6_HUMAN|CHCHD6|CHCM1
Q86WJ1	CHD1L	GO:0006974	Chromodomain-helicase-DNA-binding p	ALC1|CHD1L|CHD1L_HUMAN
O14757	CHEK1	GO:0006974; GO:0000077	Serine/threonine-protein kinase Chk1	CHEK1|CHK1|CHK1_HUMAN
O96017	CHEK2	GO:0006974; GO:0000077; GO:000	Serine/threonine-protein kinase Chk2	CDS1|CHEK2|CHK2|CHK2_HUMAN|RAD53
Q99828	CIB1	GO:0006974; GO:0006302	Calcium and integrin-binding protein 1	CIB|CIB1|CIB1_HUMAN|KIP|PRKDCIP
O15516	CLOCK	GO:0000077	Circadian locomoter output cycles prot	BHLHE8|CLOCK|CLOCK_HUMAN|KIAA0334
Q9HAW4	CLSPN	GO:0000077	Claspin	CLSPN|CLSPN_HUMAN
Q2NKJ3	CTC1	GO:0006974	CST complex subunit CTC1	C17orf68|CTC1|CTC1_HUMAN
P16410	CTLA4	GO:0006974	Cytotoxic T-lymphocyte protein 4	CD152|CTLA4|CTLA4_HUMAN
B3KSJ7	DCLRE1C	GO:0006302	cDNA FLJ36438 fis, clone THYMU20121	B3KSJ7_HUMAN|DCLRE1C
P35638	DDIT3	GO:0006974	DNA damage-inducible transcript 3 pro	CHOP|CHOP10|DDIT3|DDIT3_HUMAN|GADD153
Q92499	DDX1	GO:0006302	ATP-dependent RNA helicase DDX1	DDX1|DDX1_HUMAN
Q9NZJ0	DTL	GO:0006974	Denticleless protein homolog	CDT2|CDW1|DCAF2|DTL|DTL_HUMAN|L2DTL|RAMP
Q8TDB6	DTX3L	GO:0006974; GO:0006302	E3 ubiquitin-protein ligase DTX3L	BBAP|DTX3L|DTX3L_HUMAN
Q92630	DYRK2	GO:0006974	Dual specificity tyrosine-phosphorylatic	DYRK2|DYRK2_HUMAN
Q01094	E2F1	GO:0000077	Transcription factor E2F1	E2F1|E2F1_HUMAN|RBBP3
Q9H6Z9	EGLN3	GO:0006974	Egl nine homolog 3	EGLN3|EGLN3_HUMAN
K7EK97	ERCC1	GO:0006302	DNA excision repair protein ERCC-1	ERCC1|K7EK97_HUMAN
Q92889	ERCC4	GO:0000724	DNA repair endonuclease XPF	ERCC11|ERCC4|XPF|XPF_HUMAN
Q13216	ERCC8	GO:0006974	DNA excision repair protein ERCC-8	CKN1|CSA|ERCC8|ERCC8_HUMAN
Q99502	EYA1	GO:0006302	Eyes absent homolog 1	EYA1|EYA1_HUMAN
Q99504	EYA3	GO:0006302	Eyes absent homolog 3	EYA3|EYA3_HUMAN
Q6NZ36	FAAP20	GO:0006974	Fanconi anemia-associated protein of 2	C1orf86|FAAP20|FAP20_HUMAN|FP7162
Q6UWZ7	FAM175A	GO:0006302	BRCA1-A complex subunit Abraxas	ABRA1|CCDC98|F175A_HUMAN|FAM175A|UNQ496/PRO1013
Q9Y2M0	FAN1	GO:0000724	Fanconi-associated nuclease 1	FAN1|FAN1_HUMAN|KIAA1018|MTMR15
C9JSE3	FANCG	GO:0006974	Fanconi anemia group G protein	C9JSE3_HUMAN|FANCG
Q9NW38	FANCL	GO:0006974	E3 ubiquitin-protein ligase FANCL	FANCL|FANCL_HUMAN|PHF9
Q5XUX0	FBXO31	GO:0006974	F-box only protein 31	FBX14|FBX31|FBX31_HUMAN|FBXO31|PP2386
P0C2W1	FBXO45	GO:0006974	F-box/SPRY domain-containing protein	FBSP1_HUMAN|FBX45|FBXO45
Q9NRD1	FBXO6	GO:0000077	F-box only protein 6	FBG2|FBS2|FBX6|FBX6_HUMAN|FBXO6
Q969H0	FBXW7	GO:0006974	F-box/WD repeat-containing protein 7	FBW7|FBX30|FBXW7|FBXW7_HUMAN|SEL10
P39748	FEN1	GO:0006302	Flap endonuclease 1	FEN1|FEN1_HUMAN|RAD2
Q9NZ56	FMN2	GO:0006974	Formin-2	FMN2|FMN2_HUMAN
O00409	FOXN3	GO:0000077	Forkhead box protein N3	C14orf116|CHES1|FOXN3|FOXN3_HUMAN
Q12778	FOXO1	GO:0006974	Forkhead box protein O1	FKHR|FOXO1|FOXO1A|FOXO1_HUMAN
O43524	FOXO3	GO:0006974	Forkhead box protein O3	FKHRL1|FOXO3|FOXO3A|FOXO3_HUMAN

A6NCE0	FOXO6	GO:0006974	Forkhead box protein O6	A6NCE0_HUMAN|FOXO6
P36915	GNL1	GO:0006974	Guanine nucleotide-binding protein-like	GNL1|GNL1_HUMAN|HSR1
P16104	H2AFX	GO:0006974; GO:0000077; GO:000	Histone H2AX	H2AFX|H2AX|H2AX_HUMAN
H3BNH8	H3BNH8	GO:0006974	Uncharacterized protein	H3BNH8_HUMAN
O95714	HERC2	GO:0006974	E3 ubiquitin-protein ligase HERC2	HERC2|HERC2_HUMAN
Q9BQA5	HINFP	GO:0000077	Histone H4 transcription factor	HINFP|HINFP_HUMAN|MIZF|ZNF743
O60921	HUS1	GO:0006974; GO:0000724; GO:000	Checkpoint protein HUS1	HUS1|HUS1_HUMAN
Q8NHY5	HUS1B	GO:0000077	Checkpoint protein HUS1B	HUS1B|HUS1B_HUMAN
Q9Y6K9	IKBKG	GO:0006974	NF-kappa-B essential modulator	FIP3|IKBKG|NEMO|NEMO_HUMAN
Q9NRY2	INIP	GO:0006974	SOSS complex subunit C	C9orf80|HSPC043|HSPC291|INIP|SOSSC_HUMAN|SSBIP1
Q9ULG1	INO80	GO:0000724; GO:0006302	DNA helicase INO80	INO80|INO80A|INO80_HUMAN|INOC1|KIAA1259
Q68E01	INTS3	GO:0006974	Integrator complex subunit 3	C1orf193|C1orf60|INT3_HUMAN|INTS3
Q9NVH2	INTS7	GO:0000077	Integrator complex subunit 7	C1orf73|INT7_HUMAN|INTS7
Q14653	IRF3	GO:0006974	Interferon regulatory factor 3	IRF3|IRF3_HUMAN
Q92985	IRF7	GO:0006974	Interferon regulatory factor 7	IRF7|IRF7_HUMAN
Q92993	KAT5	GO:0006302	Histone acetyltransferase KAT5	HTATIP|KAT5|KAT5_HUMAN|TIP60
Q15004	KIAA0101	GO:0006974	PCNA-associated factor	KIAA0101|L5|NS5ATP9|PAF|PAF15_HUMAN
O60870	KIN	GO:0006974	DNA/RNA-binding protein KIN17	BTCD|KIN|KIN17|KIN17_HUMAN
P18858	LIG1	GO:0000724; GO:0006302	DNA ligase 1	DNLI1_HUMAN|LIG1
P49917	LIG4	GO:0006302	DNA ligase 4	DNLI4_HUMAN|LIG4
P07948	LYN	GO:0006974	Tyrosine-protein kinase Lyn	JTK8|LYN|LYN_HUMAN
Q9BQ69	MACROD1	GO:0006974	O-acetyl-ADP-ribose deacetylase MACR	LRP16|MACD1_HUMAN|MACROD1
A1Z1Q3	MACROD2	GO:0006974	O-acetyl-ADP-ribose deacetylase MACR	C20orf133|MACD2_HUMAN|MACROD2
Q9UI95	MAD2L2	GO:0006302	Mitotic spindle assembly checkpoint pr	MAD2B|MAD2L2|MD2L2_HUMAN|REV7
Q96JY0	MAEL	GO:0006974	Protein maelstrom homolog	MAEL|MAEL_HUMAN
P28482	MAPK1	GO:0006974	Mitogen-activated protein kinase 1	ERK2|MAPK1|MK01_HUMAN|PRKM1|PRKM2
E7EX54	MAPK14	GO:0000077	Mitogen-activated protein kinase 14	E7EX54_HUMAN|MAPK14
B3KR49	MAPK3	GO:0006974	cDNA FLJ33690 fis, clone BRAWH20029	B3KR49_HUMAN|hCG_1983753|MAPK3
P49137	MAPKAPK2	GO:0006974	MAP kinase-activated protein kinase 2	MAPK2_HUMAN|MAPKAPK2
Q96GX5	MASTL	GO:0006974	Serine/threonine-protein kinase greatw	GW|GWL|GWL_HUMAN|MASTL|THC2
P33993	MCM7	GO:0006974	DNA replication licensing factor MCM7	CDC47|MCM2|MCM7|MCM7_HUMAN
Q9UJA3	MCM8	GO:0006974; GO:0000724	DNA helicase MCM8	C20orf154|MCM8|MCM8_HUMAN
Q9NXL9	MCM9	GO:0006974; GO:0000724	DNA helicase MCM9	C6orf61|MCM9|MCM9_HUMAN|MCMDC1
Q9ULC4	MCTS1	GO:0006974	Malignant T-cell-amplified sequence 1	MCT1|MCTS1|MCTS1_HUMAN
Q14676	MDC1	GO:0000724; GO:0006302	Mediator of DNA damage checkpoint p	KIAA0170|MDC1|MDC1_HUMAN|NFBD1
O00255	MEN1	GO:0006974	Menin	MEN1|MEN1_HUMAN|SCG2
Q29983	MICA	GO:0006974	MHC class I polypeptide-related sequer	MICA|MICA_HUMAN|PERB11.1
Q9NYL2	MLTK	GO:0000077	Mitogen-activated protein kinase kinas	HCCS4|MLTK|MLTK_HUMAN|ZAK
Q96T76	MMS19	GO:0006974	MMS19 nucleotide excision repair prot	MMS19|MMS19L|MMS19_HUMAN
Q6ZRQ5	MMS22L	GO:0000724	Protein MMS22-like	C6orf167|MMS22L|MMS22_HUMAN
P41218	MNDA	GO:0006974	Myeloid cell nuclear differentiation ant	MNDA|MNDA_HUMAN
Q9UBU8	MORF4L1	GO:0000724	Mortality factor 4-like protein 1	FWP006|HSPC008|HSPC061|MO4L1_HUMAN|MORF4L1|MRG15|PP368
P49959	MRE11A	GO:0006974; GO:0000724; GO:000	Double-strand break repair protein MR	HNGS1|MRE11|MRE11A|MRE11_HUMAN
P43246	MSH2	GO:0006302	DNA mismatch repair protein Msh2	MSH2|MSH2_HUMAN
P01106	MYC	GO:0006974	Myc proto-oncogene protein	BHLHE39|MYC|MYC_HUMAN
Q96AH0	NABP1	GO:0006974; GO:0000724	SOSS complex subunit B2	NABP1|OBFC2A|SOSB2_HUMAN|SSB2
Q9BQ15	NABP2	GO:0006974; GO:0000724	SOSS complex subunit B1	LP3587|NABP2|OBFC2B|SOSB1_HUMAN|SSB1
O60934	NBN	GO:0000077; GO:0000724; GO:000	Nibrin	NBN|NBN_HUMAN|NBS|NBS1|P95
Q14686	NCOA6	GO:0006974	Nuclear receptor coactivator 6	AIB3|KIAA0181|NCOA6|NCOA6_HUMAN|RAP250|TRBP
Q96PY6	NEK1	GO:0006974	Serine/threonine-protein kinase Nek1	KIAA1901|NEK1|NEK1_HUMAN
Q13469	NFATC2	GO:0006974	Nuclear factor of activated T-cells, cyto	NFAC2_HUMAN|NFAT1|NFATC2|NFATP
C9JWV4	NHEJ1	GO:0006302	Non-homologous end-joining factor 1	C9JWV4_HUMAN|NHEJ1
Q6KC79	NIPBL	GO:0006974	Nipped-B-like protein	IDN3|NIPBL|NIPBL_HUMAN
Q8IXT1	NOXIN	GO:0006974	Nitric oxide-inducible gene protein	C11orf82|NOXIN|NOXIN_HUMAN
E5RFJ1	NSMCE2	GO:0000724	E3 SUMO-protein ligase NSE2	E5RFJ1_HUMAN|NSMCE2
O60285	NUAK1	GO:0006974	NUAK family SNF1-like kinase 1	ARK5|KIAA0537|NUAK1|NUAK1_HUMAN|OMPHK1
Q96FW1	OTUB1	GO:0006974	Ubiquitin thioesterase OTUB1	HSPC263|OTB1|OTU1|OTUB1|OTUB1_HUMAN
Q86YC2	PALB2	GO:0000724	Partner and localizer of BRCA2	FANCN|PALB2|PALB2_HUMAN
Q5XG87	PAPD7	GO:0006302	DNA polymerase sigma	PAPD7|PAPD7_HUMAN|POLS|TRF4
Q86W56	PARG	GO:0006974	Poly(ADP-ribose) glycohydrolase	PARG|PARG_HUMAN
P09874	PARP1	GO:0006302	Poly [ADP-ribose] polymerase 1	ADPRT|PARP1|PARP1_HUMAN|PPOL
Q9UKK3	PARP4	GO:0006974	Poly [ADP-ribose] polymerase 4	ADPRTL1|KIAA0177|PARP4|PARP4_HUMAN|PARPL
Q8IXQ6	PARP9	GO:0006302	Poly [ADP-ribose] polymerase 9	BAL|BAL1|PARP9|PARP9_HUMAN
O43189	PHF1	GO:0006974	PHD finger protein 1	PCL1|PHF1|PHF1_HUMAN
H0YE55	PIDD	GO:0006974	p53-induced protein with a death doma	H0YE55_HUMAN|PIDD
Q9H4B4	PLK3	GO:0006974	Serine/threonine-protein kinase PLK3	CNK|FNK|PLK3|PLK3_HUMAN|PRK
Q13794	PMAIP1	GO:0006974	Phorbol-12-myristate-13-acetate-induc	APR_HUMAN|NOXA|PMAIP1
P06746	POLB	GO:0006974	DNA polymerase beta	DPOLB_HUMAN|POLB
O75807	PPP1R15A	GO:0006974	Protein phosphatase 1 regulatory subu	GADD34|PPP1R15A|PR15A_HUMAN
F5GX40	PRKDC	GO:0006302	DNA-dependent protein kinase catalyti	F5GX40_HUMAN|PRKDC
E7ES96	PSEN1	GO:0006974	Presenilin-1	E7ES96_HUMAN|PSEN1
O00487	PSMD14	GO:0000724	26S proteasome non-ATPase regulatory	POH1|PSDE_HUMAN|PSMD14
Q14997	PSME4	GO:0006974	Proteasome activator complex subunit	KIAA0077|PSME4|PSME4_HUMAN
Q06124	PTPN11	GO:0000077	Tyrosine-protein phosphatase non-rece	PTN11_HUMAN|PTP2C|PTPN11|SHPTP2
O60671	RAD1	GO:0006974; GO:0000077	Cell cycle checkpoint protein RAD1	RAD1|RAD1_HUMAN|REC1
D6RHU1	RAD17	GO:0006974; GO:0000077	Cell cycle checkpoint protein RAD17	D6RHU1_HUMAN|RAD17
C9J0Q4	RAD18	GO:0006974	E3 ubiquitin-protein ligase RAD18	C9J0Q4_HUMAN|RAD18
O60216	RAD21	GO:0006302	Double-strand-break repair protein rad	HR21|KIAA0078|NXP1|RAD21|RAD21_HUMAN
Q9H4I0	RAD21L1	GO:0006302	Double-strand-break repair protein rad	RAD21L|RAD21L1|RD21L_HUMAN
K7ENJ0	RAD23A	GO:0006974	UV excision repair protein RAD23 homc	K7ENJ0_HUMAN|RAD23A
Q5W0S5	RAD23B	GO:0006974	UV excision repair protein RAD23 homc	Q5W0S5_HUMAN|RAD23B
Q92878	RAD50	GO:0006974; GO:0000724; GO:000	DNA repair protein RAD50	RAD50|RAD50_HUMAN
Q06609	RAD51	GO:0006974; GO:0000724; GO:000	DNA repair protein RAD51 homolog 1	RAD51|RAD51A|RAD51_HUMAN|RECA

Q96B01	RAD51AP1	GO:0000724	RAD51-associated protein 1	PIR51|R51A1_HUMAN|RAD51AP1
F5GX95	RAD52	GO:0000724; GO:0006302	DNA repair protein RAD52 homolog	F5GX95_HUMAN|RAD52
Q9Y620	RAD54B	GO:0000724	DNA repair and recombination protein	RA54B_HUMAN|RAD54B
Q92698	RAD54L	GO:0000724	DNA repair and recombination protein	RAD54A|RAD54L|RAD54_HUMAN
Q99638	RAD9A	GO:0006974; GO:0000077	Cell cycle checkpoint control protein RA	RAD9A|RAD9A_HUMAN
B4DX60	RAD9B	GO:0000077	Cell cycle checkpoint control protein RA	B4DX60_HUMAN|hCG_41292|RAD9B
Q9NS23	RASSF1	GO:0006974	Ras association domain-containing prot	RASF1_HUMAN|RASSF1|RDA32
Q15291	RBBP5	GO:0006974	Retinoblastoma-binding protein 5	RBBP5|RBBP5_HUMAN|RBQ3
Q99708	RBBP8	GO:0000724	DNA endonuclease RBBP8	COM1_HUMAN|CTIP|RBBP8
Q9BSD3	RHNO1	GO:0000077	RAD9, HUS1, RAD1-interacting nuclear	C12orf32|HKMT1188|RHINO|RHNO1|RHNO1_HUMAN
Q5UIP0	RIF1	GO:0006974	Telomere-associated protein RIF1	RIF1|RIF1_HUMAN
Q8IYW5	RNF168	GO:0006974; GO:0006302	E3 ubiquitin-protein ligase RNF168	RN168_HUMAN|RNF168
Q8NCN4	RNF169	GO:0006974	E3 ubiquitin-protein ligase RNF169	KIAA1991|RN169_HUMAN|RNF169
F8WEW6	RNF8	GO:0006974; GO:0006302	E3 ubiquitin-protein ligase RNF8	F8WEW6_HUMAN|RNF8
I3L2M5	RPA1	GO:0000724; GO:0006302	Replication protein A 70 kDa DNA-bindi	I3L2M5_HUMAN|RPA1
P15927	RPA2	GO:0000724; GO:0006302	Replication protein A 32 kDa subunit	REPA2|RFA2_HUMAN|RPA2|RPA32|RPA34
P35244	RPA3	GO:0000724; GO:0006302	Replication protein A 14 kDa subunit	REPA3|RFA3_HUMAN|RPA14|RPA3
Q13156	RPA4	GO:0000077	Replication protein A 30 kDa subunit	RFA4_HUMAN|RPA4
Q71UM5	RPS27L	GO:0006974	40S ribosomal protein S27-like	RPS27L|RS27L_HUMAN
P23396	RPS3	GO:0006974	40S ribosomal protein S3	OK/SW-cl.26|RPS3|RS3_HUMAN
Q9Y6P5	SESN1	GO:0006974	Sestrin-1	PA26|SESN1|SESN1_HUMAN|SEST1
Q7Z333	SETX	GO:0006302	Probable helicase senataxin	ALS4|KIAA0625|SCAR1|SETX|SETX_HUMAN
Q86XK3	SFR1	GO:0000724	Swi5-dependent recombination DNA re	C10orf78|MEI5|MEIR5|SFR1|SFR1_HUMAN
E9PJN2	SGK1	GO:0006974	Serine/threonine-protein kinase Sgk1	E9PJN2_HUMAN|SGK1
P60896	SHFM1	GO:0000724	26S proteasome complex subunit DSS1	DSS1|DSS1_HUMAN|SHFDG1|SHFM1
Q96EB6	SIRT1	GO:0006974	NAD-dependent protein deacetylase sir	SIR1_HUMAN|SIR2L1|SIRT1
Q9Y6E7	SIRT4	GO:0006974	NAD-dependent protein deacetylase sir	SIR2L4|SIR4_HUMAN|SIRT4
Q9BQ83	SLX1A	GO:0000724	Structure-specific endonuclease subuni	GIYD1|GIYD2|SLX1|SLX1A|SLX1B|SLX1_HUMAN
Q8IY92	SLX4	GO:0000724	Structure-specific endonuclease subuni	BTBD12|KIAA1784|KIAA1987|SLX4|SLX4_HUMAN
O60264	SMARCA5	GO:0006302	SWI/SNF-related matrix-associated acti	SMARCA5|SMCA5_HUMAN|SNF2H|WCRF135
Q8IY18	SMC5	GO:0000724	Structural maintenance of chromosome	KIAA0594|SMC5|SMC5L1|SMC5_HUMAN
C9JMN1	SMC6	GO:0000724	Structural maintenance of chromosome	C9JMN1_HUMAN|SMC6
P00441	SOD1	GO:0006302	Superoxide dismutase [Cu-Zn]	SOD1|SODC_HUMAN
Q8TC71	SPATA18	GO:0006974	Mitochondria-eating protein	MIEAP|MIEAP_HUMAN|SPATA18
Q5MJ70	SPDYA	GO:0006974	Speedy protein A	SPDY1|SPDYA|SPDYA_HUMAN|SPY1
Q14159	SPIDR	GO:0006974; GO:0000724	DNA repair-scaffolding protein	KIAA0146|SPIDR|SPIDR_HUMAN
Q9H040	SPRTN	GO:0006974	SprT-like domain-containing protein Sp	C1orf124|DVC1|SPRTN|SPRTN_HUMAN|UNQ1880/PRO4323
Q15831	STK11	GO:0006974	Serine/threonine-protein kinase STK11	LKB1|PJS|STK11|STK11_HUMAN
Q1ZZU3	SWI5	GO:0000724	DNA repair protein SWI5 homolog	C9orf119|SAE3|SWI5|SWI5_HUMAN
Q6NVH7	SWSAP1	GO:0000724	ATPase SWSAP1	C19orf39|SWAP1_HUMAN|SWSAP1
P21675	TAF1	GO:0006974	Transcription initiation factor TFIID sub	BA2R|CCG1|CCGS|TAF1|TAF1_HUMAN|TAF2A
Q16594	TAF9	GO:0006974	Transcription initiation factor TFIID sub	TAF2G|TAF9|TAF9_HUMAN|TAFII31
Q7L7X3	TAOK1	GO:0006974	Serine/threonine-protein kinase TAO1	KIAA1361|MAP3K16|MARKK|TAOK1|TAOK1_HUMAN
Q9UL54	TAOK2	GO:0006974	Serine/threonine-protein kinase TAO2	KIAA0881|MAP3K17|PSK|PSK1|TAOK2|TAOK2_HUMAN|UNQ2971/PRO7431
Q9H2K8	TAOK3	GO:0006974	Serine/threonine-protein kinase TAO3	DPK|JIK|KDS|MAP3K18|TAOK3|TAOK3_HUMAN
Q9NUW8	TDP1	GO:0006302	Tyrosyl-DNA phosphodiesterase 1	TDP1|TYDP1_HUMAN
O95551	TDP2	GO:0006302	Tyrosyl-DNA phosphodiesterase 2	AD-022|EAP2|TDP2|TTRAP|TYDP2_HUMAN
Q5H9I0	TFDP3	GO:0006974	Transcription factor Dp family member	DP4|HCA661|TFDP3|TFDP3_HUMAN
Q9UNS1	TIMELESS	GO:0006974	Protein timeless homolog	TIM|TIM1|TIMELESS|TIMELESS1|TIM_HUMAN
H3BQ83	TIPIN	GO:0006974; GO:0000077	TIMELESS-interacting protein	H3BQ83_HUMAN|TIPIN
O75663	TIPRL	GO:0000077	TIP41-like protein	TIPRL|TIPRL_HUMAN
Q9UKI8	TLK1	GO:0006974	Serine/threonine-protein kinase tousle	KIAA0137|TLK1|TLK1_HUMAN
Q86UE8	TLK2	GO:0006974	Serine/threonine-protein kinase tousle	TLK2|TLK2_HUMAN
Q96HA7	TONSL	GO:0000724	Tonsoku-like protein	IKBR|NFKBIL2|TONSL|TONSL_HUMAN
P11388	TOP2A	GO:0006974	DNA topoisomerase 2-alpha	TOP2|TOP2A|TOP2A_HUMAN
Q92547	TOPBP1	GO:0006974	DNA topoisomerase 2-binding protein 1	KIAA0259|TOPB1_HUMAN|TOPBP1
Q9NS56	TOPORS	GO:0006974	E3 ubiquitin-protein ligase Topors	LUN|TOPORS|TOPRS_HUMAN|TP53BPL
P04637	TP53	GO:0006974; GO:0006302	Cellular tumor antigen p53	P53|P53_HUMAN|TP53
Q12888	TP53BP1	GO:0006974; GO:0000724; GO:000	Tumor suppressor p53-binding protein	TP53BP1|TP53B_HUMAN
Q9Y2A0	TP53TG1	GO:0006974	TP53-target gene 1 protein	P53TG1|T53G1_HUMAN|TP53AP1|TP53TG1
O15350	TP73	GO:0006974	Tumor protein p73	P73|P73_HUMAN|TP73
Q14669	TRIP12	GO:0006974	E3 ubiquitin-protein ligase TRIP12	KIAA0045|TRIP12|TRIPC_HUMAN|ULF
Q15645	TRIP13	GO:0006302	Pachytene checkpoint protein 2 homol	PCH2|PCH2_HUMAN|TRIP13
P63146	UBE2B	GO:0006974	Ubiquitin-conjugating enzyme E2 B	RAD6B|UBE2B|UBE2B_HUMAN
P61088	UBE2N	GO:0000724	Ubiquitin-conjugating enzyme E2 N	BLU|UBE2N|UBE2N_HUMAN
Q9NPD8	UBE2T	GO:0006974	Ubiquitin-conjugating enzyme E2 T	HSPC150|PIG50|UBE2T|UBE2T_HUMAN
O95071	UBR5	GO:0006974	E3 ubiquitin-protein ligase UBR5	EDD|EDD1|HYD|KIAA0896|UBR5|UBR5_HUMAN
Q96RL1	UIMC1	GO:0006302	BRCA1-A complex subunit RAP80	RAP80|RXRIP110|UIMC1|UIMC1_HUMAN
Q9Y5T5	USP16	GO:0006974	Ubiquitin carboxyl-terminal hydrolase 1	MSTP039|UBP16_HUMAN|USP16
Q96RU2	USP28	GO:0006974; GO:0000077	Ubiquitin carboxyl-terminal hydrolase 2	KIAA1515|UBP28_HUMAN|USP28
Q96K76	USP47	GO:0006974	Ubiquitin carboxyl-terminal hydrolase 4	UBP47_HUMAN|USP47
Q9UKW4	VAV3	GO:0006974	Guanine nucleotide exchange factor VA	VAV3|VAV3_HUMAN
P55072	VCP	GO:0006974; GO:0006302	Transitional endoplasmic reticulum ATP	TERA_HUMAN|VCP
Q9BTA9	WAC	GO:0006974	WW domain-containing adapter protein	KIAA1844|WAC|WAC_HUMAN
Q14191	WRN	GO:0006974; GO:0006302	Werner syndrome ATP-dependent helic	RECQ3|RECQL2|WRN|WRN_HUMAN
P98170	XIAP	GO:0006974	E3 ubiquitin-protein ligase XIAP	API3|BIRC4|IAP3|XIAP|XIAP_HUMAN
O43543	XRCC2	GO:0000724	DNA repair protein XRCC2	XRCC2|XRCC2_HUMAN
O43542	XRCC3	GO:0006974	DNA repair protein XRCC3	XRCC3|XRCC3_HUMAN
Q13426	XRCC4	GO:0006302	DNA repair protein XRCC4	XRCC4|XRCC4_HUMAN
P13010	XRCC5	GO:0006302	X-ray repair cross-complementing prote	G22P2|XRCC5|XRCC5_HUMAN
P12956	XRCC6	GO:0006302	X-ray repair cross-complementing prote	G22P1|XRCC6|XRCC6_HUMAN
P46937	YAP1	GO:0006974	Yorkie homolog	YAP1|YAP1_HUMAN|YAP65
P25490	YY1	GO:0006974; GO:0000724	Transcriptional repressor protein YY1	INO80S|TYY1_HUMAN|YY1

Q9NUA8	ZBTB40	GO:0006974	Zinc finger and BTB domain-containing	KIAA0478|ZBT40_HUMAN|ZBTB40
Q68DK2	ZFYVE26	GO:0000724	Zinc finger FYVE domain-containing pro	KIAA0321|ZFY26_HUMAN|ZFYVE26
Q9HA38	ZMAT3	GO:0006974	Zinc finger matrin-type protein 3	PAG608|WIG1|ZMAT3|ZMAT3_HUMAN
Q96PM9	ZNF385A	GO:0006974	Zinc finger protein 385A	HZF|RZF|Z385A_HUMAN|ZNF385|ZNF385A
Q5FWF4	ZRANB3	GO:0006974	DNA annealing helicase and endonucle	ZRAB3_HUMAN|ZRANB3
Q19AV6	ZSWIM7	GO:0000724	Zinc finger SWIM domain-containing pr	SWS1|ZSWIM7|ZSWM7_HUMAN

Supplementary Table S2: Primary antibodies

Antibody target	Species	Catalog number (supplier)	Application*
53BP1	rabbit	Ab21083 (Abcam)	IF
Actin (AC-15)	mouse	Clone #A-5441 (Sigma)	IB
ATM (2C1)	mouse	GTX70103 (GeneTex)	IB
pATM S1981	rabbit	2152-1 (Epitomics)	IB
Cdh1	mouse	MA5-11496 (Neomarkers)	IB
Cdh1	mouse	sc-56312 (Santa Cruz)	IB
Cdh1	mouse	Ab3242 (Abcam)	IP/IB
Claspin	rabbit	Gift from Dr. R. Freire	IB
CtIP (14-1)	mouse	gift from Richard Baer	IB
CtIP (612L)	rabbit	gift from Richard Baer	IP
CtIP (D-4)	mouse	sc-271339 (Santa Cruz)	IB
CtIP (T-16)	goat	sc-5970 (Santa Cruz)	IB
Chk1 (G4)	mouse	sc-8408 (Santa Cruz)	IB
pChk1 S345	rabbit	2341(Cell Signaling)	IB
Chk2	rabbit	gift from Grant Stewart IB	IB
pChk2 T68 (C13C1)	rabbit	2197P (Cell Signaling)	IB
Cyclin B1 (GNS1)	mouse	sc-245 (Santa Cruz)	IB
Cyclin B1	mouse	05-373 (Upstate)	IB
FK2	mouse	PW8810 (Enzo life sciences)	IB
FLAG	mouse	F3165 (Sigma)	IB
GFP	rabbit	Ab290 (Abcam)	IB
GFP	mouse	sc-9996 (Santa Cruz)	IB
pHistone-H3 S10	rabbit	#06570 (Upstate)	FC
HA	mouse	sc-7392 (Santa Cruz)	IP and IB
γH2AX (JBW301)	mouse	05-636 (Millipore)	IF and FC
γH2AX (20E3)	rabbit	9718 (Cell Signaling)	IB and IF
KAP1	mouse	sc-81411 (Santa Cruz)	IB
pKAP1 pS824	rabbit	A300-767A (Bethyl)	IB
MPM-2	mouse	05-368 (Millipore)	FC
Mre11	mouse	GTX70212 (GeneTex)	IB
Mre11	rabbit	NB100-142 (Novus)	IB
p53 (DO-1)	mouse	sc-126 (Santa Cruz)	IB
Plk1	rabbit	#06-813 (Millipore)	IB
Rad51 (H-92)	rabbit	Sc-8349 (Santa Cruz)	IB
Rad51	rabbit	Ab63801 (Abcam)	IF
RPA2 (Ab-3)	mouse	NA19L (Calbiochem)	IF and IB

pRPA S4/S8 (BL647)	rabbit	A300-245A (Bethyl)	IB
TFIIH (S-19)	rabbit	sc-293 (Santa Cruz)	IB

*IB: Immunoblotting, IF: Immunofluorescence, IP: Immunoprecipitation, FC: flow cytometry

Supplementary Table S3

APC/C substrate analysis:

APC/C target	Gene symbol	Reference
P15-PAF	KIAA0101	(Emanuele *et al*, 2011)
CKAP2	CKAP2	(Seki & Fang, 2007)
KIFC1	KIFC1/HSET	(Zhao *et al*, 2008)
Aurora A	AURKA	(Littlepage & Ruderman, 2002; Taguchi *et al*, 2002)
Cyclin B	CCNB	(Pfleger *et al*, 2001; Glotzer *et al*, 1991)
Cenp-F	CENPF	(Gurden *et al*, 2010)
Kif11/Eg5	KIF11	(Zhao *et al*, 2008)
Plk1	PLK	(Lindon & Pines, 2004)
ECT2	ECT2	(Pfleger *et al*, 2001; Liot *et al*, 2011)
Thymidine kinase	TK1	(Ke *et al*, 2005)
Anillin	ANLN	(Zhao & Fang, 2005)
GTSE-1	GTSE-1	(Michael *et al*, 2008)
UbcH10	UBCH10	(Rape & Kirschner, 2004)
Bub1	BUB1	(Qi & Yu, 2007)
Aurora B	AURKB	(Nguyen *et al*, 2005; Stewart & Fang, 2005)
Kif2C/MCAK	KIF2C	(Zhao *et al*, 2008)
NDC80/Hec1	NDC80	(Li *et al*, 2011)
Thymidylate kinase	DTYMK	(Ke *et al*, 2005)

Supplemental references:

Emanuele MJ, Ciccia A, Elia AEH & Elledge SJ (2011) Proliferating cell nuclear antigen (PCNA)-associated KIAA0101/PAF15 protein is a cell cycle-regulated anaphase-promoting complex/cyclosome substrate. *Proc. Natl. Acad. Sci. U.S.A.* **108:** 9845–9850

Glotzer M, Murray AW & Kirschner MW (1991) Cyclin is degraded by the ubiquitin pathway. *Nature* **349:** 132–138

Gurden MDJ, Holland AJ, van Zon W, Tighe A, Vergnolle MA, Andres DA, Spielmann HP, Malumbres M, Wolthuis RMF, Cleveland DW & Taylor SS (2010) Cdc20 is required for the post-anaphase, KEN-dependent degradation of centromere protein F. *J. Cell. Sci.* **123:** 321–330

Ke P-Y, Kuo Y-Y, Hu C-M & Chang Z-F (2005) Control of dTTP pool size by anaphase promoting complex/cyclosome is essential for the maintenance of genetic stability. *Genes Dev.* **19:** 1920–1933

Li L, Zhou Y, Wang G-F, Liao S-C, Ke Y-B, Wu W, Li X-H, Zhang R-L & Fu Y-C (2011) Anaphase-promoting complex/cyclosome controls HEC1 stability. *Cell Prolif.* **44:** 1–9

Lindon C & Pines J (2004) Ordered proteolysis in anaphase inactivates Plk1 to contribute to proper mitotic exit in human cells. *J. Cell Biol.* **164:** 233–241

Liot C, Seguin L, Siret A, Crouin C, Schmidt S & Bertoglio J (2011) APC(cdh1) mediates degradation of the oncogenic Rho-GEF Ect2 after mitosis. *PLoS ONE* **6:** e23676

Littlepage LE & Ruderman JV (2002) Identification of a new APC/C recognition domain, the A box, which is required for the Cdh1-dependent destruction of the kinase Aurora-A during mitotic exit. *Genes Dev*. **16:** 2274–2285

Liu Z, Yuan F, Ren J, Cao J, Zhou Y, Yang Q & Xue Y (2012) GPS-ARM: computational analysis of the APC/C recognition motif by predicting D-boxes and KEN-boxes. *PLoS ONE* **7:** e34370

Michael S, Travé G, Ramu C, Chica C & Gibson TJ (2008) Discovery of candidate KEN-box motifs using cell cycle keyword enrichment combined with native disorder prediction and motif conservation. *Bioinformatics* **24:** 453–457

Nguyen HG, Chinnappan D, Urano T & Ravid K (2005) Mechanism of Aurora-B degradation and its dependency on intact KEN and A-boxes: identification of an aneuploidy-promoting property. *Mol*. *Cell*. *Biol*. **25:** 4977–4992

Pfleger CM, Lee E & Kirschner MW (2001) Substrate recognition by the Cdc20 and Cdh1 components of the anaphase-promoting complex. *Genes Dev*. **15:** 2396–2407

Qi W & Yu H (2007) KEN-box-dependent degradation of the Bub1 spindle checkpoint kinase by the anaphase-promoting complex/cyclosome. *J*. *Biol*. *Chem*. **282:** 3672–3679

Rape M & Kirschner MW (2004) Autonomous regulation of the anaphase-promoting complex couples mitosis to S-phase entry. *Nature* **432:** 588–595

Seki A & Fang G (2007) CKAP2 is a spindle-associated protein degraded by APC/C-Cdh1 during mitotic exit. *J*. *Biol*. *Chem*. **282:** 15103–15113

Stewart S & Fang G (2005) Destruction box-dependent degradation of aurora B is mediated by the anaphase-promoting complex/cyclosome and Cdh1. *Cancer Res*. **65:** 8730–8735

Taguchi SI, Honda K, Sugiura K, Yamaguchi A, Furukawa K & Urano T (2002) Degradation of human Aurora-A protein kinase is mediated by hCdh1. *FEBS Lett*. **519:** 59–65

Zhao W-M & Fang G (2005) Anillin is a substrate of anaphase-promoting complex/cyclosome (APC/C) that controls spatial contractility of myosin during late cytokinesis. *J*. *Biol*. *Chem*. **280:** 33516–33524

Zhao W-M, Coppinger JA, Seki A, Cheng X-L, Yates JR & Fang G (2008) RCS1, a substrate of APC/C, controls the metaphase to anaphase transition. *Proc*. *Natl*. *Acad*. *Sci*. *U.S.A*. **105:** 13415–13420

4 Discussion

4.1 APC/C^{Cdh1} targets CtIP for degradation after mitotic exit

The precise regulation of DSB repair pathways is pivotal to ensure genome stability. DSB repair through HR is limited to S/G_2 phases when the intact sister chromatid is available to provide sequence homology. This cell cycle-dependent regulation of HR occurs at many different levels and mainly applies to proteins involved in DNA-end resection, the first step of HR. Human CtIP is essential for the initiation of DNA-end resection, and its function in this process is controlled by various post-translational modifications including phosphorylation, ubiquitylation, and acetylation. Moreover, CtIP protein levels are low during G_1 and increased during S/G_2 phase while mRNA levels are rather constant [295]. Nevertheless, the mechanisms controlling CtIP protein fluctuations remained elusive so far.

We initiated our study by recapitulating the observation that CtIP protein levels fluctuate during cell cycle progression. Therefore we synchronized cells using different approaches and followed CtIP levels over time, confirming that CtIP protein levels are high during S/G_2/M phases, but rapidly decline following mitotic exit. Treatment with the proteasome inhibitor MG-132 counteracted the decrease of CtIP levels, indicative for a proteasome-dependent degradation of CtIP. It is known that the E3 ubiquitin ligase APC/C orchestrates the exit from mitosis by targeting substrates for degradation and that it remains active throughout G_1. Thus, it represents a good candidate to explain CtIP down-regulation at this stage of the cell cycle. We confirmed this hypothesis by using the APC/C inhibitor proTAME, which stabilized CtIP in G_1, as well as Plk1, a well-studied APC/C substrate [176, 309]. APC/C binds its substrates through the cell cycle-dependent and mutually exclusive association with two co-activators, Cdc20 and Cdh1 [124]. Cdc20 is associated with APC/C during early mitosis and principally regulates mitotic progression, whereas Cdh1 is active from late mitosis to the G_1/S transition and shows a broad spectrum of substrates [310]. The timing of CtIP degradation suggests that Cdh1 is the responsible co-activator mediating CtIP recognition. In fact, proteins targeted by Cdc20 are promptly degraded during mitosis, whereas CtIP is detectable during mitosis and rather follows the degradation pattern of Cdh1 substrates [147, 166, 171]. Accordingly, we showed that Cdh1 depletion results in CtIP stabilization and decreased CtIP polyubiquitylation. Moreover, after overexpressing tagged versions of

CtIP and Cdh1 in HEK293T cells, we used co-immunoprecipitation experiments to show that the two proteins interact *in vivo*. This interaction was confirmed by pull-down experiments, in which a bacterially expressed GST-CtIP construct was used to pull-down endogenous Cdh1 from HeLa nuclear extracts.

Cdh1 and Cdc20 recognize short destruction motifs, the so-called KEN and D-boxes, in disordered regions of their substrate proteins. Analysis of the primary amino acid sequence of CtIP revealed the presence of two putative KEN boxes in the central region of the protein and five putative D-boxes: two in the N- and three in the C-terminus of the protein. The two KEN boxes are highly conserved throughout evolution, whereas all D-boxes are only partially conserved. To identify which motif is mediating CtIP-Cdh1 interaction, we substituted the respective lysine residue of both KEN boxes with alanine (CtIP-K179A and -K467A). In the case of other substrates, mutation of the first amino acid of a KEN box was demonstrated to completely abrogate the recognition by Cdh1 [311]. Using this approach, we showed that the KEN box at position 467-469 in CtIP is required for the interaction with Cdh1. Moreover, pull-down experiments using a GST-CtIP fragment only containing the two KEN boxes, excluded a major role for the various D-boxes in the interaction. Interestingly, the KEN box motif in CtIP perfectly matches the updated consensus sequence ([D/N]-K-E-N-x-x-P) that was based on the analysis of 46 previously validated KEN boxes [148]. Various studies reported that Cdh1 preferentially binds its substrates through the recognition of KEN boxes, but the efficient ubiquitylation of a substrate harboring both D- and KEN boxes seems to depend on the presence of both degrons [312, 313]. In fact, the Apc10 subunit of the APC/C complex plays a role in stabilizing the interaction between APC/C^{Cdh1} and the target protein by binding to D-boxes present in the substrate [131, 144]. In our study, we did not further address an auxiliary role for the D-boxes in CtIP degradation, however they could potentially be involved in the processivity of CtIP polyubiquitylation by APC/C^{Cdh1}. Based on our interaction data, we generated stable cell lines inducibly expressing GFP-tagged wild-type (wt) or K467A mutant CtIP. Using an *in vivo* ubiquitylation assay, we observed that polyubiquitylation was severely reduced in the K467A mutant when compared to wild-type CtIP. Moreover, live-cell microscopy experiments performed in asynchronous cells confirmed that CtIP-wt was degraded following mitotic exit, whereas CtIP-K467A was more stable in G_1.

It has been reported that CtIP is post-translationally modified during cell cycle progression and after DNA damage. These modifications include phosphorylation,

ubiquitylation and acetylation [307, 314, 315]. Thus, one could speculate whether APC/C^{Cdh1}-dependent degradation of CtIP during G_1 is required for the removal of modified CtIP. In this manner, cell cycle- and damage-dependent modified CtIP would be erased altogether and only the newly expressed and naïve CtIP would be present at the beginning of a new cell cycle. For example, we observed that in response to DNA damage, cells expressing the CtIP-K467A mutant were faster in initiating resection of DSBs compared to cells expressing CtIP-wt. Intriguingly, the K467A mutant could be differently modified than CtIP-wt and therefore have a functional advantage after damage detection. Nevertheless the uncontrolled activity of CtIP, resulting in unscheduled DNA-end resection, would force DSB repair towards HR increasing the chances of forming complex chromosomal rearrangements [296].

In the above-mentioned cell cycle synchronization experiments, we noticed that CtIP migrated much slower on SDS-PAGE in samples prepared from cells arrested in M phase by nocodazole than in samples from untreated cells. The mobility shift in CtIP was most likely not caused by prolonged mitosis enforced by the nocodazole treatment as we obtained a similar migration pattern of CtIP in mitotic extracts using different synchronization protocols. Interestingly, we observed that the shift was abrogated in lysates from nocodazole-arrested cells treated with λ-phosphatase, indicating that CtIP is hyperphosphorylated during mitosis. It was shown that DSBs induced in mitosis are not repaired and that key DDR factor such as 53BP1 and BRCA1 are not recruited to sites of DNA damage [316-318]. Moreover, it has been reported recently that this phenomenon is, at least partially, mediated by inhibitory phosphorylation of RNF8 and 53BP1 [319]. We therefore speculate that CtIP hyperphosphorylation during mitosis is an inhibitory mechanism protecting cells from unwanted DNA-end resection. In fact, DSBs detected during mitosis are only repaired during the next G_1 phase and inheritance of resected DSBs would force the cell to use error-prone repair mechanisms, such as alt-NHEJ [320-322]. Alternatively, it is possible that CtIP hyperphosphorylation protects the protein from being bound by the APC/C during mitosis, and that degradation can only take place after post-mitotic dephosphorylation has occurred. Similarly, it has been shown that Cdc6 and Skp2, two APC/C^{Cdh1} substrates, are protected from degradation by CDK2-dependent phosphorylation [323, 324].

Finally, our study showed that inhibition of APC/C by using a small molecule inhibitor results in a stabilization of CtIP after mitotic exit and during G_1. Even if the activity of CtIP is posed under CDK-dependent control, stabilization of CtIP could

result in an increased frequency of aberrant resection of DSBs occurring in G_1. Especially in the light of the recent discovery that Plk3 can (mis-)activate CtIP during G_1 by mediating the phosphorylation of Ser-327 and Thr-847 to repair complex DSBs, although at the cost of chromosome translocations and large-scale genome deletions [299]. Therefore, it appears to be vital to keep CtIP levels low during G_1. With a two-layered control over CtIP activity, based on both reduced CtIP protein levels and required phosphorylation events, c-NHEJ would be the favored DSB repair pathway during G_1. Nevertheless, a low amount of CtIP molecules could be needed to address complex DSBs formed during G_1, whereas excessive CtIP levels could result in genomic instability. So far, we did not address the question whether cells expressing CtIP-K467A are more prone to resect DSBs during G_1, although it would be extremely interesting to express the CtIP-K467A mutant under the control of the endogenous CtIP promoter. With this approach it would be possible to follow the behavior of the recombinant protein over several cell cycles and challenge cells in different phases of the cell cycle with genotoxic agents.

4.2 APC/C^{Cdh1} reduces CtIP levels after DNA damage in G_2

Besides its predominant role in degrading specific substrate proteins during mitotic exit and G_1 phase, APC/C^{Cdh1} was also implicated in the response to DNA damage occurring in G_2 phase of the cell cycle [82, 191]. Damage-dependent activation of the APC/C results in a stabilization of the G_2/M checkpoint and eventually in the establishment of a senescence state [195, 196]. Interestingly, we discovered that APC/C^{Cdh1} also negatively regulates CtIP protein levels in response to DSBs prior to mitotic entry. Moreover, we observed that APC/C-mediated degradation of CtIP is dose-dependent, occurring most efficiently after high levels of DNA damage. This implies that especially under conditions provoking high amounts of DNA damage, such as those inflicted by high-dose irradiation, premature APC/C^{Cdh1} activation may contribute to determine cell fate and genomic integrity. Remarkably, and in contrast to previous findings, we found that Claspin was readily degraded in an APC/C-dependent manner in irradiated G2 cells [82]. Under normal conditions, Claspin is required for checkpoint-mediated cell cycle arrest in response to DNA damage. However, it has been proposed that DNA damage-induced senescence suppresses checkpoint signaling and, according to our data, APC/C-dependent degradation of Claspin could be an initiating molecular event for checkpoint inactivation in order to

promote senescence [325]. APC/C inhibition in irradiated G_2 cell resulted in a stabilization of CtIP and a decrease in ATM-mediated Chk2 phosphorylation. This could be explained by the notion that progressive DNA-end resection is promoting the switch from the ATM/Chk2 to the ATR/Chk1 signaling cascade [17, 73]. The stabilization of CtIP resulted in an increase of RPA2 phosphorylation, which serves as an indirect readout for DNA-end resection. Nevertheless, we did not observe an increase in Chk1 phosphorylation, suggesting that the downstream signaling of both branches of the G_2/M DNA damage checkpoint is impaired in those cells. Interestingly, the hyper-resection phenotype upon APC/C inhibition in irradiated G_2 cells was also observed in our cells expressing the CtIP-K467A mutant.

We did not further investigate whether increased RPA phosphorylation, and, thus, increased formation of ssDNA, was due to either a higher number of DSBs undergoing normal resection or same number of DSBs undergoing more extensive resection. It has been proposed that during G_2 phase, HR is responsible for the repair of 15-30% of IR-induced DSBs emerging during G_2, whereas the majority of the DSBs is addressed by NHEJ [326-328]. On the one hand, it is possible to speculate that an over-active CtIP mutant could increase the number of resected DNA breaks, and this should result in an increased number of RPA foci observed in irradiated cells expressing the CtIP-K467A mutant. Alternatively, if after damage CtIP would not be degraded, the protein would have the potential of continuously start resecting new DSBs. We therefore hypothesize that, especially in presence of many DSBs, cells try to limit the number of DSBs repaired via the onerous HR pathway. To this end, the degradation of the factor responsible for the initiation of DNA-end resection would shift DSB repair in direction of NHEJ pathways. Furthermore, shortly resected DSBs are the required intermediate for the alt-NHEJ pathway. It would therefore be interesting to investigate whether CtIP-K467A-expressing cells favor the use of mutagenic alt-NHEJ, over the more faithful c-NHEJ repair pathway [236, 329]. On the other hand, a more extensive resection of the same number of DSBs would result in the same number of foci in CtIP-K467A- and CtIP-wt-expressing cells, but those in CtIP-K467A-expressing cells should be bigger or brighter. This question could be addressed using a ChIP-based approach in which, after a DSB has been induced at a precise location, RPA-bound DNA could be immunoprecipitated using an RPA antibody and the extent of resection analyzed using primers annealing at different distances from the break site [330]. CtIP is mainly responsible for initiating DNA-end resection and not for the expansion of the resected tracts. Nevertheless, CtIP is

required to restrain Exo1 activity *in vitro* and mis-regulation of CtIP could result in uncontrolled Exo1-dependent resection *in vivo* [331].

In the live-cell microscopy experiments, we noted that IR-induced CtIP-K467A foci persisted much longer than CtIP-wt foci, indicating that APC/C^{Cdh1} may be involved in the removal of CtIP from DSBs. A similar mechanism was proposed for the degradation of chromatin-bound PTEN during mitosis [332]. Interestingly, Apc3, a structural subunit of the APC/C complex, has been shown to interact with MDC1 in a damage-dependent manner [333], MDC1 directly binds to γH2AX and, thus, is one of the first proteins recruited to DSBs [21, 334]. Although the role of this interaction has never been elucidated, MDC1 may recruit APC/C to sites of DSBs to subsequently facilitate the clearance of CtIP and other DDR factors. Moreover, it was shown that the prolyl-isomerase PIN1 isomerizes CtIP after DNA damage, thereby promoting its proteasome-dependent degradation and limiting its activity [307]. CtIP isomerization could therefore be a mechanism to facilitate CtIP recognition by the APC/C^{Cdh1} complex or a different as yet undefined E3 ligase. However, we did not experimentally address this question.

Remarkably, using a GFP reporter assay we observed that expression of the CtIP-K467A mutant resulted in a similar decrease in HR as seen in the resection-deficient CtIP-T847A mutant. In line with this data, and previous results showing reduced numbers of IR-induced Rad51 foci upon Cdh1 depletion, Rad51 loading onto chromatin is impaired in CtIP-K467A-expressing cells. Taken together, these findings suggest that excessive resection of DSB generates stretches of ssDNA that are ineffective to produce recombinogenic Rad51-ssDNA filaments. Moreover, decreased HR and Rad51 loading on chromatin could also be due to the prolonged presence of CtIP on chromatin, which would sterically hinder Rad51 recruitment. Finally, other components of the HR repair pathway could be under control of the APC/C complex, or a related mechanism, and stabilization of CtIP alone does not lead to a functional outcome because the downstream factors are anyways degraded or not functional.

To conclude our study, we tested the survival of CtIP-K467A-expressing cells after treatment with different genotoxic agents (such as doxorubicin and IR) and the PARP inhibitor olaparib. Even if these cells were less capable in repairing DSBs in different assays, they were only mildly sensitive towards olaparib treatment, which caused hypersensitivity in cells expressing the resection-deficient mutant CtIP-T847A. Moreover, CtIP-K467A-expressing cells were not sensitive to IR or doxorubicin, however low doses of these agents cause lesions that are mainly repaired in a CtIP-

independent manner [261]. Altogether, these results indicate that cells can partially tolerate an increase in DNA-end resection but most likely DSB repair would occur through mutagenic repair pathways. Cells will therefore survive the genotoxic treatment, but at the cost of acquiring mutations [296, 299]. Nevertheless, this hypothesis would need to be addressed experimentally.

5 Conclusions and perspectives

In my PhD thesis I have discovered a novel role for the APC/C^{Cdh1} E3 ubiquitin ligase in regulating CtIP stability and, hence, controlling DSB repair. CtIP plays a pivotal role during DSB repair by initiating DNA-end resection and channeling the repair to HR. Based on our data, we hypothesize that APC/C^{Cdh1}-mediated degradation of CtIP, both during G_1 and after DNA damage in G_2, contributes in choosing the appropriate DSB repair pathway. In G_1, due to the absence of the sister chromatids, cells prefer to fix DSBs by using the c-NHEJ repair pathway, therefore DNA-end resection events are limited by the low levels of CtIP. Differently, after detection of a lesion in G_2, cells initiate repair of a subset of DSBs through the error-free HR, but subsequently limit DNA-end resection by promoting CtIP degradation and hence addressing the remaining DSBs using the faster NHEJ pathway. In fact, excessive HR has been suggested to compromise genome stability [335, 336]. For example, in budding yeast, the inability of completing HR potentially leads to the accumulation of repair intermediates, which cause genomic instability and cell death [337]. Interestingly, work form several laboratories proposed that p53 plays direct role in suppressing HR [338]. One could therefore speculate that p53-dependent activation of APC/C^{Cdh1} and the subsequent degradation of CtIP is part of this anti-recombinogenic mechanism. Moreover, under DNA damage conditions, p53 promotes the maturation of several miRNAs with growth-suppressive functions [339]. We have recently shown that after prolonged DNA damage induction this mechanism results in a miR-19a/b-dependent decrease in CtIP protein and mRNA levels [293].

In response to excessive genotoxic stress during S/G_2, cells quickly have to decide whether it is favorable to either transiently arrest the cell cycle and repair the lesions or to irreversibly withdraw from the cell cycle. It has been shown, that the p53- and p21-dependent import of cyclin B1 in the nucleus and its subsequent degradation in an APC/C-dependent manner commit the cells to establish a senescence state [195, 196]. In fact, in order to retain the ability to re-enter the cell cycle after the activation of the G_2/M checkpoint, cells need to maintain high levels of cell cycle regulators, such as cyclin B1. Interestingly, U2OS cells are impaired in their capability of importing cyclin B1 to the nucleus, therefore they maintain recovery competence much longer than non-transformed cells [197, 340]. Since in U2OS cells, similarly to other transformed cells [341], cyclin B1 is excluded from the nucleus, it is possible to speculate that these cells could specifically exploit the fast and Cdc14B-

dependent activation of the APC/C complex, without the risk of degrading this important cell cycle regulator. Therefore, some cancer cells could use this mechanism to increase their resistance towards genotoxic treatments, by rapidly dampening HR to favor the use of more efficient DNA repair pathways. To test whether this hypothesis holds true, the short- and long-term responses of transformed and untransformed cells should be compared. Moreover a better understanding of the DNA damage-dependent targets of the APC/C complex is needed. To this end, exploiting an APC/C inhibitor such as proTAME in different SILAC studies could be extremely informative. Finally, a characterization of the factors that limit APC/C activity to a defined subset of substrates after DNA damage, will help to understand this regulatory mechanism.

In conclusion, the APC/C is a multisubunit ubiquitin ligase that plays a central role in ensuring the timely progression of the cell cycle. The co-activators Cdh1 and Cdc20 bind to APC/C at different stages of the cell cycle, thereby directing APC/C activity towards defined substrates. Cdc20 expression is positively correlated with human cancers, whereas a possible tumor suppressor role for Cdh1 is suggested for some cancers [342]. The APC/C^{Cdc20} complex is essential for the completion of mitosis: efficient depletion of Cdc20 in cultured cells results in apoptosis, whereas knock-out of Cdc20 causes mouse embryonic lethality at the two-cell stage [167-169]. For these reasons, the APC/C complex has been proposed to be a good therapeutic target for killing cancer cells by prolonged and irreversible mitotic arrest [168, 343]. To date, two APC/C inhibitors have been developed: proTAME and apcin [309, 344]. On one hand, proTAME inhibits APC/C activity by preventing Cdc20 and Cdh1 binding to the APC/C core [309]. On the other hand, apicin binds in close proximity to the WD-40 domain of Cdc20 and inhibits the ability of the co-activator to interact with substrates [344]. Since both inhibitors irreversibly block mitotic exit, by interfering with APC/C function in different ways, the synergistic use of the two drugs achieved the best inhibition of APC/C activity [344]. Residual activity of the APC/C complex would enable cells to escape the mitotic arrest [309, 345], but could be insufficient to ensure the DDR-related functions of APC/C hence resulting in genome instability. Therefore, exploiting APC/C inhibitors to specifically kill cancer cells is an appealing strategy, but the emerging role of the APC/C^{Cdh1} in maintaining genome stability has to be taken into consideration.

6 References

1. Oxford Dictionaries - Definition of Cancer. Available at: http://www.oxforddictionaries.com [Accessed December 5, 2014].
2. National Cancer Institute - What Is Cancer?. Available at: http://www.cancer.gov/cancertopics/cancerlibrary/what-is-cancer [Accessed December 5, 2014].
3. GLOBOCAN 2012 Fact Sheets by Cancer. Available at: http://globocan.iarc.fr/Pages/fact_sheets_cancer.aspx [Accessed December 5, 2014].
4. Wikipedia, the free encyclopedia - War on Cancer. Available at: https://en.wikipedia.org/wiki/War_on_Cancer [Accessed December 5, 2014].
5. Hanahan, D., and Weinberg, R. A. (2000). The hallmarks of cancer. Cell *100*, 57–70.
6. Hanahan, D., and Weinberg, R. A. (2011). Hallmarks of cancer: the next generation. Cell *144*, 646–674.
7. Jackson, S. P., and Bartek, J. (2009). The DNA-damage response in human biology and disease. Nature *461*, 1071–1078.
8. Hoeijmakers, J. H. (2001). Genome maintenance mechanisms for preventing cancer. Nature *411*, 366–374.
9. Cooke, M. S., Evans, M. D., Dizdaroglu, M., and Lunec, J. (2003). Oxidative DNA damage: mechanisms, mutation, and disease. FASEB J. *17*, 1195–1214.
10. Lindahl, T. (1993). Instability and decay of the primary structure of DNA. Nature *362*, 709–715.
11. Salk, J. J., Fox, E. J., and Loeb, L. A. (2010). Mutational heterogeneity in human cancers: origin and consequences. Annu Rev Pathol *5*, 51–75.
12. Negrini, S., Gorgoulis, V. G., and Halazonetis, T. D. (2010). Genomic instability--an evolving hallmark of cancer. Nature Publishing Group *11*, 220–228.
13. Shiloh, Y. (2003). ATM and related protein kinases: safeguarding genome integrity. Nature Reviews Cancer *3*, 155–168.
14. Andegeko, Y., Moyal, L., Mittelman, L., Tsarfaty, I., Shiloh, Y., and Rotman, G. (2001). Nuclear retention of ATM at sites of DNA double strand breaks. J. Biol. Chem. *276*, 38224–38230.
15. Carson, C. T., Schwartz, R. A., Stracker, T. H., Lilley, C. E., Lee, D. V., and Weitzman, M. D. (2003). The Mre11 complex is required for ATM activation and the G2/M checkpoint. EMBO J. *22*, 6610–6620.
16. Gottlieb, T. M., and Jackson, S. P. (1993). The DNA-dependent protein kinase: requirement for DNA ends and association with Ku antigen. Cell *72*, 131–142.
17. Zou, L., and Elledge, S. J. (2003). Sensing DNA damage through ATRIP recognition of RPA-ssDNA complexes. Science *300*, 1542–1548.
18. Yang, X. H., and Zou, L. (2006). Recruitment of ATR-ATRIP, Rad17, and 9-1-1 complexes to DNA damage. Meth. Enzymol. *409*, 118–131.
19. Kotula, E., Faigle, W., Berthault, N., Dingli, F., Loew, D., Sun, J.-S., Dutreix, M., and Quanz, M. (2013). DNA-PK target identification reveals novel links between DNA repair signaling and cytoskeletal regulation. PLoS ONE *8*, e80313.
20. Matsuoka, S., Ballif, B. A., Smogorzewska, A., McDonald, E. R., Hurov, K. E., Luo,

J., Bakalarski, C. E., Zhao, Z., Solimini, N., Lerenthal, Y., et al. (2007). ATM and ATR Substrate Analysis Reveals Extensive Protein Networks Responsive to DNA Damage. Science *316*, 1160–1166.

21. Stucki, M., Clapperton, J. A., Mohammad, D., Yaffe, M. B., Smerdon, S. J., and Jackson, S. P. (2005). MDC1 directly binds phosphorylated histone H2AX to regulate cellular responses to DNA double-strand breaks. Cell *123*, 1213–1226.

22. Bekker-Jensen, S., and Mailand, N. (2010). Assembly and function of DNA double-strand break repair foci in mammalian cells. DNA Repair *9*, 1219–1228.

23. Mailand, N., Bekker-Jensen, S., Faustrup, H., Melander, F., Bartek, J., Lukas, C., and Lukas, J. (2007). RNF8 ubiquitylates histones at DNA double-strand breaks and promotes assembly of repair proteins. Cell *131*, 887–900.

24. Huen, M. S. Y., Grant, R., Manke, I., Minn, K., Yu, X., Yaffe, M. B., and Chen, J. (2007). RNF8 transduces the DNA-damage signal via histone ubiquitylation and checkpoint protein assembly. Cell *131*, 901–914.

25. Kolas, N. K., Chapman, J. R., Nakada, S., Ylanko, J., Chahwan, R., Sweeney, F. D., Panier, S., Mendez, M., Wildenhain, J., Thomson, T. M., et al. (2007). Orchestration of the DNA-damage response by the RNF8 ubiquitin ligase. Science *318*, 1637–1640.

26. Doil, C., Mailand, N., Bekker-Jensen, S., Menard, P., Larsen, D. H., Pepperkok, R., Ellenberg, J., Panier, S., Durocher, D., Bartek, J., et al. (2009). RNF168 binds and amplifies ubiquitin conjugates on damaged chromosomes to allow accumulation of repair proteins. Cell *136*, 435–446.

27. Stewart, G. S., Panier, S., Townsend, K., Al-Hakim, A. K., Kolas, N. K., Miller, E. S., Nakada, S., Ylanko, J., Olivarius, S., Mendez, M., et al. (2009). The RIDDLE syndrome protein mediates a ubiquitin-dependent signaling cascade at sites of DNA damage. Cell *136*, 420–434.

28. Ciccia, A., and Elledge, S. J. (2010). The DNA Damage Response: Making It Safe to Play with Knives. Mol. Cell *40*, 179–204.

29. Cimprich, K. A., and Cortez, D. (2008). ATR: an essential regulator of genome integrity. Nature Publishing Group *9*, 616–627.

30. Smith, J., Tho, L. M., Xu, N., and Gillespie, D. A. (2010). The ATM–Chk2 and ATR–Chk1 Pathways in DNA Damage Signaling and Cancer 1st ed. (Elsevier Inc.).

31. Kumagai, A., and Dunphy, W. G. (2000). Claspin, a novel protein required for the activation of Chk1 during a DNA replication checkpoint response in Xenopus egg extracts. Mol. Cell *6*, 839–849.

32. Kumagai, A., Kim, S.-M., and Dunphy, W. G. (2004). Claspin and the activated form of ATR-ATRIP collaborate in the activation of Chk1. J. Biol. Chem. *279*, 49599–49608.

33. Huehn, D., Bolck, H. A., and Sartori, A. A. (2013). Targeting DNA double-strand break signalling and repair: recent advances in cancer therapy. Swiss Med Wkly *143*, w13837.

34. Savitsky, K., Bar-Shira, A., Gilad, S., Rotman, G., Ziv, Y., Vanagaite, L., Tagle, D. A., Smith, S., Uziel, T., Sfez, S., et al. (1995). A single ataxia telangiectasia gene with a product similar to PI-3 kinase. Science *268*, 1749–1753.

35. Shiloh, Y. (1997). Ataxia-telangiectasia and the Nijmegen breakage syndrome: related disorders but genes apart. Annu. Rev. Genet. *31*, 635–662.

36. Nussenzweig, A., and Nussenzweig, M. C. (2007). A backup DNA repair pathway moves to the forefront. Cell *131*, 223–225.

37. Roy, R., Chun, J., and Powell, S. N. (2012). BRCA1 and BRCA2: different roles in a

common pathway of genome protection. 1–11.

38. Antoniou, A. C., Casadei, S., Heikkinen, T., Barrowdale, D., Pylkäs, K., Roberts, J., Lee, A., Subramanian, D., De Leeneer, K., Fostira, F., et al. (2014). Breast-cancer risk in families with mutations in PALB2. N. Engl. J. Med. *371*, 497–506.

39. Morgan, D. O. (1997). Cyclin-dependent kinases: engines, clocks, and microprocessors. Annu. Rev. Cell Dev. Biol. *13*, 261–291.

40. Malumbres, M., and Barbacid, M. (2005). Mammalian cyclin-dependent kinases. Trends Biochem Sci *30*, 630–641.

41. Pines, J. (2011). Cubism and the cell cycle: the many faces of the APC/C. Nat. Rev. Mol. Cell Biol. *12*, 427–438.

42. Wurzenberger, C., and Gerlich, D. W. (2011). Phosphatases: providing safe passage through mitotic exit. Nature Publishing Group *12*, 469–482.

43. Boutros, R., Lobjois, V., and Ducommun, B. (2007). CDC25 phosphatases in cancer cells: key players? Good targets? Nature Reviews Cancer *7*, 495–507.

44. Cánepa, E. T., Scassa, M. E., Ceruti, J. M., Marazita, M. C., Carcagno, A. L., Sirkin, P. F., and Ogara, M. F. (2007). INK4 proteins, a family of mammalian CDK inhibitors with novel biological functions. IUBMB Life *59*, 419–426.

45. Ullah, Z., Lee, C. Y., and Depamphilis, M. L. (2009). Cip/Kip cyclin-dependent protein kinase inhibitors and the road to polyploidy. Cell Div *4*, 10.

46. Chini, C. C. S., and Chen, J. (2003). Human claspin is required for replication checkpoint control. J. Biol. Chem. *278*, 30057–30062.

47. Jin, J., Shirogane, T., Xu, L., Nalepa, G., Qin, J., Elledge, S. J., and Harper, J. W. (2003). SCFbeta-TRCP links Chk1 signaling to degradation of the Cdc25A protein phosphatase. Genes Dev. *17*, 3062–3074.

48. Mailand, N., Falck, J., Lukas, C., Syljuâsen, R. G., Welcker, M., Bartek, J., and Lukas, J. (2000). Rapid destruction of human Cdc25A in response to DNA damage. Science *288*, 1425–1429.

49. Peng, C. Y., Graves, P. R., Thoma, R. S., Wu, Z., Shaw, A. S., and Piwnica-Worms, H. (1997). Mitotic and G2 checkpoint control: regulation of 14-3-3 protein binding by phosphorylation of Cdc25C on serine-216. Science *277*, 1501–1505.

50. Forrest, A., and Gabrielli, B. (2001). Cdc25B activity is regulated by 14-3-3. Oncogene *20*, 4393–4401.

51. Medema, R. H., and Macůrek, L. (2012). Checkpoint control and cancer. Oncogene *31*, 2601–2613.

52. Takai, H., Naka, K., Okada, Y., Watanabe, M., Harada, N., Saito, S., Anderson, C. W., Appella, E., Nakanishi, M., Suzuki, H., et al. (2002). Chk2-deficient mice exhibit radioresistance and defective p53-mediated transcription. EMBO J. *21*, 5195–5205.

53. Jack, M. T., Woo, R. A., Hirao, A., Cheung, A., Mak, T. W., and Lee, P. W. K. (2002). Chk2 is dispensable for p53-mediated G1 arrest but is required for a latent p53-mediated apoptotic response. Proc. Natl. Acad. Sci. U.S.A. *99*, 9825–9829.

54. Hirao, A., Kong, Y. Y., Matsuoka, S., Wakeham, A., Ruland, J., Yoshida, H., Liu, D., Elledge, S. J., and Mak, T. W. (2000). DNA damage-induced activation of p53 by the checkpoint kinase Chk2. Science *287*, 1824–1827.

55. Hirao, A., Cheung, A., Duncan, G., Girard, P.-M., Elia, A. J., Wakeham, A., Okada, H., Sarkissian, T., Wong, J. A., Sakai, T., et al. (2002). Chk2 is a tumor suppressor that regulates apoptosis in both an ataxia telangiectasia mutated (ATM)-dependent and an ATM-independent manner. Mol. Cell. Biol. *22*, 6521–6532.

56. Ferguson, A. M., White, L. S., Donovan, P. J., and Piwnica-Worms, H. (2005).

Normal cell cycle and checkpoint responses in mice and cells lacking Cdc25B and Cdc25C protein phosphatases. Mol. Cell. Biol. *25*, 2853–2860.

57. O'Connell, M. J., Raleigh, J. M., Verkade, H. M., and Nurse, P. (1997). Chk1 is a wee1 kinase in the G2 DNA damage checkpoint inhibiting cdc2 by Y15 phosphorylation. EMBO J. *16*, 545–554.

58. Agami, R., and Bernards, R. (2000). Distinct initiation and maintenance mechanisms cooperate to induce G1 cell cycle arrest in response to DNA damage. Cell *102*, 55–66.

59. Santra, M. K., Wajapeyee, N., and Green, M. R. (2009). F-box protein FBXO31 mediates cyclin D1 degradation to induce G1 arrest after DNA damage. Nature *459*, 722–725.

60. Hanel, W., and Moll, U. M. (2012). Links between mutant p53 and genomic instability. J. Cell. Biochem. *113*, 433–439.

61. Dai, C., and Gu, W. (2010). p53 post-translational modification: deregulated in tumorigenesis. Trends Mol Med *16*, 528–536.

62. Dulić, V., Kaufmann, W. K., Wilson, S. J., Tlsty, T. D., Lees, E., Harper, J. W., Elledge, S. J., and Reed, S. I. (1994). p53-dependent inhibition of cyclin-dependent kinase activities in human fibroblasts during radiation-induced G1 arrest. Cell *76*, 1013–1023.

63. el-Deiry, W. S., Harper, J. W., O'Connor, P. M., Velculescu, V. E., Canman, C. E., Jackman, J., Pietenpol, J. A., Burrell, M., Hill, D. E., and Wang, Y. (1994). WAF1/CIP1 is induced in p53-mediated G1 arrest and apoptosis. Cancer Res. *54*, 1169–1174.

64. Bunz, F., Dutriaux, A., Lengauer, C., Waldman, T., Zhou, S., Brown, J. P., Sedivy, J. M., Kinzler, K. W., and Vogelstein, B. (1998). Requirement for p53 and p21 to sustain G2 arrest after DNA damage. Science *282*, 1497–1501.

65. Imbriano, C., Gurtner, A., Cocchiarella, F., Di Agostino, S., Basile, V., Gostissa, M., Dobbelstein, M., Del Sal, G., Piaggio, G., and Mantovani, R. (2005). Direct p53 transcriptional repression: in vivo analysis of CCAAT-containing G2/M promoters. Mol. Cell. Biol. *25*, 3737–3751.

66. McKenzie, L., King, S., Marcar, L., Nicol, S., Dias, S. S., Schumm, K., Robertson, P., Bourdon, J.-C., Perkins, N., Fuller-Pace, F., et al. (2010). p53-dependent repression of polo-like kinase-1 (PLK1). cc *9*, 4200–4212.

67. Lahav, G., Rosenfeld, N., Sigal, A., Geva-Zatorsky, N., Levine, A. J., Elowitz, M. B., and Alon, U. (2004). Dynamics of the p53-Mdm2 feedback loop in individual cells. Nat. Genet. *36*, 147–150.

68. Batchelor, E., Loewer, A., Mock, C., and Lahav, G. (2011). Stimulus-dependent dynamics of p53 in single cells. Mol. Syst. Biol. *7*, 488.

69. Kuntz, K., and O'Connell, M. J. (2009). The G(2) DNA damage checkpoint: could this ancient regulator be the Achilles heel of cancer? Cancer Biol. Ther. *8*, 1433–1439.

70. Reinhardt, H. C., Aslanian, A. S., Lees, J. A., and Yaffe, M. B. (2007). p53-deficient cells rely on ATM- and ATR-mediated checkpoint signaling through the p38MAPK/MK2 pathway for survival after DNA damage. Cancer Cell *11*, 175–189.

71. Reinhardt, H. C., Hasskamp, P., Schmedding, I., Morandell, S., van Vugt, M. A. T. M., Wang, X., Linding, R., Ong, S.-E., Weaver, D., Carr, S. A., et al. (2010). DNA damage activates a spatially distinct late cytoplasmic cell-cycle checkpoint network controlled by MK2-mediated RNA stabilization. Mol. Cell *40*, 34–49.

72. Morandell, S., Reinhardt, H. C., Cannell, I. G., Kim, J. S., Ruf, D. M., Mitra, T., Couvillon, A. D., Jacks, T., and Yaffe, M. B. (2013). A reversible gene-targeting strategy identifies synthetic lethal interactions between MK2 and p53 in the DNA

damage response in vivo. CELREP *5*, 868–877.

73. Kousholt, A. N., Fugger, K., Hoffmann, S., Larsen, B. D., Menzel, T., Sartori, A. A., and Sorensen, C. S. (2012). CtIP-dependent DNA resection is required for DNA damage checkpoint maintenance but not initiation. J. Cell Biol. *197*, 869–876.

74. Cotta-Ramusino, C., McDonald, E. R., Hurov, K., Sowa, M. E., Harper, J. W., and Elledge, S. J. (2011). A DNA damage response screen identifies RHINO, a 9-1-1 and TopBP1 interacting protein required for ATR signaling. Science *332*, 1313–1317.

75. Menzel, T., Nähse-Kumpf, V., Kousholt, A. N., Klein, D. K., Lund-Andersen, C., Lees, M., Johansen, J. V., Syljuåsen, R. G., and Sørensen, C. S. (2011). scientific report. EMBO Rep *12*, 705–712.

76. Lindqvist, A., Rodríguez-Bravo, V., and Medema, R. H. (2009). The decision to enter mitosis: feedback and redundancy in the mitotic entry network. J. Cell Biol. *185*, 193–202.

77. van Vugt, M. A. T. M., Bràs, A., and Medema, R. H. (2004). Polo-like kinase-1 controls recovery from a G2 DNA damage-induced arrest in mammalian cells. Mol. Cell *15*, 799–811.

78. Seki, A., Coppinger, J. A., Jang, C.-Y., Yates, J. R., and Fang, G. (2008). Bora and the kinase Aurora a cooperatively activate the kinase Plk1 and control mitotic entry. Science *320*, 1655–1658.

79. Macurek, L., Lindqvist, A., Lim, D., Lampson, M. A., Klompmaker, R., Freire, R., Clouin, C., Taylor, S. S., Yaffe, M. B., and Medema, R. H. (2008). Polo-like kinase-1 is activated by aurora A to promote checkpoint recovery. Nature *455*, 119–123.

80. Jang, Y.-J., Ma, S., Terada, Y., and Erikson, R. L. (2002). Phosphorylation of threonine 210 and the role of serine 137 in the regulation of mammalian polo-like kinase. J. Biol. Chem. *277*, 44115–44120.

81. Smits, V. A., Klompmaker, R., Arnaud, L., Rijksen, G., Nigg, E. A., and Medema, R. H. (2000). Polo-like kinase-1 is a target of the DNA damage checkpoint. Nat. Cell Biol. *2*, 672–676.

82. Bassermann, F., Frescas, D., Guardavaccaro, D., Busino, L., Peschiaroli, A., and Pagano, M. (2008). The Cdc14B-Cdh1-Plk1 axis controls the G2 DNA-damage-response checkpoint. Cell *134*, 256–267.

83. Lobjois, V., Jullien, D., Bouché, J.-P., and Ducommun, B. (2009). The polo-like kinase 1 regulates CDC25B-dependent mitosis entry. Biochim. Biophys. Acta *1793*, 462–468.

84. Toyoshima-Morimoto, F., Taniguchi, E., and Nishida, E. (2002). Plk1 promotes nuclear translocation of human Cdc25C during prophase. EMBO Rep *3*, 341–348.

85. van Vugt, M. A. T. M., Gardino, A. K., Linding, R., Ostheimer, G. J., Reinhardt, H. C., Ong, S.-E., Tan, C. S., Miao, H., Keezer, S. M., Li, J., et al. (2010). A Mitotic Phosphorylation Feedback Network Connects Cdk1, Plk1, 53BP1, and Chk2 to Inactivate the G2/M DNA Damage Checkpoint. PLoS Biol *8*, e1000287.

86. Peschiaroli, A., Dorrello, N. V., Guardavaccaro, D., Venere, M., Halazonetis, T., Sherman, N. E., and Pagano, M. (2006). SCFbetaTrCP-mediated degradation of Claspin regulates recovery from the DNA replication checkpoint response. Mol. Cell *23*, 319–329.

87. Mailand, N., Bekker-Jensen, S., Bartek, J., and Lukas, J. (2006). Destruction of Claspin by SCFbetaTrCP restrains Chk1 activation and facilitates recovery from genotoxic stress. Mol. Cell *23*, 307–318.

88. Watanabe, N., Arai, H., Nishihara, Y., Taniguchi, M., Watanabe, N., Hunter, T., and Osada, H. (2004). M-phase kinases induce phospho-dependent ubiquitination of somatic Wee1 by SCFbeta-TrCP. Proc. Natl. Acad. Sci. U.S.A. *101*, 4419–4424.

89. Lee, D.-H., and Chowdhury, D. (2011). What goes on must come off: phosphatases gate-crash the DNA damage response. Trends Biochem Sci *36*, 569–577.

90. Lindqvist, A., de Bruijn, M., Macurek, L., Bràs, A., Mensinga, A., Bruinsma, W., Voets, O., Kranenburg, O., and Medema, R. H. (2009). Wip1 confers G2 checkpoint recovery competence by counteracting p53-dependent transcriptional repression. EMBO J. *28*, 3196–3206.

91. Fiscella, M., Zhang, H., Fan, S., Sakaguchi, K., Shen, S., Mercer, W. E., Vande Woude, G. F., O'Connor, P. M., and Appella, E. (1997). Wip1, a novel human protein phosphatase that is induced in response to ionizing radiation in a p53-dependent manner. Proc. Natl. Acad. Sci. U.S.A. *94*, 6048–6053.

92. Lu, X., Nannenga, B., and Donehower, L. A. (2005). PPM1D dephosphorylates Chk1 and p53 and abrogates cell cycle checkpoints. Genes Dev. *19*, 1162–1174.

93. Lu, X., Ma, O., Nguyen, T.-A., Jones, S. N., Oren, M., and Donehower, L. A. (2007). The Wip1 Phosphatase acts as a gatekeeper in the p53-Mdm2 autoregulatory loop. Cancer Cell *12*, 342–354.

94. d'Adda di Fagagna, F. (2008). Living on a break: cellular senescence as a DNA-damage response. Nature Reviews Cancer *8*, 512–522.

95. Kuilman, T., Michaloglou, C., Mooi, W. J., and Peeper, D. S. (2010). The essence of senescence. Genes Dev. *24*, 2463–2479.

96. Hayflick, L., and Moorhead, P. S. (1961). The serial cultivation of human diploid cell strains. Exp. Cell Res. *25*, 585–621.

97. Childs, B. G., Baker, D. J., Kirkland, J. L., Campisi, J., and van Deursen, J. M. (2014). Senescence and apoptosis: dueling or complementary cell fates? EMBO Rep.

98. Stein, G. H., Drullinger, L. F., Soulard, A., and Dulić, V. (1999). Differential roles for cyclin-dependent kinase inhibitors p21 and p16 in the mechanisms of senescence and differentiation in human fibroblasts. Mol. Cell. Biol. *19*, 2109–2117.

99. Beausejour, C. M., Krtolica, A., Galimi, F., Narita, M., Lowe, S. W., Yaswen, P., and Campisi, J. (2003). Reversal of human cellular senescence: roles of the p53 and p16 pathways. EMBO J. *22*, 4212–4222.

100. Narita, M., Nũnez, S., Heard, E., Narita, M., Lin, A. W., Hearn, S. A., Spector, D. L., Hannon, G. J., and Lowe, S. W. (2003). Rb-mediated heterochromatin formation and silencing of E2F target genes during cellular senescence. Cell *113*, 703–716.

101. Kosar, M., Bartkova, J., Hubackova, S., Hodny, Z., Lukas, J., and Bartek, J. (2011). Senescence-associated heterochromatin foci are dispensable for cellular senescence, occur in a cell type- and insult-dependent manner and follow expression of p16(ink4a). cc *10*, 457–468.

102. Campisi, J. (2013). Aging, cellular senescence, and cancer. Annu. Rev. Physiol. *75*, 685–705.

103. Dimri, G. P., Lee, X., Basile, G., Acosta, M., Scott, G., Roskelley, C., Medrano, E. E., Linskens, M., Rubelj, I., and Pereira-Smith, O. (1995). A biomarker that identifies senescent human cells in culture and in aging skin in vivo. Proc. Natl. Acad. Sci. U.S.A. *92*, 9363–9367.

104. Kurz, D. J., Decary, S., Hong, Y., and Erusalimsky, J. D. (2000). Senescence-associated (beta)-galactosidase reflects an increase in lysosomal mass during replicative ageing of human endothelial cells. Journal of Cell Science *113 (Pt 20)*, 3613–3622.

105. Erwig, L.-P., and Henson, P. M. (2008). Clearance of apoptotic cells by phagocytes. Cell Death Differ *15*, 243–250.

106. Coppé, J.-P., Patil, C. K., Rodier, F., Sun, Y., Muñoz, D. P., Goldstein, J., Nelson, P. S., Desprez, P.-Y., and Campisi, J. (2008). Senescence-associated secretory phenotypes reveal cell-nonautonomous functions of oncogenic RAS and the p53 tumor suppressor. PLoS Biol *6*, 2853–2868.

107. Jung, T., Catalgol, B., and Grune, T. (2009). The proteasomal system. Molecular Aspects of Medicine *30*, 191–296.

108. Bassermann, F., Eichner, R., and Pagano, M. (2013). Biochimica et Biophysica Acta. BBA - Molecular Cell Research, 1–13.

109. Finley, D. (2009). Recognition and processing of ubiquitin-protein conjugates by the proteasome. Annu. Rev. Biochem. *78*, 477–513.

110. Hershko, A., and Ciechanover, A. (1998). The ubiquitin system. Annu. Rev. Biochem. *67*, 425–479.

111. Peng, J., Schwartz, D., Elias, J. E., Thoreen, C. C., Cheng, D., Marsischky, G., Roelofs, J., Finley, D., and Gygi, S. P. (2003). A proteomics approach to understanding protein ubiquitination. Nat. Biotechnol. *21*, 921–926.

112. Kim, H. T., Kim, K. P., Lledias, F., Kisselev, A. F., Scaglione, K. M., Skowyra, D., Gygi, S. P., and Goldberg, A. L. (2007). Certain pairs of ubiquitin-conjugating enzymes (E2s) and ubiquitin-protein ligases (E3s) synthesize nondegradable forked ubiquitin chains containing all possible isopeptide linkages. J. Biol. Chem. *282*, 17375–17386.

113. Komander, D., and Rape, M. (2012). The Ubiquitin Code. Annu. Rev. Biochem., 1–27.

114. Kulathu, Y., and Komander, D. (2012). Atypical ubiquitylation - the unexplored world of polyubiquitin beyond Lys48 and Lys63 linkages. Nature Publishing Group *13*, 508–523.

115. Komander, D., Clague, M. J., and Urbé, S. (2009). Breaking the chains: structure and function of the deubiquitinases. 1–14.

116. Nakayama, K. I., and Nakayama, K. (2006). Ubiquitin ligases: cell-cycle control and cancer. Nature Reviews Cancer *6*, 369–381.

117. Ye, Y., and Rape, M. (2009). Building ubiquitin chains: E2 enzymes at work. 1–10.

118. Metzger, M. B., Hristova, V. A., and Weissman, A. M. (2012). HECT and RING finger families of E3 ubiquitin ligases at a glance. Journal of Cell Science *125*, 531–537.

119. Rotin, D., and Kumar, S. (2009). Physiological functions of the HECT family of ubiquitin ligases. Nature Publishing Group *10*, 398–409.

120. Deshaies, R. J., and Joazeiro, C. A. P. (2009). RING Domain E3 Ubiquitin Ligases. Annu. Rev. Biochem. *78*, 399–434.

121. Li, W., Bengtson, M. H., Ulbrich, A., Matsuda, A., Reddy, V. A., Orth, A., Chanda, S. K., Batalov, S., and Joazeiro, C. A. P. (2008). Genome-wide and functional annotation of human E3 ubiquitin ligases identifies MULAN, a mitochondrial E3 that regulates the organelle's dynamics and signaling. PLoS ONE *3*, e1487.

122. Skaar, J. R., Pagan, J. K., and Pagano, M. (2013). Mechanisms and function of substrate recruitment by F-box proteins. Nature Publishing Group *14*, 369–381.

123. Chang, L., and Barford, D. (2014). Insights into the anaphase-promoting complex: a molecular machine that regulates mitosis. Curr. Opin. Struct. Biol. *29*, 1–9.

124. Visintin, R., Prinz, S., and Amon, A. (1997). CDC20 and CDH1: a family of substrate-specific activators of APC-dependent proteolysis. Science *278*, 460–463.

125. Vodermaier, H. C., Gieffers, C., Maurer-Stroh, S., Eisenhaber, F., and Peters, J.-M. (2003). TPR Subunits of the Anaphase-Promoting Complex Mediate Binding to the

Activator Protein CDH1. Current Biology *13*, 1459–1468.

126. Kraft, C., Vodermaier, H. C., Maurer-Stroh, S., Eisenhaber, F., and Peters, J.-M. (2005). The WD40 propeller domain of Cdh1 functions as a destruction box receptor for APC/C substrates. Mol. Cell *18*, 543–553.

127. Sikorski, R. S., Boguski, M. S., Goebl, M., and Hieter, P. (1990). A repeating amino acid motif in CDC23 defines a family of proteins and a new relationship among genes required for mitosis and RNA synthesis. Cell *60*, 307–317.

128. Zhang, Z., Chang, L., Yang, J., Conin, N., Kulkarni, K., and Barford, D. (2013). The four canonical tpr subunits of human APC/C form related homo-dimeric structures and stack in parallel to form a TPR suprahelix. J. Mol. Biol. *425*, 4236–4248.

129. Carroll, C. W., Enquist-Newman, M., and Morgan, D. O. (2005). The APC subunit Doc1 promotes recognition of the substrate destruction box. Curr. Biol. *15*, 11–18.

130. Buschhorn, B. A., Petzold, G., Galova, M., Dube, P., Kraft, C., Herzog, F., Stark, H., and Peters, J.-M. (2011). Substrate binding on the APC/C occurs between the coactivator Cdh1 and the processivity factor Doc1. Nature Structural & Molecular Biology *18*, 6–13.

131. Passmore, L. A., McCormack, E. A., Au, S. W. N., Paul, A., Willison, K. R., Harper, J. W., and Barford, D. (2003). Doc1 mediates the activity of the anaphase-promoting complex by contributing to substrate recognition. EMBO J. *22*, 786–796.

132. Carroll, C. W., and Morgan, D. O. (2002). The Doc1 subunit is a processivity factor for the anaphase-promoting complex. Nat. Cell Biol. *4*, 880–887.

133. Chang, L., Zhang, Z., Yang, J., McLaughlin, S. H., and Barford, D. (2014). Molecular architecture and mechanism ofthe anaphase-promoting complex. Nature *513*, 388–393.

134. Dube, P., Herzog, F., Gieffers, C., Sander, B., Riedel, D., Müller, S. A., Engel, A., Peters, J.-M., and Stark, H. (2005). Localization of the coactivator Cdh1 and the cullin subunit Apc2 in a cryo-electron microscopy model of vertebrate APC/C. Mol. Cell *20*, 867–879.

135. Kimata, Y., Baxter, J. E., Fry, A. M., and Yamano, H. (2008). A role for the Fizzy/Cdc20 family of proteins in activation of the APC/C distinct from substrate recruitment. Mol. Cell *32*, 576–583.

136. Matsumoto, M. L., Wickliffe, K. E., Dong, K. C., Yu, C., Bosanac, I., Bustos, D., Phu, L., Kirkpatrick, D. S., Hymowitz, S. G., Rape, M., et al. (2010). K11-Linked Polyubiquitination in Cell Cycle Control Revealed by a K11 Linkage-Specific Antibody. Mol. Cell *39*, 477–484.

137. Wickliffe, K. E., Lorenz, S., Wemmer, D. E., Kuriyan, J., and Rape, M. (2011). The mechanism of linkage-specific ubiquitin chain elongation by a single-subunit E2. Cell *144*, 769–781.

138. Jin, L., Williamson, A., Banerjee, S., Philipp, I., and Rape, M. (2008). Mechanism of ubiquitin-chain formation by the human anaphase-promoting complex. Cell *133*, 653–665.

139. Kirkpatrick, D. S., Hathaway, N. A., Hanna, J., Elsasser, S., Rush, J., Finley, D., King, R. W., and Gygi, S. P. (2006). Quantitative analysis of in vitro ubiquitinated cyclin B1 reveals complex chain topology. Nat. Cell Biol. *8*, 700–710.

140. Williamson, A., Wickliffe, K. E., Mellone, B. G., Song, L., Karpen, G. H., and Rape, M. (2009). Identification of a physiological E2 module for the human anaphase-promoting complex. Proc. Natl. Acad. Sci. U.S.A. *106*, 18213–18218.

141. Wu, T., Merbl, Y., Huo, Y., Gallop, J. L., Tzur, A., and Kirschner, M. W. (2010). UBE2S drives elongation of K11-linked ubiquitin chains by the anaphase-promoting complex. Proc. Natl. Acad. Sci. U.S.A. *107*, 1355–1360.

142. Garnett, M. J., Mansfeld, J., Godwin, C., Matsusaka, T., Wu, J., Russell, P., Pines, J., and Venkitaraman, A. R. (2009). UBE2S elongates ubiquitin chains on APC/C substrates to promote mitotic exit. Nat. Cell Biol. *11*, 1363–1369.

143. Meyer, H.-J., and Rape, M. (2014). Enhanced protein degradation by branched ubiquitin chains. Cell *157*, 910–921.

144. da Fonseca, P. C. A., Kong, E. H., Zhang, Z., Schreiber, A., Williams, M. A., Morris, E. P., and Barford, D. (2011). Structures of APC/C^{Cdh1} with substrates identify Cdh1 and Apc10 as the D-box co-receptor. Nature *470*, 274–278.

145. Glotzer, M., Murray, A. W., and Kirschner, M. W. (1991). Cyclin is degraded by the ubiquitin pathway. Nature *349*, 132–138.

146. Liu, Z., Yuan, F., Ren, J., Cao, J., Zhou, Y., Yang, Q., and Xue, Y. (2012). GPS-ARM: Computational Analysis of the APC/C Recognition Motif by Predicting D-Boxes and KEN-Boxes. PLoS ONE *7*, e34370.

147. Pfleger, C. M., and Kirschner, M. W. (2000). The KEN box: an APC recognition signal distinct from the D box targeted by Cdh1. Genes Dev. *14*, 655–665.

148. He, J., Chao, W. C. H., Zhang, Z., Yang, J., Cronin, N., and Barford, D. (2013). Insights into Degron Recognition by APC/C Coactivators from the Structure of an Acm1-Cdh1 Complex. Mol. Cell, 1–12.

149. Littlepage, L. E., and Ruderman, J. V. (2002). Identification of a new APC/C recognition domain, the A box, which is required for the Cdh1-dependent destruction of the kinase Aurora-A during mitotic exit. Genes Dev. *16*, 2274–2285.

150. Peters, J.-M. (2006). The anaphase promoting complex/cyclosome: a machine designed to destroy. Nat. Rev. Mol. Cell Biol. *7*, 644–656.

151. Hsu, J. Y., Reimann, J. D. R., Sørensen, C. S., Lukas, J., and Jackson, P. K. (2002). E2F-dependent accumulation of hEmi1 regulates S phase entry by inhibiting APC^{Cdh1}. Nat. Cell Biol. *4*, 358–366.

152. Reimann, J. D., Freed, E., Hsu, J. Y., Kramer, E. R., Peters, J. M., and Jackson, P. K. (2001). Emi1 is a mitotic regulator that interacts with Cdc20 and inhibits the anaphase promoting complex. Cell *105*, 645–655.

153. Kraft, C., Herzog, F., Gieffers, C., Mechtler, K., Hagting, A., Pines, J., and Peters, J.-M. (2003). Mitotic regulation of the human anaphase-promoting complex by phosphorylation. EMBO J. *22*, 6598–6609.

154. Shteinberg, M., Protopopov, Y., Listovsky, T., Brandeis, M., and Hershko, A. (1999). Phosphorylation of the cyclosome is required for its stimulation by Fizzy/cdc20. Biochem. Biophys. Res. Commun. *260*, 193–198.

155. Kramer, E. R., Scheuringer, N., Podtelejnikov, A. V., Mann, M., and Peters, J. M. (2000). Mitotic Regulation of the APC Activator Proteins CDC20 and CDH1. Mol. Biol. Cell *11*, 1555–1569.

156. Lukas, C., Sørensen, C. S., Kramer, E., Santoni-Rugiu, E., Lindeneg, C., Peters, J.-M., Bartek, J., and Lukas, J. (1999). Accumulation of cyclin B1 requires E2F and cyclin-A-dependent rearrangement of the anaphase-promoting complex. Nature *401*, 815–818.

157. Cross, F. R. (2003). Two redundant oscillatory mechanisms in the yeast cell cycle. Developmental Cell *4*, 741–752.

158. Moshe, Y., Boulaire, J., Pagano, M., and Hershko, A. (2004). Role of Polo-like kinase in the degradation of early mitotic inhibitor 1, a regulator of the anaphase promoting complex/cyclosome. Proc. Natl. Acad. Sci. U.S.A. *101*, 7937–7942.

159. Hansen, D. V., Loktev, A. V., Ban, K. H., and Jackson, P. K. (2004). Plk1 regulates activation of the anaphase promoting complex by phosphorylating and triggering

$SCF^{\beta TrCP}$-dependent destruction of the APC Inhibitor Emi1. Mol. Biol. Cell *15*, 5623–5634.

160. Lénárt, P., Petronczki, M., Steegmaier, M., Di Fiore, B., Lipp, J. J., Hoffmann, M., Rettig, W. J., Kraut, N., and Peters, J.-M. (2007). The small-molecule inhibitor BI 2536 reveals novel insights into mitotic roles of polo-like kinase 1. Curr. Biol. *17*, 304–315.

161. Di Fiore, B., and Pines, J. (2007). Emi1 is needed to couple DNA replication with mitosis but does not regulate activation of the mitotic APC/C. J. Cell Biol. *177*, 425–437.

162. Kops, G. J. P. L., Weaver, B. A. A., and Cleveland, D. W. (2005). On the road to cancer: aneuploidy and the mitotic checkpoint. Nature Reviews Cancer *5*, 773–785.

163. Primorac, I., and Musacchio, A. (2013). Panta rhei: The APC/C at steady state. J. Cell Biol. *201*, 177–189.

164. Mansfeld, J., Collin, P., Collins, M. O., Choudhary, J. S., and Pines, J. (2011). APC15 drives the turnover of MCC-CDC20 to make the spindle assembly checkpoint responsive to kinetochore attachment. Nat. Cell Biol. *13*, 1234–1243.

165. Yang, M., Li, B., Tomchick, D. R., Machius, M., Rizo, J., Yu, H., and Luo, X. (2007). $p31^{comet}$ blocks Mad2 activation through structural mimicry. Cell *131*, 744–755.

166. Clute, P., and Pines, J. (1999). Temporal and spatial control of cyclin B1 destruction in metaphase. Nat. Cell Biol. *1*, 82–87.

167. Li, M., York, J. P., and Zhang, P. (2007). Loss of Cdc20 causes a securin-dependent metaphase arrest in two-cell mouse embryos. Mol. Cell. Biol. *27*, 3481–3488.

168. Huang, H.-C., Shi, J., Orth, J. D., and Mitchison, T. J. (2009). Evidence that mitotic exit is a better cancer therapeutic target than spindle assembly. Cancer Cell *16*, 347–358.

169. Wolthuis, R., Clay-Farrace, L., van Zon, W., Yekezare, M., Koop, L., Ogink, J., Medema, R., and Pines, J. (2008). Cdc20 and Cks direct the spindle checkpoint-independent destruction of cyclin A. Mol. Cell *30*, 290–302.

170. Sullivan, M., and Morgan, D. O. (2007). Finishing mitosis, one step at a time. Nature Publishing Group *8*, 894–903.

171. Hagting, A., Elzen, Den, N., Vodermaier, H. C., Waizenegger, I. C., Peters, J.-M., and Pines, J. (2002). Human securin proteolysis is controlled by the spindle checkpoint and reveals when the APC/C switches from activation by Cdc20 to Cdh1. J. Cell Biol. *157*, 1125–1137.

172. Jaspersen, S. L., Charles, J. F., and Morgan, D. O. (1999). Inhibitory phosphorylation of the APC regulator Hct1 is controlled by the kinase Cdc28 and the phosphatase Cdc14. Curr. Biol. *9*, 227–236.

173. Stegmeier, F., and Amon, A. (2004). Closing mitosis: the functions of the Cdc14 phosphatase and its regulation. Annu. Rev. Genet. *38*, 203–232.

174. Sigl, R., Wandke, C., Rauch, V., Kirk, J., Hunt, T., and Geley, S. (2009). Loss of the mammalian APC/C activator FZR1 shortens G1 and lengthens S phase but has little effect on exit from mitosis. Journal of Cell Science *122*, 4208–4217.

175. Garcí-Higuera, I., Manchado, E., Dubus, P., Cañamero, M., Méndez, J., Moreno, S., and Malumbres, M. (2008). Genomic stability and tumour suppression by the APC/C cofactor Cdh1. Nature Publishing Group *10*, 802–811.

176. Lindon, C., and Pines, J. (2004). Ordered proteolysis in anaphase inactivates Plk1 to contribute to proper mitotic exit in human cells. J. Cell Biol. *164*, 233–241.

177. Rape, M., Reddy, S. K., and Kirschner, M. W. (2006). The Processivity of Multiubiquitination by the APC Determines the Order of Substrate Degradation. Cell

124, 89–103.

178. Wirth, K. G., Ricci, R., Giménez-Abián, J. F., Taghybeeglu, S., Kudo, N. R., Jochum, W., Vasseur-Cognet, M., and Nasmyth, K. (2004). Loss of the anaphase-promoting complex in quiescent cells causes unscheduled hepatocyte proliferation. Genes Dev. *18*, 88–98.

179. Bashir, T., Dorrello, N. V., Amador, V., Guardavaccaro, D., and Pagano, M. (2004). Control of the SCF(Skp2-Cks1) ubiquitin ligase by the APC/C(Cdh1) ubiquitin ligase. Nature *428*, 190–193.

180. Wei, W., Ayad, N. G., Wan, Y., Zhang, G.-J., Kirschner, M. W., and Kaelin, W. G. (2004). Degradation of the SCF component Skp2 in cell-cycle phase G1 by the anaphase-promoting complex. Nature *428*, 194–198.

181. Li, M., Shin, Y.-H., Hou, L., Huang, X., Wei, Z., Klann, E., and Zhang, P. (2008). The adaptor protein of the anaphase promoting complex Cdh1 is essential in maintaining replicative lifespan and in learning and memory. Nat. Cell Biol. *10*, 1083–1089.

182. Albanese, C., Johnson, J., Watanabe, G., Eklund, N., Vu, D., Arnold, A., and Pestell, R. G. (1995). Transforming p21ras mutants and c-Ets-2 activate the cyclin D1 promoter through distinguishable regions. J. Biol. Chem. *270*, 23589–23597.

183. Miller, J. J. (2006). Emi1 stably binds and inhibits the anaphase-promoting complex/cyclosome as a pseudosubstrate inhibitor. Genes Dev. *20*, 2410–2420.

184. Rape, M., and Kirschner, M. W. (2004). Autonomous regulation of the anaphase-promoting complex couples mitosis to S-phase entry. Nature *432*, 588–595.

185. Listovsky, T., Oren, Y. S., Yudkovsky, Y., Mahbubani, H. M., Weiss, A. M., Lebendiker, M., and Brandeis, M. (2004). Mammalian Cdh1/Fzr mediates its own degradation. EMBO J. *23*, 1619–1626.

186. Fukushima, H., Ogura, K., Wan, L., Lu, Y., Li, V., Gao, D., Liu, P., Lau, A. W., Wu, T., Kirschner, M. W., et al. (2013). SCF-Mediated Cdh1 Degradation Defines a Negative Feedback System that Coordinates Cell-Cycle Progression. CELREP *4*, 803–816.

187. Benmaamar, R., and Pagano, M. (2005). Involvement of the SCF complex in the control of Cdh1 degradation in S-phase. cc *4*, 1230–1232.

188. Lehman, N. L., Tibshirani, R., Hsu, J. Y., Natkunam, Y., Harris, B. T., West, R. B., Masek, M. A., Montgomery, K., van de Rijn, M., and Jackson, P. K. (2007). Oncogenic regulators and substrates of the anaphase promoting complex/cyclosome are frequently overexpressed in malignant tumors. The American Journal of Pathology *170*, 1793–1805.

189. Fujita, T., Liu, W., Doihara, H., and Wan, Y. (2008). Regulation of Skp2-p27 axis by the Cdh1/anaphase-promoting complex pathway in colorectal tumorigenesis. The American Journal of Pathology *173*, 217–228.

190. Fujita, T., Liu, W., Doihara, H., Date, H., and Wan, Y. (2008). Dissection of the APC^{Cdh1}-Skp2 cascade in breast cancer. Clin. Cancer Res. *14*, 1966–1975.

191. Sudo, T., Ota, Y., Kotani, S., Nakao, M., Takami, Y., Takeda, S., and Saya, H. (2001). Activation of Cdh1-dependent APC is required for G1 cell cycle arrest and DNA damage-induced G2 checkpoint in vertebrate cells. EMBO J. *20*, 6499–6508.

192. Mocciaro, A., Berdougo, E., Zeng, K., Black, E., Vagnarelli, P., Earnshaw, W., Gillespie, D., Jallepalli, P., and Schiebel, E. (2010). Vertebrate cells genetically deficient for Cdc14A or Cdc14B retain DNA damage checkpoint proficiency but are impaired in DNA repair. J. Cell Biol. *189*, 631–639.

193. Lee, J., Kim, J. A., Barbier, V., Fotedar, A., and Fotedar, R. (2009). DNA damage triggers p21WAF1-dependent Emi1 down-regulation that maintains G2 arrest. Mol. Biol. Cell *20*, 1891–1902.

194. Wiebusch, L., and Hagemeier, C. (2010). p53- and p21-dependent premature APC/C-Cdh1 activation in G2 is part of the long-term response to genotoxic stress. Oncogene *29*, 3477–3489.

195. Johmura, Y., Shimada, M., Misaki, T., Naiki-Ito, A., Miyoshi, H., Motoyama, N., Ohtani, N., Hara, E., Nakamura, M., Morita, A., et al. (2014). Necessary and Sufficient Role for a Mitosis Skip in Senescence Induction. Mol. Cell, 1–12.

196. Krenning, L., Feringa, F. M., Shaltiel, I. A., van den Berg, J., and Medema, R. H. (2014). Transient Activation of p53 in G2 Phase Is Sufficient to Induce Senescence. Mol. Cell, 1–14.

197. Müllers, E., Cascales, H. S., Jaiswal, H., Saurin, A. T., and Lindqvist, A. (2014). Nuclear translocation of Cyclin B1 marks the restriction point for terminal cell cycle exit in G2 phase. cc *13*, 2733–2743.

198. Takahashi, A., Imai, Y., Yamakoshi, K., Kuninaka, S., Ohtani, N., Yoshimoto, S., Hori, S., Tachibana, M., Anderton, E., Takeuchi, T., et al. (2012). DNA Damage Signaling Triggers Degradation of Histone Methyltransferases through APC/C^{Cdh1} in Senescent Cells. Mol. Cell *45*, 123–131.

199. Frankenberg-Schwager, M., and Frankenberg, D. (1990). DNA double-strand breaks: their repair and relationship to cell killing in yeast. Int. J. Radiat. Biol. *58*, 569–575.

200. Champoux, J. J. (2001). DNA topoisomerases: structure, function, and mechanism. Annu. Rev. Biochem. *70*, 369–413.

201. Gaj, T., Gersbach, C. A., and Barbas, C. F., III (2013). ZFN, TALEN, and CRISPR/Cas-based methods for genome engineering. Trends in Biotechnology *31*, 397–405.

202. Jung, D., Giallourakis, C., Mostoslavsky, R., and Alt, F. W. (2006). Mechanism and control of V(D)J recombination at the immunoglobulin heavy chain locus. Annu. Rev. Immunol. *24*, 541–570.

203. Stavnezer, J., Guikema, J. E. J., and Schrader, C. E. (2008). Mechanism and Regulation of Class Switch Recombination. Annu. Rev. Immunol. *26*, 261–292.

204. Mimitou, E. P., and Symington, L. S. (2009). DNA end resection: many nucleases make light work. DNA Repair *8*, 983–995.

205. Mimitou, E. P., and Symington, L. S. (2011). DNA end resection--unraveling the tail. DNA Repair *10*, 344–348.

206. Blackwood, J. K., Rzechorzek, N. J., Bray, S. M., Maman, J. D., Pellegrini, L., and Robinson, N. P. (2013). End-resection at DNA double-strand breaks in the three domains of life. Biochem. Soc. Trans. *41*, 314–320.

207. Chapman, J. R., Taylor, M. R. G., and Boulton, S. J. (2012). Playing the End Game: DNA Double-Strand Break Repair Pathway Choice. Mol. Cell *47*, 497–510.

208. Gudas, J. M., Li, T., Nguyen, H., Jensen, D., Rauscher, F. J., and Cowan, K. H. (1996). Cell cycle regulation of BRCA1 messenger RNA in human breast epithelial cells. Cell Growth Differ. *7*, 717–723.

209. Yamamoto, A., Taki, T., Yagi, H., Habu, T., Yoshida, K., Yoshimura, Y., Yamamoto, K., Matsushiro, A., Nishimune, Y., and Morita, T. (1996). Cell cycle-dependent expression of the mouse Rad51 gene in proliferating cells. Molecular & general genetics : MGG *251*, 1–12.

210. Ferretti, L. P., Lafranchi, L., and Sartori, A. A. (2013). Controlling DNA-end resection: a new task for CDKs. Front Genet *4*, 99.

211. Aylon, Y., Liefshitz, B., and Kupiec, M. (2004). The CDK regulates repair of double-strand breaks by homologous recombination during the cell cycle. EMBO J. *23*,

4868–4875.

212. Ira, G., Pellicioli, A., Balijja, A., Wang, X., Fiorani, S., Carotenuto, W., Liberi, G., Bressan, D., Wan, L., Hollingsworth, N. M., et al. (2004). DNA end resection, homologous recombination and DNA damage checkpoint activation require CDK1. Nature *431*, 1011–1017.

213. Jazayeri, A., Falck, J., Lukas, C., Bartek, J., Smith, G. C. M., Lukas, J., and Jackson, S. P. (2006). ATM- and cell cycle-dependent regulation of ATR in response to DNA double-strand breaks. Nat. Cell Biol. *8*, 37–45.

214. Deans, A. J., Khanna, K. K., McNees, C. J., Mercurio, C., Heierhorst, J., and McArthur, G. A. (2006). Cyclin-dependent kinase 2 functions in normal DNA repair and is a therapeutic target in BRCA1-deficient cancers. Cancer Res. *66*, 8219–8226.

215. Lieber, M. R. (2010). The Mechanism of Double-Strand DNA Break Repair by the Nonhomologous DNA End-Joining Pathway. Annu. Rev. Biochem. *79*, 181–211.

216. Rothkamm, K., Krüger, I., Thompson, L. H., and Lobrich, M. (2003). Pathways of DNA double-strand break repair during the mammalian cell cycle. Mol. Cell. Biol. *23*, 5706–5715.

217. Ghezraoui, H., Piganeau, M., Renouf, B., Renaud, J.-B., Sallmyr, A., Ruis, B., Oh, S., Tomkinson, A. E., Hendrickson, E. A., Giovannangeli, C., et al. (2014). Chromosomal Translocations in Human Cells Are Generated by Canonical Nonhomologous End-Joining. Mol. Cell, 1–14.

218. Bétermier, M., Bertrand, P., and Lopez, B. S. (2014). Is non-homologous end-joining really an inherently error-prone process? PLoS Genet *10*, e1004086.

219. Uematsu, N., Weterings, E., Yano, K. I., Morotomi-Yano, K., Jakob, B., Taucher-Scholz, G., Mari, P. O., van Gent, D. C., Chen, B. P. C., and Chen, D. J. (2007). Autophosphorylation of DNA-PKCS regulates its dynamics at DNA double-strand breaks. J. Cell Biol. *177*, 219–229.

220. Kim, J. S. (2005). Independent and sequential recruitment of NHEJ and HR factors to DNA damage sites in mammalian cells. J. Cell Biol. *170*, 341–347.

221. Neal, J. A., and Meek, K. (2011). Choosing the right path: does DNA-PK help make the decision? Mutation Research - Fundamental and Molecular Mechanisms of Mutagenesis *711*, 73–86.

222. Kurimasa, A., Kumano, S., Boubnov, N. V., Story, M. D., Tung, C. S., Peterson, S. R., and Chen, D. J. (1999). Requirement for the kinase activity of human DNA-dependent protein kinase catalytic subunit in DNA strand break rejoining. Mol. Cell. Biol. *19*, 3877–3884.

223. Kienker, L. J., Shin, E. K., and Meek, K. (2000). Both V(D)J recombination and radioresistance require DNA-PK kinase activity, though minimal levels suffice for V(D)J recombination. Nucleic Acids Research *28*, 2752–2761.

224. Yoo, S., and Dynan, W. S. (1999). Geometry of a complex formed by double strand break repair proteins at a single DNA end: recruitment of DNA-PKcs induces inward translocation of Ku protein. Nucleic Acids Research *27*, 4679–4686.

225. DeFazio, L. G., Stansel, R. M., Griffith, J. D., and Chu, G. (2002). Synapsis of DNA ends by DNA-dependent protein kinase. EMBO J. *21*, 3192–3200.

226. Meek, K., Douglas, P., Cui, X., Ding, Q., and Lees-Miller, S. P. (2007). trans Autophosphorylation at DNA-dependent protein kinase's two major autophosphorylation site clusters facilitates end processing but not end joining. Mol. Cell. Biol. *27*, 3881–3890.

227. Moshous, D., Callebaut, I., de Chasseval, R., Corneo, B., Cavazzana-Calvo, M., Le Deist, F., Tezcan, I., Sanal, O., Bertrand, Y., Philippe, N., et al. (2001). Artemis, a novel DNA double-strand break repair/V(D)J recombination protein, is mutated in

human severe combined immune deficiency. Cell *105*, 177–186.

228. Ma, Y., Pannicke, U., Schwarz, K., and Lieber, M. R. (2002). Hairpin opening and overhang processing by an Artemis/DNA-dependent protein kinase complex in nonhomologous end joining and V(D)J recombination. Cell *108*, 781–794.

229. Ma, Y., Pannicke, U., Lu, H., Niewolik, D., Schwarz, K., and Lieber, M. R. (2005). The DNA-dependent protein kinase catalytic subunit phosphorylation sites in human Artemis. J. Biol. Chem. *280*, 33839–33846.

230. Kurosawa, A., and Adachi, N. (2010). Functions and regulation of Artemis: a goddess in the maintenance of genome integrity. J. Radiat. Res. *51*, 503–509.

231. Ramsden, D. A. (2011). Polymerases in nonhomologous end joining: building a bridge over broken chromosomes. Antioxid. Redox Signal. *14*, 2509–2519.

232. Ahnesorg, P., Smith, P., and Jackson, S. P. (2006). XLF interacts with the XRCC4-DNA ligase IV complex to promote DNA nonhomologous end-joining. Cell *124*, 301–313.

233. Deriano, L., and Roth, D. B. (2013). Modernizing the Nonhomologous End-Joining Repertoire: Alternative and Classical NHEJ Share the Stage. Annu. Rev. Genet. *47*, 433–455.

234. Boulton, S. J., and Jackson, S. P. (1996). Saccharomyces cerevisiae Ku70 potentiates illegitimate DNA double-strand break repair and serves as a barrier to error-prone DNA repair pathways. EMBO J. *15*, 5093–5103.

235. Kabotyanski, E. B., Gomelsky, L., Han, J. O., Stamato, T. D., and Roth, D. B. (1998). Double-strand break repair in Ku86- and XRCC4-deficient cells. Nucleic Acids Research *26*, 5333–5342.

236. Zhang, Y., and Jasin, M. (2010). An essential role for CtIP in chromosomal translocation formation through an alternative endjoining pathway. Nature Structural & Molecular Biology *18*, 80–84.

237. Chiruvella, K. K., Liang, Z., and Wilson, T. E. (2013). Repair of double-strand breaks by end joining. Cold Spring Harbor Perspectives in Biology *5*, a012757.

238. Boboila, C., Jankovic, M., Yan, C. T., Wang, J. H., Wesemann, D. R., Zhang, T., Fazeli, A., Feldman, L., Nussenzweig, A., Nussenzweig, M., et al. (2010). Alternative end-joining catalyzes robust IgH locus deletions and translocations in the combined absence of ligase 4 and Ku70. Proc. Natl. Acad. Sci. U.S.A. *107*, 3034–3039.

239. Guirouilh-Barbat, J., Rass, E., Plo, I., Bertrand, P., and Lopez, B. S. (2007). Defects in XRCC4 and KU80 differentially affect the joining of distal nonhomologous ends. Proc. Natl. Acad. Sci. U.S.A. *104*, 20902–20907.

240. Simsek, D., and Jasin, M. (2010). Alternative end-joining is suppressed by the canonical NHEJ component Xrcc4-ligase IV during chromosomal translocation formation. Nature Structural & Molecular Biology *17*, 410–416.

241. Rass, E., Grabarz, A., Plo, I., Gautier, J., Bertrand, P., and Lopez, B. S. (2009). Role of Mre11 in chromosomal nonhomologous end joining in mammalian cells. Nature Structural & Molecular Biology *16*, 819–824.

242. Xie, A., Kwok, A., and Scully, R. (2009). Role of mammalian Mre11 in classical and alternative nonhomologous end joining. Nature Structural & Molecular Biology *16*, 814–818.

243. Simsek, D., Brunet, E., Wong, S. Y.-W., Katyal, S., Gao, Y., McKinnon, P. J., Lou, J., Zhang, L., Li, J., Rebar, E. J., et al. (2011). DNA ligase III promotes alternative nonhomologous end-joining during chromosomal translocation formation. PLoS Genet *7*, e1002080.

244. Boboila, C., Oksenych, V., Gostissa, M., Wang, J. H., Zha, S., Zhang, Y., Chai, H.,

Lee, C.-S., Jankovic, M., Saez, L.-M. A., et al. (2012). Robust chromosomal DNA repair via alternative end-joining in the absence of X-ray repair cross-complementing protein 1 (XRCC1). Proc. Natl. Acad. Sci. U.S.A. *109*, 2473–2478.

245. Stark, J. M., Pierce, A. J., Oh, J., Pastink, A., and Jasin, M. (2004). Genetic Steps of Mammalian Homologous Repair with Distinct Mutagenic Consequences. Mol. Cell. Biol. *24*, 9305–9316.

246. Moynahan, M. E., and Jasin, M. (2010). Mitotic homologous recombination maintains genomic stability and suppresses tumorigenesis. Nature Publishing Group *11*, 196–207.

247. Pedersen, B. S., and De, S. (2013). Loss of heterozygosity preferentially occurs in early replicating regions in cancer genomes. Nucleic Acids Research *41*, 7615–7624.

248. Mao, Z., Bozzella, M., Seluanov, A., and Gorbunova, V. (2008). DNA repair by nonhomologous end joining and homologous recombination during cell cycle in human cells. cc *7*, 2902–2906.

249. Karanam, K., Kafri, R., Loewer, A., and Lahav, G. (2012). Quantitative live cell imaging reveals a gradual shift between DNA repair mechanisms and a maximal use of HR in mid S phase. Mol. Cell *47*, 320–329.

250. Elliott, B., Richardson, C., and Jasin, M. (2005). Chromosomal translocation mechanisms at intronic alu elements in mammalian cells. Mol. Cell *17*, 885–894.

251. Byrne, M., Wray, J., Reinert, B., Wu, Y., Nickoloff, J., Lee, S.-H., Hromas, R., and Williamson, E. (2014). Mechanisms of oncogenic chromosomal translocations. Ann. N. Y. Acad. Sci. *1310*, 89–97.

252. Weinstock, D. M., Elliott, B., and Jasin, M. (2006). A model of oncogenic rearrangements: differences between chromosomal translocation mechanisms and simple double-strand break repair. Blood *107*, 777–780.

253. Symington, L. S., and Gautier, J. (2011). Double-Strand Break End Resection and Repair Pathway Choice. Annu. Rev. Genet. *45*, 110301100158074.

254. Mimitou, E. P., and Symington, L. S. (2008). Sae2, Exo1 and Sgs1 collaborate in DNA double-strand break processing. Nature *455*, 770–774.

255. Zhu, Z., Chung, W.-H., Shim, E. Y., Lee, S. E., and Ira, G. (2008). Sgs1 Helicase and Two Nucleases Dna2 and Exo1 Resect DNA Double-Strand Break Ends. Cell *134*, 981–994.

256. Shibata, A., Moiani, D., Arvai, A. S., Perry, J., Harding, S. M., Genois, M.-M., Maity, R., van Rossum-Fikkert, S., Kertokalio, A., Romoli, F., et al. (2013). DNA Double-Strand Break Repair Pathway Choice Is Directed by Distinct MRE11 Nuclease Activities. Mol. Cell, 1–12.

257. Garcia, V., Phelps, S. E. L., Gray, S., and Neale, M. J. (2011). Bidirectional resection of DNA double-strand breaks by Mre11 and Exo1. Nature *479*, 241–244.

258. Cannavó, E., and Cejka, P. (2014). Sae2 promotes dsDNA endonuclease activity within Mre11–Rad50–Xrs2 to resect DNA breaks. Nature, 1–16.

259. Clerici, M., Mantiero, D., Guerini, I., Lucchini, G., and Longhese, M. P. (2008). The Yku70-Yku80 complex contributes to regulate double-strand break processing and checkpoint activation during the cell cycle. EMBO Rep *9*, 810–818.

260. D'Amours, D., and Jackson, S. P. (2002). The Mre11 complex: at the crossroads of dna repair and checkpoint signalling. Nat. Rev. Mol. Cell Biol. *3*, 317–327.

261. Sartori, A. A., Lukas, C., Coates, J., Mistrik, M., Fu, S., Bartek, J., Baer, R., Lukas, J., and Jackson, S. P. (2007). Human CtIP promotes DNA end resection. Nature *450*, 509–514.

262. Wang, H., Li, Y., Truong, L. N., Shi, L. Z., Hwang, P. Y.-H., He, J., Do, J., Cho, M. J., Li, H., Negrete, A., et al. (2014). CtIP Maintains Stability at Common Fragile Sites and Inverted Repeats by End Resection-Independent Endonuclease Activity. Mol. Cell.

263. Makharashvili, N., Tubbs, A. T., Yang, S.-H., Wang, H., Barton, O., Zhou, Y., Deshpande, R. A., Lee, J.-H., Lobrich, M., Sleckman, B. P., et al. (2014). Catalytic and Noncatalytic Roles of the CtIP Endonuclease in Double-Strand Break End Resection. Mol. Cell.

264. Symington, L. S. (2014). DNA repair: Making the cut. Nature.

265. Gravel, S., Chapman, J. R., Magill, C., and Jackson, S. P. (2008). DNA helicases Sgs1 and BLM promote DNA double-strand break resection. Genes Dev. *22*, 2767–2772.

266. Symington, L. S. (2014). End resection at double-strand breaks: mechanism and regulation. Cold Spring Harbor Perspectives in Biology *6*.

267. Oakley, G. G., and Patrick, S. M. (2010). Replication protein A: directing traffic at the intersection of replication and repair. Front Biosci (Landmark Ed) *15*, 883–900.

268. Cejka, P., Cannavó, E., Polaczek, P., Masuda-Sasa, T., Pokharel, S., Campbell, J. L., and Kowalczykowski, S. C. (2010). DNA end resection by Dna2-Sgs1-RPA and its stimulation by Top3-Rmi1 and Mre11-Rad50-Xrs2. Nature *467*, 112–116.

269. Niu, H., Chung, W.-H., Zhu, Z., Kwon, Y., Zhao, W., Chi, P., Prakash, R., Seong, C., Liu, D., Lu, L., et al. (2010). Mechanism of the ATP-dependent DNA end-resection machinery from Saccharomyces cerevisiae. Nature *467*, 108–111.

270. Chen, H., Lisby, M., and Symington, L. S. (2013). RPA coordinates DNA end resection and prevents formation of DNA hairpins. Mol. Cell *50*, 589–600.

271. Sung, P., and Klein, H. (2006). Mechanism of homologous recombination: mediators and helicases take on regulatory functions. Nat. Rev. Mol. Cell Biol. *7*, 739–750.

272. Krejci, L., Altmannova, V., Spirek, M., and Zhao, X. (2012). Homologous recombination and its regulation. Nucleic Acids Research *40*, 5795–5818.

273. McIlwraith, M. J., McIlwraith, M. J., Vaisman, A., Liu, Y., Fanning, E., Woodgate, R., and West, S. C. (2005). Human DNA polymerase eta promotes DNA synthesis from strand invasion intermediates of homologous recombination. Mol. Cell *20*, 783–792.

274. Sebesta, M., Burkovics, P., Juhasz, S., Zhang, S., Szabo, J. E., Lee, M. Y. W. T., Haracska, L., and Krejci, L. (2013). Role of PCNA and TLS polymerases in D-loop extension during homologous recombination in humans. DNA Repair *12*, 691–698.

275. Schwartz, E. K., and Heyer, W.-D. (2011). Processing of joint molecule intermediates by structure-selective endonucleases during homologous recombination in eukaryotes. Chromosoma *120*, 109–127.

276. Bizard, A. H., and Hickson, I. D. (2014). The dissolution of double Holliday junctions. Cold Spring Harbor Perspectives in Biology *6*, a016477.

277. Andersen, S. L., and Sekelsky, J. (2010). Meiotic versus mitotic recombination: two different routes for double-strand break repair: the different functions of meiotic versus mitotic DSB repair are reflected in different pathway usage and different outcomes. Bioessays *32*, 1058–1066.

278. Huertas, P., Cortés-Ledesma, F., Sartori, A. A., Aguilera, A., and Jackson, S. P. (2008). CDK targets Sae2 to control DNA-end resection and homologous recombination. Nature *455*, 689–692.

279. Penkner, A., Portik-Dobos, Z., Tang, L., Schnabel, R., Novatchkova, M., Jantsch, V., and Loidl, J. (2007). A conserved function for a Caenorhabditis elegans Com1/Sae2/CtIP protein homolog in meiotic recombination. EMBO J. *26*

280. Limbo, O., Chahwan, C., Yamada, Y., de Bruin, R. A. M., Wittenberg, C., and Russell, P. (2007). Ctp1 is a cell-cycle-regulated protein that functions with Mre11 complex to control double-strand break repair by homologous recombination. Mol. Cell *28*, 134–146.

281. Meloni, A. R., Smith, E. J., and Nevins, J. R. (1999). A mechanism for Rb/p130-mediated transcription repression involving recruitment of the CtBP corepressor. Proc. Natl. Acad. Sci. U.S.A. *96*, 9574–9579.

282. Schaeper, U., Subramanian, T., Lim, L., Boyd, J. M., and Chinnadurai, G. (1998). Interaction between a cellular protein that binds to the C-terminal region of adenovirus E1A (CtBP) and a novel cellular protein is disrupted by E1A through a conserved PLDLS motif. J. Biol. Chem. *273*, 8549–8552.

283. Wong, A. K., Ormonde, P. A., Pero, R., Chen, Y., Lian, L., Salada, G., Berry, S., Lawrence, Q., Dayananth, P., Ha, P., et al. (1998). Characterization of a carboxy-terminal BRCA1 interacting protein. Oncogene *17*, 2279–2285.

284. Chinnadurai, G. (2009). The transcriptional corepressor CtBP: a foe of multiple tumor suppressors. Cancer Res. *69*, 731–734.

285. Fusco, C., Reymond, A., and Zervos, A. S. (1998). Molecular cloning and characterization of a novel retinoblastoma-binding protein. Genomics *51*, 351–358.

286. Liu, F., and Lee, W.-H. (2006). CtIP activates its own and cyclin D1 promoters via the E2F/RB pathway during G1/S progression. Mol. Cell. Biol. *26*, 3124–3134.

287. Chen, P.-L., Liu, F., Cai, S., Lin, X., Li, A., Chen, Y., Gu, B., Lee, E. Y.-H. P., and Lee, W.-H. (2005). Inactivation of CtIP leads to early embryonic lethality mediated by G1 restraint and to tumorigenesis by haploid insufficiency. Mol. Cell. Biol. *25*, 3535–3542.

288. Chinnadurai, G. (2006). CtIP, a candidate tumor susceptibility gene is a team player with luminaries. Biochimica et Biophysica Acta (BBA) - Reviews on Cancer *1765*, 67–73.

289. Koipally, J., and Georgopoulos, K. (2002). Ikaros-CtIP interactions do not require C-terminal binding protein and participate in a deacetylase-independent mode of repression. J. Biol. Chem. *277*, 23143–23149.

290. Rebollo, A., and Schmitt, C. (2003). Ikaros, Aiolos and Helios: transcription regulators and lymphoid malignancies. Immunol. Cell Biol. *81*, 171–175.

291. Ott, G., Rosenwald, A., and Campo, E. (2013). Understanding MYC-driven aggressive B-cell lymphomas: pathogenesis and classification. Blood *122*, 3884–3891.

292. Jin, H. Y., Oda, H., Lai, M., Skalsky, R. L., Bethel, K., Shepherd, J., Kang, S. G., Liu, W.-H., Sabouri-Ghomi, M., Cullen, B. R., et al. (2013). MicroRNA-17~92 plays a causative role in lymphomagenesis by coordinating multiple oncogenic pathways. EMBO J. *32*, 2377–2391.

293. Hühn, D., Kousholt, A. N., Sorensen, C. S., and Sartori, A. A. (2014). miR-19, a component of the oncogenic miR-17~92 cluster, targets the DNA-end resection factor CtIP. Oncogene *0*.

294. Fu, Q., Chow, J., Bernstein, K. A., Makharashvili, N., Arora, S., Lee, C. F., Person, M. D., Rothstein, R., and Paull, T. T. (2013). Phosphorylation-regulated transitions in oligomeric state control the activity of the Sae2 DNA repair enzyme. Mol. Cell. Biol.

295. Yu, X., and Baer, R. (2000). Nuclear localization and cell cycle-specific expression of CtIP, a protein that associates with the BRCA1 tumor suppressor. J. Biol. Chem. *275*, 18541–18549.

296. Huertas, P., and Jackson, S. P. (2009). Human CtIP mediates cell cycle control of DNA end resection and double strand break repair. J. Biol. Chem. *284*, 9558–9565.

297. Huertas, P. (2010). DNA resection in eukaryotes: deciding how to fix the break. Nature Structural & Molecular Biology *17*, 11–16.

298. Wang, H., Shi, L. Z., Wong, C. C. L., Han, X., Hwang, P. Y.-H., Truong, L. N., Zhu, Q., Shao, Z., Chen, D. J., Berns, M. W., et al. (2013). The interaction of CtIP and Nbs1 connects CDK and ATM to regulate HR-mediated double-strand break repair. PLoS Genet *9*, e1003277.

299. Barton, O., Naumann, S. C., Diemer-Biehs, R., Künzel, J., Steinlage, M., Conrad, S., Makharashvili, N., Wang, J., Feng, L., Lopez, B. S., et al. (2014). Polo-like kinase 3 regulates CtIP during DNA double-strand break repair in G1. J. Cell Biol. *206*, 877–894.

300. Yu, X., and Chen, J. (2004). DNA damage-induced cell cycle checkpoint control requires CtIP, a phosphorylation-dependent binding partner of BRCA1 C-terminal domains. Mol. Cell. Biol. *24*, 9478–9486.

301. Chen, L., Nievera, C. J., Lee, A. Y.-L., and Wu, X. (2008). Cell cycle-dependent complex formation of BRCA1.CtIP.MRN is important for DNA double-strand break repair. J. Biol. Chem. *283*, 7713–7720.

302. Yu, X., Wu, L. C., Bowcock, A. M., Aronheim, A., and Baer, R. (1998). The C-terminal (BRCT) domains of BRCA1 interact in vivo with CtIP, a protein implicated in the CtBP pathway of transcriptional repression. J. Biol. Chem. *273*, 25388–25392.

303. Buis, J., Stoneham, T., Spehalski, E., and Ferguson, D. O. (2012). Mre11 regulates CtIP-dependent double-strand break repair by interaction with CDK2. Nature Structural & Molecular Biology.

304. Polato, F., Callen, E., Wong, N., Faryabi, R., Bunting, S., Chen, H.-T., Kozak, M., Kruhlak, M. J., Reczek, C. R., Lee, W.-H., et al. (2014). CtIP-mediated resection is essential for viability and can operate independently of BRCA1. Journal of Experimental Medicine *211*, 1027–1036.

305. Reczek, C. R., Szabolcs, M., Stark, J. M., Ludwig, T., and Baer, R. (2013). The interaction between CtIP and BRCA1 is not essential for resection-mediated DNA repair or tumor suppression. J. Cell Biol. *201*, 693–707.

306. You, Z., Shi, L. Z., Zhu, Q., Wu, P., Zhang, Y.-W., Basilio, A., Tonnu, N., Verma, I. M., Berns, M. W., and Hunter, T. (2009). CtIP links DNA double-strand break sensing to resection. Mol. Cell *36*, 954–969.

307. Steger, M., Murina, O., Hühn, D., Ferretti, L. P., Walser, R., Hänggi, K., Lafranchi, L., Neugebauer, C., Paliwal, S., Janscak, P., et al. (2013). Prolyl Isomerase PIN1 Regulates DNA Double-Strand Break Repair by Counteracting DNA End Resection. Mol. Cell *50*, 333–343.

308. Liou, Y.-C., Zhou, X. Z., and Lu, K. P. (2011). Prolyl isomerase Pin1 as a molecular switch to determine the fate of phosphoproteins. Trends Biochem Sci.

309. Zeng, X., Sigoillot, F., Gaur, S., Choi, S., Pfaff, K. L., Oh, D.-C., Hathaway, N., Dimova, N., Cuny, G. D., and King, R. W. (2010). Pharmacologic inhibition of the anaphase-promoting complex induces a spindle checkpoint-dependent mitotic arrest in the absence of spindle damage. Cancer Cell *18*, 382–395.

310. Eguren, M., Manchado, E., and Malumbres, M. (2011). Non-mitotic functions of the Anaphase-Promoting Complex. Seminars in Cell & Developmental Biology *22*, 572–578.

311. Ke, P. Y., and Chang, Z. F. (2003). Mitotic Degradation of Human Thymidine Kinase 1 Is Dependent on the Anaphase-Promoting Complex/Cyclosome-Cdh1-Mediated Pathway. Mol. Cell. Biol. *24*, 514–526.

312. Burton, J. L., and Solomon, M. J. (2001). D box and KEN box motifs in budding yeast Hsl1p are required for APC-mediated degradation and direct binding to Cdc20p and

Cdh1p. Genes Dev. *15*, 2381–2395.

313. Barford, D. (2011). Structural insights into anaphase-promoting complex function and mechanism. Philosophical Transactions of the Royal Society B: Biological Sciences *366*, 3605–3624.

314. You, Z., and Bailis, J. M. (2010). DNA damage and decisions: CtIP coordinates DNA repair and cell cycle checkpoints. Trends Cell Biol. *20*, 402–409.

315. Kaidi, A., Weinert, B. T., Choudhary, C., and Jackson, S. P. (2010). Human SIRT6 promotes DNA end resection through CtIP deacetylation. Science *329*, 1348–1353.

316. Giunta, S., Belotserkovskaya, R., and Jackson, S. P. (2010). DNA damage signaling in response to double-strand breaks during mitosis. J. Cell Biol. *190*, 197–207.

317. Zhang, W., Peng, G., Lin, S.-Y., and Zhang, P. (2011). DNA damage response is suppressed by the high cyclin-dependent kinase 1 activity in mitotic mammalian cells. Journal of Biological Chemistry *286*, 35899–35905.

318. Nelson, G., Buhmann, M., and Zglinicki, von, T. (2009). DNA damage foci in mitosis are devoid of 53BP1. cc *8*, 3379–3383.

319. Orthwein, A., Fradet-Turcotte, A., Noordermeer, S. M., Canny, M. D., Brun, C. M., Strecker, J., Escribano-Diaz, C., and Durocher, D. (2014). Mitosis Inhibits DNA Double-Strand Break Repair to Guard Against Telomere Fusions. Science.

320. Giunta, S., and Jackson, S. P. (2011). Give me a break, but not in mitosis: the mitotic DNA damage response marks DNA double-strand breaks with early signaling events. cc *10*, 1215–1221.

321. Lukas, C., Savic, V., Bekker-Jensen, S., Doil, C., Neumann, B., Pedersen, R. S., Grøfte, M., Chan, K. L., Hickson, I. D., Bartek, J., et al. (2011). 53BP1 nuclear bodies form around DNA lesions generated by mitotic transmission of chromosomes under replication stress. Nat. Cell Biol. *13*, 243–253.

322. Heijink, A. M., Krajewska, M., and van Vugt, M. A. T. M. (2013). The DNA damage response during mitosis. Mutation Research - Fundamental and Molecular Mechanisms of Mutagenesis *750*, 45–55.

323. Rodier, G., Coulombe, P., Tanguay, P.-L., Boutonnet, C., and Meloche, S. (2008). Phosphorylation of Skp2 regulated by CDK2 and Cdc14B protects it from degradation by APC(Cdh1) in G1 phase. EMBO J. *27*, 679–691.

324. Mailand, N., and Diffley, J. F. X. (2005). CDKs promote DNA replication origin licensing in human cells by protecting Cdc6 from APC/C-dependent proteolysis. Cell *122*, 915–926.

325. Gabai, V. L., O'Callaghan-Sunol, C., Meng, L., Sherman, M. Y., and Yaglom, J. (2008). Triggering senescence programs suppresses Chk1 kinase and sensitizes cells to genotoxic stresses. Cancer Res. *68*, 1834–1842.

326. Shibata, A., Conrad, S., Birraux, J., Geuting, V., Barton, O., Ismail, A., Kakarougkas, A., Meek, K., Taucher-Scholz, G., Lobrich, M., et al. (2011). Factors determining DNA double-strand break repair pathway choice in G2 phase. EMBO J. *30*, 1079–1092.

327. Mao, Z., Bozzella, M., Seluanov, A., and Gorbunova, V. (2008). Comparison of nonhomologous end joining and homologous recombination in human cells. DNA Repair *7*, 1765–1771.

328. Beucher, A., Birraux, J., Tchouandong, L., Barton, O., Shibata, A., Conrad, S., Goodarzi, A. A., Krempler, A., Jeggo, P. A., and Lobrich, M. (2009). ATM and Artemis promote homologous recombination of radiation-induced DNA double-strand breaks in G2. EMBO J. *28*, 3413–3427.

329. Bennardo, N., Cheng, A., Huang, N., and Stark, J. M. (2008). Alternative-NHEJ is a

mechanistically distinct pathway of mammalian chromosome break repair. PLoS Genet *4*, e1000110.

330. Yamane, A., Robbiani, D. F., Resch, W., Bothmer, A., Nakahashi, H., Oliveira, T., Rommel, P. C., Brown, E. J., Nussenzweig, A., Nussenzweig, M. C., et al. (2013). RPA accumulation during class switch recombination represents 5“-3” DNA-end resection during the S-G2/M phase of the cell cycle. CELREP *3*, 138–147.

331. Eid, W., Steger, M., El-Shemerly, M., Ferretti, L. P., Pena-Diaz, J., König, C., Valtorta, E., Sartori, A. A., and Ferrari, S. (2010). DNA end resection by CtIP and exonuclease 1 prevents genomic instability. EMBO Rep, 1–7.

332. Choi, B. H., Pagano, M., Huang, C., and Dai, W. (2014). Cdh1, a Substrate-recruiting Component of Anaphase-promoting Complex/Cyclosome (APC/C) Ubiquitin E3 Ligase, Specifically Interacts with Phosphatase and Tensin Homolog (PTEN) and Promotes Its Removal from Chromatin. J. Biol. Chem. *289*, 17951–17959.

333. Coster, G., Hayouka, Z., Argaman, L., Strauss, C., Friedler, A., Brandeis, M., and Goldberg, M. (2007). The DNA damage response mediator MDC1 directly interacts with the anaphase-promoting complex/cyclosome. J. Biol. Chem. *282*, 32053–32064.

334. Jungmichel, S., and Stucki, M. (2010). MDC1: The art of keeping things in focus. Chromosoma *119*, 337–349.

335. Richardson, C., Stark, J. M., Ommundsen, M., and Jasin, M. (2004). Rad51 overexpression promotes alternative double-strand break repair pathways and genome instability. Oncogene *23*, 546–553.

336. Guirouilh-Barbat, J., Lambert, S., Bertrand, P., and Lopez, B. S. (2014). Is homologous recombination really an error-free process? Front Genet *5*, 175.

337. Gangloff, S., Soustelle, C., and Fabre, F. (2000). Homologous recombination is responsible for cell death in the absence of the Sgs1 and Srs2 helicases. Nat. Genet. *25*, 192–194.

338. Bertrand, P., Saintigny, Y., and Lopez, B. S. (2004). p53's double life: transactivation-independent repression of homologous recombination. Trends in Genetics *20*, 235–243.

339. Suzuki, H. I., Yamagata, K., Sugimoto, K., Iwamoto, T., Kato, S., and Miyazono, K. (2009). Modulation of microRNA processing by p53. Nature *460*, 529–533.

340. Krenning, L., and Medema, R. H. (2014). Enter the nucleus to exit the cycle. cc *13*, 2651–2652.

341. Smeets, M. F., Mooren, E. H., and Begg, A. C. (1994). The effect of radiation on G2 blocks, cyclin B expression and cdc2 expression in human squamous carcinoma cell lines with different radiosensitivities. Radiother Oncol *33*, 217–227.

342. Zhang, J., Wan, L., Dai, X., Sun, Y., and Wei, W. (2014). Functional characterization of Anaphase Promoting Complex/Cyclosome (APC/C) E3 ubiquitin ligases in tumorigenesis. BBA - Reviews on Cancer *1845*, 1–17.

343. Taniguchi, K., Momiyama, N., Ueda, M., Matsuyama, R., Mori, R., Fujii, Y., Ichikawa, Y., Endo, I., Togo, S., and Shimada, H. (2008). Targeting of CDC20 via small interfering RNA causes enhancement of the cytotoxicity of chemoradiation. Anticancer Res. *28*, 1559–1563.

344. Sackton, K. L., Dimova, N., Zeng, X., Tian, W., Zhang, M., Sackton, T. B., Meaders, J., Pfaff, K. L., Sigoillot, F., Yu, H., et al. (2014). Synergistic blockade of mitotic exit by two chemical inhibitors of the APC/C. Nature *514*, 646–649.

345. Brito, D. A., and Rieder, C. L. (2006). Mitotic checkpoint slippage in humans occurs via cyclin B destruction in the presence of an active checkpoint. Curr. Biol. *16*, 1194–1200.

7 Curriculum vitae

PERSONAL INFORMATION

Surname:	**LAFRANCHI**
Name:	**Lorenzo**
Date of Birth:	**January 22th, 1987**
Place of origin:	**Monteceneri/Medeglia, TI**

EDUCATION AND TRAINING

09/2011 - 01/2015	**Ph.D., University of Zurich, Zurich, Switzerland** Enrolled in the Cancer Biology Ph.D. program, Life Science Zurich Graduate School Employed as a PhD student in the group of Prof. A.A. Sartori, Institute of Molecular Cancer Research, UZH, Zurich *Title of the Ph.D. thesis: "APC/C^{Cdh1} contributes to maintenance of genome stability by targeting the DNA-end resection factor CtIP"*
09/2009 - 05/2011	**M.Sc. in Biochemistry, Swiss Federal Institute of Technology (ETH), Zurich, Switzerland** Trained as a M.Sc. student in the group of Prof. C.M. Azzalin, Institute of Biochemistry, ETH, Zurich *Title of the M.Sc. thesis: "Characterization of structure and functions of telomeric transcripts in S. pombe"*
10/2006 - 10/2009	**B.Sc. in Biology - Chemical direction,** Swiss Federal Institute of Technology (ETH), Zurich, Switzerland
09/2002 - 06/2006	**Maturity - Focus on Biology and Chemistry,** Liceo Cantonale Bellinzona, Switzerland

LIST OF PUBLICATIONS

Lafranchi L., de Boer H.R., de Vries E.G., Ong S.-E., Sartori A.A., and van Vugt M.A. (2014) *APC/C-Cdh1 controls CtIP stability during the cell cycle and in response to DNA damage.* EMBO J 33(23), 2860-2879

Ferretti L.P.[1], Lafranchi L.[1], and Sartori A.A. (2013) *Controlling DNA-end resection: a new task for CDKs*. Front Genet. 4:99

[1]these authors contributed equally to this work

Steger M., Murina O., Huehn D., Ferretti L.P., Walser R., Haenggi K.,Lafranchi L., Neugebauer C., Paliwal S., Janscak P., Gerrits B., Zerbe O., and Sartori A.A. (2013) *Prolyl Isomerase PIN1 Regulates DNA Double-Strand Break Repair by Counteracting DNA End Resection*. Mol Cell 50(3), 333-343

PRESENTATIONS AT SCIENTIFIC CONFERENCES

Copenhagen Bioscience Conferences “PTMs in cell signaling”, Hillerod, Denmark (September 14-18, 2014). Poster presentation: *APC/C-Cdh1 controls CtIP stability during the cell cycle and in response to DNA damage*

“Swiss Meeting on Genome Stability and Chromatin Dynamics”, Weggis, Switzerland (May 26-28, 2014). Oral presentation: *APC/C-Cdh1 at the crossroads between cell cycle regulation and DNA repair*

EMBO Conference Series “The DNA damage response in cell physiology and disease”, Cape Sounio, Greece (October 7-11, 2013). Poster presentation: *The APC/C^{Cdh1} E3 ubiquitin ligase regulates CtIP turnover*

TEACHING EXPERIENCES

University of Zurich (April 2012 and 2013) Organization and supervision of the annual practical course: “Genome Instability and Molecular Cancer Research”

University of Zurich (December 2011) Supervision of the practical course: "Classical and Molecular Genetics"

8 Acknowledgements

I would like to thank all my colleagues and friends who helped and supported me during my time as PhD student.

First of all, I would like to express my appreciation to Prof. Alessandro A. Sartori for giving me the opportunity to join his lab as a PhD student and for his supervision over the years. Moreover, I would like to thank all the present and past members of the Sartori lab for all the scientific and non-scientific interactions. I am particularly grateful to Dani for proofreading the thesis and Hella, Julia and Sarah for helping me with the German summary. I am also thankful to Martin for introducing me to lab work at the beginning of my PhD and Hella for nice days in the “small lab”.

I acknowledge and thank my thesis committee members Dr. Izabela Sumara, Prof. Claus M. Azzalin and Prof. Ian J. Frew for critical discussions and valuable suggestions.

I would also like to thank Prof. Marcel A.T. van Vugt and Rolf de Boer for the nice collaboration. Sharing and discussing data has been an enriching experience.

I wish to thank all the present and past members of the IMCR for the nice and collaborative atmosphere.

Thanks to Mauro for many coffees and theories, but also thanks to all my friends for fun and sustainment.

Un grazie immenso anche alla mia famiglia, senza la quale non avrei mai potuto raggiungere questo traguardo. Il vostro sostegno e la vostra approvazione sono stati e saranno sempre importanti per le mie scelte.

Finally, I praise Dani; for being there and for being as she is.

9 Appendix

9.1 Prolyl Isomerase PIN1 Regulates DNA Double-Strand Break Repair by Counteracting DNA End Resection

Article published in “Molecular Cell”, 2013

Authors:

Steger M., Murina O., Huehn D., Ferretti L.P., Walser R., Haenggi K., Lafranchi L., Neugebauer C., Paliwal S., Janscak P., Gerrits B., Zerbe O., and Sartori A.A.

Contributions:

I performed the GST-pulldown experiments shown and quantified in figure 2C.

Molecular Cell
Article

Prolyl Isomerase PIN1 Regulates DNA Double-Strand Break Repair by Counteracting DNA End Resection

Martin Steger,[1] Olga Murina,[1] Daniela Hühn,[1] Lorenza P. Ferretti,[1] Reto Walser,[2] Kay Hänggi,[1] Lorenzo Lafranchi,[1] Christine Neugebauer,[1] Shreya Paliwal,[1] Pavel Janscak,[1] Bertran Gerrits,[3] Giannino Del Sal,[4,5] Oliver Zerbe,[2] and Alessandro A. Sartori[1,*]
[1]Institute of Molecular Cancer Research
[2]Institute of Organic Chemistry
[3]Functional Genomics Center Zurich
University of Zurich, Winterthurerstrasse 190, CH-8057 Zürich, Switzerland
[4]Laboratorio Nazionale CIB, Area Science Park, Padriciano 99, 34149 Trieste, Italy
[5]Department of Life Sciences, University of Trieste, 34100 Trieste, Italy
*Correspondence: sartori@imcr.uzh.ch
http://dx.doi.org/10.1016/j.molcel.2013.03.023

SUMMARY

The regulation of DNA double-strand break (DSB) repair by phosphorylation-dependent signaling pathways is crucial for the maintenance of genome stability; however, remarkably little is known about the molecular mechanisms by which phosphorylation controls DSB repair. Here, we show that PIN1, a phosphorylation-specific prolyl isomerase, interacts with key DSB repair factors and affects the relative contributions of homologous recombination (HR) and nonhomologous end-joining (NHEJ) to DSB repair. We find that PIN1-deficient cells display reduced NHEJ due to increased DNA end resection, whereas resection and HR are compromised in PIN1-overexpressing cells. Moreover, we identify CtIP as a substrate of PIN1 and show that DSBs become hyperresected in cells expressing a CtIP mutant refractory to PIN1 recognition. Mechanistically, we provide evidence that PIN1 impinges on CtIP stability by promoting its ubiquitylation and subsequent proteasomal degradation. Collectively, these data uncover PIN1-mediated isomerization as a regulatory mechanism coordinating DSB repair.

INTRODUCTION

In response to DNA double-strand breaks (DSBs), cells initiate an elaborate signaling cascade known as the DNA damage response (DDR) to maintain genomic integrity (Jackson and Bartek, 2009). The DDR coordinates cell-cycle checkpoints and DNA repair or—if the damage cannot be repaired—triggers specialized programs such as apoptosis and senescence (Ciccia and Elledge, 2010). DSBs are the most cytotoxic lesions that are induced by ionizing radiation (IR) and DNA topoisomerase II poisons, such as etoposide (ETOP) and doxorubicin (Jackson and Bartek, 2009). They also frequently arise during S phase when replication forks encounter persistent single-strand breaks that are caused by camptothecin (CPT), a DNA topoisomerase I poison, or poly(ADP-ribose) polymerase (PARP) inhibitors (Pommier, 2006; Rouleau et al., 2010). Although DSBs are suitable substrates for both homologous recombination (HR) and nonhomologous end-joining (NHEJ), DSBs resulting from replication fork collapse are preferentially repaired by HR, whereas those induced by IR and ETOP are mostly addressed by NHEJ (Helleday, 2010; Shibata et al., 2011). It has been shown that NHEJ largely contributes to genomic instability and cytotoxicity in HR-defective cells treated with CPT or PARP inhibitors (Adachi et al., 2004; Eid et al., 2010; Patel et al., 2011). In contrast, HR is able to compensate to some degree for the repair of IR-induced DSBs in NHEJ mutant cells during late S/G2 phase (Beucher et al., 2009; Shibata et al., 2011).

HR is a rather slow, multistep repair process restricted to S/G2 phase when the intact sister chromatid is available to allow error-free repair (Heyer et al., 2010). Briefly, HR requires 5′ to 3′ nucleolytic degradation of DSB ends to generate long stretches of single-stranded DNA (ssDNA) - a mechanism generally described as DNA end resection. In vertebrates, DNA end resection is initiated by the collaborative action of the MRE11-RAD50-NBS1 (MRN) complex together with CtIP (Sartori et al., 2007). Subsequently, EXO1 and BLM are involved in long-range resection exposing long 3′ ssDNA tails that are immediately coated with RPA (Gravel et al., 2008). Finally, BRCA2 promotes the exchange of RPA with RAD51, allowing ssDNA-RAD51 nucleoprotein filaments to carry out homology search and DNA strand invasion (Heyer et al., 2010). In contrast, NHEJ occurs with faster kinetics and functions throughout the cell cycle (Shibata et al., 2011). Besides cell-cycle stage and DSB complexity, the division of labor between the two DSB repair pathways was shown to depend on the chromatin state around the lesion (Goodarzi et al., 2010). Mechanistically, however, DNA end resection is the key determinant of DSB repair pathway choice, because it prevents repair by NHEJ and commits cells to HR (Chapman et al., 2012).

Besides ATM-mediated phosphorylation of substrates at S/T-Q motifs in response to DSBs, phosphorylation at S/T-P

motifs is another major signaling mechanism in the regulation of cell-cycle progression and various stress responses (Matsuoka et al., 2007; Bennetzen et al., 2010). Enzymes responsible for S/T-P phosphorylation belong to a large family of proline-directed protein kinases, including cyclin-dependent kinases (CDKs) and mitogen-activated protein kinases (MAPKs) (Ubersax and Ferrell, 2007). Strikingly, CDK activity is required for DNA end resection and HR (Aylon et al., 2004; Ira et al., 2004; Huertas et al., 2008). However, it is currently unclear how, mechanistically, phosphorylation affects DSB repair pathway choice. Interestingly, a subset of proteins phosphorylated at S/T-P motifs exist in two different configurations, namely as *cis* and *trans* isoforms. The intrinsically slow interconversion between these two forms can be catalyzed by PIN1, which specifically binds phosphorylated S/T-P motifs through its WW domain and catalyzes *cis*/*trans* isomerization through its peptidylprolyl isomerase (PPIase) domain (Yaffe et al., 1997). In this way, PIN1 acts as a molecular switch to control the function of several proteins, including cell-cycle regulators and transcription factors, but so far has not been linked to DNA repair processes (Liou et al., 2011).

Here, we report that PIN1 interacts with prominent DSB repair factors including 53BP1, BRCA1-BARD1, and CtIP. Using immortalized and cancer cell lines, we find that PIN1 overexpression attenuates HR, while PIN1 depletion reduces NHEJ as a result of increased DNA end resection. We further demonstrate that PIN1-mediated isomerization of CtIP requires CtIP phosphorylation at two conserved S/T-P motifs (S276 and T315) and show that CDK2 activity is required for PIN1-CtIP interaction. We report that cells expressing a phosphomutant form of CtIP (CtIP-2A) deficient in PIN1 interaction exhibit hyperresection phenotypes similar to PIN1-deficient cells. Finally, we provide evidence that PIN1 negatively regulates CtIP protein stability by promoting CtIP polyubiquitylation and subsequent proteasomal degradation. Altogether, our findings uncover a key role for the prolyl isomerase PIN1 in controlling CtIP-dependent DNA end resection and, consequently, DSB repair.

RESULTS

PIN1 Isomerase Is Involved in the Regulation of DSB Repair

The importance of S/T-P phosphorylation in the regulation of DSB repair and the fact that PIN1 modulates the function of proteins phosphorylated at S/T-P motifs through proline isomerization prompted us to examine whether PIN1 interacts with DSB repair proteins. To this end, we performed pull-down experiments with recombinant GST-tagged PIN1, followed by mass spectrometry (MS) analysis. Besides known PIN1 substrates and many potentially novel PIN1 interaction partners, we identified several prominent DDR factors implicated in DSB repair, including BRCA1, 53BP1, and CtIP (see Figure S1 and Table S1 available online). Since all these factors were shown to be involved in DSB repair pathway choice, we examined whether PIN1 affects the repair of DSB by NHEJ or HR using cell lines bearing EJ5-GFP or DR-GFP reporter cassettes, respectively (Bennardo et al., 2008). Depletion of PIN1 decreased NHEJ frequencies to levels similar to those achieved by depleting key NHEJ factors such as XRCC4 and 53BP1 (Figure 1A) (Bunting et al., 2010). Conversely, we observed a slight but statistically significant increase in HR efficiency upon PIN1 depletion in both HEK293 and U2OS DR-GFP cells, while CtIP depletion resulted in a strong reduction in HR, as expected (Figure 1B and Figure S2A) (Sartori et al., 2007; Bennardo et al., 2008). Based on these observations, we speculated that high levels of PIN1 could interfere with HR. Indeed, transient overexpression of PIN1 caused a significant decrease in the HR reporter signal, without affecting the cell-cycle distribution (Figure 1C and Figure S2B). Importantly, the negative effect of PIN1 on HR was dependent on both substrate recognition and isomerization, as overexpression of a phospho-binding mutant (W34A) or a catalytic mutant (C113A) diminished HR to a lesser extent (1.4- and 2.0-fold, respectively) compared to wild-type (WT) (3.1-fold) (Figure 1C).

Next, we examined whether DSB signaling is altered in U2OS cells depleted for PIN1 by analyzing the phosphorylation status of prominent DDR factors after ETOP treatment. Interestingly, knockdown of PIN1 caused a marked increase in RPA2 hyperphosphorylation, indicative of increased ssDNA formation, but did not alter cell-cycle distribution profiles (Figure 1D, Figures S2C and S2D) (Sartori et al., 2007; Kousholt et al., 2012). Moreover, in agreement with increased rates of DNA end resection, we found that PIN1-depleted cells were more resistant to CPT than control-depleted cells, a phenotype which is reminiscent of NHEJ-deficient cells (Figure S2E) (Adachi et al., 2004; Eid et al., 2010; Shibata et al., 2011).

To further investigate whether loss of PIN1 indeed compromises NHEJ, we used pulsed-field gel electrophoresis (PFGE) to monitor the efficiency of *Pin1* knockout mouse embryonic fibroblasts (MEFs) in repairing ETOP-induced DSBs. *Pin1*$^{-/-}$ MEFs displayed both increased RPA2 phosphorylation and slower repair kinetics compared to PIN1-complemented cells, indicative of a defect in NHEJ caused by increased DNA resection (Figure 1E and Figure S2F). Consistent with impaired DNA end resection, we detected a clear reduction in IR-induced phosphorylation of RPA2 at S4/S8 after transient overexpression of PIN1-wt compared to mock-transfected cells or to cells overexpressing PIN1-W34A (Figure 1F and Figure S2G). Since we have identified the DNA end resection factor CtIP in our screen for PIN1 interactors (Figure S1), we addressed whether CtIP could be responsible for the observed hyperresection phenotype of PIN1-deficient cells. To this end, we depleted PIN1, CtIP, or both factors together from U2OS cells and monitored RPA foci formation in response to ETOP treatment as readout for DSB resection (Figure 1G and Figure S2H). As expected, approximately 25% of control-depleted cells exhibited RPA foci, and their formation was strictly CtIP dependent (Helleday, 2010; Shibata et al., 2011). Furthermore, and consistent with increased RPA2 phosphorylation, depletion of PIN1 led to an almost 2-fold increase in RPA-foci-positive cells. Remarkably, this increase was entirely dependent on CtIP, suggesting that PIN1 limits the resection activity of CtIP. Similarly, codepletion of CtIP partially rescued the NHEJ defect in PIN1-depleted HEK293 EJ5-GFP reporter cells, further demonstrating that PIN1 promotes NHEJ by counteracting CtIP-dependent DNA resection (Figure 1H). The fact that

Molecular Cell
PIN1 Isomerase Regulates DSB Repair

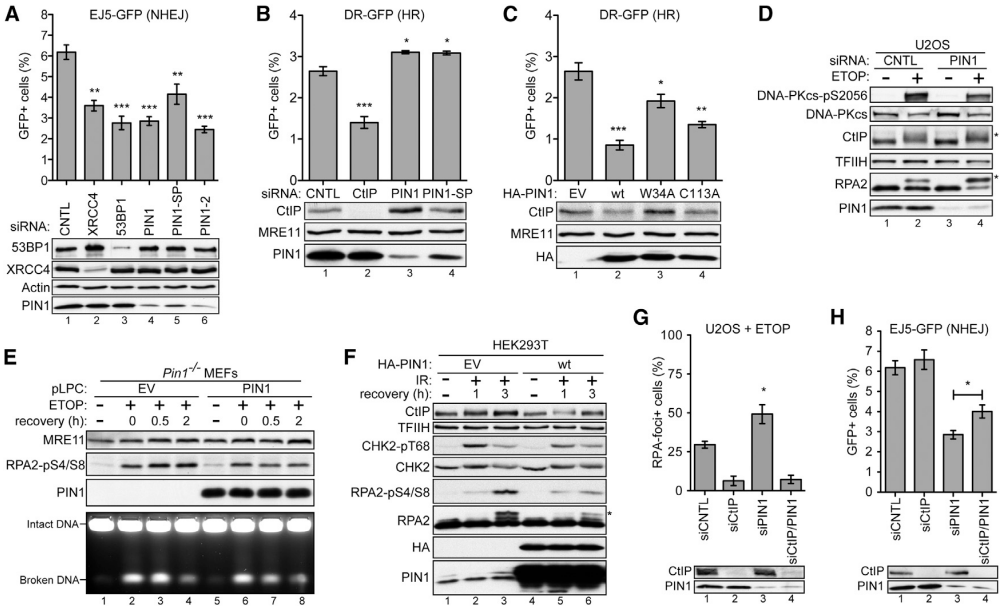

Figure 1. PIN1 Regulates DSB Repair

(A) HEK293 EJ5-GFP cells were transfected with the indicated siRNAs. Two days later, cells were transfected with the I-SceI expression plasmid and harvested after 48 hr for flow cytometry and immunoblot analysis.

(B) HEK293 DR-GFP cells were transfected with the indicated siRNAs and further processed as in (A).

(C) HEK293 DR-GFP cells were cotransfected with the indicated HA-PIN1 variants together with the I-SceI plasmid and further processed as in (A).

(D) Control- or PIN1-depleted U2OS cells were treated with etoposide (ETOP, 20 μM) for 6 hr, and whole-cell extracts were analyzed by immunoblotting. Asterisks indicate hyperphosphorylated forms of CtIP and RPA2, respectively.

(E) *Pin1*$^{-/-}$ MEFs complemented with empty vector (EV, pLPC) or PIN1 were treated with ETOP (10 μM) for 2 hr and lysed at the indicated times after ETOP removal. Whole-cell extracts were analyzed by immunoblotting, and the amount of broken DNA was assessed by PFGE followed by ethidium bromide (EtBr) staining (see also Figure S2F for quantification of the PFGE signals).

(F) HEK293T cells were transfected with empty vector (EV, pcDNA3.1) or HA-PIN1-wt for 72 hr. Cells were irradiated (30 Gy) and whole-cell extracts were prepared at indicated times and analyzed by immunoblotting. Asterisk indicates hyperphosphorylated form of RPA2.

(G) Forty-eight hours after transfection with the indicated siRNAs, U2OS cells grown on coverslips were treated with ETOP (5 μM) for 1 hr, fixed, and coimmunostained for γ-H2AX and RPA2 (see also Figure S2H). In each sample at least 50 cells were scored. Graph shows the percentage of cells exhibiting more than 10 RPA foci/nuclei. Immunoblot analysis of the same samples is shown below.

(H) Shown is NHEJ assay and immunoblot analysis after transfection with the indicated siRNAs as in (A). In (A), (B), (C), (G), and (H), data are represented as mean ± SEM (n ≥ 3). See also Figure S2.

CtIP depletion did not fully restore NHEJ could be explained by the possibility that, besides restricting the function of CtIP in DNA end resection, PIN1 may facilitate NHEJ through alternative mechanisms. For instance, we have identified 53BP1 and BRCA1 as putative PIN1 substrates (Figure S1), both playing key roles in the regulation of DSB repair pathway choice (Bunting et al., 2010).

PIN1 Interacts with CtIP Phosphorylated at Two S/T-P Motifs

To confirm the result of our MS analysis, suggesting that PIN1 and CtIP form a complex, we subjected whole-cell extracts from U2OS cells or from U2OS cells stably expressing GFP-tagged CtIP to GST-PIN1 pull-down assays. We found that both endogenous CtIP and GFP-CtIP interact with PIN1-wt but not with the PIN1-W34A mutant, indicating that the interaction is mediated by phosphorylation (Figure 2A). Consistently, treatment of extracts with λ-phosphatase prior to GST-PIN1 pull-down completely abolished the interaction with CtIP (Figures S3A and S3B). Next, we verified whether endogenous PIN1-CtIP complexes exist in cells by performing proximity ligation assays (in situ PLA), an elegant method to detect protein-protein interactions in situ (Söderberg et al., 2006). As shown in Figure 2B, we detected robust PLA signals in most of the cells, demonstrating interaction between PIN1 and CtIP. Moreover, we repeatedly observed more PLA signals per nucleus in EdU-positive cells than in EdU-negative cells, indicative of an increased PIN1-CtIP interaction during S phase (Figure 2B and Figure S3C).

Human CtIP contains in total 12 S/T-P motifs that could be targeted by proline-directed kinases (Figure S3D). To identify which of these motifs are recognized by PIN1, we tested the binding of PIN1 to a panel of serine/threonine to alanine point mutants of CtIP in a series of GST pull-down experiments

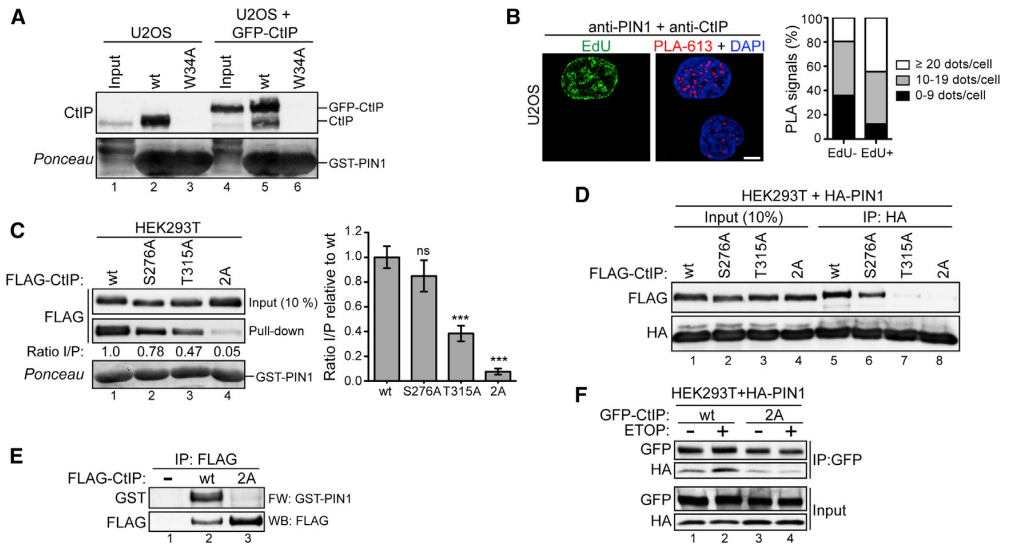

Figure 2. PIN1 Interacts with CtIP through Phosphorylated S/T-P Motifs

(A) GST-PIN1-wt or -W34A fusion proteins were immobilized on glutathione-Sepharose beads and incubated with whole-cell extracts from either U2OS cells (lanes 1–3) or U2OS cells stably expressing GFP-CtIP (lanes 4–6). Inputs and precipitated bead fractions from the pull-downs were subjected to immunoblotting with anti-CtIP antibodies.

(B) (Left) Detection of endogenous PIN1-CtIP complexes by in situ proximity ligation assay (PLA). U2OS cells were pulse labeled with 5′-ethynyl-2′-deoxyuridine (EdU, 10 μM) for 15 min, fixed, and incubated with antibodies against PIN1 and CtIP prior to detection of protein-protein interactions using a fluorescently labeled probe (PLA-613). Nuclei were visualized by DAPI staining, and EdU incorporation was detected according to the manufacturer's instructions (see also Figure S3C). (Right) Quantification of the PLA signals/cell. For both conditions, PLA signals from at least 50 cells were enumerated. Scale bar, 5 μm.

(C) (Left) GST-PIN1 pull-down assay using extracts of HEK293T cells expressing indicated FLAG-tagged versions of CtIP. The band intensities were quantified using ImageJ and represented as input/pull-down (I/P) ratios. (Right) Data are represented as mean values of densitometric quantification ± SEM ($n \geq 5$).

(D) HEK293T cells were cotransfected with HA-PIN1 and the indicated FLAG-CtIP plasmids. HA-PIN1 was immunoprecipitated from whole-cell extracts using anti-HA antibody, and immunocomplexes were analyzed by western blotting.

(E) Anti-FLAG immunoprecipitates from empty vector- or FLAG-CtIP-transfected HEK293T cells were subjected to far-western blotting using purified GST-PIN1 as a probe, followed by immunodetection with anti-GST antibody. After stripping, the same membrane was reprobed using anti-FLAG antibody.

(F) HEK293T cells were cotransfected with GFP-CtIP (wt and 2A) and HA-PIN1 for 48 hr before treatment with ETOP (10 μM) for 2 hr. Whole-cell extracts were analyzed by western blotting before (input) and after immunoprecipitation (IP) using anti-GFP antibody. See also Figure S3.

(Figures S3E–S3G). Our analysis revealed that PIN1-CtIP interaction is mainly mediated by T315 and is almost completely abolished in cells expressing a CtIP-S276A/T315A double mutant (CtIP-2A; Figure 2C). To corroborate these findings, we performed anti-HA immunoprecipitation experiments in HEK293T cells cotransfected with FLAG-CtIP and HA-PIN1 expression constructs. As expected, CtIP-wt did not interact with PIN1-W34A but was efficiently coprecipitated with PIN1-wt and PIN1-C113A (Figure S3H). Moreover, we were able to confirm that mutating either S276 or T315 to nonphosphorylatable alanine reduced the binding to PIN1, while PIN1-CtIP interaction is almost completely abolished in the CtIP-2A mutant (Figure 2D). In addition, far-western blot analysis indicated that this interaction is direct and that CtIP-T315 is more crucial for PIN1 binding than CtIP-S276 (Figure 2E and Figure S3I). Finally, we addressed whether PIN1-CtIP interaction is influenced by DNA damage and observed a slight increase in complex formation upon ETOP treatment, suggesting that CtIP phosphorylation at S276 and/or T315 may be induced upon DNA damage (Figure 2F).

CtIP-T315 Phosphorylation Promotes PIN1-CtIP Interaction

By examining the amino acid sequences surrounding S276 and T315, we noticed that both residues are highly conserved in mammals, suggesting that they are possibly targeted by proline-directed kinases in vivo (Figure S4A). In order to address whether T315 and S276 are indeed phosphorylated in vivo, we raised individual phospho-specific antibodies. As a first line of evidence, both phospho-antibodies recognized wt CtIP transiently overexpressed in cells, but not the corresponding alanine substitution mutants (Figure 3A). Second, we specifically detected CtIP-T315 after immunoprecipitating endogenous CtIP from HEK293T cells followed by immunoblotting with the anti-pT315 antibody, whereas the signal completely disappeared upon pretreatment of the extracts with λ-phosphatase (Figure 3B).

We next investigated whether CtIP-T315 phosphorylation increased after ETOP treatment but did not observe any significant changes in pT315 levels, suggesting that the enhanced binding of PIN1 to CtIP in presence of DNA damage (Figure 2F)

Molecular Cell
PIN1 Isomerase Regulates DSB Repair

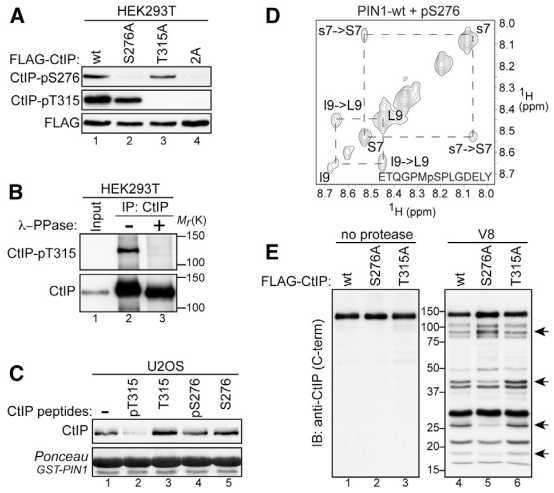

Figure 3. CtIP-T315 and CtIP-S276 Are Phosphorylated to Promote PIN1 Binding and *cis*/*trans* Isomerization

(A) Extracts from HEK293T cells transfected for 48 hr with the indicated FLAG-CtIP constructs were immunoblotted with either rabbit polyclonal antibodies raised against CtIP phosphopeptides or with anti-FLAG antibody.

(B) Extracts from HEK293T cells were treated with λ-PPase, immunoprecipitated using anti-CtIP antibody, and immunoblotted with the indicated antibodies.

(C) GST-PIN1 pull-down assays were performed using U2OS whole-cell extracts (0.5 mg) supplemented with the indicated CtIP peptides (80 μg).

(D) Shown is selected region of the two-dimensional ROESY spectra of the CtIP-pS276 peptide after incubation with purified, recombinant GST-PIN1.

(E) HEK293T cells were transfected with the indicated FLAG-CtIP constructs for 72 hr. CtIP proteins were purified using M2 magnetic beads, eluted with 3xFLAG peptides, digested with V8 protease, and analyzed by western blotting using anti-CtIP antibody. See also Figure S4 and Figure S5.

is mediated more by CtIP-S276 phosphorylation (Figure S4B). Finally, we were able to confirm the phosphorylation on T315 in vivo by MS analysis of CtIP immunoprecipitated from HEK293T cells (Figure S4C). To further substantiate our previous findings that pT315 is more crucial for PIN1 binding compared to pS276 (Figures 2C and 2D), we used synthetic CtIP phosphopeptides and examined their ability to compete for PIN1 binding in GST-PIN1 pull-down experiments. Remarkably, we found that increasing amounts of pT315 peptides completely abolished PIN1-CtIP interaction, whereas pS276 peptides and the nonphosphopeptides failed to do so, strongly suggesting that CtIP-pT315 is the preferred PIN1 binding site (Figure 3C and Figure S5A).

CtIP-S276 Phosphorylation Promotes CtIP Isomerization by PIN1

To determine whether PIN1 catalyzes *cis*/*trans* isomerization of the phosphorylated S/T-P motifs in CtIP, we applied nuclear magnetic resonance (NMR) spectroscopy to monitor exchange processes in the aforementioned CtIP phosphopeptides in the presence of recombinant PIN1 proteins (Wang et al., 2010). ROESY spectra of both phosphopeptides recorded in the absence of PIN1 were devoid of any crosspeaks that are indicative of an exchange process between the *cis* and *trans* species (data not shown). Importantly, upon addition of PIN1, we detected exchange crosspeaks in the spectrum of the CtIP-pS276 peptide, which were absent in the presence of a catalytically inactive mutant of PIN1 (C113A) and in the nonphosphorylated peptide (Figure 3D and Figures S5B–S5E). However, we could not detect any *cis*/*trans* isomerization signals in the CtIP-pT315 peptide (Figure S5F). Based on previously published data, we speculated that the presence of two consecutive proline residues in this peptide (pT-P-P) may hinder PIN1 isomerization (Lippens et al., 2007). Interestingly, we observed exchange crosspeaks in the ROESY spectrum of a modified CtIP-pT315 peptide in which the second proline was replaced with leucine (P317L; Figure S5G). In order to address whether PIN1 also isomerizes CtIP-pS276 in the setting of an intact CtIP protein, we performed limited proteolysis experiments using FLAG-CtIP purified from HEK293T cells (Stukenberg and Kirschner, 2001). In large agreement with our NMR data, V8 protease cleavage pattern of CtIP-S276A was clearly different compared to CtIP-wt and CtIP-T315A, indicating that pS276-P277 rather than pT315-P317 is isomerized in vivo (Figure 3E). Collectively, our findings support a model in which CtIP-pT315 is the major PIN1 docking site, whereas CtIP-pS276 serves as a PIN1 isomerization site.

CDK2 Activity Is Required for CtIP-T315 Phosphorylation

Next, we aimed at identifying the protein kinase(s) responsible for CtIP phosphorylation at S276 and T315 and, thus, for CtIP recognition by PIN1. Considering recent data showing that CtIP is targeted by CDKs, we examined whether CDK activity is required for CtIP-PIN1 interaction (Chapman et al., 2012). Interestingly, we found that a short treatment of cells with Roscovitine (a general CDK inhibitor), but not with RO-3306 (a selective CDK1 inhibitor), strongly reduced the binding of PIN1 to CtIP (Figure 4A and Figure S6A). Moreover, consistent with CtIP-T315 being the major PIN1 interaction site, cells treated with Roscovitine also displayed reduced phosphorylation of T315, while phosphorylation of S276 was not affected by CDK inhibition (Figures 4B and 4C). To further substantiate the role of CDKs in promoting CtIP-PIN1 interaction, we transiently expressed dominant-negative (dn) forms of CDK1, CDK2, and CDK4 in HEK293T cells and examined their effect on PIN1 binding to CtIP. As shown in Figure 4D, we observed the strongest reduction in CtIP-PIN1 complex formation in the absence of CDK2 activity, which did not affect cell-cycle distribution (Figure S6B). Furthermore, we found that overexpression of wt CDK2 resulted in a considerable increase in CtIP-PIN1 interaction (Figure S6C). Consistent with a role for CDK2 in the phosphorylation of T315, CtIP-pT315 levels steadily increased during S phase, peaked at late S/G2 phase, and were lowest in G1 (Figure S6D). From this data, we conclude that CDK2, by phosphorylating CtIP at T315, is predominantly responsible for the interaction between CtIP and PIN1.

CtIP-2A Phosphomutant Promotes Hyperresection of DSBs

To investigate the potential functions of CtIP isomerization at the cellular and molecular level, we generated stable U2OS cell

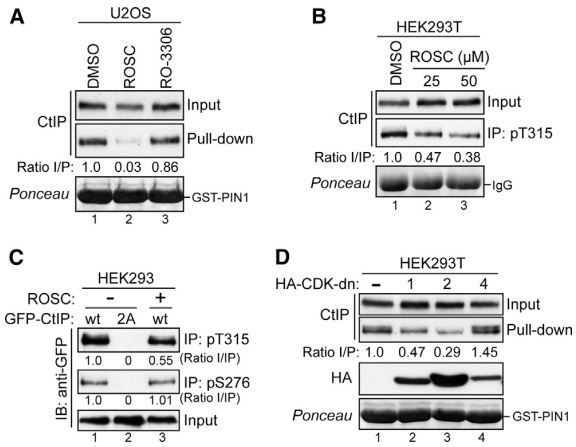

Figure 4. CtIP-PIN1 Interaction and CtIP-T315 Phosphorylation Require CDK2 Activity

(A) Extracts from U2OS cells treated for 2 hr with DMSO, R-Roscovitine (25 μM), or RO-3306 (25 μM) were subjected to GST-PIN1 pull-down assays.

(B) HEK293T cells were treated for 2 hr with DMSO or ROSC, and extracts were immunoblotted for CtIP before (input) and after immunoprecipitation (IP) using the anti-CtIP-pT315 antibody.

(C) HEK293 cells expressing GFP-CtIP (wt and 2A) were treated for 3 hr with either DMSO or ROSC (25 μM). After lysis, whole-cell extracts were immunoblotted for GFP either directly (input) or after immunoprecipitation (IP) with anti-pT315 or anti-pS276 antibodies.

(D) Extracts from HEK293T cells transfected with either pcDNA3.1 (−) or plasmids expressing HA-tagged dominant-negative (dn) mutants of CDK1, CDK2, and CDK4 for 48 hr were subjected to GST-PIN1 pull-down assays. The ratios of input versus pull-down (I/P; in A and D) and input versus IP (I/IP; in B and C) were quantified by densitometry using ImageJ. See also Figure S6.

clones that expressed siRNA-resistant GFP-tagged wt (GFP-CtIP-wt) or mutant CtIP in which both S276 and T315 were changed to nonphosphorylatable alanine (GFP-CtIP-2A) (Figures 5A and 5B). Importantly, the GFP-CtIP-2A mutant protein was still able to interact with BRCA1 and MRE11 (Figure S7A) and to localize to DSB-containing tracks generated by laser microirradiation (Figure 5C and Figure S7B). From this we concluded that PIN1 is required neither for CtIP complex formation with BRCA1 and MRN nor for CtIP recruitment to damaged chromatin that occurs exclusively in S/G2 cells (Sartori et al., 2007; Chen et al., 2008). Moreover, similar to PIN1 depletion, cells expressing CtIP-2A were slightly more CPT resistant than cells expressing CtIP-wt (Figure 5D and Figure S7C). However, the observed increase in CPT resistance could be, at least in part, due to higher expression levels of GFP-CtIP-2A compared to GFP-CtIP-wt (Figure 5A and Figure S7C). Strikingly, like PIN1-depleted cells, CtIP-2A mutant cells treated with ETOP displayed both increased RPA2 hyperphosphorylation and RPA foci formation, indicating higher rates of DSB resection (Figures 5E and 5F and Figure S7D). Since ETOP-induced DSBs are usually repaired with fast kinetics by classical NHEJ, and DNA end resection is known to counteract NHEJ, we speculated that NHEJ is compromised in CtIP-2A mutant cells (Shibata et al., 2011). To this end, we monitored the amount of broken DNA after ETOP treatment in both cell lines in the presence and absence of a DNA-PKcs inhibitor. Indeed, in both NHEJ-proficient and -deficient backgrounds, we found that CtIP-2A cells exhibited more DSBs than did CtIP-wt cells (Figure 5G and Figure S7E). This suggested that the DSB repair defect in CtIP-2A mutant cells is caused by hyperresection, thereby channeling repair into HR, which operates at slower kinetics compared to NHEJ. To further substantiate these findings, we measured the frequencies of HR and NHEJ in HEK293 GFP-reporter cells after transient transfection of CtIP-wt, CtIP-T847A, and CtIP-2A (Figures S7F–S7H). At first, overexpression of the CtIP-2A mutant coincided with a decrease in NHEJ, reflecting the fact that end resection precludes NHEJ usage. In contrast, however, CtIP-2A-expressing cells were as efficient in HR as cells expressing CtIP-wt, indicating that hyperresection may also negatively affect HR by promoting mutagenic types of homology-directed repair such as single-strand annealing (Bennardo et al., 2008). In fact, it was recently reported that depletion of DNA2, which promotes "long-range" resection, leads to increased HR using the same reporter cells (Karanja et al., 2012). Accordingly, the anticipated increase in HR due to hyperresection (e.g., in CtIP-2A cells) could be potentially outweighed by the fact that long-range resection hinders the restoration of a functional DR-GFP reporter gene.

Finally, we addressed whether PIN1 restricts CtIP-dependent DNA end resection particularly in late S/G2 phase when both HR and NHEJ are operable but most DSBs preferably undergo NHEJ (Shibata et al., 2011; Karanam et al., 2012). To this end, we exposed late S/G2 cells stably expressing either CtIP-wt or CtIP-2A to IR and measured the extent of DSB resection by monitoring the levels of hyperphosphorylated RPA2. Consistent with our previous results, we noted a significant increase in phosphorylated RPA2 in CtIP-2A mutant cells, indicative of enhanced resection (Figure 5H). Taken together, these results suggest that CtIP isomerization serves as a key regulatory mechanism restricting DSB resection in late S/G2 phase of the cell cycle.

PIN1 Controls CtIP Stability and Promotes Its Ubiquitylation

Prolyl isomerization by PIN1 was shown to play a crucial role in regulating the stability of many proteins (Liou et al., 2011). Interestingly, in many of our PIN1 depletion experiments, we have noticed increased CtIP protein levels (e.g., Figures 1B and 1D). Moreover, we repeatedly observed a reduction in the amount of CtIP after transient transfection of cells with PIN1-wt, but not with PIN1 mutants, particularly in the presence of DSBs (Figures 1C and 1F and Figure 6A). Thus, we speculated that PIN1 might indeed promote CtIP degradation. To address this idea, we treated cells expressing either CtIP-wt or CtIP-2A for 8 hr with MG132. Interestingly, by blocking the ubiquitin-proteasome pathway, we observed a more substantial increase in the levels of CtIP-wt (4.7-fold) compared to those of CtIP-2A (1.7-fold), indicating that PIN1 is at least partially responsible for CtIP degradation under these conditions (Figure 6B). Next, we exposed CtIP-wt- and CtIP-2A-expressing cells to ETOP and, at different time points after the removal of the drug, analyzed CtIP protein turnover by blocking de novo biosynthesis. Strikingly, CtIP-wt levels rapidly dropped after the recovery from ETOP, whereas CtIP-2A levels remained stable (Figure 6C and

Molecular Cell
PIN1 Isomerase Regulates DSB Repair

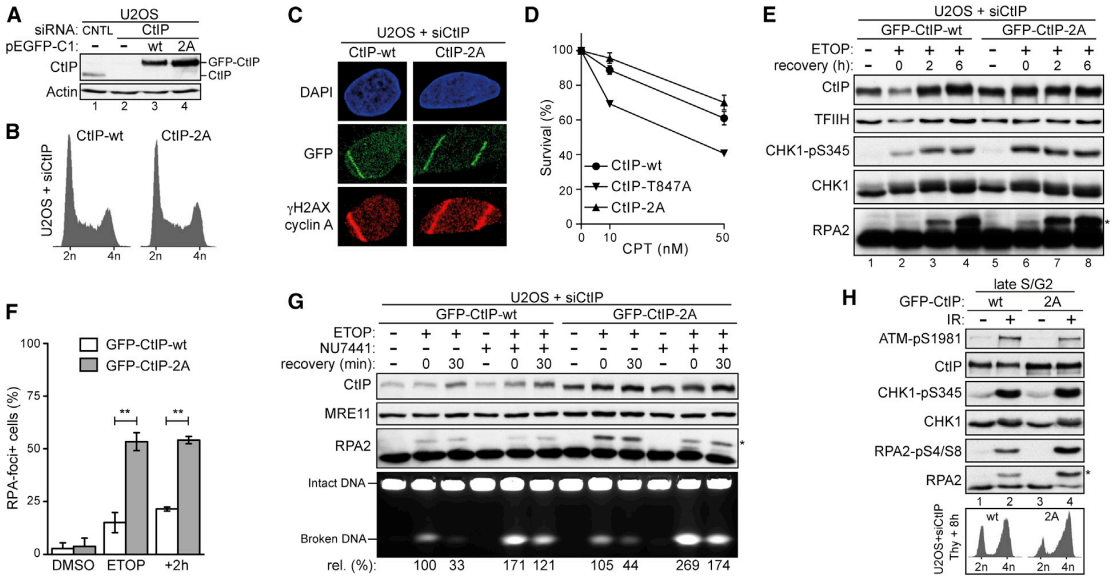

Figure 5. CtIP-2A Mutant Promotes Hyperresection of DSBs

(A) U2OS cells stably expressing siRNA-resistant GFP-tagged CtIP-wt and CtIP-2A or the empty vector (–) were transfected with CNTL or CtIP siRNA for 72 hr, and whole-cell extracts were analyzed by western blotting.

(B) The same cells as in (A) were analyzed by flow cytometry.

(C) The same cells as in (A) were sensitized with BrdU followed by laser microirradiation. After 30 min, cells were fixed, coimmunostained for γ-H2AX and cyclin A, and analyzed by fluorescence microscopy (see also Figure S7B).

(D) The same cells as in (A), including the resection-defective CtIP-T847A mutant, were transfected with CtIP siRNA for 72 hr and treated for 1 hr with either DMSO or low doses of CPT (see also Figure S7C). Survival was determined by colony formation. Data are represented as mean ± SEM (n = 3).

(E) The same cells as in (A) were treated with ETOP (5 μM) for 1 hr, released into drug-free medium for the indicated times, and analyzed by immunoblotting.

(F) The same cells as in (A) were treated with ETOP (5 μM) for 1 hr and were either immediately fixed or released into drug-free medium for 2 hr before fixation. After pre-extraction, cells were coimmunostained for RPA2 and γ-H2AX and analyzed by fluorescence microscopy (see also Figure S7D). For each condition at least 50 cells were scored. Graph shows the percentage of cells exhibiting more than 10 RPA foci per nuclei. Data are represented as mean ± SEM (n ≥ 2).

(G) The same cells as in (A) were treated with ETOP (10 μM) for 2 hr in the absence or presence of a DNA-PKcs inhibitor (NU7441, 10 μM). Cells were harvested either directly or at 30 min after the release into drug-free medium. Whole-cell extracts were analyzed by immunoblotting, and genomic DNA was analyzed by PFGE. DNA breakage in each lane was quantified using ImageJ and normalized against intact DNA. Relative amount of broken DNA in cells expressing GFP-CtIP-wt treated with ETOP was set to 100%.

(H) Same cells as in (A) were synchronized by a single thymidine block. Eight hours after the release from thymidine, cells enriched in S/G2 were irradiated at 30 Gy and, 2 hr later lysates were analyzed by immunoblotting. In (E), (G), and (H), the asterisk indicates the hyperphosphorylated form of RPA2. See also Figure S7.

Figure S8), further supporting the role of PIN1 in negatively regulating CtIP stability. Since polyubiquitylation is a requirement for proteasome-mediated protein degradation, we next addressed whether PIN1 may indeed facilitate CtIP ubiquitylation. To this end, we transfected His-Ubiquitin into HEK293 cell lines inducibly expressing GFP-CtIP and analyzed the level of CtIP polyubiquitylation after Ni-NTA pull-down (Figures 6D and 6E). Strikingly, CtIP ubiquitylation was largely abolished when PIN1 was efficiently depleted (Figure 6F). Moreover, the CtIP-2A mutant was less ubiquitylated compared to CtIP-wt (Figure 6G). Collectively, these results suggest that CtIP isomerization by PIN1 is a prerequisite for CtIP ubiquitylation and subsequent proteasomal degradation.

DISCUSSION

The PIN1 isomerase regulates a number of cellular processes but has so far not been connected to DNA repair (Liou et al., 2011). Here we report that human PIN1 interacts with key DSB repair factors and demonstrate that PIN1 is involved in the regulation of DSB repair. Our results point to a model in which PIN1 affects DSB repair by restricting DNA end resection through phosphorylation-dependent CtIP isomerization, which in turn controls CtIP stability (Figure 7). As a consequence of deregulated DNA end resection, we find that cells lacking PIN1 display reduced levels of NHEJ and potentially increased levels of mutagenic forms of homology-directed repair (e.g., single-strand annealing), while cells overexpressing PIN1 are compromised in error-free HR and repair DSBs more frequently by NHEJ. Since PIN1-mediated isomerization of p53 was shown to potentiate its activity in response to genotoxic stress, and based on the fact that p53 is a regulator of HR, our findings that PIN1 controls DSB repair pathway choice may specifically apply to cancer or immortalized cells that have lost p53 function (Zacchi et al., 2002; Zheng et al., 2002; Bertrand et al., 2004; Liou et al., 2011).

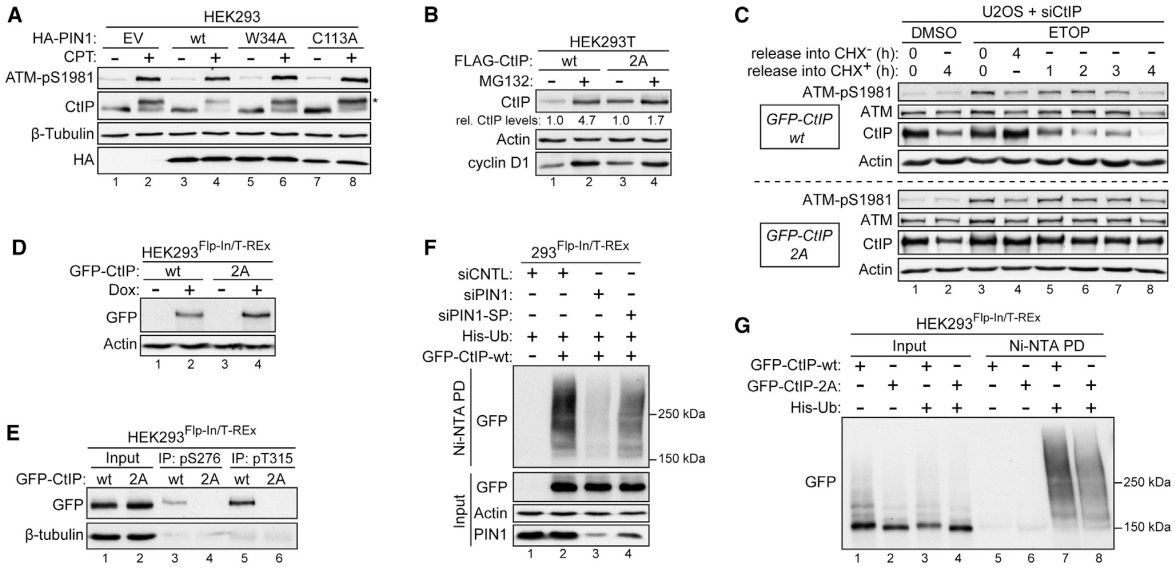

Figure 6. PIN1 Destabilizes CtIP by Promoting Its Ubiquitylation

(A) Two days after transfection with the indicated plasmids, HEK293 cells were treated with CPT (1 μM) for 2 hr and whole-cell extracts were analyzed by immunoblotting. Asterisk indicates hyperphosphorylated form of CtIP.

(B) HEK293T cells were transfected with either FLAG-CtIP-wt or FLAG-CtIP-2A. Eight hours after transfection, cells were splitted into two new plates. Twenty-four hours after plasmid transfection, cells were treated with MG132 (10 μM) for 8 hr and lysed for immunoblot analysis using the indicated antibodies. The signal intensities of CtIP bands were quantified by densitometric analysis using the ImageJ software and normalized to those of Actin. The values represent the relative increase in CtIP-wt and CtIP-2A levels upon MG132 treatment.

(C) Three days after transfection with CtIP siRNA, U2OS cells stably expressing siRNA-resistant GFP-CtIP (wt and 2A) were treated with DMSO or ETOP (10 μM). After 1 hr, cells were released into fresh medium supplemented with 200 μg/ml cycloheximide (CHX) or not for the indicated times, and lysates were analyzed by immunoblotting (see also Figure S8).

(D) HEK293/Flp-In/T-REx cells containing stably integrated GFP-CtIP constructs (wt and 2A) were cultivated in the absence or presence of doxycycline (Dox; 1 μg/ml) for 24 hr, and lysates were analyzed by immunoblotting.

(E) The same cells as in (D) were treated with Dox for 24 hr. After lysis, whole-cell extracts were analyzed by western blotting either directly (input) or after immunoprecipitation (IP) with the indicated anti-CtIP phospho-specific antibodies.

(F) Forty-eight hours after transfection with the indicated siRNAs, HEK293/Flp-In/T-REx cells were transfected with His-Ub, and the expression of GFP-CtIP-wt was simultaneously induced with Dox (except in lane 1). Eight hours after induction, cells were transfected with siRNA for a second time. Seventy-two hours after the first siRNA transfection, cells were treated with MG132 (20 μM) for 6 hr, followed by lysis in buffer containing guanidium-HCl. Ubiquitin conjugates were purified using Ni-NTA-agarose beads, eluted, and analyzed by western blotting using anti-GFP antibody.

(G) Thirty hours after transfection with His-Ub, Dox-induced HEK293/Flp-In/T-REx cells expressing either GFP-CtIP-wt or GFP-CtIP-2A were lysed in buffer containing guanidium-HCl and processed as in (F).

Besides restricting CtIP activity in DNA end resection, it is very tempting to speculate that PIN1 modulates DSB repair pathway choice through regulating the fate of other phosphoproteins. For example, based on our results and previously published data, it is very likely that PIN1 controls the function of 53BP1 and/or BRCA1: (1) we have identified both proteins in a proteomic screen for PIN1 interactors, (2) we find that depleting CtIP does not completely rescue the NHEJ defect in PIN1-deficient cells, (3) BRCA1 was shown to displace 53BP1 from DSBs to enable DNA resection by CtIP (Bunting et al., 2010), (4) PIN1 was very recently identified in a SILAC-based screen for 53BP1 interactors (Di Virgilio et al., 2013), and (5) both proteins are known to be phosphorylated at multiple S/T-P motifs, making them attractive targets for PIN1 (Jowsey et al., 2007; Johnson et al., 2009).

Regarding the mechanism of CtIP regulation by PIN1, we identify S276 and T315 as the two crucial S/T-P motifs mediating PIN1-CtIP interaction. Phosphorylated T315 emerges as the main docking site for PIN1, whereas pS276 is required for *cis/trans* isomerization. Furthermore, we find CDK2 to be the responsible kinase for the phosphorylation of T315. In contrast, phosphorylation of S276 turns out to be independent of CDK activity. In addition, we find that DNA damage stabilizes PIN1-CtIP interaction, but without upregulating T315 phosphorylation, suggesting that it is rather S276 phosphorylation that is induced by genotoxic stress. Interestingly, the amino acid sequence surrounding S276 matches the consensus motif for p38MAPK, a stress kinase reported to be activated by ATM and ATR in response to various DNA-damaging agents including DNA topoisomerase inhibitors (Manke et al., 2005; Reinhardt et al., 2007). Clearly, further investigations are needed to establish both the role of DNA damage in PIN1-mediated CtIP isomerization and the kinase responsible for S276 phosphorylation.

Molecular Cell
PIN1 Isomerase Regulates DSB Repair

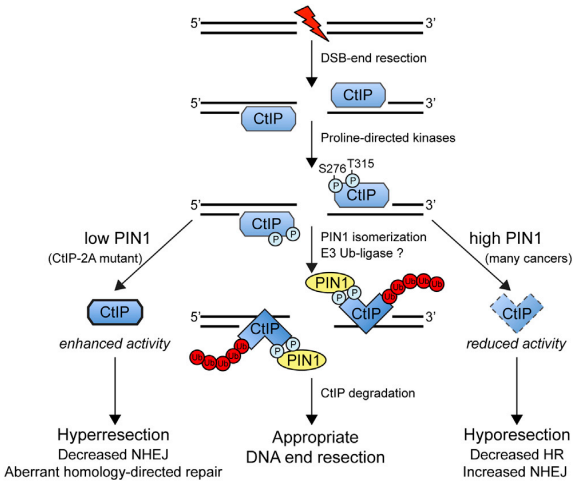

Figure 7. Hypothetical Model: How PIN1-Mediated CtIP Isomerization Controls DNA End Resection

During S/G2, CtIP together with other nucleases promotes the resection of DSBs. Following resection initiation, proline-directed kinases including CDK2 phosphorylate CtIP on T315 and S276, resulting in the binding of PIN1 to CtIP. PIN1-mediated isomerization of CtIP leads to CtIP ubiquitylation through an as-yet-unknown E3 ubiquitin ligase and subsequent CtIP degradation by the proteasome. This mechanism ensures an appropriate usage of DSB end resection. Consequently, cells with abrogated PIN1 function or inherently low PIN1 levels display reduced NHEJ and aberrant (error-prone) forms of homology-directed repair due to enhanced CtIP resection activity (hyperresection). In contrast, cells overexpressing PIN1 display reduced HR and increased NHEJ due to decreased CtIP resection activity (hyporesection). Therefore, we propose that PIN1 plays an important role in the regulation of DSB repair, particularly in late S and G2 phases of the cell cycle.

It also remains to be determined how, mechanistically, isomerization by PIN1 primes CtIP for polyubiquitylation and subsequent degradation. Interestingly, a similar regulatory mechanism involving CDK and PIN1 has recently been reported for hypoxia-induced PML degradation by a Cullin-3 (CUL3) E3 ubiquitin ligase. The authors of this study showed that phosphorylation of PML by CDK1/2 and PIN1-mediated isomerization promotes the recruitment of a CUL3-KLHL20 ubiquitin ligase to polyubiquitylate PML and trigger its degradation (Yuan et al., 2011). Alternatively, a SKP1-CUL1-F box protein (SCF)-type E3 ligase may be involved in CtIP ubiquitylation, since most F box proteins bind to a distinct sequence in their substrates, which typically needs to be phosphorylated (“phospho-degron”) (Silverman et al., 2012).

Ultimately, our findings that overexpression of PIN1 suppresses HR may have important therapeutic implications. For example, PIN1 overexpression, which is frequently found in cancers, may render those cells hypersensitive to PARP inhibition based on the concept of synthetic lethality, analogous to the situation described for BRCA mutant cancers (Bao et al., 2004; Rouleau et al., 2010; Bouwman and Jonkers, 2012). We anticipate that future studies investigating the role of PIN1 in the regulation of other DNA repair factors will provide further important clues to understand how PIN1 contributes to the maintenance of genome stability.

EXPERIMENTAL PROCEDURES

Cell Culture, siRNAs, and Plasmids

U2OS, HEK293T, *Pin1*$^{-/-}$ MEFs, and HEK293T retroviral packaging cells were grown in DMEM supplemented with 10% FCS, 100 U/ml penicillin, and 100 μg/ml streptomycin. The Flp-In T-REx HEK293 host cell line (Invitrogen) was maintained in medium supplemented with 10 μg/ml blasticidin and 300 μg/ml zeocin. Maintenance of the DR-GFP and EJ5-GFP HEK293 cell lines was done as described previously (Bennardo et al., 2008). U2OS clones stably expressing siRNA-resistant forms GFP-CtIP were generated as described previously and were cultured in DMEM supplemented with 10% FCS, standard antibiotics and 500 μg/ml G-418 (Sartori et al., 2007). Retroviral infection of *Pin1*$^{-/-}$ MEFs was carried out as described previously (Zacchi et al., 2002). IR was given using a Faxitron X-ray machine. Laser microirradiation was performed as described previously (Eid et al., 2010). Data for survival curves were generated by colony formation assays as described previously (Sartori et al., 2007). Transfection of siRNA oligos was done using Lipofectamine RNAiMAX (Invitrogen). All siRNA duplexes were purchased from Microsynth except the ON-TARGETplus SMARTpool for PIN1 (PIN1-SP [L-003291-00-0005] [Marcucci et al., 2011; Krishnan et al., 2012] Dharmacon), and the sequences (5′ to 3′) were as follows: luciferase (CNTL; CGUACGCGGAAUACUUCGA) (Sartori et al., 2007), CtIP (GCUAAAACAGGAACGAAUC) (Sartori et al., 2007), XRCC4 (AUAUGUUGGUGAACUGAGA) (Sartori et al., 2007), 53BP1 (CAGGACAGTCTTTCCACGAAT) (Meerang et al., 2011), PIN1-3′UTR (CCGU CACACAGUAUUUAUU), and PIN1-2 (GCUACAUCCAGAAGAUCAA) (Phan et al., 2007). All siRNA transfections were done with 40 nM final concentration of oligos. Plasmids were transfected by using either the standard calcium phosphate method or FuGene 6 (Roche) according to manufacturer’s instructions. The pGEX-4T3 plasmid for bacterial expression of recombinant GST-tagged PIN1 was a gift from Christopher Nelson (University of Victoria, Canada). The epitope-tagged expression vectors for human CtIP have been described previously (Yu et al., 2006; Sartori et al., 2007). The HA-tagged expression vectors for human PIN1 were described previously (Rustighi et al., 2009). The HA-tagged expression vectors for HA-CDK1-dn, HA-CDK4-dn, and HA-CDK2 (wt and dn) were purchased from Addgene (van den Heuvel and Harlow, 1993). The pcDNA3.1-6xHis-Ubiquitin plasmid was a gift from Matthias Peter (ETH Zurich, Switzerland). All PIN1 and CtIP point mutants were introduced by site-directed mutagenesis using Expand Long Template PCR System (Roche) and confirmed by sequencing.

Statistics

Statistical analyses were carried out using unpaired, two-tailed t tests. p values expressed as *$p < 0.05$, **$p < 0.005$, and ***$p < 0.0005$ were considered significant. ns indicates that the difference between the two groups is not significant.

SUPPLEMENTAL INFORMATION

Supplemental Information includes eight figures, one table, Supplemental Experimental Procedures, and Supplemental References and can be found with this article at http://dx.doi.org/10.1016/j.molcel.2013.03.023.

ACKNOWLEDGMENTS

We are very grateful to J. Stark (Department of Radiation Biology, Beckman Research Institute of City of Hope, Duarte, CA, USA) for EJ5-GFP and DR-GFP HEK293 and U2OS cell lines. We thank S. Ferrari and O. Schärer for critical reading of the manuscript. This work was supported by grants of the Swiss National Science Foundation (31003A-129747/1 to P.J. and 31003A_135507 to A.A.S.), the Promedica Stiftung (to A.A.S.), the Vontobel-Stiftung (to A.A.S.), and the “Forschungskredit” of the University of Zurich (54410102 to M.S.).

Received: October 2, 2012
Revised: February 2, 2013
Accepted: March 22, 2013
Published: April 25, 2013

Molecular Cell
PIN1 Isomerase Regulates DSB Repair

REFERENCES

Adachi, N., So, S., and Koyama, H. (2004). Loss of nonhomologous end joining confers camptothecin resistance in DT40 cells. Implications for the repair of topoisomerase I-mediated DNA damage. J. Biol. Chem. *279*, 37343–37348.

Aylon, Y., Liefshitz, B., and Kupiec, M. (2004). The CDK regulates repair of double-strand breaks by homologous recombination during the cell cycle. EMBO J. *23*, 4868–4875.

Bao, L., Kimzey, A., Sauter, G., Sowadski, J.M., Lu, K.P., and Wang, D.-G. (2004). Prevalent overexpression of prolyl isomerase Pin1 in human cancers. Am. J. Pathol. *164*, 1727–1737.

Bennardo, N., Cheng, A., Huang, N., and Stark, J.M. (2008). Alternative-NHEJ is a mechanistically distinct pathway of mammalian chromosome break repair. PLoS Genet. *4*, e1000110. http://dx.doi.org/10.1371/journal.pgen.1000110.

Bennetzen, M.V., Larsen, D.H., Bunkenborg, J., Bartek, J., Lukas, J., and Andersen, J.S. (2010). Site-specific phosphorylation dynamics of the nuclear proteome during the DNA damage response. Mol. Cell. Proteomics *9*, 1314–1323.

Bertrand, P., Saintigny, Y., and Lopez, B.S. (2004). p53's double life: transactivation-independent repression of homologous recombination. Trends Genet. *20*, 235–243.

Beucher, A., Birraux, J., Tchouandong, L., Barton, O., Shibata, A., Conrad, S., Goodarzi, A.A., Krempler, A., Jeggo, P.A., and Löbrich, M. (2009). ATM and Artemis promote homologous recombination of radiation-induced DNA double-strand breaks in G2. EMBO J. *28*, 3413–3427.

Bouwman, P., and Jonkers, J. (2012). The effects of deregulated DNA damage signalling on cancer chemotherapy response and resistance. Nat. Rev. Cancer *12*, 587–598.

Bunting, S.F., Callén, E., Wong, N., Chen, H.-T., Polato, F., Gunn, A., Bothmer, A., Feldhahn, N., Fernandez-Capetillo, O., Cao, L., et al. (2010). 53BP1 inhibits homologous recombination in Brca1-deficient cells by blocking resection of DNA breaks. Cell *141*, 243–254.

Chapman, J.R., Taylor, M.R.G., and Boulton, S.J. (2012). Playing the end game: DNA double-strand break repair pathway choice. Mol. Cell *47*, 497–510.

Chen, L., Nievera, C.J., Lee, A.Y.-L., and Wu, X. (2008). Cell cycle-dependent complex formation of BRCA1.CtIP.MRN is important for DNA double-strand break repair. J. Biol. Chem. *283*, 7713–7720.

Ciccia, A., and Elledge, S.J. (2010). The DNA damage response: making it safe to play with knives. Mol. Cell *40*, 179–204.

Di Virgilio, M., Callen, E., Yamane, A., Zhang, W., Jankovic, M., Gitlin, A.D., Feldhahn, N., Resch, W., Oliveira, T.Y., Chait, B.T., et al. (2013). Rif1 prevents resection of DNA breaks and promotes immunoglobulin class switching. Science *339*, 711–715.

Eid, W., Steger, M., El-Shemerly, M., Ferretti, L.P., Peña-Diaz, J., König, C., Valtorta, E., Sartori, A.A., and Ferrari, S. (2010). DNA end resection by CtIP and exonuclease 1 prevents genomic instability. EMBO Rep. *11*, 962–968.

Goodarzi, A.A., Jeggo, P., and Löbrich, M. (2010). The influence of heterochromatin on DNA double strand break repair: Getting the strong, silent type to relax. DNA Repair (Amst.) *9*, 1273–1282.

Gravel, S., Chapman, J.R., Magill, C., and Jackson, S.P. (2008). DNA helicases Sgs1 and BLM promote DNA double-strand break resection. Genes Dev. *22*, 2767–2772.

Helleday, T. (2010). Homologous recombination in cancer development, treatment and development of drug resistance. Carcinogenesis *31*, 955–960.

Heyer, W.-D., Ehmsen, K.T., and Liu, J. (2010). Regulation of homologous recombination in eukaryotes. Annu. Rev. Genet. *44*, 113–139.

Huertas, P., Cortés-Ledesma, F., Sartori, A.A., Aguilera, A., and Jackson, S.P. (2008). CDK targets Sae2 to control DNA-end resection and homologous recombination. Nature *455*, 689–692.

Ira, G., Pellicioli, A., Balijja, A., Wang, X., Fiorani, S., Carotenuto, W., Liberi, G., Bressan, D., Wan, L., Hollingsworth, N.M., et al. (2004). DNA end resection, homologous recombination and DNA damage checkpoint activation require CDK1. Nature *431*, 1011–1017.

Jackson, S.P., and Bartek, J. (2009). The DNA-damage response in human biology and disease. Nature *461*, 1071–1078.

Johnson, N., Cai, D., Kennedy, R.D., Pathania, S., Arora, M., Li, Y.-C., D'Andrea, A.D., Parvin, J.D., and Shapiro, G.I. (2009). Cdk1 participates in BRCA1-dependent S phase checkpoint control in response to DNA damage. Mol. Cell *35*, 327–339.

Jowsey, P., Morrice, N.A., Hastie, C.J., McLauchlan, H., Toth, R., and Rouse, J. (2007). Characterisation of the sites of DNA damage-induced 53BP1 phosphorylation catalysed by ATM and ATR. DNA Repair (Amst.) *6*, 1536–1544.

Karanam, K., Kafri, R., Loewer, A., and Lahav, G. (2012). Quantitative live cell imaging reveals a gradual shift between DNA repair mechanisms and a maximal use of HR in mid S phase. Mol. Cell *47*, 320–329.

Karanja, K.K., Cox, S.W., Duxin, J.P., Stewart, S.A., and Campbell, J.L. (2012). DNA2 and EXO1 in replication-coupled, homology-directed repair and in the interplay between HDR and the FA/BRCA network. Cell Cycle *11*, 3983–3996.

Kousholt, A.N., Fugger, K., Hoffmann, S., Larsen, B.D., Menzel, T., Sartori, A.A., and Sørensen, C.S. (2012). CtIP-dependent DNA resection is required for DNA damage checkpoint maintenance but not initiation. J. Cell Biol. *197*, 869–876.

Krishnan, N., Lam, T.T., Fritz, A., Rempinski, D., O'Loughlin, K., Minderman, H., Berezney, R., Marzluff, W.F., and Thapar, R. (2012). The prolyl isomerase Pin1 targets stem-loop binding protein (SLBP) to dissociate the SLBP-histone mRNA complex linking histone mRNA decay with SLBP ubiquitination. Mol. Cell. Biol. *32*, 4306–4322.

Liou, Y.-C., Zhou, X.Z., and Lu, K.P. (2011). Prolyl isomerase Pin1 as a molecular switch to determine the fate of phosphoproteins. Trends Biochem. Sci. *36*, 501–514.

Lippens, G., Landrieu, I., and Smet, C. (2007). Molecular mechanisms of the phospho-dependent prolyl cis/trans isomerase Pin1. FEBS J. *274*, 5211–5222.

Manke, I.A., Nguyen, A., Lim, D., Stewart, M.Q., Elia, A.E.H., and Yaffe, M.B. (2005). MAPKAP kinase-2 is a cell cycle checkpoint kinase that regulates the G2/M transition and S phase progression in response to UV irradiation. Mol. Cell *17*, 37–48.

Marcucci, R., Brindle, J., Paro, S., Casadio, A., Hempel, S., Morrice, N., Bisso, A., Keegan, L.P., Del Sal, G., and O'Connell, M.A. (2011). Pin1 and WWP2 regulate GluR2 Q/R site RNA editing by ADAR2 with opposing effects. EMBO J. *30*, 4211–4222.

Matsuoka, S., Ballif, B.A., Smogorzewska, A., McDonald, E.R., 3rd, Hurov, K.E., Luo, J., Bakalarski, C.E., Zhao, Z., Solimini, N., Lerenthal, Y., et al. (2007). ATM and ATR substrate analysis reveals extensive protein networks responsive to DNA damage. Science *316*, 1160–1166.

Meerang, M., Ritz, D., Paliwal, S., Garajova, Z., Bosshard, M., Mailand, N., Janscak, P., Hübscher, U., Meyer, H., and Ramadan, K. (2011). The ubiquitin-selective segregase VCP/p97 orchestrates the response to DNA double-strand breaks. Nat. Cell Biol. *13*, 1376–1382.

Patel, A.G., Sarkaria, J.N., and Kaufmann, S.H. (2011). Nonhomologous end joining drives poly(ADP-ribose) polymerase (PARP) inhibitor lethality in homologous recombination-deficient cells. Proc. Natl. Acad. Sci. USA *108*, 3406–3411.

Phan, R.T., Saito, M., Kitagawa, Y., Means, A.R., and Dalla-Favera, R. (2007). Genotoxic stress regulates expression of the proto-oncogene Bcl6 in germinal center B cells. Nat. Immunol. *8*, 1132–1139.

Pommier, Y. (2006). Topoisomerase I inhibitors: camptothecins and beyond. Nat. Rev. Cancer *6*, 789–802.

Reinhardt, H.C., Aslanian, A.S., Lees, J.A., and Yaffe, M.B. (2007). p53-deficient cells rely on ATM- and ATR-mediated checkpoint signaling through the p38MAPK/MK2 pathway for survival after DNA damage. Cancer Cell *11*, 175–189.

Rouleau, M., Patel, A., Hendzel, M.J., Kaufmann, S.H., and Poirier, G.G. (2010). PARP inhibition: PARP1 and beyond. Nat. Rev. Cancer *10*, 293–301.

Rustighi, A., Tiberi, L., Soldano, A., Napoli, M., Nuciforo, P., Rosato, A., Kaplan, F., Capobianco, A., Pece, S., Di Fiore, P.P., and Del Sal, G. (2009).

Molecular Cell

PIN1 Isomerase Regulates DSB Repair

The prolyl-isomerase Pin1 is a Notch1 target that enhances Notch1 activation in cancer. Nat. Cell Biol. *11*, 133–142.

Sartori, A.A., Lukas, C., Coates, J., Mistrik, M., Fu, S., Bartek, J., Baer, R., Lukas, J., and Jackson, S.P. (2007). Human CtIP promotes DNA end resection. Nature *450*, 509–514.

Shibata, A., Conrad, S., Birraux, J., Geuting, V., Barton, O., Ismail, A., Kakarougkas, A., Meek, K., Taucher-Scholz, G., Löbrich, M., and Jeggo, P.A. (2011). Factors determining DNA double-strand break repair pathway choice in G2 phase. EMBO J. *30*, 1079–1092.

Silverman, J.S., Skaar, J.R., and Pagano, M. (2012). SCF ubiquitin ligases in the maintenance of genome stability. Trends Biochem. Sci. *37*, 66–73.

Söderberg, O., Gullberg, M., Jarvius, M., Ridderstråle, K., Leuchowius, K.-J., Jarvius, J., Wester, K., Hydbring, P., Bahram, F., Larsson, L.-G., and Landegren, U. (2006). Direct observation of individual endogenous protein complexes in situ by proximity ligation. Nat. Methods *3*, 995–1000.

Stukenberg, P.T., and Kirschner, M.W. (2001). Pin1 acts catalytically to promote a conformational change in Cdc25. Mol. Cell *7*, 1071–1083.

Ubersax, J.A., and Ferrell, J.E., Jr. (2007). Mechanisms of specificity in protein phosphorylation. Nat. Rev. Mol. Cell Biol. *8*, 530–541.

van den Heuvel, S., and Harlow, E. (1993). Distinct roles for cyclin-dependent kinases in cell cycle control. Science *262*, 2050–2054.

Wang, Y., Liu, C., Yang, D., Yu, H., and Liou, Y.-C. (2010). Pin1At encoding a peptidyl-prolyl cis/trans isomerase regulates flowering time in Arabidopsis. Mol. Cell *37*, 112–122.

Yaffe, M.B., Schutkowski, M., Shen, M., Zhou, X.Z., Stukenberg, P.T., Rahfeld, J.U., Xu, J., Kuang, J., Kirschner, M.W., Fischer, G., et al. (1997). Sequence-specific and phosphorylation-dependent proline isomerization: a potential mitotic regulatory mechanism. Science *278*, 1957–1960.

Yu, X., Fu, S., Lai, M., Baer, R., and Chen, J. (2006). BRCA1 ubiquitinates its phosphorylation-dependent binding partner CtIP. Genes Dev. *20*, 1721–1726.

Yuan, W.-C., Lee, Y.-R., Huang, S.-F., Lin, Y.-M., Chen, T.-Y., Chung, H.-C., Tsai, C.-H., Chen, H.-Y., Chiang, C.-T., Lai, C.-K., et al. (2011). A Cullin3-KLHL20 Ubiquitin ligase-dependent pathway targets PML to potentiate HIF-1 signaling and prostate cancer progression. Cancer Cell *20*, 214–228.

Zacchi, P., Gostissa, M., Uchida, T., Salvagno, C., Avolio, F., Volinia, S., Ronai, Z., Blandino, G., Schneider, C., and Del Sal, G. (2002). The prolyl isomerase Pin1 reveals a mechanism to control p53 functions after genotoxic insults. Nature *419*, 853–857.

Zheng, H., You, H., Zhou, X.Z., Murray, S.A., Uchida, T., Wulf, G., Gu, L., Tang, X., Lu, K.P., and Xiao, Z.-X.J. (2002). The prolyl isomerase Pin1 is a regulator of p53 in genotoxic response. Nature *419*, 849–853.

9.2 Controlling DNA-end resection: a new task for CDKs

Mini review article published in “Frontiers in Genetics”, 2013

Authors:
Lorenza P. Ferretti, Lorenzo Lafranchi, Alessandro A. Sartori

Contributions:
LPF and LL contributed equally to this work.

frontiers in
GENETICS

MINI REVIEW ARTICLE
published: 03 June 2013
doi: 10.3389/fgene.2013.00099

Controlling DNA-end resection: a new task for CDKs

***Lorenza P. Ferretti*†, *Lorenzo Lafranchi*† *and Alessandro A. Sartori**

Institute of Molecular Cancer Research, Faculty of Medicine, University of Zurich, Zurich, Switzerland

Edited by:
Antonio Porro, Ecole Polytechnique Federale de Lausanne, Switzerland

Reviewed by:
Travis H. Stracker, Institute for Research in Biomedicine, Spain
Boris Pfander, Max-Planck Society, Germany

***Correspondence:**
Alessandro A. Sartori, Institute of Molecular Cancer Research, Faculty of Medicine, University of Zurich, Winterthurerstrasse 190, CH-8057 Zürich, Switzerland
e-mail: sartori@imcr.uzh.ch

†*These authors have contributed equally to this work.*

DNA double-strand breaks (DSBs) are repaired by two major pathways: homologous recombination (HR) and non-homologous end-joining (NHEJ). The choice between HR and NHEJ is highly regulated during the cell cycle. DNA-end resection, an evolutionarily conserved process that generates long stretches of single-stranded DNA, plays a critical role in pathway choice, as it commits cells to HR, while, at the same time, suppressing NHEJ. As erroneous DSB repair is a major source of genomic instability-driven tumorigenesis, DNA-end resection factors, and in particular their regulation by post-translational modifications, have become the subject of extensive research over the past few years. Recent work has implicated phosphorylation at S/T-P motifs by cyclin-dependent kinases (CDKs) as a major regulatory mechanism of DSB repair. Intriguingly, CDK activity was found to be critically important for the coordinated and timely execution of DNA-end resection, and key players in this process were subsequently identified as CDK substrates. In this mini review, we provide an overview of the current understanding of how the DNA-end resection machinery in yeast and human cells is controlled by CDK-mediated phosphorylation.

Keywords: DNA double-strand break repair, DNA-end resection, homologous recombination, cyclin-dependent kinase, phosphorylation, CtIP/Sae2, PIN1

INTRODUCTION

In order to preserve genome integrity, cells employ a complex surveillance network that detects, signals and repairs DNA lesions. These intricate and highly regulated pathways are collectively termed the DNA damage response (DDR; Zhou and Elledge, 2000). One major hallmark of the DDR represents the activation of checkpoints to temporarily delay cell cycle progression through inhibition of cyclin-dependent kinase (CDK) activity. In the budding yeast *Saccharomyces cerevisiae*, a single CDK, Cdc28 (or Cdk1), drives both G1/S and G2/M transitions, whereas in metazoan four CDKs are responsible for cell cycle progression (Morgan, 1997). CDK activity is modulated by association with regulatory subunits known as cyclins, the levels of which oscillate during the cell cycle (King et al., 1996). G1 phase is controlled by CDK4 and CDK6 in complex with D-type cyclins, whereas CDK2-cyclin E is essential for G1/S transition and the assembly of the DNA replication machinery. CDK2-cyclin A is required for proper completion of DNA replication and progression through S phase. Toward the end of interphase, cyclin A associates with CDK1 to facilitate S/G2 transition before CDK1-cyclin B complexes drive cells through mitosis (Morgan, 1997; Malumbres and Barbacid, 2005). CDKs belong to a large family of proline-directed kinases (which also includes MAPKs and GSK3) that exclusively phosphorylate serines or threonines immediately preceding a proline (S/T-P motifs) (Hanks and Hunter, 1995; Errico et al., 2010). CDK substrate specificity is increased by direct binding of the cyclin subunit to conserved RxL motifs present in certain CDK targets (Harper and Adams, 2001). A recent study showed that 50% of CDK2-cyclin A targets carried at least one RxL motif distal to the phosphorylation site (Chi et al., 2008).

In accordance with reduced CDK activity as a consequence of DNA damage-induced checkpoint activation, S/T-P motifs are largely dephosphorylated in response to DNA double-strand breaks (DSBs) (Bennetzen et al., 2010; Beli et al., 2012). However, in apparent contrast to this, CDK activity is strictly required for accurate processing and repair of DSBs in S/G2 phase, indicating that at least some DDR factors are primed by CDK phosphorylation prior to checkpoint activation (Enserink and Kolodner, 2010; Chapman et al., 2012). DSBs are highly deleterious lesions with the potential to cause cell death or genomic instability leading to cancer. DSBs can arise spontaneously as a result of replication fork collapse or can be induced by exogenous DNA-damaging agents including ionizing radiation and certain anti-cancer drugs (Jackson and Bartek, 2009). In order to repair DSBs, all organisms rely on two major pathways: non-homologous end-joining (NHEJ) and homologous recombination (HR). NHEJ functions throughout the cell cycle and religates broken ends without the need of extensive processing (Lieber, 2010). HR, instead, requires an undamaged template for faithful DSB repair, usually the sister chromatid, and is therefore restricted to S/G2 phase (Heyer et al., 2010). HR is initiated by 5′-3′ degradation of the DSB ends to generate 3′-single-stranded DNA (ssDNA) overhangs. This evolutionarily conserved process, termed DNA-end resection, requires the coordinated action of several nucleases and helicases (**Figure 1**; Mimitou and Symington, 2009; Blackwood et al., 2013). Recent work in yeast and human cells has established that DNA recombination and particularly DNA-end resection are highly regulated by various kinases including Mec1/ATR, Tel1/ATM, Rad53/CHK1, Cdc5/PLK1, and, as reviewed here, CDKs (Longhese et al., 2010; Chapman et al., 2012; Finn et al., 2012; Krejci et al., 2012).

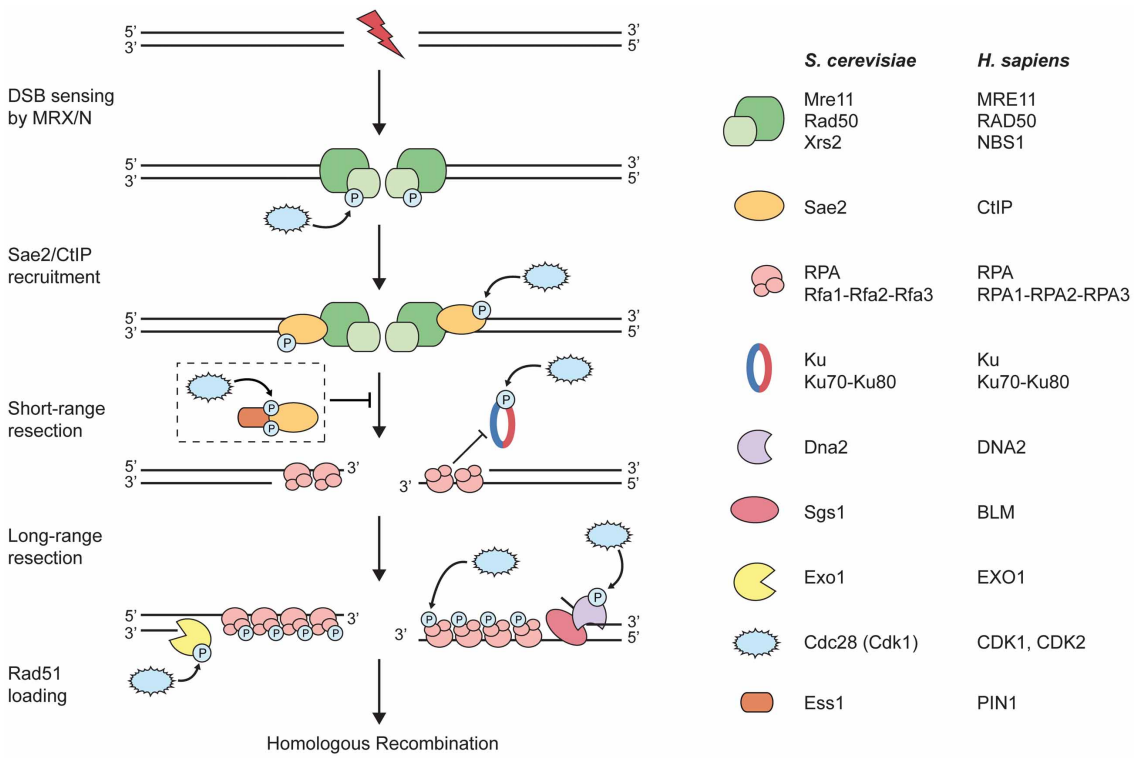

FIGURE 1 | CDKs target components of the DNA-end resection machinery. Upon induction of a DNA double-strand break (DSB), the MRX/N complex rapidly localizes to the damaged site. During S and G2 phases of the cell cycle, DSB repair via homologous recombination (HR) is initiated by DNA-end resection. At first, short-range resection is carried out by the MRX/N complex and Sae2/CtIP; the two factors collaborate in the initial end trimming creating short 3′-ssDNA overhangs, which are immediately coated by replication protein A (RPA). Importantly, processed DSB ends are no longer suitable substrates for Ku binding and, thus, for the repair by non-homologous end-joining. Next, long-range resection is catalyzed either by the 5′-3′ exonuclease Exo1 or the helicase Sgs1/BLM in conjunction with the endonuclease Dna2. Subsequently, RPA is removed from ssDNA and replaced by the Rad51 recombinase that is required for strand invasion of the sister chromatid and further downstream steps in HR (not depicted in the figure). The dashed box depicts the proposed inhibitory role of PIN1 during DNA-end resection: PIN1 binds and subsequently isomerizes phosphorylated CtIP, thereby promoting its degradation by the proteasome and, hence, counteracting resection and HR. Note that both short- and long-range resection factors are potentially regulated by CDK phosphorylation (please refer to the main text for details).

CDK SUBSTRATES IN DNA-END RESECTION

In 2004, two studies in *S. cerevisiae* described for the first time that Cdk1 is essential for DSB repair pathway choice by promoting DNA-end resection in G2 phase (Aylon et al., 2004; Ira et al., 2004). These findings were later confirmed in human cells, showing that ssDNA-dependent activation of the ATR checkpoint pathway in response to DSBs is restricted to S/G2 and requires CDK activity (Jazayeri et al., 2006). Similarly, inhibition of CDK2 in mammalian cells was shown to impair HR and delay DSB signaling (Deans et al., 2006). Based on these key findings, it was proposed that DNA-end resection is governed by CDK-mediated phosphorylation (**Figure 1**) (Ira et al., 2004). However, it was only until the last few years that components of the resection machinery were identified as CDK substrates.

MRX/MRN

Genetic studies in *S. cerevisiae* have long implicated the Mre11-Rad50-Xrs2 (MRX) complex in the initial processing of DSBs (Symington and Gautier, 2011). However, as MRX exhibits both endonuclease and 3′-5′ exonuclease activities *in vitro* (Paull, 2010), it still remains unclear how MRX catalyzes 5′-3′ nucleolytic degradation of DNA ends *in vivo*. New clues came from a recent study suggesting that DNA-end resection could occur with bidirectional polarity, as opposed to the unidirectional model shown in **Figure 1**. Accordingly, Mre11 endonuclease first creates a nick in the strand to be resected up to 300 nucleotides away from the DSB that, in a second step, serves as an entry point for resection by Mre11 3′-5′ exonuclease toward the DSB end and by Exo1 5′-3′ exonuclease away from the DSB (Garcia et al., 2011).

None of the MRX subunits have so far been reported as Cdk1 substrates. Moreover, an *mre11* mutant in which all six S/T-P motifs have been mutagenized did not exhibit any major phenotypes attributable to a resection defect. The same holds true for an *xrs2* mutant in which both CDK consensus motifs (S/T-P-x-K/R) were mutated (Ira et al., 2004). Notably, however, three additional S/T-P motifs in Xrs2 were found to be phosphorylated

in a proteomic study, raising the possibility of it being indeed a Cdk1 substrate (Albuquerque et al., 2008). In human cells, akin to the situation in yeast, only the NBS1 subunit of the MRN complex was found to be phosphorylated in a cell-cycle-dependent manner (**Figure 1**; Olsen et al., 2010). Additionally, two groups reported that CDKs phosphorylate NBS1 at serine 432 in S phase (Falck et al., 2012; Wohlbold et al., 2012). Surprisingly, while Falck et al. concluded that NBS1-S432 phosphorylation promotes DNA-end resection, Wohlbold et al. reported normal resection in the absence of NBS1-S432 phosphorylation. Although it is rather difficult to reconcile these contradicting results, they have most likely emanated from the different NBS1-deficient cells used for complementation studies. Thus, it remains to be clarified whether Xrs2/NBS1 phosphorylation by CDKs is a conserved mechanism to promote DNA-end resection by MRX/N.

Sae2/CtIP

SAE2 (or *COM1*) was originally identified as being required to complete meiotic recombination in *S. cerevisiae* (McKee and Kleckner, 1997; Prinz et al., 1997). Subsequent genetic and biochemical studies in yeast and mammalian cells have shown that Sae2 and its human counterpart CtIP cooperates with the MRX/N nuclease to initiate resection of DSBs (**Figure 1**; Sartori et al., 2007; Symington and Gautier, 2011). There are three potential CDK phosphorylation sites in Sae2 and 12 in CtIP. Remarkably, phosphorylation of a single S/T-P motif in the C-terminus of both proteins (Sae2-S267/CtIP-T847) by CDK is required to promote resection (Huertas et al., 2008; Huertas and Jackson, 2009). Consistent with a role of Cdk1 in positively regulating Sae2 function, mutation of a RxL cyclin-binding motif present upstream of S267 caused comparable DNA damage hypersensitivity to that of *sae2-S267A* cells (Huertas et al., 2008). Moreover, in cells expressing a phospho-mimicking mutant (Sae2-S267E/CtIP-T847E), resection is permitted even in absence of Cdk1 activity; however, not to the same extent as in normal cells. Therefore, it was proposed that additional Cdk1 sites, on Sae2/CtIP itself or on other proteins, are required for optimal resection (Huertas, 2010). Despite the fact that the precise mechanism of how S267/T847 phosphorylation "activates" Sae2/CtIP is still unclear, it is of major importance for both meiotic and mitotic recombination (Manfrini et al., 2010; Nicolette et al., 2010).

Prior to the identification of CtIP-T847 as a CDK site, phosphorylation of S327 was shown to occur exclusively during S/G2 and to be a pre-requisite for CtIP-BRCA1 interaction (Yu and Chen, 2004; Yu et al., 2006). Furthermore, it was recently shown that CtIP-S327 phosphorylation is CDK2-dependent and facilitated by MRE11, which directly interacts with CDK2 and CtIP, thereby bringing CDK2 in proximity with its substrate (Buis et al., 2012). Although evidence for a direct role of CtIP-S327 phosphorylation in resection is still missing, the BRCA1-CtIP complex was recently reported to facilitate the removal of the 53BP1 effector protein RIF1 from DSBs in S/G2, thereby channeling DSB repair into HR (Escribano-Díaz et al., 2013). Moreover, it was recently reported that phosphorylation of a cluster of five additional S/T-P motifs located in the central region of CtIP is important for DNA-end resection (Wang et al., 2013). Mechanistically, phosphorylation of this cluster is needed for the association of CtIP with NBS1, which promotes DNA damage-induced CtIP phosphorylation by ATM (You et al., 2009; Wang et al., 2013). It is important to note, however, that Wang et al. did not directly address whether any of these clustered phosphosites in CtIP are indeed targeted by CDKs *in vivo*.

KU

When DSBs arise in the cell, Ku—a heterodimer composed of Ku70 and Ku80—is usually loaded onto duplex DNA ends. During the repair process, Ku serves as a docking site for many NHEJ proteins, including DNA-PKcs and DNA ligase IV, to rejoin the broken ends (Lieber, 2010). It has been shown that DNA-end resection and HR are constrained during G1 due to both efficient NHEJ and low CDK activity (Aylon et al., 2004; Jazayeri et al., 2006). Interestingly, in the absence of Ku, Cdk1 activity is dispensable for the initiation of resection by MRX-Sae2, but is still needed for long-range resection by Exo1 or Sgs1-Dna2 (Clerici et al., 2008). Therefore, Ku is thought to antagonize DNA-end resection and has to be removed from the ends in order to permit HR. These data also indicate that CDK activity promotes resection by restraining the recruitment of Ku to DSBs, raising the question whether Ku itself is a potential CDK substrate (**Figure 1**). However, removal of all putative Cdk1 phosphorylation sites on Ku70 and 3 out of 4 sites on Ku80 failed to elicit any DSB repair phenotype in *S. cerevisiae*, suggesting that the negative regulation of Ku by Cdk1 is most likely indirect (Zhang et al., 2009). Ku binding to DNA ends also attenuates resection and HR in mammalian cells (Shao et al., 2012; Tomimatsu et al., 2012). Furthermore, Ku70 was reported as a binding partner and substrate of CDK2-cyclin A, and Ku70-T455 was identified as a CDK target site by mass spectrometry (Müller-Tidow et al., 2004; Chi et al., 2008; Olsen et al., 2010); but whether or not Ku phosphorylation by CDKs has an impact on DNA-end resection has yet to be determined.

EXO1

Exonuclease 1 (Exo1) belongs to the RAD2/XPG family of structure-specific 5′ nucleases and has been implicated in multiple genome maintenance pathways including DNA repair and telomere maintenance (Tran et al., 2004). Exo1 is dispensable for initial resection in yeast and human cells but acts in a separate pathway from Sgs1-Dna2/BLM-DNA2 to promote extensive 5′-3′ DSB resection (**Figure 1**; Symington and Gautier, 2011). Moreover, Exo1-dependent resection and its recruitment to DSBs depends on both MRX/N and Sae2/CtIP and is blocked by the presence of Ku (Eid et al., 2010; Sun et al., 2012; Tomimatsu et al., 2012). Although DNA damage-induced phosphorylation of Exo1 has been reported to attenuate its activity in both yeast and human cells (Morin et al., 2008; Bolderson et al., 2010), probably by controlling its stability (El-Shemerly et al., 2005), there is currently no published data available whether Exo1 is a CDK target. However, several S/T-P sites in human EXO1 were repeatedly found to be phosphorylated using mass spectrometry analyses (El-Shemerly et al., 2008; Chen et al., 2009; Shiromizu et al., 2013). Indeed, some of these sites are phosphorylated by CDKs in S/G2 phase, thereby stimulating DNA-end resection by EXO1 and

promoting DSB repair by HR while at the same time suppressing NHEJ (S. Burma, personal communication).

Sgs1-Dna2/BLM-DNA2

Sgs1 and its human ortholog BLM are members of the RecQ family of 3′-5′ DNA helicases and are involved in the suppression of crossovers by promoting the dissolution of Holliday junction intermediates (Bernstein et al., 2010). The role for Sgs1 in conjunction with the Dna2 nuclease in the generation of long stretches of ssDNA during HR was discovered because of its redundancy with Exo1 (**Figure 1**; Gravel et al., 2008; Mimitou and Symington, 2008; Zhu et al., 2008). Although there is currently no data available on CDK-mediated phosphorylation of Sgs1, BLM is phosphorylated at various S/T-P motifs by mitotic kinases including CDK1 (Beausoleil et al., 2004; Leng et al., 2006; Dephoure et al., 2008; Olsen et al., 2010). However, these modifications are more likely to be involved in the regulation of BLM's function in the separation of sister chromatids during mitosis rather than in DNA-end resection (Chan and Hickson, 2011). In contrast, Cdk1-mediated phosphorylation of *S. cerevisiae* Dna2 at T4, S17, and S237 stimulates its recruitment to DSBs and DNA-end resection (Chen et al., 2011). Consistent with the redundancy observed between Dna2- and Exo1-dependent resection pathways, *dna2-T4A/S17A/S237A* cells only resect DSBs in the presence of functional Exo1. Interestingly, T4 and S17 lie within a bipartite nuclear localization signal, suggesting a timely regulated nuclear import of Dna2 upon phosphorylation during G1/S transition (Kosugi et al., 2009). Remarkably, human DNA2 lacks the entire N-terminal region of yeast Dna2 including all three S/T-P sites, suggesting that CDK-mediated regulation of long-range resection in human cells differs from yeast.

RPA

Replication protein A (RPA) is an evolutionarily conserved, heterotrimeric complex consisting of RPA1, RPA2, and RPA3. Owing to its high ssDNA binding affinity, RPA is required for most aspects of DNA metabolism including replication, repair and recombination (Oakley and Patrick, 2010). Following resection, RPA wraps around the generated 3′-ssDNA overhangs to protect the DNA against nuclease degradation and to prevent hairpin formation that would impede Rad51 filament assembly (**Figure 1**; Holloman, 2011). *In vitro* studies have also implicated RPA in promoting long-range resection through stimulation of both Exo1- and Sgs1-Dna2-dependent pathways (Cejka et al., 2010; Niu et al., 2010; Nimonkar et al., 2011; Cannavo et al., 2013). Furthermore, under DNA-damaging conditions, RPA-coated ssDNA serves to recruit the Mec1/ATR kinase, a critical event in checkpoint activation (Zou and Elledge, 2003). RPA2 contains a flexible N-terminal domain that is differentially phosphorylated at multiple residues during the cell cycle and in response to genotoxic stress. Two residues within this region, S23 and S29, are phosphorylated by CDK2-cyclin A and CDK1-cyclin B at the G1/S boundary and during mitosis, respectively (**Figure 1**); however, they are not conserved in yeast (Oakley and Patrick, 2010). In response to DSBs, ATR-mediated phosphorylation of RPA2-S33 induces phosphorylation of RPA2-S23/S29, and both act synergistically to stimulate phosphorylation of additional residues closer to the N-terminus by DNA-PK (Anantha et al., 2007; Liaw et al., 2011). Although DNA damage-induced RPA2 hyper-phosphorylation seems critical for Rad51 recruitment and HR in response to replication stress, it is not essential for HR as measured by an I-SceI-based reporter assay (Shi et al., 2010; Serrano et al., 2013). Moreover, dephosphorylation of RPA2 by the PP4 phosphatase complex has also been reported to facilitate HR (Lee et al., 2010). However, a direct role of CDK-mediated RPA phosphorylation in DNA-end resection has not yet been demonstrated.

CHROMATIN BINDING AND REMODELLING FACTORS

DNA-end resection occurs in the context of chromatin, which constitutes a natural barrier to all kind of DNA transactions including DSB repair (Price and D'Andrea, 2013; Tsabar and Haber, 2013). Last year, three groups described a role of the *S. cerevisiae* chromatin-remodeling factor Fun30 (and its human counterpart SMARCAD1) in the repair of DSBs by HR (Chen et al., 2012; Costelloe et al., 2012; Eapen et al., 2012). Fun30/SMARCAD1 physically associates with DSB ends and, by weakening the histone-DNA interactions in nucleosomes, establishes a DNA conformation that facilitates both Sgs1- and Exo1-dependent resection. Furthermore, it was shown that Fun30 function in resection becomes less important in cells lacking the histone-bound Rad9 checkpoint protein, suggesting that Fun30 helps to overcome the inhibitory effect of Rad9 on DNA-end resection (Chen et al., 2012). Interestingly, both Fun30 and Rad9 were identified as Cdk1 substrates and reported to be phosphorylated at multiple S/T-P sites (Ubersax et al., 2003; Albuquerque et al., 2008). Moreover, loss of Rad9 has been reported to partially bypass the requirement for Cdk1 in resection (Lazzaro et al., 2008). This inhibitory mechanism is likely to be evolutionarily conserved as 53BP1, the mammalian ortholog of Rad9 (Wang et al., 2002), suppresses resection to promote NHEJ and immunoglobulin class switching (Bunting et al., 2010; Bothmer et al., 2011). Accordingly, multiple CDK consensus sites in SMARCAD1 and 53BP1 were repeatedly found to be phosphorylated (Beausoleil et al., 2004; Linding et al., 2007; Bennetzen et al., 2010; Olsen et al., 2010; Shiromizu et al., 2013). Further experiments are required to establish whether some of the CDK sites in Fun30/SMARCAD1 and Rad9/53BP1 play a role in the regulation of DNA-end resection and, thus, in DSB repair pathway choice.

CONCLUDING REMARKS

While the role of CDKs in regulating DNA-end resection is a given fact, we are only beginning to understand the mechanistic consequences of these phosphorylation events for individual repair factors, e.g., on protein-protein interactions, intracellular localization, or protein stability. Another important question to address in the future is how DNA-end resection is limited in order to generate confined tracts of ssDNA that are suitable for homology search by the Rad51 recombinase leading to productive HR. In other words, there must be additional regulatory mechanisms providing a switch between activation and inhibition of DNA-end resection to coordinate DSB repair pathways in a spatiotemporal manner.

Novel insights are provided by a recent study showing that PIN1, a phosphorylation-specific peptidyl-prolyl cis/trans isomerase, counteracts DNA-end resection in human cells (Steger et al., 2013). PIN1 was previously shown to isomerize phosphorylated S/T-P peptide bonds, thereby controlling the function of a subset of CDK substrates involved in diverse cellular processes (Liou et al., 2011). In a proteomic screen for PIN1 substrates, Steger et al. identified several prominent DSB repair proteins including BRCA1, 53BP1 and CtIP. Interestingly, PIN1-mediated isomerization of CtIP requires the phosphorylation of CtIP at two S/T-P sites: CtIP-pT315 (by CDK) serves as the major binding site for PIN1, whereas CtIP-pS276 (by an unknown proline-directed kinase) is isomerized by PIN1. Following isomerization, CtIP gets ubiquitylated and subsequently degraded by the proteasome. In this way, PIN1 is proposed to limit DNA-end resection, thereby possibly contributing to fine-tune the coordination of HR and NHEJ during S and G2 phases of the cell cycle (**Figure 1**; Karanam et al., 2012). So far, no direct connection has been made between PIN1 and the regulation of DSB repair in *S. cerevisiae*, studies of which are hampered by the fact that yeast PIN1 (Ess1) is essential for viability (Siepe and Jentsch, 2009). Future studies will have to determine whether phosphorylation-dependent regulation by PIN1 in concert with CDKs applies to other DSB repair proteins apart from CtIP and, thus, represents a general feature of the DDR.

ACKNOWLEDGMENTS

We wish to thank D. Hühn and P. Cejka for critical reading of the manuscript and helpful discussions. We also would like to apologize to all authors whose significant contributions could not be cited due to space limitations. This applies in particular to studies on DNA-end resection in *Schizosaccharomyces pombe* and in *Xenopus laevis* egg extracts. Alessandro A. Sartori is supported by the Vontobel-Stiftung. Lorenza P. Ferretti and Lorenzo Lafranchi are supported by grants of the Swiss National Science Foundation (31003A_135507) and the Promedica Stiftung.

REFERENCES

Albuquerque, C. P., Smolka, M. B., Payne, S. H., Bafna, V., Eng, J., and Zhou, H. (2008). A multidimensional chromatography technology for in-depth phosphoproteome analysis. *Mol. Cell. Proteomics* 7, 1389–1396. doi: 10.1074/mcp.M700468-MCP200

Anantha, R. W., Vassin, V. M., and Borowiec, J. A. (2007). Sequential and synergistic modification of human RPA stimulates chromosomal DNA repair. *J. Biol. Chem.* 282, 35910–35923. doi: 10.1074/jbc.M704645200

Aylon, Y., Liefshitz, B., and Kupiec, M. (2004). The CDK regulates repair of double-strand breaks by homologous recombination during the cell cycle. *EMBO J.* 23, 4868–4875. doi: 10.1038/sj.emboj.7600469

Beausoleil, S. A., Jedrychowski, M., Schwartz, D., Elias, J. E., Villén, J., Li, J., et al. (2004). Large-scale characterization of HeLa cell nuclear phosphoproteins. *Proc. Natl. Acad. Sci. U.S.A.* 101, 12130–12135. doi: 10.1073/pnas.0404720101

Beli, P., Lukashchuk, N., Wagner, S. A., Weinert, B. T., Olsen, J. V., Baskcomb, L., et al. (2012). Proteomic investigations reveal a role for RNA processing factor THRAP3 in the DNA damage response. *Mol. Cell* 46, 212–225. doi: 10.1016/j.molcel.2012.01.026

Bennetzen, M. V., Larsen, D. H., Bunkenborg, J., Bartek, J., Lukas, J., and Andersen, J. S. (2010). Site-specific phosphorylation dynamics of the nuclear proteome during the DNA damage response. *Mol. Cell. Proteomics* 9, 1314–1323. doi: 10.1074/mcp.M900616-MCP200

Bernstein, K. A., Gangloff, S., and Rothstein, R. (2010). The RecQ DNA helicases in DNA repair. *Annu. Rev. Genet.* 44, 393–417. doi: 10.1146/annurev-genet-102209-163602

Blackwood, J. K., Rzechorzek, N. J., Bray, S. M., Maman, J. D., Pellegrini, L., and Robinson, N. P. (2013). End-resection at DNA double-strand breaks in the three domains of life. *Biochem. Soc. Trans.* 41, 314–320. doi: 10.1042/BST20120307

Bolderson, E., Tomimatsu, N., Richard, D. J., Boucher, D., Kumar, R., Pandita, T. K., et al. (2010). Phosphorylation of Exo1 modulates homologous recombination repair of DNA double-strand breaks. *Nucleic Acids Res.* 38, 1821–1831. doi: 10.1093/nar/gkp1164

Bothmer, A., Robbiani, D. F., Di Virgilio, M., Bunting, S. F., Klein, I. A., Feldhahn, N., et al. (2011). Regulation of DNA end joining, resection, and immunoglobulin class switch recombination by 53BP1. *Mol. Cell* 42, 319–329. doi: 10.1016/j.molcel.2011.03.019

Buis, J., Stoneham, T., Spehalski, E., and Ferguson, D. O. (2012). Mre11 regulates CtIP-dependent double-strand break repair by interaction with CDK2. *Nat. Struct. Mol. Biol.* 19, 246–252. doi: 10.1038/nsmb.2212

Bunting, S. F., Callen, E., Wong, N., Chen, H.-T., Polato, F., Gunn, A., et al. (2010). 53BP1 inhibits homologous recombination in Brca1-deficient cells by blocking resection of DNA breaks. *Cell* 141, 243–254. doi: 10.1016/j.cell.2010.03.012

Cannavo, E., Cejka, P., and Kowalczykowski, S. C. (2013). Relationship of DNA degradation by *Saccharomyces cerevisiae* exonuclease 1 and its stimulation by RPA and Mre11-Rad50-Xrs2 to DNA end resection. *Proc. Natl. Acad. Sci. U.S.A.* 110, E1661–E1668. doi: 10.1073/pnas.1305166110

Cejka, P., Cannavo, E., Polaczek, P., Masuda-Sasa, T., Pokharel, S., Campbell, J. L., et al. (2010). DNA end resection by Dna2-Sgs1-RPA and its stimulation by Top3-Rmi1 and Mre11-Rad50-Xrs2. *Nature* 467, 112–116. doi: 10.1038/nature09355

Chan, K. L., and Hickson, I. D. (2011). New insights into the formation and resolution of ultra-fine anaphase bridges. *Semin. Cell Dev. Biol.* 22, 906–912. doi: 10.1016/j.semcdb.2011.07.001

Chapman, J. R., Taylor, M. R. G., and Boulton, S. J. (2012). Playing the end game: DNA double-strand break repair pathway choice. *Mol. Cell* 47, 497–510. doi: 10.1016/j.molcel.2012.07.029

Chen, R. Q., Yang, Q. K., Lu, B. W., Yi, W., Cantin, G., Chen, Y. L., et al. (2009). CDC25B mediates rapamycin-induced oncogenic responses in cancer cells. *Cancer Res.* 69, 2663–2668. doi: 10.1158/0008-5472.CAN-08-3222

Chen, X., Cui, D., Papusha, A., Zhang, X., Chu, C. D., Tang, J., et al. (2012). The Fun30 nucleosome remodeller promotes resection of DNA double-strand break ends. *Nature* 489, 576–580. doi: 10.1038/nature11355

Chen, X., Niu, H., Chung, W.H., Zhu, Z., Papusha, A., Shim, E. Y., et al. (2011). Cell cycle regulation of DNA double-strand break end resection by Cdk1-dependent Dna2 phosphorylation. *Nat. Struct. Mol. Biol.* 18, 1015–1019. doi: 10.1038/nsmb.2105

Chi, Y., Welcker, M., Hizli, A. A., Posakony, J. J., Aebersold, R., and Clurman, B. E. (2008). Identification of CDK2 substrates in human cell lysates. *Genome Biol.* 9:R149. doi: 10.1186/gb-2008-9-10-r149

Clerici, M., Mantiero, D., Guerini, I., Lucchini, G., and Longhese, M. P. (2008). The Yku70-Yku80 complex contributes to regulate double-strand break processing and checkpoint activation during the cell cycle. *EMBO Rep.* 9, 810–818. doi: 10.1038/embor.2008.121

Costelloe, T., Louge, R., Tomimatsu, N., Mukherjee, B., Martini, E., Khadaroo, B., et al. (2012). The yeast Fun30 and human SMARCAD1 chromatin remodellers promote DNA end resection. *Nature* 489, 581–584. doi: 10.1038/nature11353

Deans, A. J., Khanna, K. K., McNees, C. J., Mercurio, C., Heierhorst, J., and McArthur, G. A. (2006). Cyclin-dependent kinase 2 functions in normal DNA repair and is a therapeutic target in BRCA1-deficient cancers. *Cancer Res.* 66, 8219–8226. doi: 10.1158/0008-5472.CAN-05-3945

Dephoure, N., Zhou, C., Villén, J., Beausoleil, S. A., Bakalarski, C. E., Elledge, S. J., et al. (2008). A quantitative atlas of mitotic phosphorylation. *Proc. Natl. Acad. Sci. U.S.A.* 105, 10762–10767. doi: 10.1073/pnas.0805139105

Eapen, V. V., Sugawara, N., Tsabar, M., Wu, W.-H., and Haber, J. E. (2012). The *Saccharomyces*

cerevisiae chromatin remodeler Fun30 regulates DNA end resection and checkpoint deactivation. *Mol. Cell. Biol.* 32, 4727–4740. doi: 10.1128/MCB.00566-12

Eid, W., Martinn, S., El-Shemerly, M., Ferretti, L. P., Peña-Diaz, J., König, C., et al. (2010). DNA end resection by CtIP and exonuclease 1 prevents genomic instability. *EMBO Rep.* 11, 962–968. doi: 10.1038/embor.2010.157

El-Shemerly, M., Hess, D., Pyakurel, A. K., Moselhy, S., and Ferrari, S. (2008). ATR-dependent pathways control hEXO1 stability in response to stalled forks. *Nucleic Acids Res.* 36, 511–519. doi: 10.1093/nar/gkm1052

El-Shemerly, M., Janscak, P., Hess, D., Jiricny, J., and Ferrari, S. (2005). Degradation of human exonuclease 1b upon DNA synthesis inhibition. *Cancer Res.* 65, 3604–3609. doi: 10.1158/0008-5472.CAN-04-4069

Enserink, J. M., and Kolodner, R. D. (2010). An overview of Cdk1-controlled targets and processes. *Cell Div.* 5:11. doi: 10.1186/1747-1028-5-11

Errico, A., Deshmukh, K., Tanaka, Y., Pozniakovsky, A., and Hunt, T. (2010). Identification of substrates for cyclin dependent kinases. *Adv. Enzyme Regul.* 50, 375–399. doi: 10.1016/j.advenzreg.2009.12.001

Escribano-Díaz, C., Orthwein, A., Fradet-Turcotte, A., Xing, M., Young, J. T. F., Tkáč, J., et al. (2013). A cell cycle-dependent regulatory circuit composed of 53BP1-RIF1 and BRCA1-CtIP controls dna repair pathway choice. *Mol. Cell* 49, 872–883. doi: 10.1016/j.molcel.2013.01.001

Falck, J., Forment, J. V., Coates, J., Mistrik, M., Lukas, J., Bartek, J., et al. (2012). CDK targeting of NBS1 promotes DNA-end resection, replication restart and homologous recombination. *EMBO Rep.* 13, 561–568. doi: 10.1038/embor.2012.58

Finn, K., Lowndes, N. F., and Grenon, M. (2012). Eukaryotic DNA damage checkpoint activation in response to double-strand breaks. *Cell. Mol. Life Sci.* 69, 1447–1473. doi: 10.1007/s00018-011-0875-3

Garcia, V., Phelps, S. E. L., Gray, S., and Neale, M. J. (2011). Bidirectional resection of DNA double-strand breaks by Mre11 and Exo1. *Nature* 479, 241–244. doi: 10.1038/nature10515

Gravel, S., Chapman, J. R., Magill, C., and Jackson, S. P. (2008). DNA helicases Sgs1 and BLM promote DNA double-strand break resection. *Genes Dev.* 22, 2767–2772. doi: 10.1101/gad.503108

Hanks, S. K., and Hunter, T. (1995). Protein kinases 6. The eukaryotic protein kinase superfamily: kinase (catalytic) domain structure and classification. *FASEB J.* 9, 576–596.

Harper, J. W., and Adams, P. D. (2001). Cyclin-dependent kinases. *Chem. Rev.* 101, 2511–2526. doi: 10.1021/cr0001030

Heyer, W.-D., Ehmsen, K. T., and Liu, J. (2010). Regulation of homologous recombination in eukaryotes. *Annu. Rev. Genet.* 44, 113–139. doi: 10.1146/annurev-genet-051710-150955

Holloman, W. K. (2011). Unraveling the mechanism of BRCA2 in homologous recombination. *Nat. Struct. Mol. Biol.* 18, 748–754. doi: 10.1038/nsmb.2096

Huertas, P. (2010). DNA resection in eukaryotes: deciding how to fix the break. *Nat. Struct. Mol. Biol.* 17, 11–16. doi: 10.1038/nsmb.1710

Huertas, P., and Jackson, S. P. (2009). Human CtIP mediates cell cycle control of DNA end resection and double strand break repair. *J. Biol. Chem.* 284, 9558–9565. doi: 10.1074/jbc.M808906200

Huertas, P., Cortés-Ledesma, F., Sartori, A. A., Aguilera, A., and Jackson, S. P. (2008). CDK targets Sae2 to control DNA-end resection and homologous recombination. *Nature* 455, 689–692. doi: 10.1038/nature07215

Ira, G., Pellicioli, A., Balijja, A., Wang, X., Fiorani, S., Carotenuto, W., et al. (2004). DNA end resection, homologous recombination and DNA damage checkpoint activation require CDK1. *Nature* 431, 1011–1017. doi: 10.1038/nature02964

Jackson, S. P., and Bartek, J. (2009). The DNA-damage response in human biology and disease. *Nature* 461, 1071–1078. doi: 10.1038/nature08467

Jazayeri, A., Falck, J., Lukas, C., Bartek, J., Smith, G. C. M., Lukas, J., et al. (2006). ATM- and cell cycle-dependent regulation of ATR in response to DNA double-strand breaks. *Nat. Cell Biol.* 8, 37–45. doi: 10.1038/ncb1337

Karanam, K., Kafri, R., Loewer, A., and Lahav, G. (2012). Quantitative live cell imaging reveals a gradual shift between DNA repair mechanisms and a maximal use of HR in mid S phase. *Mol. Cell* 47, 320–329. doi: 10.1016/j.molcel.2012.05.052

King, R. W., Deshaies, R. J., Peters, J. M., and Kirschner, M. W. (1996). How proteolysis drives the cell cycle. *Science* 274, 1652–1659. doi: 10.1126/science.274.5293.1652

Kosugi, S., Hasebe, M., Tomita, M., and Yanagawa, H. (2009). Systematic identification of cell cycle-dependent yeast nucleocytoplasmic shuttling proteins by prediction of composite motifs. *Proc. Natl. Acad. Sci. U.S.A.* 106, 10171–10176. doi: 10.1073/pnas.0900604106

Krejci, L., Altmannova, V., Spirek, M., and Zhao, X. (2012). Homologous recombination and its regulation. *Nucleic Acids Res.* 40, 5795–5818. doi: 10.1093/nar/gks270

Lazzaro, F., Sapountzi, V., Granata, M., Pellicioli, A., Vaze, M., Haber, J. E., et al. (2008). Histone methyltransferase Dot1 and Rad9 inhibit single-stranded DNA accumulation at DSBs and uncapped telomeres. *EMBO J.* 27, 1502–1512. doi: 10.1038/emboj.2008.81

Lee, D.-H., Pan, Y., Kanner, S., Sung, P., Borowiec, J. A., and Chowdhury, D. (2010). A PP4 phosphatase complex dephosphorylates RPA2 to facilitate DNA repair via homologous recombination. *Nat. Struct. Mol. Biol.* 17, 365–372. doi: 10.1038/nsmb.1769

Leng, M., Chan, D. W., Luo, H., Zhu, C., Qin, J., and Wang, Y. (2006). MPS1-dependent mitotic BLM phosphorylation is important for chromosome stability. *Proc. Natl. Acad. Sci. U.S.A.* 103, 11485–11490. doi: 10.1073/pnas.0601828103

Liaw, H., Lee, D., and Myung, K. (2011). DNA-PK-dependent RPA2 hyperphosphorylation facilitates DNA repair and suppresses sister chromatid exchange. *PLoS ONE* 6:e21424. doi: 10.1371/journal.pone.0021424

Lieber, M. R. (2010). The mechanism of double-strand DNA Break Repair by the Nonhomologous DNA End-Joining Pathway. *Annu. Rev. Biochem.* 79, 181–211. doi: 10.1146/annurev.biochem.052308.093131

Linding, R., Jensen, L. J., Ostheimer, G. J., van Vugt, M. A. T. M., Jørgensen, C., Miron, I. M., et al. (2007). Systematic discovery of *in vivo* phosphorylation networks. *Cell* 129, 1415–1426. doi: 10.1016/j.cell.2007.05.052

Liou, Y.-C., Zhou, X. Z., and Lu, K. P. (2011). Prolyl isomerase Pin1 as a molecular switch to determine the fate of phosphoproteins. *Trends Biochem. Sci.* 36, 501–514. doi: 10.1016/j.tibs.2011.07.001

Longhese, M. P., Bonetti, D., Manfrini, N., and Clerici, M. (2010). Mechanisms and regulation of DNA end resection. *EMBO J.* 29, 2864–2874. doi: 10.1038/emboj.2010.165

Malumbres, M., and Barbacid, M. (2005). Mammalian cyclin-dependent kinases. *Trends Biochem. Sci.* 30, 630–641. doi: 10.1016/j.tibs.2005.09.005

Manfrini, N., Guerini, I., Citterio, A., Lucchini, G., and Longhese, M. P. (2010). Processing of meiotic DNA double strand breaks requires cyclin-dependent kinase and multiple nucleases. *J. Biol. Chem.* 285, 11628–11637. doi: 10.1074/jbc.M110.104083

McKee, A. H., and Kleckner, N. (1997). A general method for identifying recessive diploid-specific mutations in *Saccharomyces cerevisiae*, its application to the isolation of mutants blocked at intermediate stages of meiotic prophase and characterization of a new gene SAE2. *Genetics* 146, 797–816.

Mimitou, E. P., and Symington, L. S. (2008). Sae2, Exo1 and Sgs1 collaborate in DNA double-strand break processing. *Nature* 455, 770–774. doi: 10.1038/nature07312

Mimitou, E. P., and Symington, L. S. (2009). Nucleases and helicases take center stage in homologous recombination. *Trends Biochem. Sci.* 34, 264–272. doi: 10.1016/j.tibs.2009.01.010

Morgan, D. O. (1997). Cyclin-dependent kinases: engines, clocks, and microprocessors. *Annu. Rev. Cell Dev. Biol.* 13, 261–291. doi: 10.1146/annurev.cellbio.13.1.261

Morin, I., Ngo, H.-P., Greenall, A., Zubko, M. K., Morrice, N., and Lydall, D. (2008). Checkpoint-dependent phosphorylation of Exo1 modulates the DNA damage response. *EMBO J.* 27, 2400–2410. doi: 10.1038/emboj.2008.171

Müller-Tidow, C., Ji, P., Diederichs, S., Potratz, J., Bäumer, N., Köhler, G., et al. (2004). The cyclin A1-CDK2 complex regulates DNA double-strand break repair. *Mol. Cell Biol.* 24, 8917–8928. doi: 10.1128/MCB.24.20.8917-8928.2004

Nicolette, M. L., Lee, K., Guo, Z., Rani, M., Chow, J. M., Lee, S. E., et al. (2010). Mre11-Rad50-Xrs2 and Sae2 promote 5′ strand resection of DNA double-strand breaks. *Nat. Struct. Mol. Biol.* 17, 1478–1485. doi: 10.1038/nsmb.1957

Nimonkar, A. V., Genschel, J., Kinoshita, E., Polaczek, P., Campbell, J. L., Wyman, C., et al. (2011). BLM-DNA2-RPA-MRN and EXO1-BLM-RPA-MRN constitute two DNA end resection machineries for human DNA break

repair. *Genes Dev.* 25, 350–362. doi: 10.1101/gad.2003811

Niu, H., Chung, W.-H., Zhu, Z., Kwon, Y., Zhao, W., Chi, P., et al. (2010). Mechanism of the ATP-dependent DNA end-resection machinery from *Saccharomyces cerevisiae*. *Nature* 467, 108–111. doi: 10.1038/nature09318

Oakley, G. G., and Patrick, S. M. (2010). Replication protein A: directing traffic at the intersection of replication and repair. *Front. Biosci.* 15, 883–900.

Olsen, J. V., Vermeulen, M., Santamaria, A., Kumar, C., Miller, M. L., Jensen, L. J., et al. (2010). Quantitative phosphoproteomics reveals widespread full phosphorylation site occupancy during mitosis. *Sci. Signal* 3, ra3. doi: 10.1126/scisignal.2000475

Paull, T. T. (2010). Making the best of the loose ends: Mre11/Rad50 complexes and Sae2 promote DNA double-strand break resection. *DNA Repair (Amst.)* 9, 1283–1291. doi: 10.1016/j.dnarep.2010.09.015

Price, B. D., and D'Andrea, A. D. (2013). Chromatin remodeling at DNA double-strand breaks. *Cell* 152, 1344–1354. doi: 10.1016/j.cell.2013.02.011

Prinz, S., Amon, A., and Klein, F. (1997). Isolation of COM1, a new gene required to complete meiotic double-strand break-induced recombination in *Saccharomyces cerevisiae*. *Genetics* 146, 781–795.

Sartori, A. A., Lukas, C., Coates, J., Mistrik, M., Fu, S., Bartek, J., et al. (2007). Human CtIP promotes DNA end resection. *Nature* 450, 509–514. doi: 10.1038/nature06337

Serrano, M. A., Li, Z., Dangeti, M., Musich, P. R., Patrick, S., Roginskaya, M., et al. (2013). DNA-PK, ATM and ATR collaboratively regulate p53-RPA interaction to facilitate homologous recombination DNA repair. *Oncogene* 32, 2452–2462. doi: 10.1038/onc.2012.257

Shao, Z., Davis, A. J., Fattah, K. R., So, S., Sun, J., Lee, K.-J., et al. (2012). Persistently bound Ku at DNA ends attenuates DNA end resection and homologous recombination. *DNA Repair (Amst.)* 11, 310–316. doi: 10.1016/j.dnarep.2011.12.007

Shi, W., Feng, Z., Zhang, J., Gonzalez-Suarez, I., Vanderwaal, R. P., Wu, X., et al. (2010). The role of RPA2 phosphorylation in homologous recombination in response to replication arrest. *Carcinogenesis* 31, 994–1002. doi: 10.1093/carcin/bgq035

Shiromizu, T., Adachi, J., Watanabe, S., Murakami, T., Kuga, T., Muraoka, S., et al. (2013). Identification of missing proteins in the neXtProt database and unregistered phosphopeptides in the PhosphoSitePlus database as part of the chromosome-centric human proteome project. *J. Proteome Res.* doi: 10.1021/pr300825v. [Epub ahead of print].

Siepe, D., and Jentsch, S. (2009). Prolyl isomerase Pin1 acts as a switch to control the degree of substrate ubiquitylation. *Nat. Cell Biol.* 11, 967–972. doi: 10.1038/ncb1908

Steger, M., Murina, O., Hühn, D., Ferretti, L. P., Walser, R., Hänggi, K., et al. (2013). Prolyl isomerase PIN1 regulates DNA double-strand break repair by counteracting DNA end resection. *Mol. Cell* 50, 333–343. doi: 10.1016/j.molcel.2013.03.023

Sun, J., Lee, K.-J., Davis, A. J., and Chen, D. J. (2012). Human Ku70/80 protein blocks exonuclease 1-mediated DNA resection in the presence of human Mre11 or Mre11/Rad50 protein complex. *J. Biol. Chem.* 287, 4936–4945. doi: 10.1074/jbc.M111.306167

Symington, L. S., and Gautier, J. (2011). Double-strand break end resection and repair pathway choice. *Annu. Rev. Genet.* 45, 247–271. doi: 10.1146/annurev-genet-110410-132435

Tomimatsu, N., Mukherjee, B., Deland, K., Kurimasa, A., Bolderson, E., Khanna, K. K., et al. (2012). Exo1 plays a major role in DNA end resection in humans and influences double-strand break repair and damage signaling decisions. *DNA Repair (Amst.)* 11, 441–448. doi: 10.1016/j.dnarep.2012.01.006

Tran, P. T., Erdeniz, N., Symington, L. S., and Liskay, R. M. (2004). EXO1-A multi-tasking eukaryotic nuclease. *DNA Repair (Amst.)* 3, 1549–1559. doi: 10.1016/j.dnarep.2004.05.015

Tsabar, M., and Haber, J. E. (2013). Chromatin modifications and chromatin remodeling during DNA repair in budding yeast. *Curr. Opin. Genet. Dev.* 23, 166–173. doi: 10.1016/j.gde.2012.11.015

Ubersax, J. A., Woodbury, E. L., Quang, P. N., Paraz, M., Blethrow, J. D., Shah, K., et al. (2003). Targets of the cyclin-dependent kinase Cdk1. *Nature* 425, 859–864. doi: 10.1038/nature02062

Wang, B., Matsuoka, S., Carpenter, P. B., and Elledge, S. J. (2002). 53BP1, a mediator of the DNA damage checkpoint. *Science* 298, 1435–1438. doi: 10.1126/science.1076182

Wang, H., Shi, L. Z., Wong, C. C. L., Han, X., Hwang, P. Y.-H., Truong, L. N., et al. (2013). The interaction of CtIP and Nbs1 connects CDK and ATM to regulate HR-mediated double-strand break repair. *PLoS Genet.* 9:e1003277. doi: 10.1371/journal.pgen.1003277

Wohlbold, L., Merrick, K. A., De, S., Amat, R., Kim, J. H., Larochelle, S., et al. (2012). Chemical genetics reveals a specific requirement for cdk2 activity in the DNA damage response and identifies nbs1 as a cdk2 substrate in human cells. *PLoS Genet.* 8:e1002935. doi: 10.1371/journal.pgen.1002935

You, Z., Shi, L. Z., Zhu, Q., Wu, P., Zhang, Y.-W., Basilio, A., et al. (2009). CtIP links DNA double-strand break sensing to resection. *Mol. Cell* 36, 954–969. doi: 10.1016/j.molcel.2009.12.002

Yu, X., and Chen, J. (2004). DNA damage-induced cell cycle checkpoint control requires CtIP, a phosphorylation-dependent binding partner of BRCA1 C-terminal domains. *Mol. Cell Biol.* 24, 9478–9486. doi: 10.1128/MCB.24.21.9478-9486.2004

Yu, X., Fu, S., Lai, M., Baer, R., and Chen, J. (2006). BRCA1 ubiquitinates its phosphorylation-dependent binding partner CtIP. *Genes Dev.* 20, 1721–1726. doi: 10.1101/gad.1431006

Zhang, Y., Shim, E. Y., Davis, M., and Lee, S. E. (2009). Regulation of repair choice: Cdk1 suppresses recruitment of end joining factors at DNA breaks. *DNA Repair (Amst.)* 8, 1235–1241. doi: 10.1016/j.dnarep.2009.07.007

Zhou, B. B., and Elledge, S. J. (2000). The DNA damage response: putting checkpoints in perspective. *Nature* 408, 433–439. doi: 10.1038/35044005

Zhu, Z., Chung, W.-H., Shim, E. Y., Lee, S. E., and Ira, G. (2008). Sgs1 helicase and two nucleases Dna2 and Exo1 resect DNA double-strand break ends. *Cell* 134, 981–994. doi: 10.1016/j.cell.2008.08.037

Zou, L., and Elledge, S. J. (2003). Sensing DNA damage through ATRIP recognition of RPA-ssDNA complexes. *Science* 300, 1542–1548.

Conflict of Interest Statement: The authors declare that the research was conducted in the absence of any commercial or financial relationships that could be construed as a potential conflict of interest.

Received: 09 April 2013; paper pending published: 19 April 2013; accepted: 16 May 2013; published online: 03 June 2013.

*Citation: Ferretti LP, Lafranchi L and Sartori AA (2013) Controlling DNA-end resection: a new task for CDKs. Front. Genet. **4**:99. doi: 10.3389/fgene.2013.00099*

This article was submitted to Frontiers in Cancer Genetics, a specialty of Frontiers in Genetics.